

POLITECNICO DI TORINO

**Corso di Laurea Magistrale
in Ingegneria Civile, indirizzo Strutture**

Tesi di Laurea Magistrale

**Numerical simulation of a grouted
joint in an integral composite
framed bridge**



Relatore

Prof. Rosario Ceravolo

Co-Relatore

M.Sc. Florian Oberhaidinger

Candidato Matricola

Lucia Ferrini s250643

A.A 2019/2020



Summary

ABSTRACT	5
1.GROUTED JOINT FOR INTEGRAL FRAMED COMPOSITE BRIDGES, SUITABLE FOR HOT DIP-GALVANIZING	6
1.1 INTEGRAL COMPOSITE FRAMED BRIDGES AND REFERENCE BRIDGE	6
1.1.1 DESCRIPTION OF THE BRIDGE GEOMETRY	10
1.1.2 CONSTRUCTIVE STAGED	11
1.1.3 HOT-DIP GALVANIZING	15
1.2 GENERAL DESCRIPTION OF THE GROUTED JOINT	18
1.2.1 JOINT GEOMETRY	19
1.2.2 ASSEMBLY	21
1.2.3 BEARING BEHAVIOUR OF THE JOINT	24
1.2.4 GROUTED CONCRETE	28
1.2.5 SIMPLIFIED HAND CALCULATION	29
1.2.6 PARAMETRICAL STUDIES	31
2.FINITE ELEMENT METHOD AND MODELING	35
2.1 FINITE ELEMENT METHOD	35
2.1.1 DSM: DIRECT STIFFNESS METHOD	37
2.1.2 VARIATIONAL FORMULATION	39
2.1.3 ISOPARAMETRIC FINITE ELEMENT	43
2.1.4 FEM MODELLING: MESH, LOADS AND BCs	48
2.2 THE SOFTWARE ABAQUS	56
2.2.1 GENERAL DESCRIPTION OF ABAQUS SOFTWARE	56
2.2.2 MODEL COMPOSITION	57
2.2.3 MODULE PART	57
2.2.4 MODULE PROPERTIES	58
2.2.5 MODULE ASSEMBLY	59
2.2.6 MODULE MESH	60
2.2.7 MODULE STEP	61
2.2.8 MODULE INTERACTION	63
2.2.9 MODULE LOAD	67
2.2.10 MODULE JOB	68
3 MODELING	69
3.1 GENERAL PROPERTIES OF FE-MODELS	69
3.1.1 MATERIAL	69
3.1.2 ELEMENT	73
3.2 GLOBAL MODEL OF THE BRIDGE	74
3.2.1 MODEL OF ONLY ONE GIRDER	75
3.2.2 MODEL OF THE ENTIRE DECK	80
3.2.3 MODEL OF THE ENTIRE DECK WITH THE EFFECT OF THE ABUTMENTS	85
3.4 BASIC MODEL FOR THE PARAMETER STUDIES	93
3.4.1 GEOMETRY OF STEEL PARTS	93
3.4.2 CONCRETE	94
3.4.3 BASIC MODEL	97
3.4.4 VARIATION MODELS FOR THE PARAMETER STUDIES	101

4 RESULTS	103
4.1 THE WHOLE BRIDGE	103
4.1.1 COMPARISON OF THE DISPLACEMENT	103
4.1.2 COMPARISON OF THE REACTION FORCES	104
4.1.3 COMPARISON OF THE BENDING MOMENT	105
4.2 THE WHOLE BRIDGE WITH THE EFFECT OF ABUTMENTS	109
4.2.1 COMPARISON OF THE UDL	109
4.2.2 COMPARISON OF THE TS	111
4.3 SIMPLIFIED MODEL	112
4.3.1 SIMPLIFIED MODEL RESULTS	112
4.4 JOINT BASIC MODEL	115
4.4.1 RESULTS OF BASIC MODEL: ELASTIC ANALYSIS	116
4.4.2 RESULTS OF MODEL 2: INFLUENCE OF THE ADDITION OF HORIZONTAL STIFFENER	123
4.4.3 RESULTS OF MODEL 3: PLASTIC ANALYSIS	125
4.4.4 MODEL1-MODEL4: INFLUENCE OF TW IN THE ELASTIC ANALYSIS	130
4.4.5 MODEL3-MODEL5: INFLUENCE OF HW IN THE PLASTIC ANALYSIS	137
4.4.6 MODEL5-MODEL6: INFLUENCE OF TW IN THE PLASTIC ANALYSIS	142
5 CONCLUSIONS	148
BIBLIOGRAPHY	149

Abstract

Hot-dip galvanizing is a profitable and sustainable procedure to protect steel components from corrosion: in the past, hot-dip galvanized steel components for bridges have been avoided largely because of concerns regarding the fatigue behaviour. Current research has shown that hot-dip galvanized components can be used for bridge constructions under certain conditions: the results are new alternative solutions instead of the anti-corrosion coatings of bridge constructions and they show how new technique are available, as the usage of hot-dip-galvanized steel components. It could improve the sustainability and profitability of prefabricated composite bridges. One of the dominant problem linked to hot galvanizing is the limited length of the deck that can be galvanized. In order to overcome this problem, the main ambition was that to create grouted joint suitable for hot dip galvanizing structures. One aim is to avoid welding on site. The technical University of Munich has begun to study and develop this new type of joint. The aim of this thesis is the numerical simulation of a particular grouted joint in order to define its own geometry and its behaviour, and also to investigate how the stresses are exactly distributed inside of it and, at the end, to highlight how the presence of the joint affects the entire behaviour of the bridge under investigation. The purpose of this thesis is the creation of a parametric model of the joint that allows to understand and investigate which is the best geometry to choose. To achieve this goal, the behaviour of the whole bridge without internal joints is first analysed by creating a 3D model on Abaqus. The model is validated by comparing the results with that obtained from the analysis of the same bridge modelled on Sofistik. Sofistik model is important to define M_{\max} , M_{\min} and shear force on joint. Knowing that, it is possible to design the parametric 3D model of the joint on Abaqus: it allows to understand the most important parameters that have to be define. The geometry of the model should be studied first in the elastic field and after in the plastic field, introducing the perfectly plastic-elastic law for steel and after even some control parameters for concrete. In this way, it is possible to investigate completely the behaviour of the joint. Once create the model, the subsequent step could be to insert the joint into the whole bridge and analysed what is its effect on the entire structure. After all these investigations, it could be interest to go on with the studies: the next step could be to analyse the response of the joint in nonlinear field, under the effect of creep and shrinkage, for example.

1.GROUTED JOINT FOR INTEGRAL FRAMED COMPOSITE BRIDGES, SUITABLE FOR HOT DIP-GALVANIZING

This chapter contains general and basic information about integral composite frame bridges, hot dip galvanizing and the grouted joint.

1.1 Integral composite framed bridges and reference bridge

In a first general analysis, Bridges can be classified according to their static scheme as follows:

- a. Girder bridges;
- b. Arched bridges;
- c. Frame bridges;
- d. Cable-stayed bridges;
- e. Suspension bridges;

Girder Bridge: the main structural elements for supporting the deck of these bridges are simple girders. The two most common cross sections of steel girder bridges are plate- and box-cross section. A girder may be made of concrete or steel. The girders themselves are the primary support for the deck, and are responsible for transferring the load down to the foundation. Material type, shape, loads and weight affect the bearing capacity. Many short-span bridges, especially in rural areas, use concrete box girders. Due to the properties of the moment of inertia of the section, the height of the girders is the most significant factor to influence its load capacity. Longer spans, more traffic, or wider spacing of the girders will all directly result in a deeper beam. (Technology, 2012)

Arch bridges: it has abutments at each end shaped as a curved arch. It works by transferring the weight of the bridge and its loads partially into a horizontal thrust restrained by the abutments at either side. A viaduct, or a long-span bridge, may be made from a series of arches. In truss and arch bridges, the girders are still the main support for the deck, but the load is transferred through the truss or arch to the foundation. These designs allow bridges to span larger distances without requiring the depth of the beam to increase beyond what is practical. (Troyano, 2003)

Frame bridges: this type of bridge has an intermediate behaviour between the arched bridges and beam bridges; in fact, it is a special structure that results very suitable for prefabrication: these bridges can be composed by a single frame or by continuous frames. A particular typology of this kind of bridge is the rigid-frame bridge: the superstructure and substructure are rigidly connected to act as a continuous unit. Typically, the structure is cast monolithically, making the structure continuous from deck to foundation and the connections between members are rigid connections which transfer bending moment, axial forces and shear forces. A bridge design consisting of a rigid frame

can provide significant structural benefits, but can also be difficult to design and construct: the starting point for the construction of frame bridges was the very high-quality design of the frames compared with the single-span girder bridges implemented until then. The advantages of frame bridges, such as high stiffness, favourable transmission of horizontal loads and simple construction without bearings, are discussed subsequently. (Transportation) (Marx)

Cable-stayed bridges: it has one or more pylons, from which support the bridge deck: a distinctive feature are the cables, which run directly from the tower to the deck, normally forming a fan-like pattern or a series of parallel lines. The cable-stayed bridge is optimal for spans longer than cantilever bridges and shorter than suspension bridges. (American, 2017)

Suspension bridges: it is a type of bridge in which the deck is hung below suspension cables on vertical suspenders. The suspension cables must be anchored at each end of the bridge, since any load applied to the bridge is transformed into a tension in these main cables. The main cables continue beyond the pillars to deck-level supports, and further continue to connections with anchors in the ground. (York, 2013)

After a brief description of all typologies, the focus is now on composite frame bridges, with particular static scheme and behaviour: the integral types. There is a differentiation between the integral and the semi-integral construction method. Integral construction method: it means a direct and integral connection between superstructure and sub-constructions, and abutments respectively. Semi-integral construction method: the bridge components are structurally separated and the abutments are for instance separated by bearings and joints. However, it is important to underline that the integral bridges feature a monolithic connection of the sub-constructions, abutments and piers to the superstructure. Together they form rigid frames without bearings and joints, which would separate the components from each other. Modern materials, such as high-strength concrete can be used to build pier walls. Fully integral bridges are monolithically connected to the supports and abutments in all axes of the substructure and the temperature dilatations have to be entirely compensated by centric tensile or compressive forces in the superstructure. Through the almost complete deformation dilatation under constraint, the occurring forces are independent of the bridge length but depend linearly on the axial stiffness of the superstructure. Tensile and compressive forces introduced by the superstructure are absorbed by the abutments, whereas, in the longitudinal direction of the bridge, almost no loads are exerted on the piers. Therefore, the abutments of integral bridges have a very high horizontal load-bearing capacity: a certain flexibility of the abutments remains, which is why on very short integral bridges almost no horizontal forces from temperature occur. The longer the length is, the lower the influence of the abutment's stiffness is; horizontal forces due to temperature and, consequently, the high effort of their introduction, approximate the theoretic limit value of $N =$

EAaTΔT. Therefore, fully integral bridge is primarily suitable for very short and also very long bridges; however, axial stiffness of the superstructures had to be kept as low as possible: this is achieved by reducing the cross-section's surfaces in case of short span widths and reducing crack formation by avoiding pre-stressing. The superstructure expands or shortens nearly without hindrance because the bending-resistant connected piers deform largely in the longitudinal direction of the bridge. (Condoleo, 2011) Often containment structures are analysed representing the soil essentially as a load: it means that the stiffness of the soil is not modelled in this case. The design proceeds considering only limiting active and passive lateral earth, if movements or deflections of the structure are insufficient to collect the limiting values, intermediate values of earth pressure occur. The lateral earth pressure depends on the strain in the soil, which in turn depends on the structure movement; they depend on the stiffness of both structure and soil, and on lateral earth pressures. This is the reason why, an analysis, which somehow reflects this loop, is required, unless the hypothesis of limiting earth pressures can be deemed conservative and acceptable. In some retaining structures, use of restrict earth pressures can be checkable in either cases, conservative or no conservative. In fact, for example, during the summer expansion of the superstructure in an integral bridge, lateral earth pressures on the abutments can nearing the theoretical passive state, especially in the upper portion where horizontal displacements are largest and pressures can be an order of magnitude greater than those experienced by non-integral bridge abutments. For some integral bridge arrangements, it is sufficient to carry out the design on the basis of some assumed lateral earth pressure distribution, while or others, the soil stiffness plays a more significant part in the behaviour of the system and an analysis which models the behaviour of both soil and structure and a soil-structure interaction analysis (SSI), is required. (Rhodes, 2018)

After all this information is possible to say that the main advantages of framed composite bridges are:

- a. The greater structural effectiveness: these bridges have a huge number of degree of constraints and it means that bending and cutting stresses of the structures making up the bridge has more uniform trend and lower peak values;
- b. Lower maintenance costs: eliminating joints and support devices, in addition to involving a lower initial cost of the bridge, it determines also a lower cost of extraordinary maintenance of the product during the time;
- c. Longer useful life: these continuous solutions increase durability and therefore the useful life of the structure: in fact, the missing of the expansion joint removes a pathway for the penetration of water;
- d. The greater reserve of resistance: the hyperstaticity of the static scheme employed allows the bridge to have a greater capacity curve;

One major purpose to build integral bridges is the will to create slender and transparent bridge structures through astute design. If piers and abutments do not require bridge bearings, the sub-constructions can be simplified, since it is no longer necessary to provide storage and floor space for the jacks. This operation allows also a slenderer design of piers, because their accessibility does not have to be guaranteed. Leaving out bearings and joints has some important advantages, in particular with regard to building maintenance:

- Sustainable construction, due to the elimination of technology susceptible to failure;
- Low maintenance, easy building inspection;
- Lower construction cost, due to savings on bearings and employment of simpler building components;

Once eliminating the bearings, it is not necessary anymore, to provide access to them for the purpose of inspection, maintenance, and replacement; at the same time, having not to offer accessibility and floor space for the jacks simplifies the construction of piers. In fact, the pier can thus be pre-fabricated and then mounted. Therefore, costs can be drastically reduced. Integral abutments can be constructed in a simpler design, which makes them less prone to damages. Another important aspect is that the construction reduces noise because there are no more joints to be crossed. It has thus proved to be of benefit also in urban areas. As said above, once eliminating the bearings, it is not necessary anymore, to provide access to them for the purpose of inspection, maintenance, and replacement; at the same time, having not to offer accessibility and floor space for the jacks simplifies the construction of piers. In fact, the pier can thus be pre-fabricated and then mounted. Therefore, costs can be drastically reduced. Integral abutments can be constructed in a simpler design, which makes them less prone to damages. Another important aspect is that the construction reduces noise because there are no more joints to be crossed. It has thus proved to be of benefit also in urban areas. For the investigations, carried out in this thesis, a reference bridge is considered. This bridge was designed by the structural engineer office SSF and is already built in Germany.

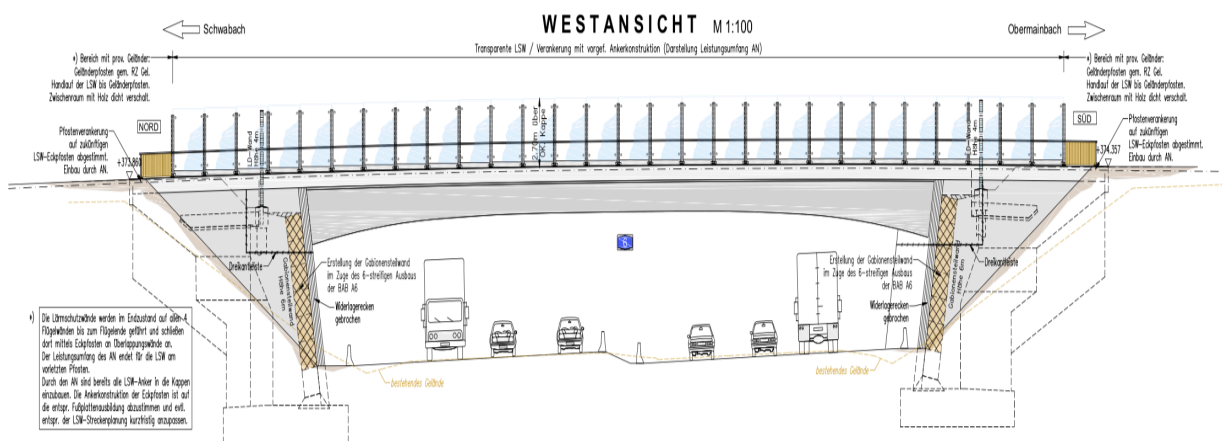


Figure 1 The Bridge under investigation

1.1.1 Description of the bridge geometry

The bridge under investigation is an integral composite framed bridge: it is an only one-span bridge of total length of 42.210 meters and variable cross section. The transversal length is 12 meters and it is split in 4 girders of 3 meters width each one; all the girders have steel box section with precast concrete slab of constant width above, and a second concrete slab casts in situ. The box section of each of the 4 girders is composed by four pieces of different thickness welded to each other:

- Top flange: it has constant thickness of 12 mm over the whole span;
- Bottom flange: it has variable thickness. In the 5.5 meters close to the abutments the thickness is 55 mm and in the remain part it is 30 mm;
- Two lateral webs: they have variable thickness. The initial width is 22 mm in the 6 meters near the abutments; after that it becomes 16 mm for another 5 meters on both sides and the remain part has $t = 12$ mm;

It is important to say that the bridge span is perfectly symmetrical with respect to the centreline section and that the precast slab is fixed to the box section thanks to reinforcements welded on the top flanges. Following these guidelines, the structure has been modelled through these four different cross sections along the span length:

Querschnitt Träger 1-4 M=1:25

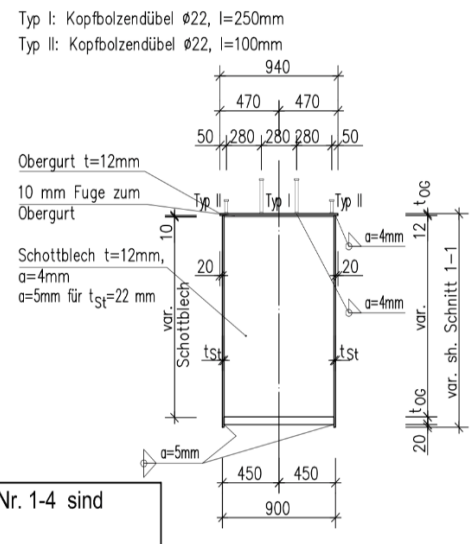


Figure 2 Transversal section of the steel box girder

Two important approximations have been done in this first modelling step:

1. Perfect flatness of the span;
2. Perfect orthogonality of the girders regarding the abutments connections;

In fact, it is necessary to report that in the real physical problem, the ground under the bridge is not perfectly flat and there is a gap between the two abutments: the span altitude at the abutments is respectively + 373.951 meters on the left side and +374.292 meters on the other side. Moreover, as it is evident from the planimetry in the figure, the four girders are not perfectly orthogonal to the abutments. Nevertheless, given that the height gap is not too relevant and so also the transverse inclination angle, it is held to be true adopting the simplifications introduced previously, because they are not considered significant for what it is interesting to calculate.

1.1.2 Constructive staged

This is an integral bridge and it means that the span has to work together with the abutments in operating conditions. Indeed, it is fundamental to respect the true and real constructive phases in the bridge modelling, in order to obtain the real and exact displacement, strain and stress fields. In this case, the construction of the bridge is simulated in the following way:

- Construction phase 0:

Each single girder is considered simply supported by the abutments and the load in this stage is the only dead load of the steel box section and of the precast concrete slab. There is only one reagent section in the entire span, composed by the precast concrete slab and the steel box section.

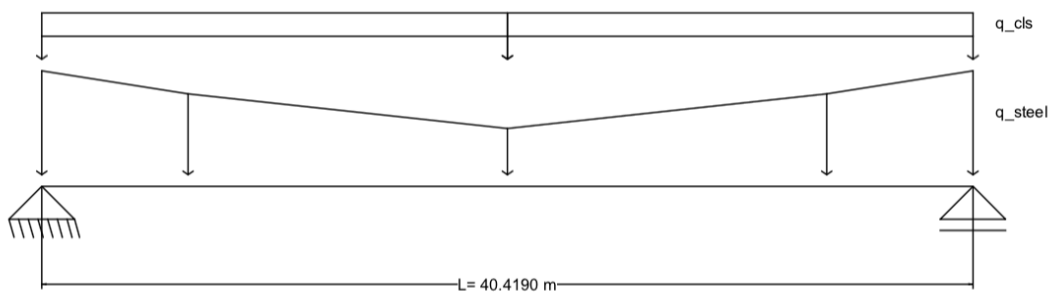


Figure 3 Dead load of the steel box section and the precast concrete slab

- Construction phase 1:

After the installation of the span, the second slab is cast in situ, but not everywhere: it is thrown only in the 8 meters close to the two abutments. It is important to underline that in this phase the reagent section is still the same of the previous step and the girder is always simply supported and the edge, until the second slab concrete has hardened. The dead load of the slab cast in situ is now added to the previous load only in the concerned regions.

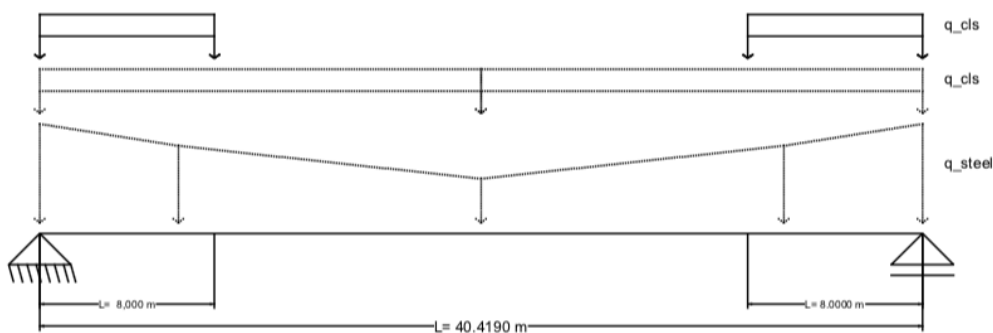


Figure 4 Dead load of the second slab cast in situ near the abutments

- Construction phase 2:

Once the concrete has hardened, the girder changes its static scheme: in this phase, the span works together with the abutments and it is possible to consider this new static scheme, Encastre-Encastre. The remaining part of the secondo slab is now cast and so in the model calculation the dead load of this part is added. There are now two different reagent sections to deal with:

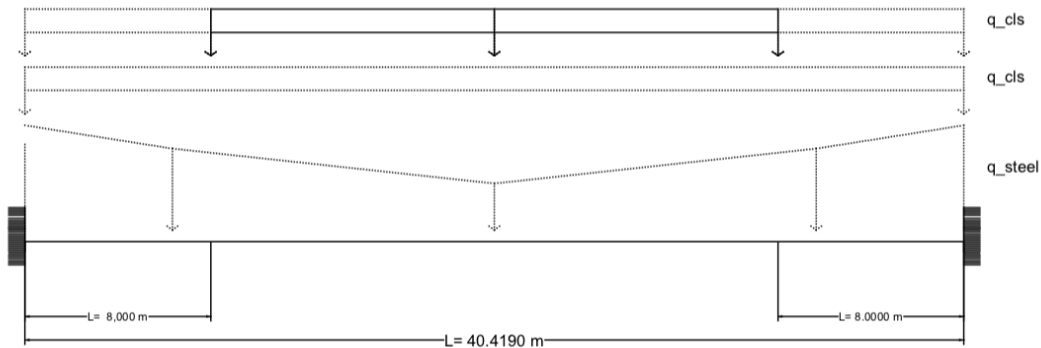


Figure 5 Dead load of the second part of the second slab cast in situ

- Construction phase 3:

In this step, the entire girder works with the same permanent cross section and with the final static scheme connected to the abutments. Now, it is possible to add the loads carried out by the superstructure, according to what was established in the project design:

- a) Noise protection wall

$$q = 0.6 \frac{kN}{m}$$

$$p_y = 0.45 \cdot 0.65 \cdot 25.00 + 0.6 = 7.9 \frac{kN}{m}$$

$$m_z = 0.45 \cdot 0.65 \cdot 25.00 \cdot 0.23 \pm 0.6 \cdot 0.22 = \pm 1.8 \frac{kN}{m}$$

- b) Kerb:

$$p_y = 0.23 \cdot 25.00 = 5.8 \frac{kN}{m^2} \quad (\text{Left})$$

$$p_y = 0.24 \cdot 25.00 = 6.0 \frac{kN}{m^2} \quad (\text{Right})$$

- c) Road Surface

$$p_y = 0.08 \cdot 25.00 + 0.5 = 2.5 \frac{kN}{m^2}$$

- d) Drainage system

$$p_y = \pi \cdot 0.1^2 \cdot 10.00 + 0.25 = 0.56 \frac{kN}{m}$$

This load is applied as a surface load on a 20cm wide strip $p_y = \frac{0.56}{0.20} = 2.8 \frac{kN}{m^2}$

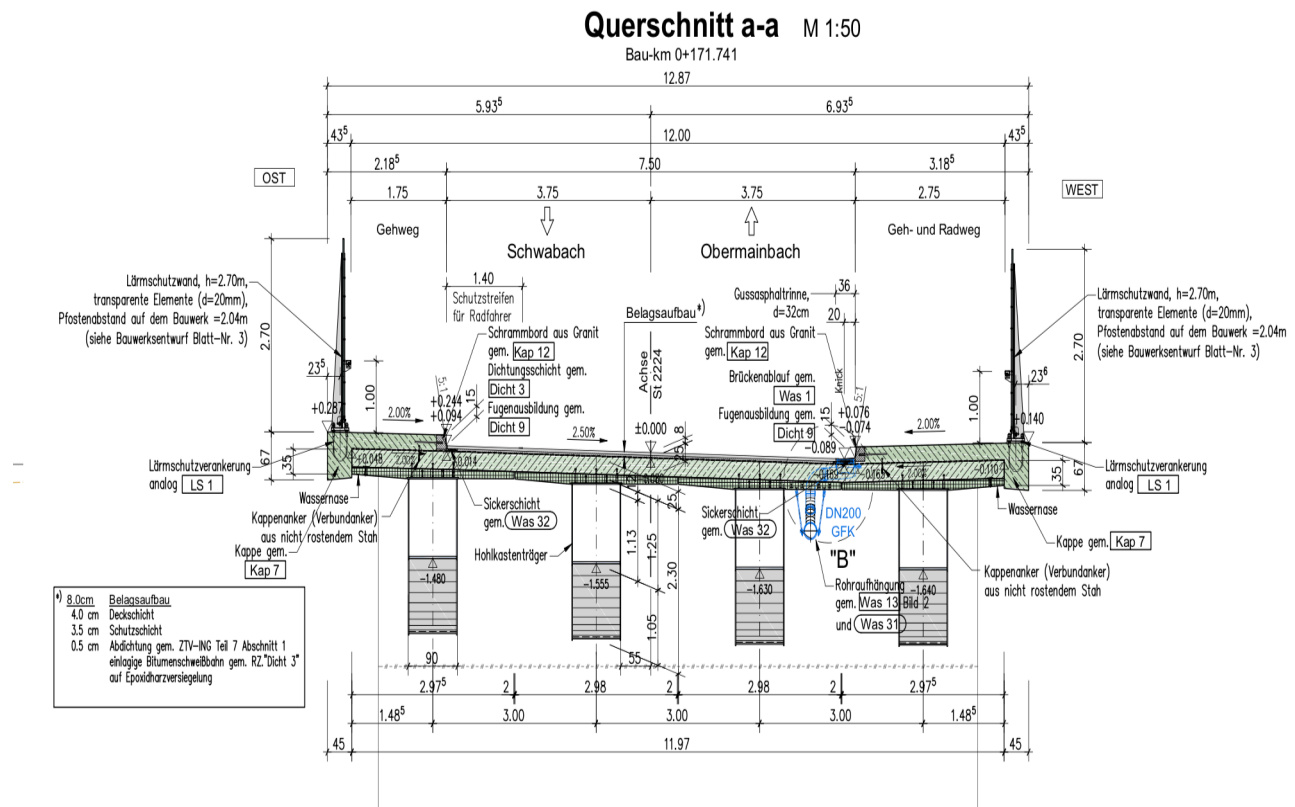


Figure 6 Transverse section of the bridge

After the analysis of the stresses due to the construction phases, the next step is to consider the behaviour of the bridge under the traffic load. According to the Euro code EN 1991-2 ‘Traffic loads on Bridges’ chapter, the general organisation for road bridges verification is the next:

TRAFFIC LOAD MODELS:

- Vertical Forces: LM1, LM2, LM3, LM4;
- Horizontal Forces: braking and acceleration, centrifugal and transverse;

GROUPS OF LOADS:

- gr1a, gr1b, gr2, gr3, gr4, gr5;
- Characteristic, frequent and quasi permanent values;

The difference load model ‘LM’ are created to do specific analysis in order to study any types of stresses:

LM1: Uniform distributed loads and tandem system, used for main model and local verification;

LM2: Single axial load used for semi-local and local verification;

LM3: Set of special vehicles used for general and local verification;

LM4: Crow loading $q = 5.00 \frac{kN}{m^2}$ used for general verification;

The different kind of loads are applied on the carriageways according to the follow information and to the introduction of the concept of 'Lane':

Division of the carriageway into notional lanes

Carriageway width w	Number of notional lanes	Width of a notional lane w_l	Width of the remaining area
$w < 5,4 \text{ m}$	$n_l = 1$	3 m	$w - 3 \text{ m}$
$5,4 \text{ m} \leq w < 6 \text{ m}$	$n_l = 2$	$\frac{w}{2}$	0
$6 \text{ m} \leq w$	$n_l = \text{Int}\left(\frac{w}{3}\right)$	3 m	$w - 3 \times n_l$

NOTE For example, for a carriageway width equal to 11m, $n_l = \text{Int}\left(\frac{w}{3}\right) = 3$, and the width of the remaining area is $11 - 3 \times 3 = 2 \text{ m}$.



Figure 7 Division of the carriageways

The Load Model 1, that is usually used in the first analysis, consists in the application of different surfaces loads in each different lane, to maximize the effect in the bridge, according to the position of the most loaded lane: in fact, lots of combinations have to be done in order to find the worse position of the most charged lane.

The main load model (LM1)

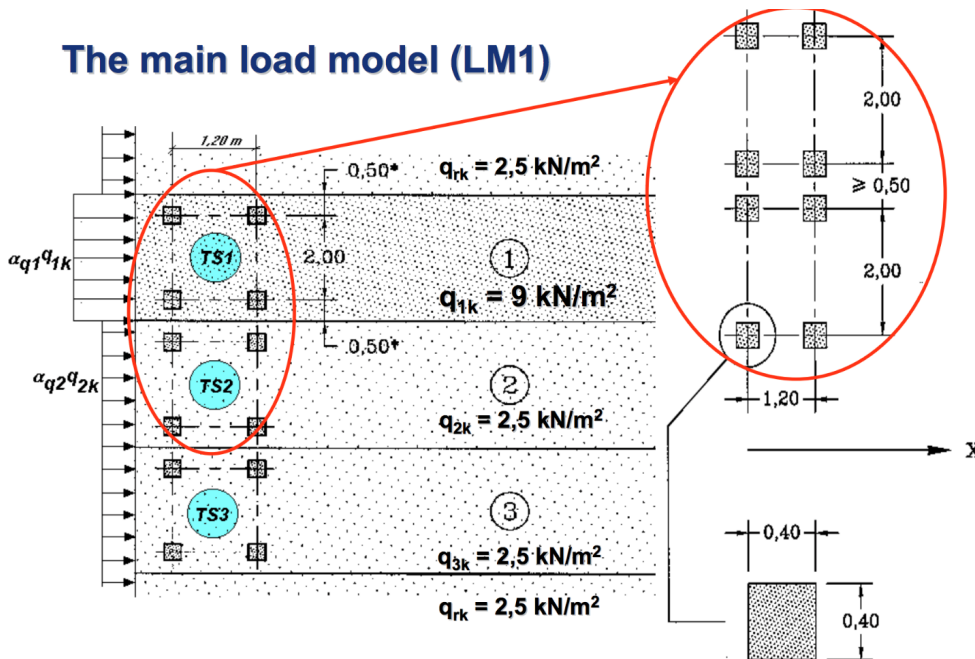


Figure 8 Load Model 1

In this case the worse combination is analyzed before thanks to Sofistik model, to avoid computational afford.

1.1.3 Hot-dip galvanizing

In general, bridges are designed and dimensioned taking into account a life span of 100 years; they should maintain the required suitability for use, withstand the changes, and demand as little maintenance as possible. Regarding the conceptual design, the following aspects are considered leading:

- a) Cost-effectiveness: the costs for planning, the materials, the maintenance and repair, the manufacture of the substructure and superstructure are taken into account;
- b) Simple design: it usually reduces planning and construction costs;
- c) Fast construction: construction time is an essential economic factor. In fact, a long-time of traffic closures or obstructions could be in some cases even more expensive than the building costs;
- d) Longevity and maintenance costs: maintenance and repair costs of a bridge over the total lifespan can in many cases be higher than the initial costs. Their cost depends on the system and adopted material; however, they should be an important factor for the design of a bridge: with limited technical effort, considerable costs can be saved;
- e) Aesthetics: visible surface and geometry of the buildings have a great influence on the perception. Even if the external aspect of bridges is not the main focus, it can significantly disturb the perception of the surroundings;

The most important thing is to reduce the cost of construction and of maintenance during the entire bridge life. In order to do that, one of the most important aspect of steel decks is to prevent any mechanism of corrosion. In fact, one of the main causes of damage to road bridges, especially in the composite steel-concrete ones, is the corrosion and it could be done by the following sources:

- Increased use of new and more aggressive defrosting salts;
- Delayed or absence of maintenance measures to protect against corrosion;
- Bridges last more than 100 years;
- A classical organic cladding must be renewed at least 2/3 times during the life of the bridge;

The corrosion problem could be avoided in pre-stressed structures and reinforced concrete construction, using Pre-stressing or reinforcing steel either internally direct or indirect contact with concrete and in the case of external tendons, cladding tubes surround the steel to protect it against corrosion. Till today, most steel bridges have used organic protect coatings from high polymer materials: although these coatings are effective, experience has shown that they have to be renewed every 25 - 30 years. Based on a desired service life of 100 years, in addition to the first coating, at least 3 further renewal coatings are required, which not only cause material and labour costs, but usually cause traffic closure, which in turn are very expensive. Nowadays, some new anti-corrosive

techniques have been developed to improve the durability of the structure and to reduce maintenance costs. The choice of the best anti-corrosive technology is an important preventive measure for designers and builders: the steel protection from corrosion represents a fundamental aim in affirming sustainable development. An alternative to organic coatings is galvanizing, especially hot-dip galvanizing, in which the steel components, that have to be protected against corrosion, are immersed in a molten zinc, with an iron-zinc layer forming on the surface that protects the component. Hot-dip galvanizing is a traditional corrosion protection process that has been used successfully for many years and can easily achieve protection periods of over 100 years. Around 2 million tons of steel are hot-dip galvanized in Germany every year. The process is used in various areas, and the following are the most significant in the field of civil engineering:

- Traffic engineering: street furniture, crash barriers, vehicle construction;
- Metal crafts: railings, gates, gratings and individual buildings;
- Steel construction: industrial construction, parking garages in steel and composite construction;
- Facades: substructures and fasteners for example;

Of course, there are many more applications for hot-dip galvanized steel components. A study, conducted by the Technical University of Munich, made it possible to estimate maintenance costs over the years for the different choice of protection adopted: organic coating and hot galvanized. Indeed, looking at the economical German background, it is possible to see that there is at least one viaduct for each kilometre of highway in Germany: this is the reason why the studies about bridges and their maintenance have always been so important. It is a question of high economic weight: for example, taking into account 80 km of a highway, it is probable to find out around 100 bridges of a wide variety of lengths. Discovering a less expensive way of doing maintenance is becoming a well-founded issue to solve.

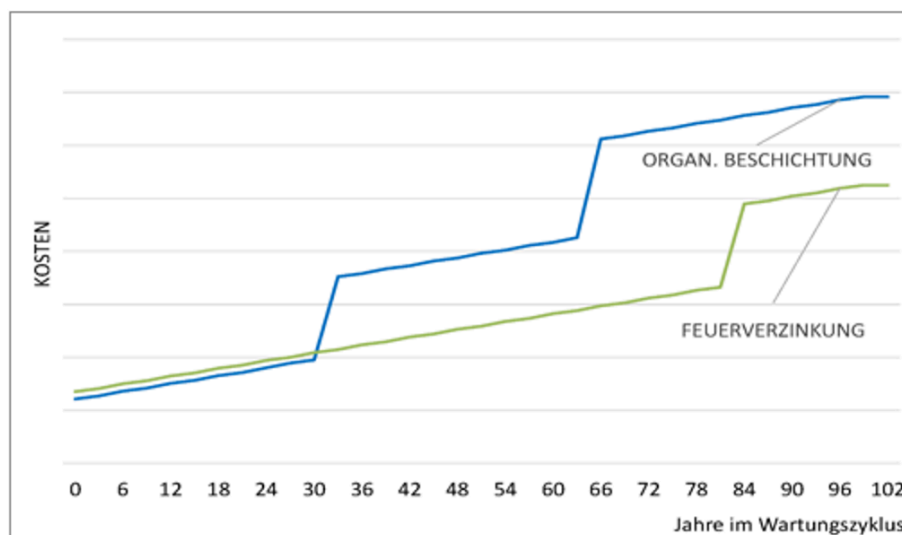


Figure 9 Comparison of the costs of different anti-corrosion technique

From the graph, it appears that preservation has to be done on bridges covered by organic cladding every 33 years: that's why hot galvanized has been designed as protection from corrosion in bridges construction. In fact, the galvanized coating is not simply deposited, as happens to the organic coating: the zinc binds to steel by means of metallurgical reaction and the coating obtained by immersion in a bath of fused zinc at 450° guarantees a very resistant long-lasting protection. This technique is relevant because it allows all the surface of the structure to be protected: in fact, making hollows profiles, the fluid can also penetrate inside, covering the internal layers. Moreover, it is impact resistant and this property takes on an important role for the various in situ construction operations that the structure may undergo. It protects the artefact with a dual mechanism: the barrier effect and the cathodes protection. The first mechanism allows the steel surface to be protected against the external environment and the second one allows the steel to be still protected in case of scratches, nicks or small damaged areas, because zinc acts as a sacrificial anode. In the common atmosphere exposition, this kind of coating could survive more than 50 years, realizing a performance unmatched by other protection system: it means that no maintenance is required on the structure for decades. It is recommended to use this technique with steel S355 with high-level of Si. Hot galvanizing is used in the composite steel-concrete structures and so it is important also to consider the reaction between zinc and concrete: zinc remains passive due to its low pH. and it means that galvanized steel is less susceptible to corrosion due to concrete carbonation. Going down in detail, surface zinc layer that is up to $300\text{ }\mu\text{m}$ thick is considered enough to protect a component from atmospheric influences for over 100 years. As said, hot-dip galvanizing is characterized by immersing a component in a molten zinc melt: but in order to get the zinc layer as clean and uniform as possible, however, a component, entering the zinc bath, has to go through a number of steps to be degreased and cleaned. In fact, workers have to adhere to some constructive constraints and pretreat the component. The process can protect both the smallest components and meter-long steel girders from corrosion. One of the main disadvantages is related to the limit of the size of the hot galvanizing bands: in fact, it also limits the size of the pieces that can be immersed. Repeated drafts of the same piece are not recommended because they can cause irregular heating and therefore great thermal stress absolutely not required. (Pernice, 2014) (Ricciolino, 2013) The zinc factories are the causes of important problems, such as maximum dimensions and limited weight, when a piece is galvanized. In fact, the only solution given to this problem in the past years, was to have galvanized steel girders with welding butts in the middle length range, that had to be subsequently repaired by spray galvanizing: this solution, not only leads to additional manufacturing costs, but also to additional maintenance and repair costs, since these impacts have bad results in terms of the life span of the corrosion protection compared to hot-dip galvanized components. In hot-dip galvanizing structure, in order to protect itself against corrosion

as an economical and efficient solution, new construction forms must be developed that are tailored to the boundary conditions of the zinc bath sizes and work without additional welding shocks and spray galvanizing. If such structures are available, hot-dip galvanized composite and composite prefabricated bridges have every requirement to become an attractive and extremely economical solution for bridges in the medium length range. It can be assumed that the proportion of hot-dip galvanized steel composite constructions for the length range in question can be increased considerably with a design that is suitable for galvanizing. (Rossi, 2014) Recently, there were concerns about the fatigue resistance of hot-dip galvanized components, which is why the method has only been used very little in bridge construction to date. Only in recent years has a research project on the behavior of hot-dip galvanized components under fatigue load, which was developed in cooperation between the TU Dortmund, the MPA-Darmstadt and the Institute for Corrosion Protection Dresden GmbH, demonstrated that hot-dip galvanizing for use is cyclical suitable bridge components. There are already a large number of bridges worldwide that were made with hot-dip galvanized steel girders and are still in good condition even after many years.

1.2 General description of the grouted joint

The solution to the previous problem is given by special **grouted joint**, designed and developed to avoid the use of welded areas in the steel decks and to prevent the problem of the fixed dimension of hot- galvanized pieces of steel. In this way, in fact, it is possible to have span longer than 16 meters, which is the limit of the zinc bath. In fact, the aim of the previous studies conducted at the chair of metal construction at the Technical University of Munich, was to create a method for the deletion of weld-free potting joints for hot-dip galvanized bridges. The idea, behind this project, was that to create a way to tie together two different pieces of hot-galvanized steel, in a simple constructive phase, as shown in the following figures. The aim of the design was to develop an assembly joint for the box cross-section of a prefabricated composite bridge, which takes advantage of the positive properties of the tie between steel and concrete and which can be studied as maintenance-free as possible so that both screwing and assembly welding can be avoided. The galvanizing-compatible casting joint should be designed and dimensioned so that it can be used for hollow boxes in bridges in the medium span range. That project is intended to provide an order of magnitude for the internal forces and the dimensions by which one can orient oneself. However, the connection technology should be prepared in such a way that it can also be adapted to other combinations of internal sizes and geometries. It consists of a steel and concrete combination: the steel is previously subjected to hot galvanizing and the concrete is cast immediately after the assembly of the two pieces.

1.2.1 Joint geometry

The general geometry of the joint itself is described in the following pictures.

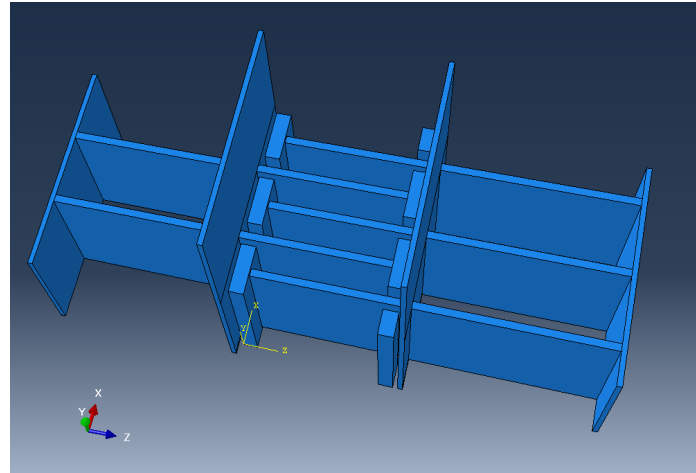


Figure 10 General 3D model of the joint

This is only the steel parts of the joint: this has been surrounded by the bridge and it has concrete inside as explained better in the next chapter. In fact, since the position of the joints along the span can be decided only once the whole bridge has modelled and once it is possible to know the soliciting actions due to all the load combinations applied to the model, the focus is now only on the geometry.

Analyzing only the right part, the elements are the following:

- a) 1 Diaphragm;
- b) 3 T-stubs welded to the diaphragm;
- c) 3 steel webs welded behind the diaphragm;
- d) 1 stiffener element, that is the end element of the joint;

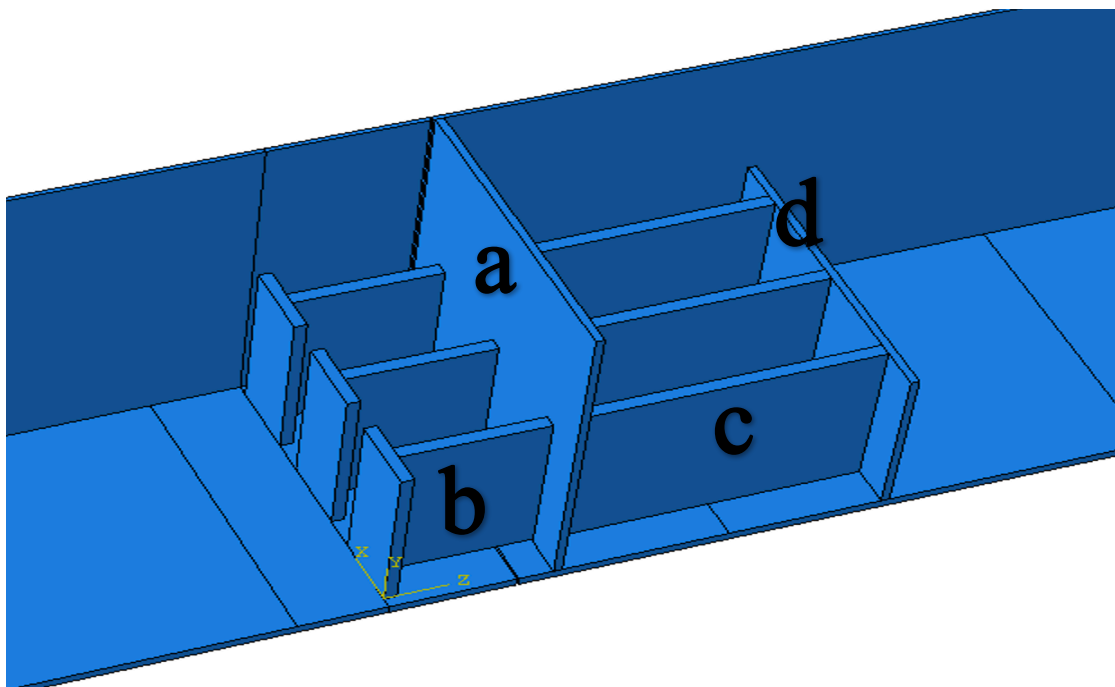


Figure 11 Joint-1

The diaphragm (a) has the same height of the total full available section of the steel box at the point in which the union is inserted. The relevant knowledge is that the two different parts are assembly near each other, and the concrete is cast to create the connection between the T-stubs in the space between the two full-height diaphragms. The geometry of the element is not known and this is one of the topic of this thesis: find out the best geometry, studying the behavior of the joint under the different load conditions. The following pictures allow us to understand which quantities are involved for the complete joint design:

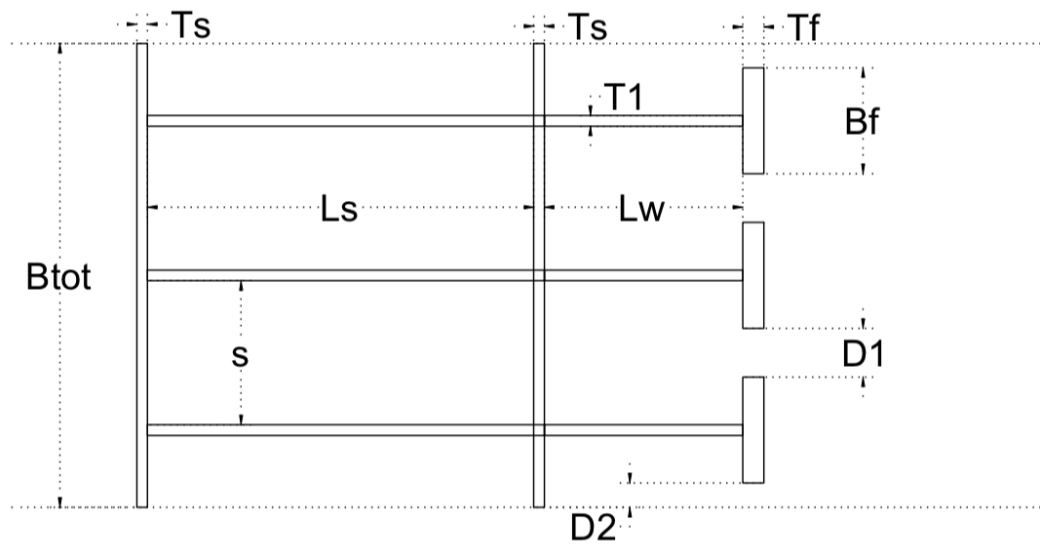


Figure 12 Geometrical parameters of the Joint 1

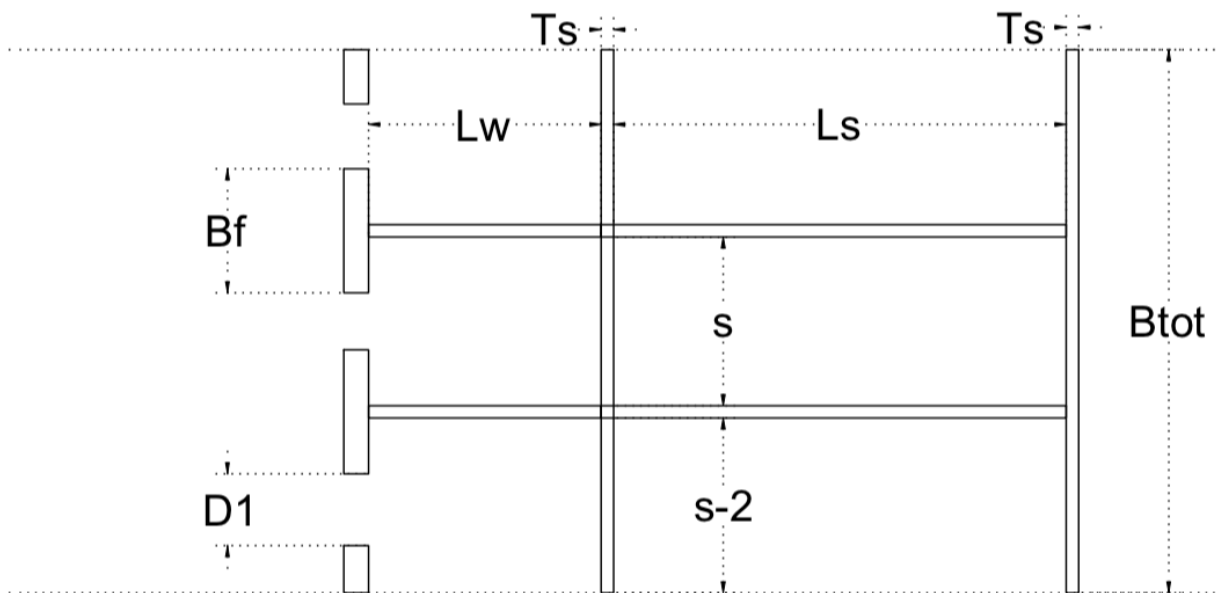


Figure 13 Geometrical parameters of the Joint 2

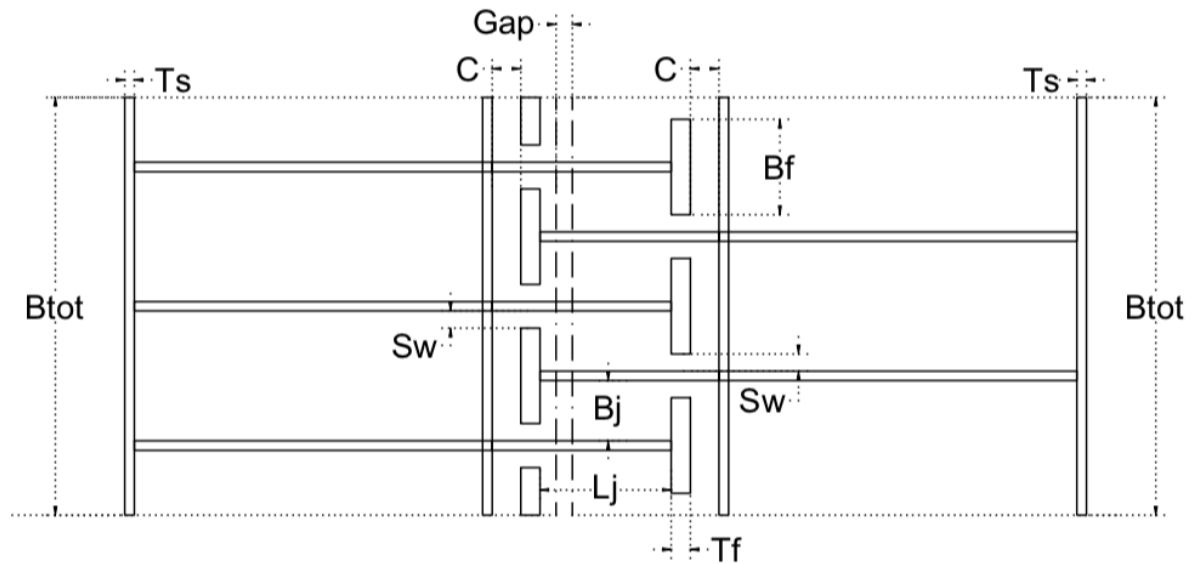


Figure 14 Geometrical parameters inside the joint

1.2.2 Assembly

After a brief description of the single steel parts of the joint, it is really important to understand how these elements are inserted inside the whole bridge. The following pictures show brief and simplified explanation of the joint assembly.

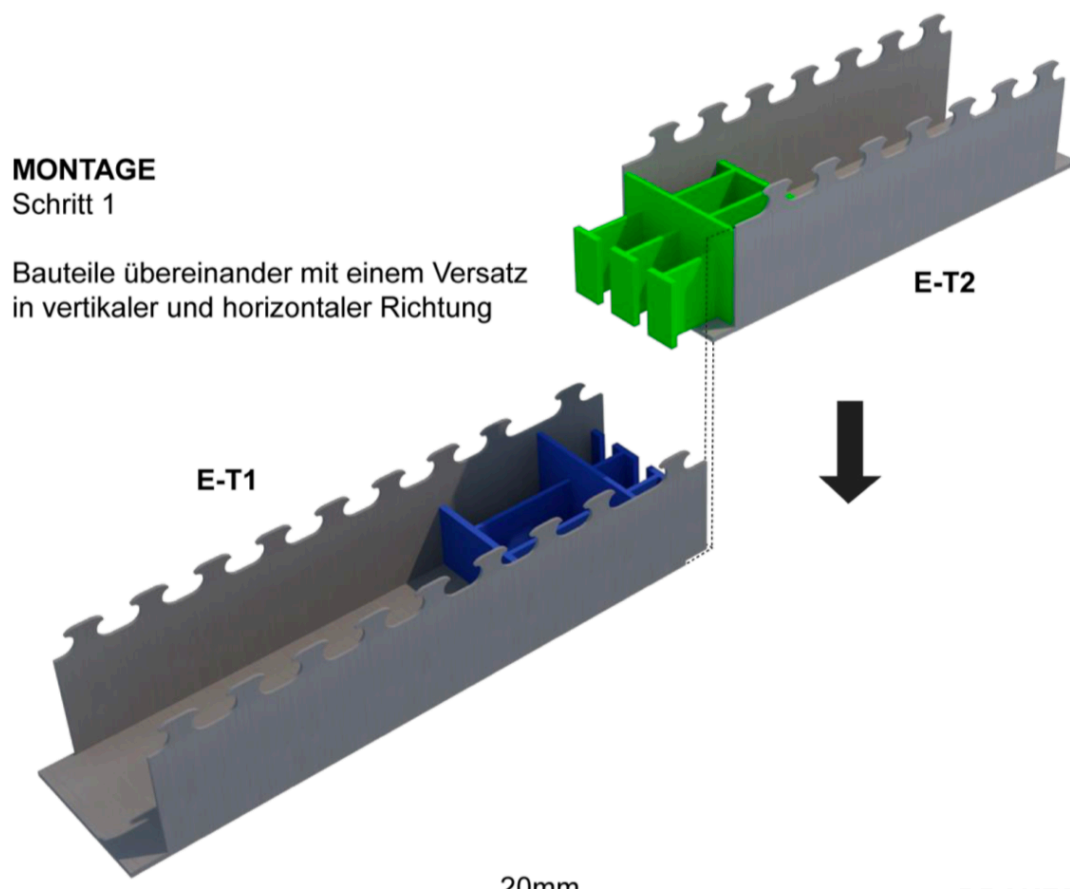


Figure 15 Assembly. Step 1: Components on the top of each other with an offset in vertical and horizontal direction

According to the pictures 12, 13 and 15, the steel parts on the right side are called all together Joint1 and the steel parts on the left, Joint2. The first phase of assembly is the vertical align of the two different joints, included the respectively bridge's parts. The second phase, instead, is the horizontal alignment, as shown in the following picture.

MONTAGE

Schritt 2

Das Bauteil E-T2 wird vertikal abgesenkt
bis die Unterkanten der Bodenplatten
niveaugleich aufliegen

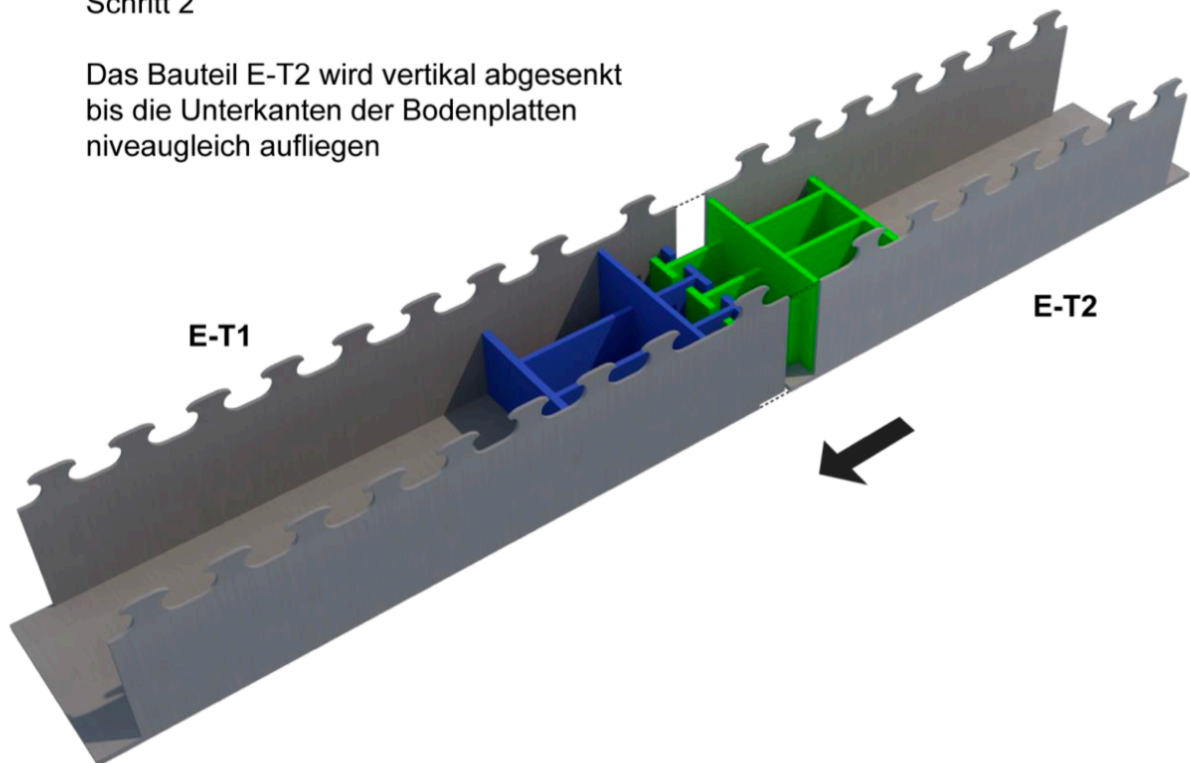


Figure 16 Assembly. Step 2: The component E-T2 is lowered vertically until the bottom edges of the floor panels lie on the same level

The third part is the concrete casting: the concrete is inserted between the diaphragms of the joint1 and the Joint2, respectively. This third phase is important because the joints start to work together from now on.

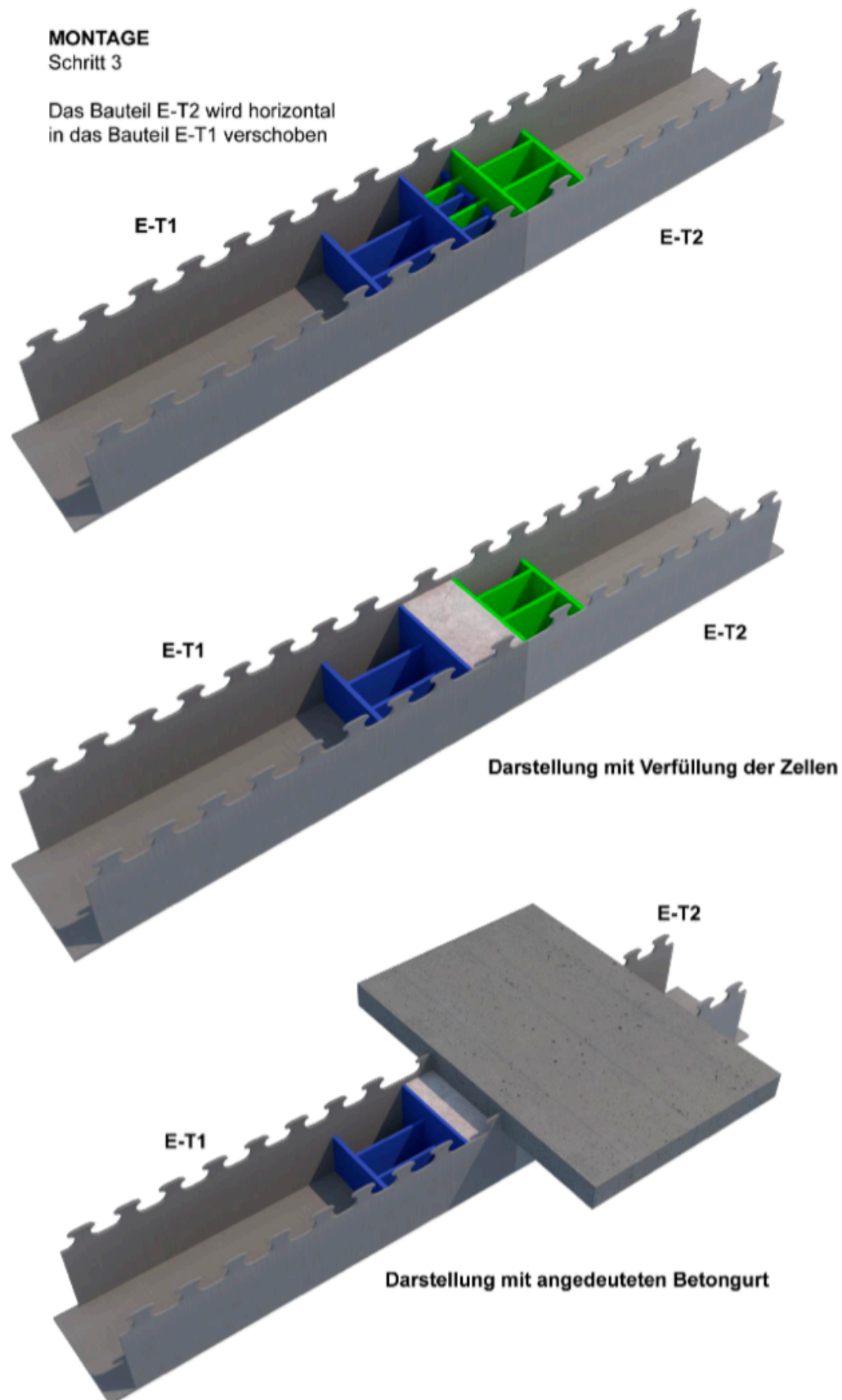


Figure 17 Assembly. Step 3: The component E-T2 becomes horizontal and it is moved into the component E-T1 and the concrete is cast inside the joint

1.2.3 Bearing behaviour of the joint

According to a global referring system, the entire joint is subjected to a bending moment, M_x , and to a shear force, V_z . These soliciting actions can assume different values according to the loads combinations applied on the bridge, during modelling. Of course, in the design process should be take into account the worst case for both positive and negative bending moment, while only the major cutting force in modulus will be considered for the shear verification.

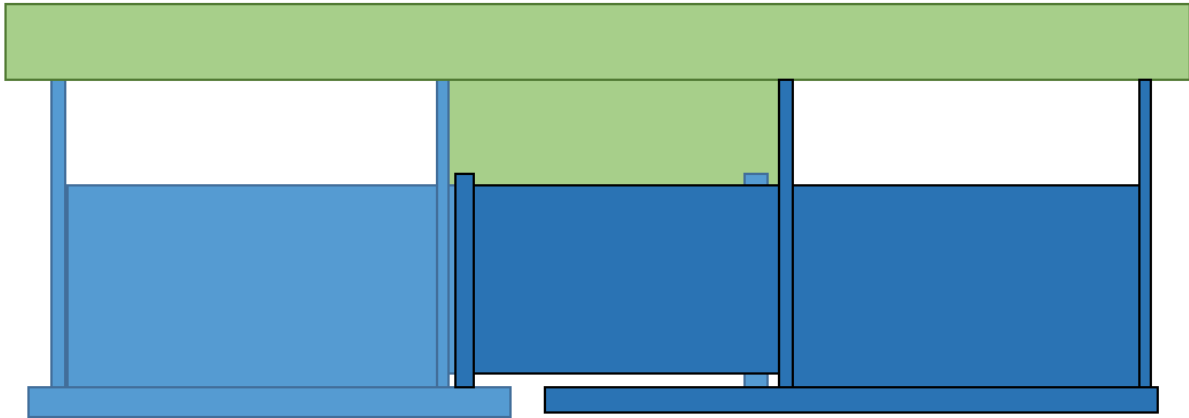


Figure 18 Lateral view of the joint

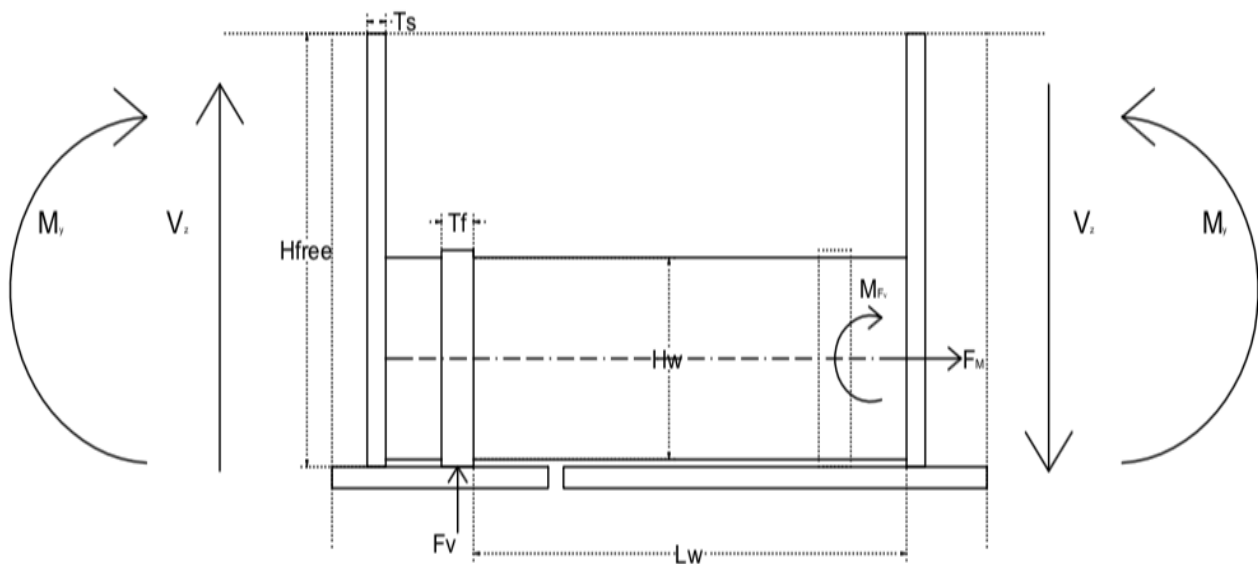


Figure 19 Application of Shear force and Bending Moment in a longitudinal view

This picture shows how the forces described above, are applied on the whole joint. Now to explain in the better way how the joint behaves, it is important to considered separately the bending moment and the shear force, to investigate how these actions are spreading inside the joints, through each element.

The bending moment transmission:

The global bending moment is considered as couple of forces: F_c that is the compression in concrete slab and F_t that is the tension in joint. In this first approach, the concrete slabs are considered completely compressed, and the application point of the resultant of compression force is considered in the middle of the entire concrete slabs thickness at first.

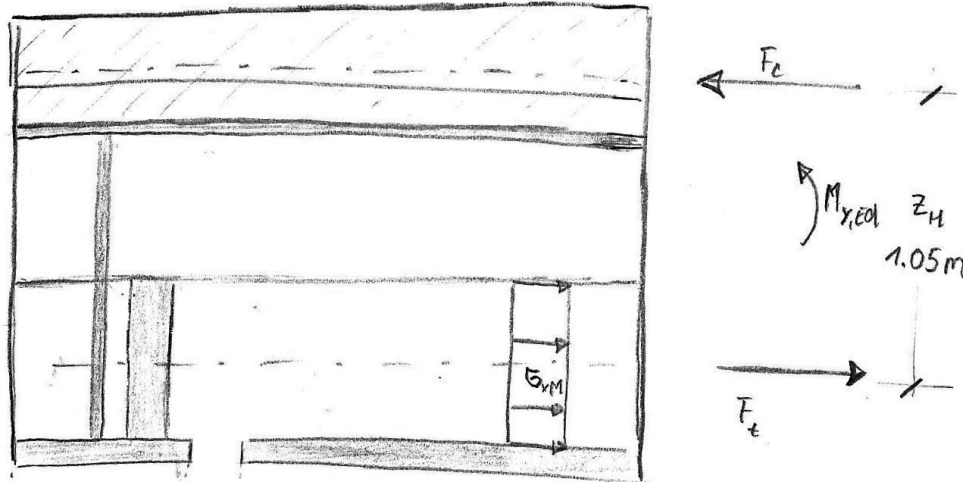


Figure 20 Simplified approach

In this preliminary study, it is important to analyze in detail the relationship between the geometric parameters involved and the tensions that develop inside the joint. Let's start considering the stresses inside the steel parts, due to the bending moment and after, their transmission to the concrete. In the steel, the force and the stress due to the bending moment are the following:

$$F_M = \frac{M_x}{3 \cdot z_M}$$

$$\sigma_{s,M} = \frac{F_M}{(t_w \cdot h_w)}$$

Let's continue considering the stresses inside the concrete. In this case, the simplified scheme is:

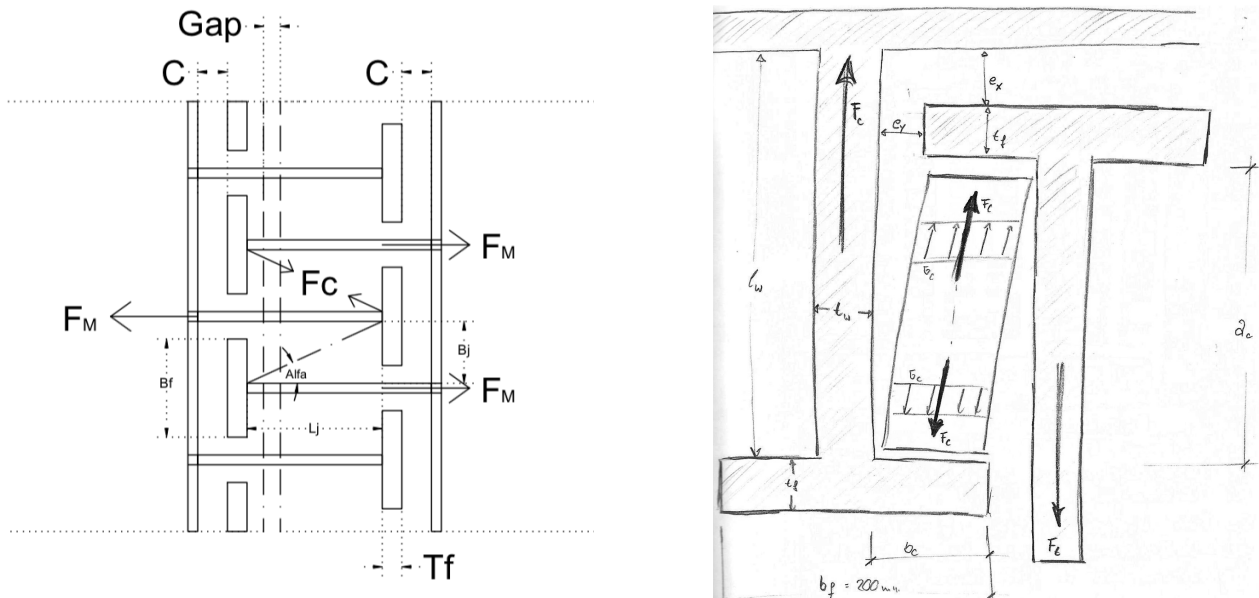


Figure 21 Distribution of tensile force between T-stub and concrete

F_M is the tensile force in the webs and due to this force, a new one is generated inside the concrete, F_C . This is a compression force and the concrete behaves as a strut.

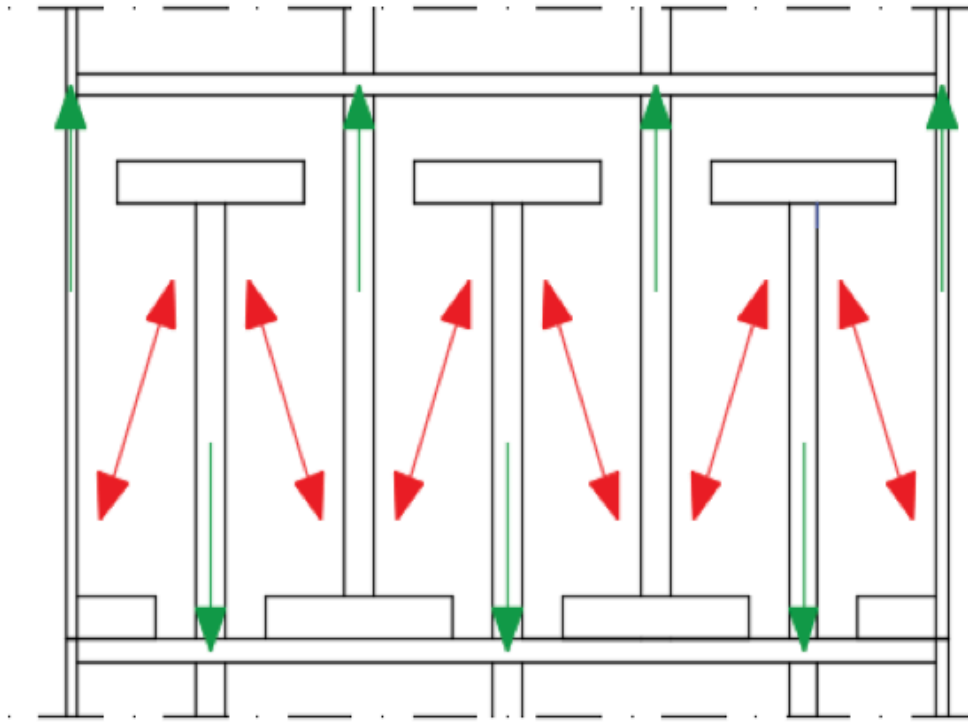


Figure 22 Spreading of stresses due to bending moment

The approximation in this calculation is to consider that the concrete behaves in a uniaxial way, while the real joint has a biaxial behavior due to contact between concrete and the T-flange and the T-web, in the transverse direction.

$$F_C = \frac{T}{2 \cdot \cos \alpha} \quad \sigma_c = \frac{F_C}{A_{cls}}$$

Geometric parameters:

$$\tan \alpha = \frac{b_j}{L_j} \quad \text{and} \quad B_w = \frac{B_f - t_f}{2}$$

Final verification on concrete:

$$\sigma_c < \frac{110}{1.5} \cdot 0.85 \text{ MPa}$$

The shear transmission:

It is important to underline that the shear force caused two different kind of stresses inside the joint's element. The first one is the tangential stress in the T-webs:

$$F_v = \frac{V_z}{3} \quad \tau_s = \frac{F_v}{t_w \cdot h_w}$$

To study the second effect it is important, before to describe how the shear is adsorbed by each part of the joint. In fact, the shear force is spreading inside each element, according to this picture:

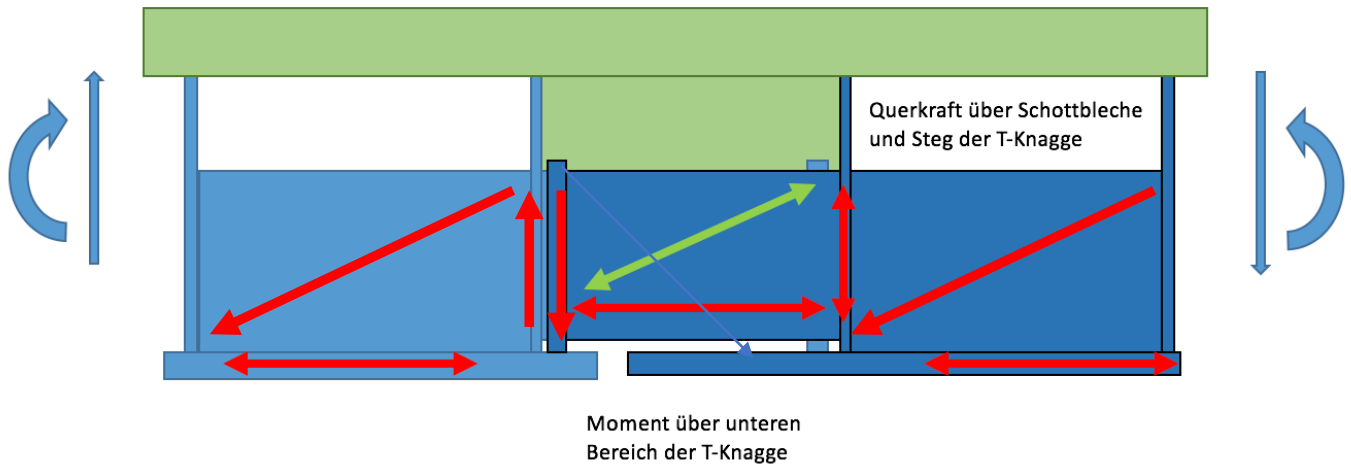


Figure 23 Spreads of the shear force along the joint

A simplified scheme can be the one represents in the following picture, in which the transmission of the shear between on side of the joint to the other is taken into account.

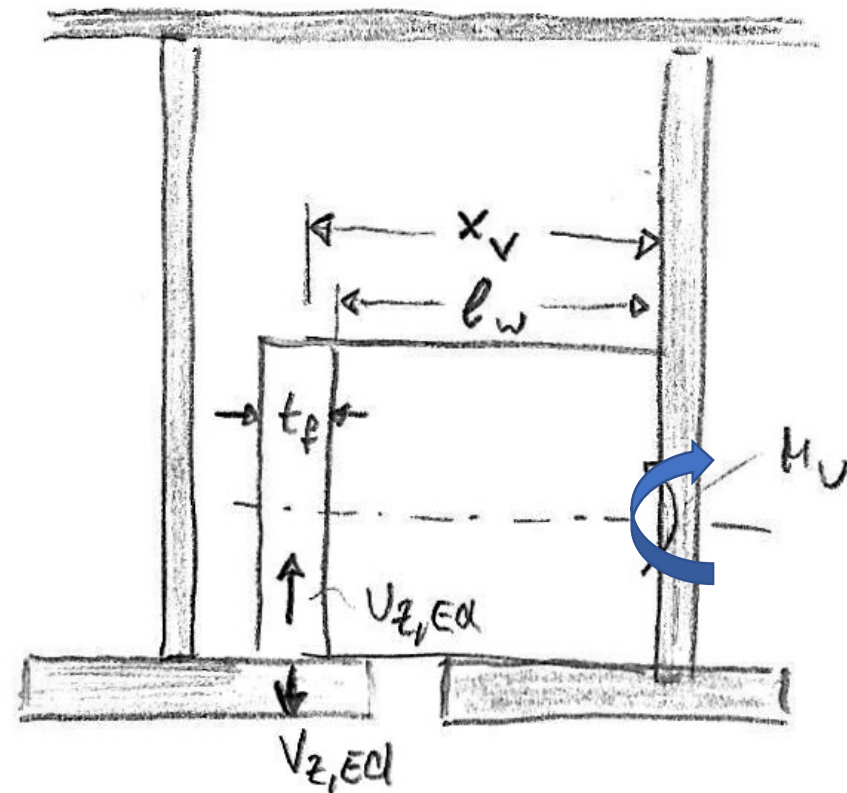


Figure24 Cantilever for shear transmission from the Joint 1 to the Joint 2

Effect of the shear in the cantilever in relation with L_w , t_w and h_w :

$$M_{Fv} = F_v \cdot \left(L_w + \frac{t_f}{2} \right)$$

$$\sigma_{s.Mfv} = \frac{M_{Fv}}{W} = \frac{M_{Fv}}{t_w \cdot h_w^2} \cdot 6$$

After this, the final step is considered the combination of the effects, due to both the solicitation actions and doing the final verification on steel:

$$\sigma_{S.tot} = \sigma_{s.M} + \sigma_{s.Mfv} < 355 \text{ MPa}$$

$$\tau_s < \frac{355}{\sqrt{3}} \text{ MPa}$$

1.2.4 Grouted concrete

In this chapter, it is important to spend some time explaining the biaxial behavior of concrete and on its benefits. In the past, in fact, a huge amount of experimental studies into the biaxial strength of concrete have been done. The issue in this investigation was usually relegated to the application of the load in a correct way. The thing that should be underline is the improvement of compression strength of a specimens under biaxial stresses, while the biaxial tensile strength of concrete is approximately equal to its uniaxial tensile strength. In our case, of course, the biaxial compression strength is the key of a correct design of the joint, so it could be guaranteed as much as possible the biaxial behavior.

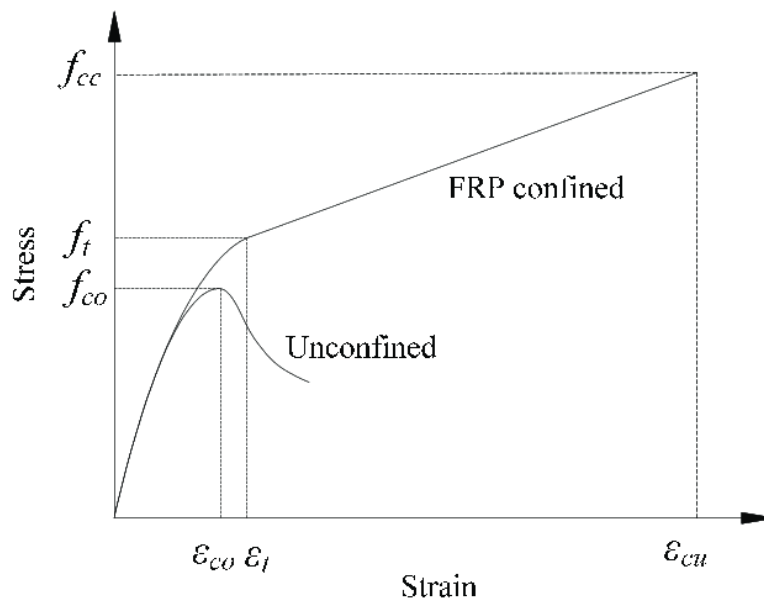


Figure 25 Difference in concrete behavior

This picture has pure didactic purpose, but it shows how the fiber reinforced concrete confined behaves better than the unconfined one. In details, the influence of the loading case on the concrete compression strength is explained through Kupfel's experiments. In fact, he was one of the most important scholar of this topic:

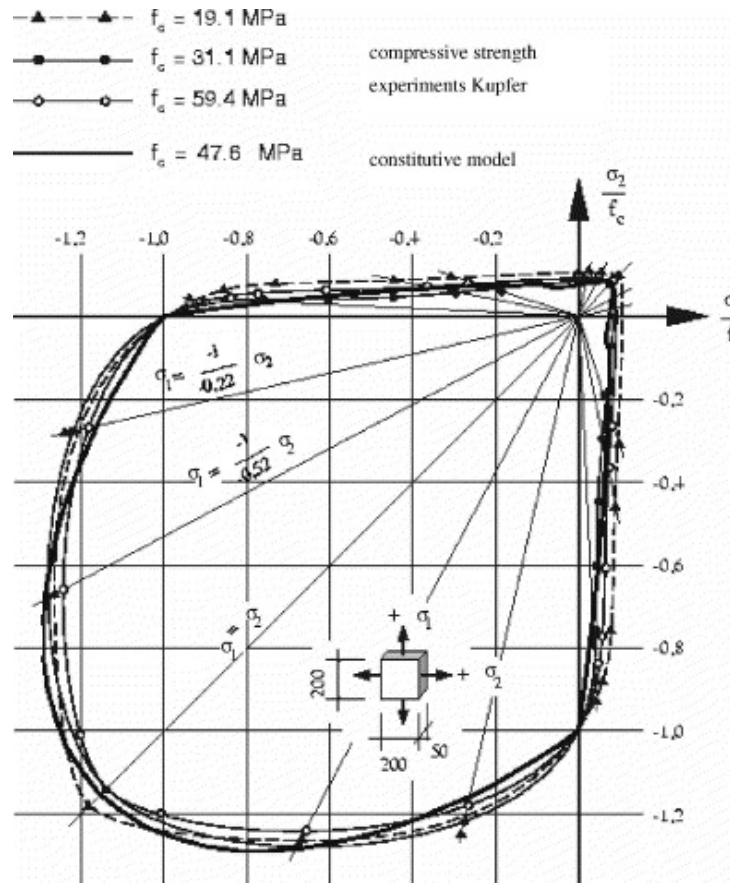


Figure 26 Kupfer's results

The interest part for our investigations is the follow:

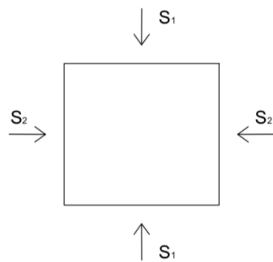


Figure 27 Biaxial state

In case of compression-compression, if the $\sigma_1 = \sigma_2$ the compressive strength of the concrete can increase more than 10 %. If the $\sigma_2 = 0.5 \sigma_1$, it could increase over the 20%. Unfortunately, on the other and, even a small tensile lateral stress can be extremely dangerous, because the compressive strength can rapidly decrease in the orthogonal direction. This is the reason, why in the ridge under investigation it is important to be sure to have exactly the first kind of behavior and avoid the tensile stresses in the transversal direction as much as possible. (1969)

1.2.5 Simplified hand calculation

In this chapter, a rapid and manual calculation has been done, in order to have some results to compare with the FE model and provide the reliability of it. A basic geometry has been considered in this chapter. In the first manual approach, the normal stresses in the T-webs generated by the bending

moment are considered to be uniformly distributed along the entire section, and the tensile force due to the moment is considered at the same time divided by three. In this first preliminary approach, some approximations have been done: it has been considered the section at 12m from the abutments, instead of that one at 12.2095m, where probably the joint starts. The second assumption is related to the bending moment and shear force applied at the boundaries: $M_x \approx 10000 \text{ kNm}$ and $V_y \approx 1200 \text{ kN}$, according with the general results obtained from verification to the ultimate limit states, on the Sofistik model. According to that, the height of the joint is chosen approximately as a half of the total available height, and the lever arm can be estimated. The lever arm of the section in which the t-webs are located is calculated doing the same assumption described before: considering the concrete all reagent in compression and the tensile force applied in the barycenter of the T-web.

$$F_M = \frac{M_x}{z_1 * 3} \approx \frac{10000}{1.032 * 3} \approx 3230 \text{ kN}$$

$$\sigma_{33} = \frac{M_x}{z_1 * 3} \cdot \frac{1}{t_w * h_w} \approx \frac{10000}{1.032 * 3} \cdot \frac{1}{0.03 * 0.5705} \approx 188,722 \text{ MPa}$$

However, this could not be the real behavior and the real distribution of the stresses on the T-webs. Indeed, let's suppose that the tensile force is not applied in the barycenter of the section but above, to $\frac{2}{3} h_w$, the total lever arm increases and the tensile force applied decreases:

$$F_M = \frac{M_x}{z_2 * 3} \approx \frac{10000}{1.1248 * 3} \approx 2963 \text{ kN}$$

The most relevant effects are underlined in the stresses that arise in the section under investigation. The first scheme could be changed and adapted to the second one, as shown in the next picture, in which the same tensile force is now applied to the barycenter of the section and a new moment arises after this transportation:

$$M_{F_M} = F_M * e = 2963 * \left(\frac{h_w}{2} - \frac{h_w}{3} \right) \approx 282 \text{ kNm}$$

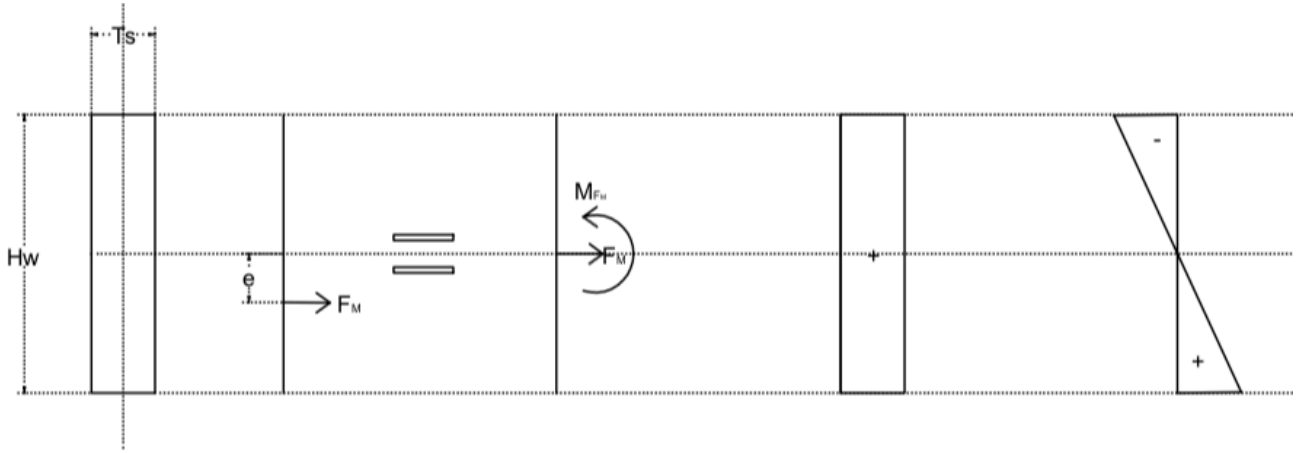


Figure 28 Stresses on T-webs

It is possible now to calculate the stress on the bottom of the T-web section and the stress on the top section according to this formulation:

$$\sigma_{33} = \frac{N}{A_s} \pm \frac{M_x}{J_x} \cdot \frac{h_w}{2}$$

So, in conclusion, it is possible to obtain the following stresses:

$$\sigma_{33_{bottom}} = \frac{F_M}{t_w * h_w} + \frac{M_{FM}}{J_s} * \frac{h_w}{2} \approx 173,123 + 173,287 \approx 346,575 \text{ MPa}$$

$$\sigma_{33_{top}} = \frac{F_M}{t_w * h_w} - \frac{M_{FM}}{J_s} * \frac{h_w}{2} \approx 173,123 - 173,287 \approx 0 \text{ MPa}$$

These results are really important and they are analyzed after the creation of the 3D model, through the finite element program Abaqus.

1.2.6 Parametrical studies

The joint has been modelled using an input file in python: in this way, in fact, it was possible to create a parametric model due to its uncertain geometry. Before doing the joint model, a parametric investigation has been conducted in order to understand how the geometry influences the stresses in the elements:

- Effect of the bending moment: thickness of the web and height of the web;
- Effect of the shear: transverse section of the web;
- Effect of the combination of the effect;
- Effect of the shear in the cantilever: length of the joint and thickness of the flange;
- Effect of the tensile force on the concrete: strut and tie verification;

- Effect of the stress in concrete due to geometry: length of the web, of the flange and angle α ;

After this list, it is easier to describe the procedure adopted to study the best geometry of the joint. A Matlab input file has been generated in order to study how these parameters affect the results applying theoretical formulations. There is a fixed parameter that is $B_{tot}=876.0$ mm: all the others have to be chosen carefully. The first thing is the introduction of a geometrical relation between B_{tot} , B_f , t_w and S_w . In fact, these parameters are highly dependent on each other:

$$B_f = \frac{B_{tot} - 2 \cdot t_1 - 6 \cdot S_w}{3}$$

It is possible in the first instance to fix $S_w = 30$ mm, whereas there must be sufficient space at each point for concrete penetration. In this way, it is possible to find a close dependence between B_f and t_w .

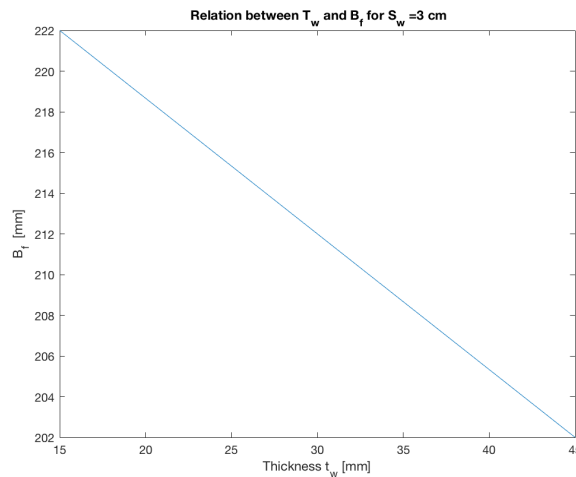


Figure 29 Relation between thickness of web and width of flange

Another pure geometric relation can be created between B_j , B_f , t_w and S_w . $B_j = \frac{b_f - t_w}{2} + S_w$

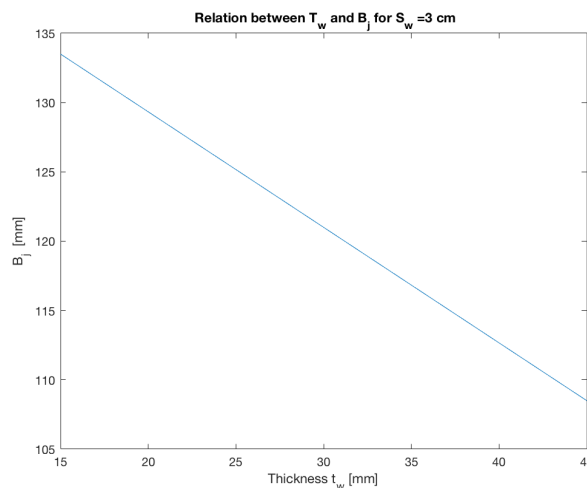


Figure 30 Relation between thickness of web and width of the concrete

According to other parametric studies, conducted in parallel, it is possible to do the following considerations:

- Utilization factor η as a function of the length of the web L_w ;
- Axial stress in web increases linearly;
- Cantilever of shear force increases linearly as the web gets longer;

In fact, the concrete stress increases inversely proportional to the cosine of α :

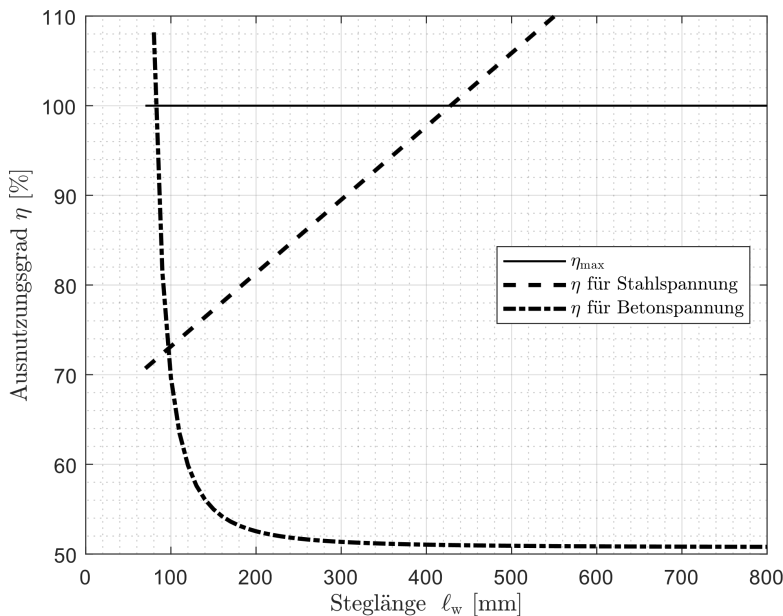
$$\sigma_c(L_w) \propto \frac{1}{\cos \alpha}$$

Where α can be geometrically defined, according to this formulation:

$$\alpha = \arctan\left(\frac{B_j}{L_j}\right) \propto \arctan\left(\frac{1}{L_w}\right)$$

So, it is possible to obtain the final proportionality:

$$\sigma_c(l_w) \propto \frac{1}{\cos\left(\arctan\left(\frac{1}{l_w}\right)\right)}$$



Parameter		Wert
Stahlgüte	$f_{y,k} =$	355 $\frac{\text{N}}{\text{mm}^2}$
Betondruckfestigkeit	$f_{c,k} =$	110 $\frac{\text{N}}{\text{mm}^2}$
Stoßhöhe	$h_{St} =$	575 mm
Stegdicke	$t_w =$	25 mm
Flanschbreite	$b_f =$	200 mm
Flanschdicke	$t_f =$	40 mm
Abstand Flansch - Schott	$e_x =$	20 mm

Figure 31 Relation between efficiency of steel and concrete and t-web length

In this graphic, it is possible to see that the efficiency factor η for the concrete stress is not decreased significantly anymore after the values of $L_w \approx 300$ mm. It is now possible to find another geometrical relation: $L_w = L_j + t_f + C$. The length of the joint L_j is strictly dependent on L_w , t_f and C . Allowing the concrete to penetrate everywhere, the parameter C is fixed: $C = 20.0$ mm. According to all these formulations, it is possible to have a better idea on which are probably the parameters that influence the tensions inside the joint.

The governing variables could probably be t_f , t_w and h_w :

- t_f Influences σ_c :

In fact, the thickness of the flange influences the trend of the tension inside the concrete and it influences the length B_j , directly related to the angle α ;

- t_w Influences σ_s : in fact, it is the most important parameters for controlling the stresses due to the bending moment;

- h_w Influences especially σ_s but also σ_c as decompression:

In fact, the height of the joint could play an important role in the definition of the stresses inside the steel due to the global shear force considered as a local moment in the webs. The increase of the height could change the lever arm and so also the tension force carried out by the T-stubs;

2. FINITE ELEMENT METHOD AND MODELING

2.1 Finite Element Method

This Chapter presents an overview of what the master thesis covers and it contains a specific description of the main concepts and general features of the finite element method. In the field of structural mechanics this method allows analyst to deal with a wide variety of problems: one-dimensional, two- dimensional and three-dimensional problems, axisymmetric problems, beams calculation, frames, plates and shells, static and dynamic problems and non-linear calculations as geometric and material non-linear. It is not a valid method only for structural analysis, but its validity also extends to other branches of computational mechanics, that can be distinguished according to the physical scale in the following way:

- Nano mechanics;
- Micromechanics;
- Continuum mechanics (Solid and Structures, Fluids, Multi physics);
- Systems;

In any case, continuum mechanics problems may be subdivided according to whether inertial effects are taken into account or not:

- Statics: Time Invariant or Quasi-static;
- Dynamics;

In static analysis, inertial forces are ignored or neglected. Static problems may be sub-classified into time invariant and quasi-static. In quasi-static problems such as foundation settlement, creep flow, rate-dependent plasticity or fatigue cycling, a more realistic estimation of time is required but inertial forces are neglected because motions are slow. In dynamics, the time dependence is explicitly considered because the calculation of inertial (and/or damping) forces requires derivatives respect to actual time to be taken. There are two different types of static analysis: Linear and Nonlinear. The first one deals with static problems in which the response of the structure is linear in the cause-and-effect sense. For example: if the applied forces are doubled, the displacements and internal stresses also double. Problems outside this domain are classified as nonlinear. The term FEM, nowadays, involves a broad spectrum of techniques that share common features. There are two sub classification that fit applications to structural mechanics well; these are:

- FEM FORMULATION → Displacement
- FEM SOLUTION → Stiffness

This particular combination is called the Direct Stiffness Method or DSM. Processes that use FEM involve carrying out a sequence of steps in some way. Those sequences take two canonical configurations, depending on the environment in which FEM is used and the main objective: model-

based simulation of physical systems, or numerical approximation to mathematical problems. First of all was the Physical FEM: the process of idealization and discretization is carried out at the same time to produce discrete model: the solution step is handled by an equation solver often customized to each fem programs. Physical fem discretisation may be developed and adjusted without reference to mathematical models, but it may be constructed simply from experimental measurements. This is the reason why, after that was developed the Mathematical FEM: this is often an ordinary differential equation “ODE” or a partial differential equation “PDE” in space and time. In this case the discrete finite element model is generated from a variational or weak form of the mathematical model. In both of these two models the solution error is the amount by which the discrete solution fails to satisfy the discrete equations. This error is relatively unimportant when using computers and especially direct linear equation solvers for the solution step. More relevant is the discretisation error which is the amount by which the discrete solution fails to satisfy the mathematical model. These two methods are complementary: and this synergy is the reason behind the power and the acceptance of the method. As said before, Physical FEM was the first one and after came mathematical FEM to provide the necessary theoretical underpinning to extend FEM beyond structural analysis. A classification of computational solid and structural mechanics is based on the discretization method by which the continuum mathematical model is discretized in the space, converted to a discrete model of finite number of degrees of freedom. In fact, continuum mechanics studies bodies at the macroscopic level, using continuum models in which microstructure is homogenized by averaging. Structural mechanics is a branch of solid mechanics in which systems are studied by decomposition: its behaviour is the same of its own components plus the interaction between the components. In this case the components are broken down into subcomponents and so on. The system model is obtained by going through the reverse process: from component equations to substructure equations and from those to the complete structure equations. Once each single component has been generated, the assembly process is governed by the classical principles of Newtonian Mechanics, which provide the necessary inter-component “Glue”. In fact, the basic concept in the physical interpretation is the “breakdown” of a complex mechanical system into simpler, disjoint components called finite elements or simply elements. The mechanical response of an element is closely related and defined by the number of degrees of freedom: these are represented as the values of the unknown functions as a set of node points. The element response is defined by algebraic equations constructed from mathematical or experimental arguments. The response of the original system is considered to be approximated by that of the discrete model constructed by connecting or assembling all the elements. The breakdown-assembly concept occurs every time an engineer considers many artificial or natural systems: if the behaviour of the system is too complex, the aim is to divide it into simpler manageable subsystems.

In the FE model, such “primitive pieces” are called elements: the behaviour of the whole system is the same of the individual elements plus their interactions. FE modelling is more than the chosen mesh and pre-processing part of analysis; the analyst must understand the classic analysis tools and he should always have the analytical solution of the problem to compare the results obtained by the program. In fact, despite finite element method essence is the same for all the FE programs, a given type element might have different kind of behaviour in each different FE programs due to some special restriction, some special features or maybe related to different input data defaults. Overall the aim of FE analysis is the choosing of the elements of such a type and size that deformation of the structure over the region spanned by an element is closely approximated by deformation modes that element can represent. (Felippa, 2001)

2.1.1 DSM: Direct Stiffness Method

The direct stiffness method, DSM, is the most common implementation of the finite element method. The important feature of this method is that all the elements area treated alike, regardless of their complexity. The power of FE method is its versatility; the structures analysed may have arbitrary shapes, supports and loads. The FE’s theory includes matrix manipulations, numerical integrations, equation solving and other automatically procedures. The DSM steps can be applied to a simple plane truss structure or to more complex problems. In fact, it is possible to start modelling simpler element, like as the two-node bar (also called linear spring) element that is the simplest structural finite element, and finally learn how to model more complex element and structures like as a six-node triangle that models thin plates, that displays intermediate complexity and the most geometrically complex finite element (at least as regards number of degrees of freedom) that is the curved, three-dimensional, 64-node “brick” element.

Examples of various types of elements







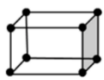
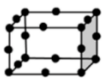


	Element Name	Element Shape	
		First Order	Second Order
1D Elements Line Element	Spring, Damper Beam, Truss		
2D Elements Surface Element	Shell, Plane2D	 	 
3D Elements Volume element	Hexahedral		
	Tetrahedral		

Figure 32 Examples of various types of elements

The advantage of starting with the simplest element is that computations can be entirely done by hand

as long as the structure contains just a few elements and this allows various steps of the solution procedure to be carefully examined and understood before passing to the computer implementation. Doing hand computations on more complex finite element systems rapidly becomes impossible. The method has two major stages: breakdown, and assembly plus solution.

- | | | |
|---------------------------------|---|---|
| 1. <i>Breakdown</i> | { | <i>Disconnection</i>
<i>Localization</i>
<i>Element formation</i> |
| 2. <i>Assembly and solution</i> | { | <i>Globalization</i>
<i>Merge</i>
<i>Application of Boundary conditions</i>
<i>Solution</i>
<i>Recovery of derived quantities</i> |

In fact, often the users, using fem programs, have to deal with pre-processing phase that consists in describing loads, supports, materials and choosing the better mesh. Post-Processing is usually carried out by the software. The ‘Disconnection’ and ‘Localization’ are conceptual steps and they are implicitly carried out either through the user-provided problem definition. The DMS processing actually begins at the element-stiffness equation forming step. The disconnection step allows to discard all known loads and supports and after that it is possible to disconnect or disassemble the structure into several components. The localization step is important to reduce clutter and to give order to the elements that are therefore identified and ordered. Matrix symbolism for this set of equations is

$$[K]\{D\} = \{R\}$$

Where:

D: is the vector unknowns;

R: is the vector of known loads;

K: is the matrix of known constants;

In the stress analysis K is called “Stiffness Matrix”. The keys points of the stiffness method analysis are nodal forces and displacements. In fact, the finite element method calculates nodal displacement $\{D\}$ and after that it uses this displacement to calculate strain $\{\epsilon\}$ and stress $\{\sigma\}$ vector; in this case therefore, if the displacements are wrong also strains and stresses could have the same mistakes. The displacement field is one of the most important ingredient in this kind of analysis because, as said above, the displacements are the primary unknowns and they are called the degrees of freedom or state variables of the system. In this way, the boundary conditions tell which components of $\{D\}$ and $\{R\}$ are actual knows and which are not. This information is used in the first step of the analysis, at

the beginning, to discard unnecessary variables and to make the calculation less expensive. In localization phase this equation is settled for each member and subsequently it must be done member to member; in fact, the first step in the stage of assembly and solution is the globalization, which should be done exactly for each single part of the system. In this step of the analysis each member stiffness equation is referred to the global system so it can be subsequently merged into the master stiffness. Actually, assembly involves joining together the stiffness equation of every single element into the global stiffness equation: this is the reason why the specific equation must be referred to a common coordinate system. Next step is the solution and it is executed by two phases: applying boundary conditions and solving the problems for the unknown nodal displacements. In fact, the general equation is modified applying boundary conditions that define which components of joint displacements and forces have to be take into account in the calculation: it is carried out by adding zero rows and columns in the appropriate position to complete the force and displacement vectors. These modifies equations are submitted to a linear equation solver which turns back the unknown nodal displacements. Post processing may follow the solution step in order to determine quantities such as internal forces and stresses that are recovered from the displacement solution: in fact, the structural engineering usually is not interested in displacement but maybe in the reaction forces at supports or in the internal member forces. As shown above, the key operation of the assembly process is the merge of individual members: it can be physically interpreted as the combination of that element in the process of fabricating the whole structure. It has two main rules:

- Compatibility of nodal displacements;
- Force equilibrium;

The first rule allows the touching joint to have the same displacement and the second one means that the sum of all forces arriving at node balances the external forces applied to that specific nodes. The practical computer implementation of direct stiffness method assembly process departs significantly from 'Augment and add' technique:

1. Member stiffness matrix are not expanded;
2. The master stiffness matrix is stored using format that takes advantage of symmetry;

(Cook, 1995)

2.1.2 Variational formulation

The application of variational principles (Virtual work principle) allows the determination of the links between the loads and displacements in each single element; indeed, the resolute technique of the serial number calculation allows to reach the discretized solution. The main idea of each kind of PDE method (Differential Equation of Derivatives Partial) is that of discretizing a continuous problem to have limited degrees of freedom. The classical method to solve PDE problems is the finite difference

method. Galërkin method allows to solve a continuous problem, delivering it in a discrete space determining a numerical approximate solution. The solving process of differential equations using finite element method can be described in the following steps:

- Variational formulation of the problem;
- Discretization using finite elements;
- Solution of discretized problem;

The Fem is viewed as a procedure for obtaining numerical approximations to the solution of boundary value problems posed over a domain Ω . As mentioned above, the first analysis step carried out by a structural engineer is to replace the actual physical structure with a mathematical model. The construction of structural and continuum finite elements using a variational formulation is based on the total potential energy; this method has the important advantage of being readily extendible to more complicated problems, such as variable cross section or section with more than two nodes. The first step to do this kind of analysis is to divide the continuous in one-dimensional, bi-dimensional or three-dimensional element through lines or imaginaries surfaces. It is done by the following procedure:

- The assumption that these elements, that have been created, are connected to each other in finite numbers of points on their own borders;
- The choice of specific set of functions, that could be the ‘Shape Functions’, due to the description of internal movement of each single element according to its nodal displacement;
- The constitutive law allows the congruence of the movements within the element to be verified;
- The problem is solved imposing equilibrium between internal forces and applied loads, in order to obtain a particular solution for the problem;

It is clearly visible that some approximations have been done to make the problem easier to solve: the functions don’t guarantee displacements continuity in adjacent elements, but only at joints; the forces equilibrium is only verified globally, while it is possible to have local violation of equilibrium, within the element or in its border lines. In addition, the choice of the degrees of freedom of the system and of the shape functions determines the approximation of the description of element and so also the effectiveness of the calculation. As said above, the internal displacements field of an element is usually expressed by polynomial functions that are easily derivable. In fact, the degree of approximations depends on the number of element used to describe the structure and on the degree of the polynomial chosen: the displacements fields in fact has to obey to some rules to guarantee the convergence of the results: it has to be continuous within the element and has to be of degree ‘n’, where n is the derivative order requested by the specific element. These functions should be able to describe the rigid motion of the element without deformation energy, they should be capable to

describe a constant strain state and the continuity between adjacent elements is expected where there are no discontinuities. The description of the displacement field could be done by two different functions:

1. Polynomial series;
2. Shape functions;

The “Shape functions” are unknown functions and they must have unit values in the considered node and zero values on the rest of the nodes. Matrix symbolism for the relationship between the displacement field and the nodal displacements is the follow:

$$\{u\} = [N]\{d\}$$

Where:

U: is the vector of the unknown displacement field;

N: is the matrix of the shape functions;

D: is the vector of the nodal displacements;

This equation describes the displacements of each single point within the element starting from the nodal displacements. It is possible to obtain also the subsequently relation between strain and nodal displacements:

$$\{\varepsilon\} = [\partial]\{u\} = [\partial][N]\{d\} = [B]\{d\}$$

Where:

ε : is the vector of the unknown strain field;

B: is the strain-displacement matrix, composed by the derivatives of the shape functions;

It is possible to calculate also the stress field through the follow formulation:

$$\{\sigma\} = [E]\{\varepsilon\} = [E][B]\{d\}$$

Where:

σ : is the vector of the unknown stress field;

E: is the matrix of the elastic module of the element;

The finite element formulation is developed by the application of the principle of virtual work: it is important to underline the assumption of being in small-displacement situation, in order to use the non-deformed shape for the calculation of the structure. It states that the virtual work done by a real forces system following the application of a virtual displacement in the equilibrium configuration is zero; it means that the virtual works of deformation done by the internal forces is the same of the works done by the external forces: $\partial L_i = \partial L_e$

It is important to define these three different symbols:

D: It is the differential;

∂ : It is the partial derivative;

δ : It is the infinitesimal variation of the position of a specific point;

Considering a three-dimensional element, in an orthogonal Cartesian referring system (X,Y,Z), of infinitesimal volume of edge dx,dy,dz , as shown in the picture below.

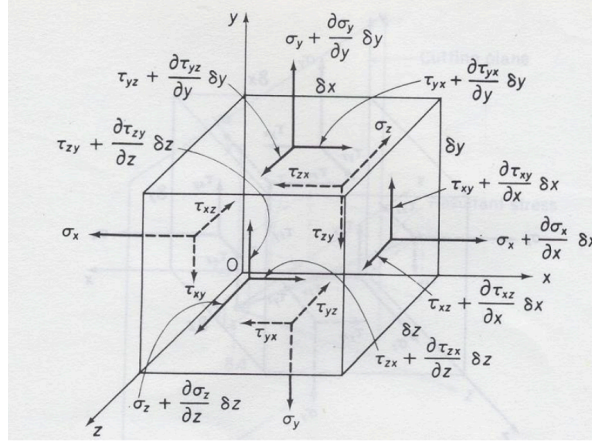


Figure 33 Three-dimensional stresses

It is possible to write the final equation obtained through the application of the principle of the virtual works:

$$\int_V \rho [N]^T [N] dV \{\ddot{d}\} + \int_V [B]^T [E] [B] dV \{d\} = \int_V [N]^T \{f\} dV + \int_S [N]^T \{\phi\} dS + \sum_{i=1}^N [N]^T \{f\}_i$$

Applying the previous equation to the general one, it is possible to get the following formulation for the global stiffness matrix:

$$[K] = \int_V [B]^T [E] [B] dV$$

In the elastic linear analysis, it is possible to calculate the agent forces knowing the displacement field and the stiffness matrix of the whole system, according to the previous formulation:

$$[K]\{D\} = \{f\}$$

In the finite element analysis, however, it is necessary to solve the inverse problem:

$$\{d\} = [K]^{-1}\{f\}$$

This formulation required the knowing of the inverse stiffness matrix $[K]^{-1}$: this is the reason why it is essential to use linear system solvers, that can be of two different types:

1. Direct methods: they use an exact algorithm to solve the equations. They are very accurate when the matrix order of size is not too remarkable, because the number of operations required is given by the number of the degrees of freedoms of the system and by the typology of K;

2. Iterative methods: they use iterative algorithm to solve the equations and the solution is provided unless an error occurs. They require an uncertain number of operations: calculation ends when convergence criteria are satisfied or an iteration limit is reached;

The speed of program execution is strongly influenced by the way in which global stiffness coefficients k_{ij} are stored: its format depends mostly on how nodes and elements are numbered. The global stiffness matrix is usually sparse and it means that it contains huge quantities of zeros and sometimes it could become wasteful to store and manipulate so many zeros. It is absolutely important to have the 'bandwidth' small, because it means that nonzero coefficients cluster in a narrow band along the diagonal and usually there are some zero coefficients within the band, but the most are outside. The biggest difference between a model with nodes in a 'good arrangement' and a model with nodes in a 'poor arrangement' is the number of strike required by the two systems when the matrix K is processed by a direct equation solver. This assembly-reduction process is like a 'wave' that moves along the structure: a solver, in fact, that works in this way is called 'wave front' equation solver. The wave front is a measure of the number of coefficients being manipulated in one of the reduction steps: the computation time of a direct solution is roughly proportional to nb^2 , where n is the order of size of K and b is the bandwidth. Three-dimensional structures have a larger b because of the high connectivity among each degree of freedom, while slender structures have a low b and low connectivity between the degrees of freedom. As long as the structure of the finite element model is not changed the direct method need to be done only once, regardless of the number of load vectors. On the other way, an iterative solver must treat each different load case as a new problem. In contrast, iterative solvers may be best on parallel-processing computers: they may be also best for some nonlinear problems in which K changes from the load step i , to load step $i+1$, because in these problems the solution d_i may be a good starting approximation for the calculation of d_{i+1} . A direct solver works very well for the most important problems and in the most current software it is the only solution algorithm available and it is used as a 'black box'.

2.1.3 Isoparametric finite element

The main goal of the isoparametric finite element is to create a relation between the internal displacements of each single element u, v, z and the nodal displacements in a direct way through the use of interpolation functions that are expressed in a local system for every single member and they are usually called ξ, η, ζ . In fact, the development of element matrices and equations expressed in terms of global coordinates could become a difficult task, especially in complex structures and these difficulties increase with high order elements or with element equipped with large number of nodes. A simpler computer formulation, in fact, is required specifically for 2D and 3D elements. In fact, isoparametric finite element allows very accurate, higher-order elements of arbitrary shape to be

developed and programmed with a minimum of effort: the addition of incompatible displacement modes to Isoparametric elements in 1971 was an important, but minor extension to the formulation [5]. To do that it is necessary to introduce a new local coordinate system and it is a natural coordinate system in which elements sides are always defined by $\xi = \pm 1$; $\eta = \pm 1$; $\zeta = \pm 1$ regardless of the shape of physical size of the element and its orientation in the global coordinate system X, Y, Z . There is a relation between the natural coordinate system and the global for each element of a specific structure and it is called ‘transformation mapping’: in fact, the internal displacements $u(x, y, z)$, $v(x, y, z)$, $w(x, y, z)$ are usually represented by polynomial functions in the global Cartesian referring system and the interpolation between these global coordinates and the local ones is at the base of the finite element isoparametric formulation. In the most general case, there should be three relations:

$$\begin{aligned} x(\xi, \eta, \zeta) &= \sum_n h_n(\xi, \eta, \zeta) x_n \\ \{x, y, z\} &\leftrightarrow f\{\xi, \eta, \zeta\} \leftrightarrow y(\xi, \eta, \zeta) = \sum_n h_n(\xi, \eta, \zeta) y_n \\ z(\xi, \eta, \zeta) &= \sum_n h_n(\xi, \eta, \zeta) z_n \end{aligned}$$

where x, y, z are the coordinate in the global system of a generic point of the element, x_n, y_n, z_n are the coordinates of the nodes of the elements, where n is the number of all nodes, and h_n are the interpolation functions defined in the local system of the element and normalized in the range ± 1 . These functions are unknown: they only have to respect the rule that their value must be one in the considered node and zero in all the others. This formulation makes it possible to have non-rectangular elements or elements with curved sides, ‘infinite’ elements for unbounded media and singularity elements for fracture mechanics. There are two possible interpolations:

- Geometric interpolation;
- Displacement interpolation;

An element is called isoparametric when it has the same interpolation points for the geometry and displacements too, otherwise it is called sub-parametric when the order of size of geometry interpolation is less than the one used for displacement interpolation and the element is called super-parametric when geometric interpolation has an order of size bigger than the displacement interpolation. The shape functions $N(i)$ are written in terms of the element reference system and the “natural” coordinate, in this example, ‘ ξ ’ has a range of Isoparametric $\xi = \pm 1.0$. The isoparametric and global reference systems are related by the following elementary equation:

$$X(\xi) = N_1(\xi)x_1 + N_2(\xi)x_2 + N_3(\xi)x_3$$

The validity of this equation can be verified at values of $\xi = -1$, $\xi = 0$ and $\xi = 1$. The global displacement can now be expressed in terms of the fundamental isoparametric shape functions:

$$u(\xi) = N_1(\xi)u_1 + N_2(\xi)u_2 + N_3(\xi)u_3$$

It should be noticed that the sum of the shape functions is equal to 1.0 for all values of ξ ; therefore, rigid-body displacement of the element is possible. This is a fundamental requirement of all displacement approximations for all types of finite elements. The strain-displacement equation for this one-dimensional element is:

$$\varepsilon_x = \frac{\partial u(\xi)}{\partial x} = \frac{du(\xi)}{dx} = \frac{du(\xi)}{d\xi} \frac{d\xi}{dx}$$

For any value of ' ξ ', the following equations can be written:

$$\frac{du(\xi)}{d\xi} = N(\xi)u$$

$$\frac{dx}{d\xi} = N(\xi)x = J(\xi)$$

It is possible to obtain the follow strain formulation:

$$\varepsilon_x = \frac{\partial u(\xi)}{\partial x} = \frac{du(\xi)}{dx} = \frac{du(\xi)}{d\xi} \frac{d\xi}{dx} = \frac{1}{J(\xi)} N(\xi)u = B(\xi)u$$

And:

$$dx = N(\xi)xd\xi = J(\xi)d\xi$$

After all these manipulations, the 3 by 3 element stiffness can now be expressed in terms of the natural system:

$$K = \int_{-1}^{+1} B(\xi)^T E B(\xi) J(\xi) d\xi$$

The distinctive trait of this final equation is that it cannot be evaluated in closed form but it can be accurately calculated by numerical integration. The Gauss numerical integration is the most accurate of all the traditional methods: it is better suited to numerical analysis and it evaluates the integral of a function as the sum of a finite number of terms:

$$I = \int_{-1}^{+1} f(\xi) d\xi = \sum_{i=1}^n w_i f(\xi_i)$$

Where:

w_i It is the weight factor and $f(\xi_i)$ is the value of the function in the point called Gauss point.

These points are at $\xi = 0$, $\xi = \pm a$ and $\xi = \pm b$ and there exist tabulations of Gauss points locations and corresponding weights for values of degrees $2n-1$.

The following formulation shows is the best way to do gauss integration:

$f = c_1 + c_2 \xi$ is exactly integrated by one-point rule

$f = c_1 + c_2 \xi + c_3 \xi^2$ is exactly integrated by a two-point rule and so on.

Of course, accuracy improves as more Gauss points are used, but it should be kept in mind that for many elements, lower order of integration produces more accurate results than higher order integration.

Polynomial degree of f	Number of integration points n	Integration points x_i	Associated weight factors w_i
1 st degree or lower	1	$x_1 = 0$	$w_1 = 2$
3 rd degree or lower	2	$x_1 = 1/\sqrt{3}$ $x_2 = -1/\sqrt{3}$	$w_1 = 1$ $w_2 = 1$
5 th degree or lower	3	$x_1 = \sqrt{0.6}$ $x_2 = 0$ $x_3 = -\sqrt{0.6}$	$w_1 = 5/9$ $w_2 = 8/9$ $w_3 = 5/9$

Figure 34 Gauss Points and Weights factors for Numerical Integration

After all, it is possible to distinguish the generator element from the others: it is the basic a-dimensional element that, after a coordinate transformation, gives a general isoparametric element. The 2D 6-node element is a generator element and so also the 2D 8-node element.

CST: the constant strain triangle is the earliest and simplest finite element.

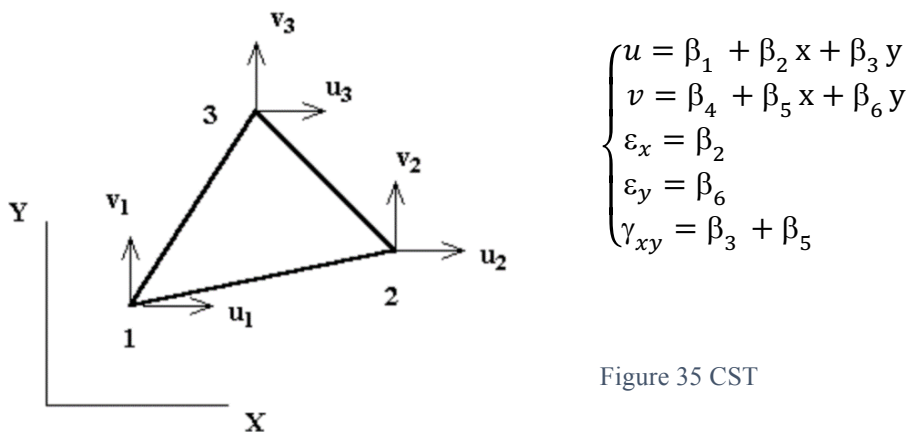


Figure 35 CST

The strain does not vary within the element: the displacement field is linear in x and y direction and so the element sides remain straight as the element deforms. This is the reason why CST element gives good results in a region of the finite element where there is a little strain gradient, otherwise it does not work well.

LST: the linear strain triangle is the earliest and simplest finite element.

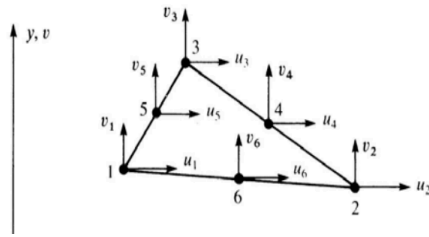
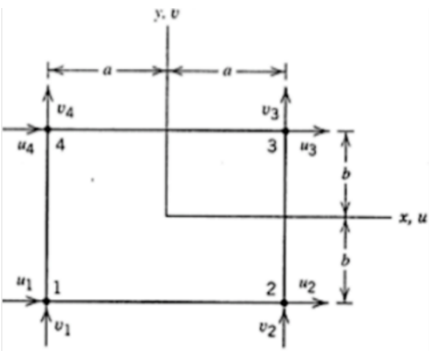


Figure 36 LST

$$\begin{cases} u = \beta_1 + \beta_2 x + \beta_3 y + \beta_4 x^2 + \beta_5 xy + \beta_6 y^2 \\ v = \beta_7 + \beta_8 x + \beta_9 y + \beta_{10} x^2 + \beta_{11} xy + \beta_{12} y^2 \\ \varepsilon_x = \beta_2 + 2\beta_4 x + \beta_5 y \\ \varepsilon_y = \beta_9 + 2\beta_{12} y + \beta_{11} x \\ \gamma_{xy} = \beta_3 + \beta_8 + \beta_5 x + 2\beta_{10} x + \beta_5 x + 2\beta_6 y + \beta_{11} y \end{cases}$$

The strain field can vary linearly with x and y within the element: the displacement field is quadratic in x and y . So LST has the same capabilities of CST and more; if the pure bending is solved using LST elements, exact solution for deflection and stress is obtained.

Q4: bilinear quadrilateral



$$\begin{cases} u = \beta_1 + \beta_2 x + \beta_3 y + \beta_4 xy \\ v = \beta_5 + \beta_6 x + \beta_7 y + \beta_8 xy \\ \varepsilon_x = \beta_2 + \beta_4 y \\ \varepsilon_y = \beta_7 + \beta_8 x \\ \gamma_{xy} = \beta_3 + \beta_6 + \beta_4 x + \beta_8 y \end{cases}$$

Figure 37 Q4

The strain field shows that ε_x is independent of x which means that Q4 element cannot exactly model a cantilever beam under transverse tip force where axial strain varies linearly with x . Q4 element cannot exactly model a state of pure bending. The physical consequence of these defects is that Q4 element is too stiff in bending because an applied moment is resisted by spurious shear stress as well as the expected flexural stress: in fact, it is possible to deduce again that the deformation mode contains spurious shear strain. This element converges properly with mesh refinement and in most problems, it works better than CST element.

Q8: quadratic quadrilateral

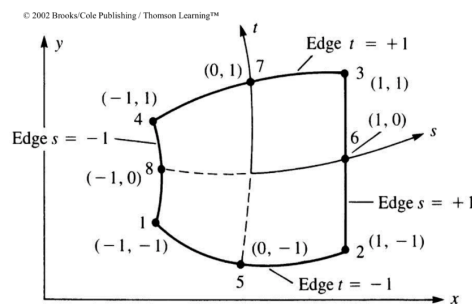


Figure 38 Q8

$$\begin{cases} u = \beta_1 + \beta_2 x + \beta_3 y + \beta_4 x^2 + \beta_5 xy + \beta_6 y^2 + \beta_7 x^2y + \beta_8 y^2x \\ v = \beta_9 + \beta_{10}x + \beta_{11}y + \beta_{12}x^2 + \beta_{13}xy + \beta_{14}y^2 + \beta_{15}x^2y + \beta_{16}y^2x \\ \varepsilon_x = \beta_2 + 2\beta_4x + \beta_5y + 2\beta_7xy + \beta_8y^2 \\ \varepsilon_y = \beta_{11} + \beta_{13}x + 2\beta_{14}y + 2\beta_{16}xy + \beta_{15}x^2 \\ \gamma_{xy} = \beta_3 + 2\beta_8xy + \beta_5x + 2\beta_6y + \beta_7x^2 + 2\beta_8xy + \beta_{10} + 2\beta_{12}x + \beta_{13}y + 2\beta_{15}xy + \beta_{16}y^2 \end{cases}$$

The strain field contains all linear terms and some quadratic terms: it means that Q8 element can represent exactly all states of constant strain and state of pure bending if it is rectangular. Non-rectangular shapes are permitted. (R.W., 1960) (Wilson E.L., 1971) (R.D., 1989) (Irons, 1968)

2.1.4 FEM modelling: Mesh, Loads and BCs

The general rules to create a correct model are:

- Use the simplest type of finite element that will do the job;
- Never use complicated or special elements, unless to be absolutely sure of their behaviour;
- Use the coarsest mesh that is deemed suitable to capture the dominant physical behaviour of the physical system;

2.1.4.1 Mesh:

It is necessary to use a relatively fine discretization in regions where high gradient of strains and stresses is expected and to employ a coarser mesh in regions where lower gradient is predicted. The regions in which it is possible to find out high gradients are:

- Near entrant corners, sharply curved edges;
- Close to concentrated loads, reactions, cracks and cut-outs;
- Within the structures with abrupt changes in thickness, material properties or cross-sectional areas;

Discretizing 3D problems, it is required to try to avoid the use of finite element with higher aspect ratio, and so elongated or skinny elements. In fact, the aspect ratio, that is the ratio between the longest dimension of the element and the shortest $AR = \frac{b}{a}$, is increasing, the inaccuracy of the solution is growing too: as a guideline, elements with aspect ratios exceeding three, should be viewed with caution and those exceeding 10 with urgency. Therefore, in 3D modelling, bricks elements should be preferred over wedges and wedges over tetrahedral: this happens because wedges and tetrahedral can produce wrong stress results.

2.1.4.2 Loads:

There are several kinds of loads that can be applied to the structures, and the most meaningful are:

- Concentrated loads and moments;
- Line loads: they result from the integration of surface loads along one transverse direction, or of volume loads along two transverse directions;

- Distributed surface loads: they are called surface tractions in continuum mechanics and they could be wind, water pressure, snow on the roofs and live load on the bridge for example;
- Distributed volume loads: they are called body forces in continuum mechanics and they could be gravity, inertial, centrifugal, and thermal forces for example;

Concentrated loads and moments must be put on a node: so, in practice, the mesh should be arranged in order to have a node at each location where a concentrated force must be applied. According to classical linear theory at a point loaded by concentrated normal force, there is:

- Finite displacement and finite stress in a beam;
- Finite displacement and infinite stress in a plate;
- Infinite displacement and stress in 2D or 3D solid;

A concentrated moment could not be applied to a node that has only translational degrees of freedom. In linear problems, loads maintain their original orientations in space, regardless of the magnitudes of the computed displacements. In nonlinear analysis, instead, it happens to deal with the ‘follower forces’: the forces whose directions change as the structure deforms. Instead, talking about distributed loads, whatever their nature is, they must always be converted to consistent nodal forces for finite element model analysis: the meaning of consistent can be done exactly through variational arguments, by requiring that the distributed loads and the nodal forces obtained produce the same external work. In fact, these nodal loads that replace distributed loading, come from FE theory and they are called ‘Work-Equivalent’ or ‘Cinematically-Equivalent’ and it means that they have the same resultant force and the same moment about an arbitrary chosen point as does the original distributed load. Two variants of this technique are described below:

1. Node by node (NbN): there is a distributed surface load acting normal to the straight boundary of the 2D finite element mesh; the load is assumed to have been integrated through the thickness normal to the surface. This method has the advantage of not requiring the error-prone computation of the centroid of the loads and it can be extended to 3D meshes as well as volume loads. It should be avoided, however, when the applied forces vary rapidly or act only over portions of the regions;
2. Element by element (EbE): in this way, distributed loads are divided over element domains: the resultant load is assigned to the centroid of the load diagram and it is allocated to the element nodes by statics. A nodal force is obtained by adding the contributions from all elements meeting at that particular node;

If it is applicable, EbE is more accurate than NbN lumping: in fact, it agrees with consistent node lumping for simple elements that possess only corner nodes.

2.1.4.3 Boundary conditions:

In structural problems formulated by the direct stiffness method, it is necessary to distinguish two different types of boundary conditions:

1. Essential: it directly involves the nodal freedom, such as displacements or rotations;
2. Natural: conditions involving applied loads are natural;

Usually essential BCs take precedence over natural BCs: the simplest essential boundary conditions are support and symmetry conditions. Supports are used to restrain structures against relative rigid body motions and this is done by attaching them to earth ground (foundations, anchors, etc.) or to a 'ground structure'. The resulting BCs are often called motion constraints. On the other hand, discovering symmetric or antisymmetric conditions could save in data preparation and computer processing time. This recognition could be done by either visualisation of the displacement field, or by imagining certain rotational or reflection motions: even though the structure may seem symmetric in shape, it must be kept in mind that the model reduction can be used only if the loading conditions are also symmetric or antisymmetric. However, if the symmetry is recognized, the size of the model is reduced: in fact, if the structures are very immense and complicated, it would be a waste of time to ignore that symmetry and work with the model of the whole structure. The conditions stated apply only to boundary nodes of the finite element model that lie in a plane of reflective symmetry of the entire structure. In general, in fact, it is important to try to lighten the model as much as possible, in order to avoid wasting time: the degrees of freedom not active must be suppressed, whether or not they are on the boundary of the model. In nonlinear analysis, the displacement boundary conditions can depend on the deformation of the structure: in this case, the most important problem is the contact problem, in which no-interpenetration conditions are enforced on flexible bodies while the extent of the contact area is unknown. (G.Ballio, 1987) (Man) (1993)

2.1.4.4 Super element concept:

A super element is an assembly of finite elements that may be regarded as an individual element for computational purposes: they could be created for modelling or processing needs. There is the following classification:

- Macro elements: these are super elements assembled with a few primitive elements;
- Substructures: these are complex assemblies of elements that result on breaking up a structure into distinguishable portions;

Both are treated exactly the same way as regards matrix processing: the basic rule is that associated with condensation of internal degrees of freedom. Sub-structuring was invented by aerospace engineers in the early 1960s for these reasons:

1. Facilitate division of labour;

2. Take advantage of repetition;
3. Overcome computer limitations;

Their development was motivated by user convenience: in hand preparation of the models, quadrilateral and bricks involve less human labour than triangles and tetrahedral. Going step further, someone can assemble components such as 'box element' for application such as box-girder bridges. Applied mathematicians, working on solution procedures for parallel computation, have developed the concept of subdomains: these are groupings of finite element that are entirely motivated by computational considerations. In fact, sub-structuring is a process of analysing a large finite element model as a collection of components and it is done following the next reasoning:

1. Divide the FE model into two or more parts by cutting along lines of nodes;
2. Create FE model of each substructure and obtain a set of reduced equations for each substructure;
3. Assemble the reduced equation sets of all substructures, to obtain global equations of all attachment of all substructures;
4. Solve the global stiffness equations to find out the displacement field. In this way, all the displacements become known for all the substructures and it is possible to go back to reaction forces and to obtain stresses in elements;

A substructure becomes appropriate when the structure is large and can be cut into substructures that do not interact strongly: after that individual substructures can be repeatedly used again. When nonlinearities, such as plastic actions, are confined to a single part of the structure it becomes necessary to use the substructure in order to take into account the real behaviour of the whole system. A related technique of super element is multiscale analysis: the whole system is first analysed as a global entity, discarding or passing over details deemed not to affect its overall behaviour. Local details are examined using the results of the global analysis in fem literature. In fact, in the global stage the way of working of the entire structure is simulated with a finite element model that necessarily ignores the details such as cut outs or joints: these details do not affect the overall behaviour of the structure, but it may be on the safety side. Such data are incorporated in a series of local analysis in retrospect: the global analysis is done with a coarse but regular mesh in order to allow the effects of the hole to be ignored; this is followed by local analysis of the region near those holes using a refined mesh. The key feature for the local analysis is the application of boundary conditions on the finer mesh boundaries: these BCs may be displacements or forces. If the displacements are used as boundary conditions, they must be interpolated from the global mesh solutions, otherwise the internal forces or stresses obtained from the entire calculation are converted to nodal forces on the fine meshes through a lumping process. Experience has shown that the stress-

boundary conditions approach generally gives more trustworthy answers; the global-local technique can be extended to more than two levels: in this case, it receives the more involving name ‘multiscale analyses’.

2.1.4.5 Static condensation:

There are two kinds of degrees of freedom:

- Internal degrees of freedom: they are not connected to the d.o.f of another super element;
- External degrees of freedom: they are connected at least to another super element;

According to the global equation:

$$[K]\{D\} = \{f\}$$

If the size of K is too large to fit into the CPU memory of the computer at hand, it is necessary to reduce the size of the matrix to solve the problem: static condensation is a process of eliminating or condensing some unknown degrees of freedom, known as secondary or slave d.o.f, and re-cast the previous equation in terms of fewer unknowns d.o.f, termed as primary unknowns or master.

2.1.4.6 Nonlinearity in stress analysis:

There could be so many types of nonlinearity and the most relevant are the following:

- Geometric nonlinearity: it means that nonlinearity arises because of significant changes in the geometry of the structure, as the presence of follower forces;
- Material nonlinearity: it comes up when the material of which the element is made of, has a nonlinear stress-strain relationship;
- Contact nonlinearity: it denotes that the contact areas between two bodies grows as applied load increases, whether the material yields or not;

In fact, it could happen that adjacent parts may make or break a contact: this contact area may change as load changes. It could also happen that elastic material may become plastic and it may not have any more linear stress-strain relation at any stress level. It is possible that part of the structure may lose stiffness due to buckling or failure of the material. In general, the abroad range of nonlinearity phenomena could be grouped in the following cases:

- Materials in which deformation depends on load rate as well as load level as creep, viscoelasticity, viscoplasticity;
- Problems with large strain as in metal-forming process;
- Linkages, mechanism and other problems which involve large rigid-body motion;
- Coupled problems as fluid-structure interactions;
- Nonlinear dynamic problems, such as nonlinear vibrations and projectile impact;

In all these cases, and also in many others, the solution cannot be obtained in a single step of analysis: several steps may be necessary and the tentative solution should be update after each step and repeat

until a convergence test is satisfied. In these situations, it happens that equation $[K]\{d\} = \{f\}$ is nonlinear because the stiffness matrix $[K]$ is function of the displacements field: the numerical methods are not able any more to solve nonlinear equation explicitly for $\{d\}$ as function of $\{f\}$. A simple way to solve nonlinear equations is called direct substitution but more often, various incremental methods are used: they used a tangent stiffness which for a single degree of freedom system is the slope of the loading curve in the P versus U plot. In SDOF problems it is possible to obtain the 'correct' curve by calculating the load P for each several values of the displacements U; on the other side, for MDOF systems it is possible to calculate the load vector only if the relation between stiffness and displacement is known. Geometric nonlinearity arises when deformations are large enough to significantly alter the way load is applied or the way the structure resist to the load; the general target of analysis is to construct the nonlinear relation between applied load and the resulting deformation and it is usually done assuming that the structure is sufficiently thin that large displacements are possible without yielding of material. Fe analysis of large-deflection problems does not require the introduction of a new set of elements: in fact, the shape functions and element library used for linear small-deflection analysis can still be used in nonlinear analysis. The software with nonlinear capability is able to keep track of the deformations and rigid-body motions of elements, so that stiffness used in the solution process correspond to the deformed configuration rather than the original configuration. On the other sides material nonlinearity arises when the relation between strain and stress is not any more described by a straight line.

2.1.4.7 3D solid models:

In a 3D model, all six possible stresses should be taken into account and the displacement field involves all three components: u, v, w. The constitutive equation is the same of the other cases:

$$\sigma = E\varepsilon + \sigma_0$$

The complete formulation could be written in the following way:

$$\begin{Bmatrix} \sigma_x \\ \sigma_y \\ \sigma_z \\ \tau_{xy} \\ \tau_{yz} \\ \tau_{xz} \end{Bmatrix} = [E]\{\varepsilon\} - \frac{E\alpha\Delta T}{1-2\nu} \begin{Bmatrix} 1 \\ 1 \\ 1 \\ 0 \\ 0 \\ 0 \end{Bmatrix}$$

The equation seen before, are still valid: the only thing that has been changed is the size of the vectors $\{u\}$ and $\{d\}$ and the order of the size of the matrix $[N]$. As a consequence of that, also the matrix $[B]$

has different dimension: it is now a 6×1 , not 3×1 anymore. The global stiffness matrix has now $3n \times 3n$ dimension, where n are the total degrees of freedom of the whole system. To prevent singularity of 'K', boundary conditions on a 3D solid must suppress six rigid-body motions.

The finite elements that can be used for 3D solids analysis are the following:

CST: Constant Strain Tetrahedron.

It behaves like constant strain triangle in the 2D case: it is accurate only when strains are almost constant over the span of an element. The element is poor in representing fields of bending or twisting.

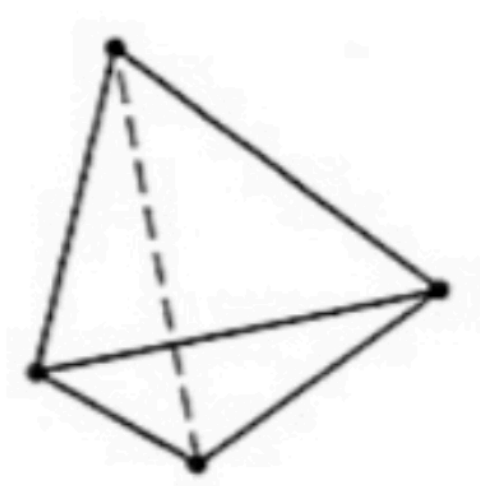


Figure 39 CST

LST: Linear Strain Tetrahedron.

It has 10 nodes and it has a strain field that is linear in the coordinates.

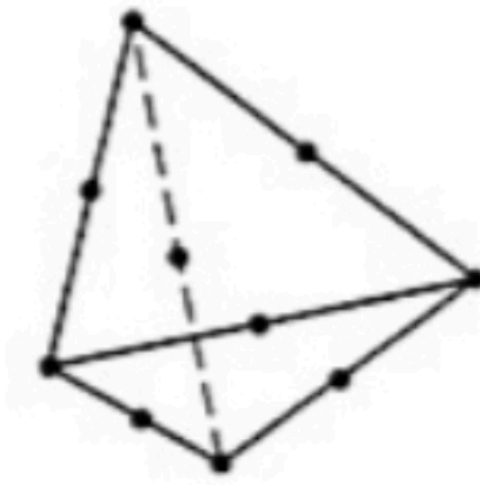


Figure 40 LST

Trilinear Hexahedron.

It is an 8-node brick and it has displacement field composed by the product of three linear polynomials $(C_1 + C_2x) \cdot (C_3 + C_4y) \cdot (C_5 + C_6z)$ in which C_i are constants. The hexahedral element can be of arbitrary shape if it is formulated as an isoparametric element:

$$N_i = \frac{1}{8} \cdot (1 \pm \xi) \cdot (1 \pm \eta) \cdot (1 \pm \zeta) \quad i=1:8$$

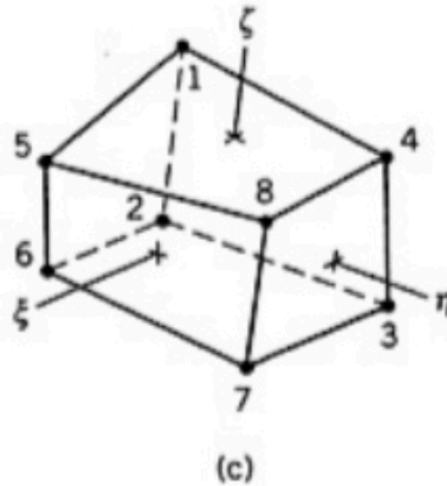


Figure 41 Trilinear Hexahedron

Trilinear hexahedron cannot model beam action well because its sides remain straight as the element deforms.

Quadratic Hexahedron.

It has 20 nodes: if the element is rectangular it can model linear strain fields exactly. In this case B is a 6x60 rectangular matrix: if K is integrated by 2by2by2 Gauss quadrature rule, three ‘hourglass’ instabilities are possible. This possibility is avoided in commercial software by using a stabilization device, a special rule of 14 points or even a 3by3by3 rule (27 points) to integrate K.

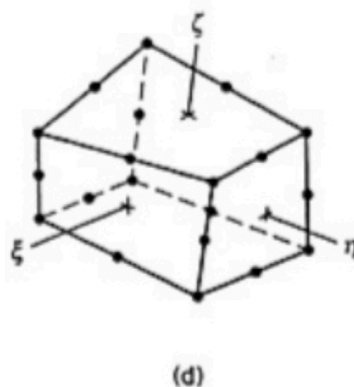


Figure 42 Quadratic Hexahedron

2.2 The Software Abaqus

The whole bridge and joint under investigation in this thesis are studied and modelled in Abaqus: Abaqus is used for all FE investigations in the present thesis.

2.2.1 General description of Abaqus software

Abaqus is a software for finite element analysis; it has got great modelling skills and a wide application fields. It is used to numerical simulation of static and dynamic response of structures and numerical simulation of single structural components; it allows to solve problems not strictly related to structural engineering: static and dynamics issues, static linear and nonlinear analysis, materials characterized by complex constitutive bonds, contact problems, fracture mechanics behaviour etc. It uses finite element method to solve structural mechanics problems. The basic idea of the method is that to discretize the structure in question into several elements, in which the unknown quantities are the nodal grid displacements. Within the range of configurations admissible by the kinematic approximation adopted, equilibrium is imposed by means of an energetic approach in terms of the virtual works principle. The finite element method is widespread and uses thanks to its versatility that allows to treat complex geometry problems more easily. The analysis procedure uses by Abaqus software consists of three main steps:

1. Pre-Processing;
2. Simulation;
3. Post-Processing;

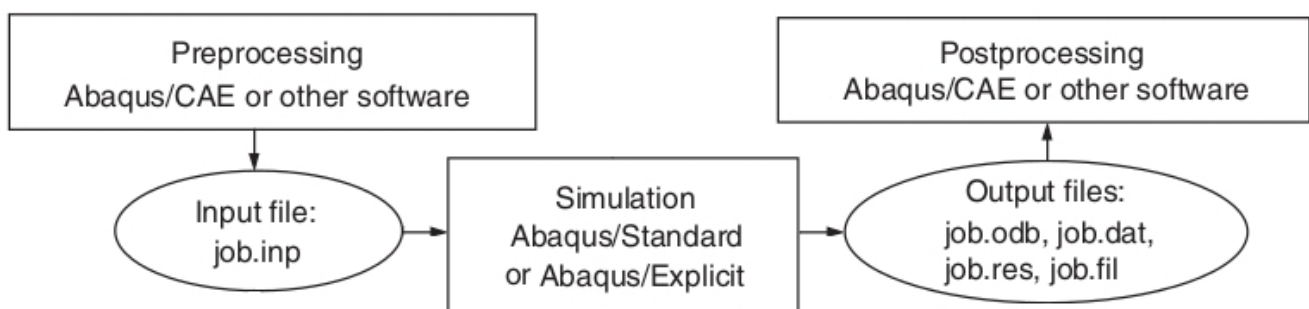


Figure 43 Abaqus's analysis step procedure

Pre-Processing: in this step, the physical problem is transformed into an input file on Abaqus, containing a complete and accurate description of the whole numerical model: exactly geometry of each part, properties of assignment materials, parts assembly, the entire mesh, load cases and boundary conditions, and the choice of analysis to be performed and the quantities requested in output. This kind of work can be done previously through some programming software (like Python or Matlab), using .inp file, .py file, or it can be directly done in Abaqus's prompt area, using .cae file. The model is usually created graphically with Abaqus/CAE, ie the Complete Abaqus Environment

which provides a simple interface for model creation and it is divided into modules each of which defines a logical aspect of modelling process: parts, properties, sections, assembly, constraints, loads, boundary conditions.

Simulation: in this step, the problem set and defined in the previous step is resolved by Abaqus/Standard or by Abaqus/Explicit. The results are saved in .dat file in which there are information on modelling and especially on the operations carried out by the software during processing. Depending on the complexity of the problem analysed and on the computer power, this step can take from seconds to days to complete the analysis.

Post-Processing: in this step, once the simulation has been performed, it's possible to view the results obtained through the program graphic interface or through a compatible program capable of reading the output file. At the end of the calculation, the displacements, the stresses or other fundamental variables required when necessary, were calculated: Abaqus has a huge variety of displaying results options, including animations, deformed graphs and the possibility of exporting data in .txt files; it also offers the chance to creating x-y graphs with desired grades. (Abaqus, 2013)

2.2.2 Model composition

The important information is: geometry, elements section properties, materials, loads, boundary conditions, type of analysis and requested output. It is important to keep in mind that the approximations in the choice of the geometry of the model, the behaviour of the material, the boundary conditions and the loads, determine how close or less the numerical solution will be to the physical problem. Before describing how the model is actually created, bear in mind the fact that unlike other finite element software, Abaqus does not use measurement units. Therefore, it is necessary to be careful and the choice of length should be consistent with the choice of material properties and loads.

2.2.3 Module Part

The Part module offers to create single part drawing its geometry directly through Abaqus/CAE. There are several ways to create a part in Abaqus/CAE: create the part using the tools available in the Part module or import the part from a file containing geometry stored in a third-party format. The Part module allows the analyst to do the following things:

- a. Create deformable, discrete rigid, analytical rigid, or Eulerian parts;
- b. Create the features that define the geometry of the part: solids, shells, wires, cuts, and rounds;
- c. Use the Feature manipulation toolset to edit, delete, suppress, resume, and regenerate a part's features;
- d. Assign the reference point to a rigid part;

- e. Use the Sketcher to create, edit, and manage the two-dimensional sketches that form the profile of a part's features. These profiles can be extruded, revolved, or swept to create part geometry;
- f. Use the Set toolset, the Partition toolset, and the Datum toolset. These toolsets operate on the part in the current viewport and allow you to create sets, partitions, and datum geometry, respectively;

Below it is a brief description of the various types of parts that can be created:

Deformable: a deformable part represents an element that can deform under load, which can be mechanical, thermal, or electrical. By default, Abaqus/CAE creates parts that are deformable. Any arbitrarily shaped axisymmetric, two-dimensional, or three-dimensional part that can be created or be imported can be specified as a deformable part;

Discrete rigid: a discrete rigid part is used to simulate the behavior of an element that can be rigid and is used in contact analyses to model bodies that cannot deform. As deformable body, a discrete rigid part can be any arbitrary shape;

Analytical rigid: an analytical rigid part is similar to a discrete rigid part. It is used to represent a rigid surface in a contact analysis. Unlike the two previous cases, the shape of an analytical rigid part is not arbitrary and must be formed from a set of sketched lines, arcs, and parabolas;

Eulerian: Eulerian parts do not deform during an analysis; instead, the material within the part, deforms under load and can flow across the rigid element boundaries. This is the reason why Eulerian parts are used to define a domain in which material can flow for an Eulerian analysis;

2.2.4 Module Properties

Once each part has been created, the following step is to create a material, with own properties and assign it to each element. The Property module allows analyst to perform the following tasks:

- a. Define materials;
- b. Define beam section profiles;
- c. Define sections;
- d. Assign sections, orientations, normal, and tangents to parts;
- e. Define composite layups;
- f. Define a skin reinforcement;
- g. Define inertia (point mass, rotary inertia, and heat capacitance) on a part;
- h. Define springs and dashpots between two points or between a point and ground;
- i. Define material calibrations;

A profile specifies the properties of a beam section that are related to its cross-sectional shape and size. Shape-based profiles can be created: they define the specific shape and dimensions of the beam

cross-section. Abaqus uses the information provided by the shape-based profile to calculate the engineering properties of the section. They can be created by first selecting from a list of shape options and then specifying that particular shape's dimensions. It is important that material properties have to be defined and assigned to all created parts. A material definition specifies all the property data relevant to a material. A material is defined by including a set of material behaviors: the prompt material editor is used to specify all the information that defines each material. Each material created has its own name and it is independent of any particular section: a single material can be referred to many sections as necessary. Abaqus/CAE assigns the properties of a material to a region of a part when section to which the material has been assigned is in turn associated with the element.

2.2.5 Module Assembly

Once each single part has been generated, they must be joint together through the Assembly module. Each part exists in its own independent coordinate system: it is important to use assembly module to create 'instances' and place them next to each other in a global coordinate system thus creating a single model. An instance maintains its association with the original part or model. If the geometry of a part or model changes, Abaqus/CAE automatically updates all instances of the part or model to reflect these changes. It is not allowed edit the geometry of an instance directly. The main model can contain many parts and model subassemblies, and a part or model can be instanced many times in the main model assembly. Even if the model consists of only a single part, an assembly that consists of just a single instance of that part must still create. A part instance can be thought of as a representation of the original part. Part instances can be either independent or dependent: an independent instance is effectively a copy of the part, a dependent instance is only a pointer to the part, partition, or virtual topology. As a result, a dependent instance cannot be mesh, while the original part from which the instance was derived can be mesh. In. this case Abaqus/CAE applies the same mesh to each dependent instance of the part. Dependent part instances: as said above, by default, Abaqus/CAE creates a dependent instance of a part. A dependent instance is only a pointer to the original part: it shares the geometry and the mesh of the original part. When the original part is meshed, Abaqus/CAE applies the same mesh to all dependent instances of the part. Most modifications are not allowed on a dependent part instance. However, operations that do not modify the geometry of a dependent part instance are still allowed; for example, you can create sets, apply loads and boundary conditions, and define connector section assignments. If you apply an adaptive meshing again rule to a dependent part instance in the Mesh module, Abaqus/CAE meshes again the original part and applies the new mesh to each dependent instance of the part. You cannot change the mesh attributes of an individual dependent part instance, like as the mesh seeds, mesh controls, and element types. However, you can change the mesh attributes of the original part, and Abaqus/CAE propagates the changes to all

dependent instances of the part. The advantages of dependent part instances are that they consume fewer memory resources and you need mesh the part only once. Independent part instances: on the other hand, an independent part instance is a copy of the geometry of the original part. If an independent part instance is created, it cannot be meshed; however, the independent instance can be meshed. In addition to meshing, most other operations can be performed on an independent instance. The disadvantages of independent instances are that they consume more memory resources, and you must mesh each independent instance individually. It is not possible to create both a dependent and an independent instance of the same part. As a result, if there is a dependent instance of a part, all subsequent instances must be dependent. The same argument applies to independent instances. Instances of mesh parts are always dependent.

2.2.6 Module Mesh

The Mesh module allows to generate meshes on parts and assemblies created within Abaqus/CAE. Various levels of automation and control are available so it is possible to create a mesh that meets the needs of the analysis. As with creating parts and assemblies, the process of assigning mesh attributes to the model—such as seeds, mesh techniques, and element types—is feature based. As a result, the parameters that define a part or an assembly can be modified, and the mesh attributes specified within the Mesh module are regenerated automatically. The Mesh module provides the following features:

- a. Tools for prescribing mesh density at local and global levels;
- b. Model coloring that indicates the meshing technique assigned to each region in the model;
- c. A variety of mesh controls, such as: element shape, meshing technique, meshing algorithm and adaptive meshing again rule;
- d. A tool for assigning Abaqus/Standard, Abaqus/Explicit, or Abaqus/CFD element types to mesh elements;
- e. A tool for verifying mesh quality;
- f. Tools for refining the mesh and for improving the mesh quality;
- g. A tool for saving the meshed assembly or selected part instances as a mesh part;

In this module, it is possible to define through the ‘global seeds’ windows the dimension of the mesh elements on the borders of the parts under examination. Abaqus/CAE can use a variety of meshing techniques to mesh models of different topologies. In some cases, different meshing technique can be chosen for a model or model region. In other cases, only one technique is valid. The different meshing techniques is useful because it provides varying levels of automation and user control: there are two meshing methodologies available in Abaqus/CAE: top-down and bottom-up. Top-down meshing: it generates a mesh by working down from the geometry of a part or region to the individual mesh nodes and elements. Top-down meshing techniques is good for the mesh of one-, two-, or three-

dimensional geometry using any available element type. The resulting mesh exactly conforms to the original geometry. The rigid conformance to geometry makes top-down meshing predominantly an automated process but may make it difficult to produce a high-quality mesh on regions with complex shapes. Bottom-up meshing: it generates a mesh by working up from two-dimensional entities (geometric faces, element faces, or two-dimensional elements) to create a three-dimensional mesh. Bottom-up meshing techniques can be used to mesh only solid three-dimensional geometry using all—or nearly all—hexahedral elements. Generating a mesh using the bottom-up meshing technique is a manual process, and the resulting mesh may vary significantly from the original geometry. However, allowing the mesh to vary from geometry may allow the analyst to produce a high quality hexahedral mesh on regions with complex shapes. When the Mesh defaults color mapping is selected, Abaqus/CAE uses different colors to indicate which meshing technique, if any, is currently assigned to a region: for example, if a solid region is meshed using the structured meshing technique, the region turns green. In fact, the green color indicates that the structured meshing technique is assigned to that region, yellow indicates that the sweep meshing technique is applied to a region and if in a region it is not possible to make the mesh using the currently assigned element shape, the region turns orange. Regions that are pink or light tan have been assigned the free and bottom-up meshing techniques, respectively. If the mesh generated automatically is not so comfortable for the geometry of the problem, the Mesh module provides a set of tools that allow you to refine a mesh:

- a. Partition toolset can be used to divide geometric regions into smaller regions: the resulting partitions introduce new edges that can be seed in a different way. Therefore, partitioning and seeding can be combined to gain additional control over the mesh generation process. Partitioning can also allow to create regions to which different element types could be assigned;
- b. The Virtual Topology toolset allows to remove these small details by combining a small face with an adjacent face or by combining a small edge with an adjacent edge. In fact, in some cases, the geometric contains details such as very small faces and edges. Introducing virtual topology is a convenient method for creating a clean, well-formed mesh;

2.2.7 Module Step

The most important thing to simulate exactly the different phases of an analysis is to specify the exact order of the application of loads and boundary conditions on the structure. It is possible to model that through the module step. The Step module allows analyst to perform the following tasks:

- a. Create analysis steps;
- b. Specify output requests;
- c. Specify adaptive meshing;

d. Specify analysis controls;

Create analysis steps: within a model it is possible to define a sequence of one or more analysis steps: the step sequence provides a convenient way to underline changes in the loading and boundary conditions of the model, changes in the way parts of the model interact with each other, the removal or addition of parts, and any other changes that may occur in the model during the course of the analysis. In addition, steps allow analyst to change the analysis procedure, the data output, and various controls. Specify output requests: Abaqus writes output from the analysis to the output database; output requests, once they have been created, propagate to subsequent analysis steps. An output request defines which variables will be output during an analysis step, from which region of the model they will be output, and at what rate they will be output. Specify adaptive meshing: adaptive mesh regions and specify controls for adaptive meshing in those regions can be defined. Specify analysis controls: analyst can customize general solution controls and solver controls. In fact, Abaqus/CAE need the special initial step: it is at the beginning of all the step and it is useful to define the initial boundary conditions and the predefined fields and interactions applied since the beginning of the analysis. In each step, loads and BCs applied to the model has to be defined in order to simulate the real physical behavior and the history of the analysis. It allows analyst to define the methods of analysis and application of the loads to be performed during all the steps. In this way, the effects of the previous step are always included in the new answer as starting conditions for each new analysis step. A step can be divided into increments to make easier the solving procedure of equation system. For a general, static step as well as for many other kinds of steps, the following options can be set:

- a. Time increase: When Automatic time increase is chosen, Abaqus/CAE starts the increase using the value entered for the initial increment size. The size of subsequent time increments is adjusted based on how quickly the solution converges and this option is the default selection. On the other hand, when Fixed time increase is chosen, Abaqus/CAE uses the value entered for the initial increment size throughout the step;
- b. Maximum number of increments: Abaqus limits the number of increments in a step to the value that you enter for the maximum number of increments: if the step exceeds this number of increments, the analysis stops, and diagnostic information is reported to the Job module and written to the message file. By default, Abaqus/CAE sets the maximum number of increments to 100;
- c. Initial increment size: Abaqus starts the step using the value entered for the initial increment size;
- d. Minimum increment size: Abaqus checks for the minimum increment size only when the model is analyzed using automatic time increase: if Abaqus/CAE needs a smaller time

increment than this value to reach a convergent solution, it terminates the analysis, reports to the Job module, and writes diagnostic information to the message file. By defaults, it uses 10-5 times the total time period;

- e. Maximum increment size: Abaqus checks for the maximum increment size only when the model is analyzed using automatic time increase: Abaqus/CAE will not increase the increment size beyond this value during the analysis. By default, it sets the value to that of the total time period;

The importance of this module is that it allows to do every kind of analysis type required by the analyst. In fact, the step module distinguishes between general nonlinear steps and linear perturbation steps by indenting the names and procedure descriptions of linear perturbation steps. As specified above, general nonlinear analysis steps define sequential events: the state of the model at the end of one general step provides the initial state for the start of the next general step. On the other side, linear perturbation analysis steps provide the linear response of the model about the state reached at the end of the last general nonlinear step. For each step in the analysis this module also indicates whether Abaqus will account for nonlinear effects from large displacements and deformations. If the displacements in a model due to loading are relatively small during a step, the effects may be small enough to be ignored. However, in cases where the loads on a model result in large displacements, nonlinear geometric effects can become important: the 'Nlgeom' setting for a step determines whether Abaqus will account for geometric nonlinearity in that step.

2.2.8 Module Interaction

The Interaction module allows to define the following different type of interactions. The most relevant for the thesis are reported above:

- a. Contact interactions;
- b. Elastic foundations;
- c. Cyclic symmetry;
- d. Model change interactions;
- e. Tie constraints;
- f. Rigid body constraints;
- g. Coupling constraints;
- h. Adjust points constraints;
- i. MPC constraints;
- j. Springs and dashpots;

Interactions are step-dependent objects, which means that when they are defined, it must be indicated in which steps of the analysis they are active. The Set and Surface toolsets in the Interaction module

allow analyst to define and name regions of the model to which interactions and constraints are applied. The Reference Point toolset allows to define reference points that are used in constraints and creating assembly-level wire features. Abaqus/CAE does not recognize mechanical contact between part instances or regions of an assembly unless that contact is specified in the Interaction module; the mere physical proximity of two surfaces in an assembly is not enough to indicate any type of interaction between the surfaces. In the next step the most important contact types for civil engineering are introduced:

- a. General contact: general contact interactions allow to define contact between many or all regions of the model with a single interaction; to refine the contact domain, analyst can include or exclude specific surface pairs. Surfaces used in general contact interactions can span many disconnected regions of the model; attributes, such as contact properties, surface properties, and contact formulation, are assigned as part of the contact interaction definition but independently of the contact domain definition, which allows to use one set of surfaces for the domain definition and another set of surfaces for the attribute assignments. General contact interactions and surface-to-surface or self-contact interactions can be used together in the same analysis: only one general contact interaction can be active in a step during an analysis;
- b. Surface-to-surface contact, self-contact, and pressure penetration: surface-to-surface contact interactions describe contact between two deformable surfaces or between a deformable surface and a rigid surface, instead self-contact interactions describe contact between different areas on a single surface. If the model includes complex geometries and numerous contact interactions, it is possible to customize the variables that control the contact algorithms to obtain cost-effective solutions. These controls are intended for advanced users and should be used with great care. On the other hand, a pressure penetration interaction allows to simulate the pressure of a fluid penetrating between two surfaces involved in surface-to-surface contact. The fluid pressure is applied normal to the surfaces: a surface-to-surface contact interaction must be created to specify the master and slave surfaces for the pressure penetration; the bodies forming the joint can both be deformable, as is the case with threaded connectors, or one can be rigid, as occurs when a soft gasket is used as a seal between stiffer structures;
- c. Model change: a model change interaction allows to remove and reactivate elements during an analysis: model change interactions can be used in all Abaqus/Standard analysis procedures except for the static, Risk procedure and linear perturbation procedures;

In addition, it is possible to describe in details the most important types of interaction properties:

- a. **Contact:** a contact interaction property can define tangential behavior (friction and elastic slip) and normal behavior (hard, soft, or damped contact and separation). In addition, a contact property can contain information about damping, thermal conductance, thermal radiation, and heat generation due to friction. A contact interaction property can be referred to by a general contact, surface-to-surface contact, or self-contact interaction;
- b. **Film condition:** a film condition interaction property defines a film coefficient as a function of temperature and field variables. A film condition interaction property can be referred to only by a film condition interaction;
- c. **Fluid cavity:** a fluid cavity interaction property defines the type of fluid occupying the cavity and the fluid properties: it is possible to choose either a hydraulic fluid or a pneumatic fluid. Hydraulic fluids must include a fluid density and they may include a fluid bulk modulus, thermal expansion coefficients, and other temperature-dependent data. Pneumatic fluids must include an ideal gas molecular weight, and they may include a molar heat capacity;
- d. **Fluid exchange:** a fluid exchange interaction property defines the fluid flow between a cavity and the environment or from one cavity to another;

Constraints defined in the Interaction module define constraints on the analysis degrees of freedom, whereas constraints defined in the Assembly module define constraints only on the initial positions of instances. In the Interaction module, the degrees of freedom between regions of a model can be constrained, and constraints can be suppressed and resumed to vary the analysis model. Currently, the following types of constraints can be defined:

- a. **Tie:** a tie constraint allows to fuse together two regions even though the meshes created on the surfaces of the regions may be dissimilar;
- b. **Rigid body:** a rigid body constraint allows to constrain the motion of regions of the assembly to the motion of a reference point: the relative positions of the regions that are part of the rigid body remain constant throughout the analysis;
- c. **Coupling:** a coupling constraint allows to constrain the motion of a surface to the motion of a single point;
- d. **Adjust points:** an adjust points constraint allows to move a point or points onto a specified surface;
- e. **MPC constraint:** an MPC constraint allows to constrain the motion of the slave nodes of a region to the motion of a single point;
- f. **Shell-to-solid coupling:** a shell-to-solid coupling constraint allows to couple the motion of a shell edge to the motion of an adjacent solid face;

The contact detection tool in Abaqus/CAE provides a fast and easy way to find contact interactions and tie constraints in a three-dimensional model. The active search domain, the definitions of surfaces, and the default interaction or constraint settings can be settled as analyst prefer to do: the search works for both geometry and meshed models. Each detected interaction or constraint involves two identified surfaces, also known as a contact pair candidate and the contact detection dialog box lists each contact pair candidate and its default parameters in a tabular format: using this tabular interface, the contact pair candidates can be reviewed in order to ensure that the surface definitions are comprehensive, the master and slave assignments are appropriate, and the parameters are correct; if necessary, parameters or surface assignments can be modified in the table, and new contact pairs can be created where appropriate. Once the contact pair candidates are configured to analyst specifications, Abaqus/CAE defines all of the contact interactions and tie constraints simultaneously. The important thing in this case is the concept of master surface and slave surface: in fact, Abaqus attempts to find the closest point for each node of the soave surface on the master surface of the contact pair where the master surface's normal pass through the node on the slave surface; indeed, in this way it is possible to discretized the interaction between the points on the master surface and the slave nodes. The important thing is that Abaqus uses a strict "Master-Slave" algorithm, in which the master surface can penetrate into slave surface, otherwise the slave nodes are constrained not to penetrate into master surface and the contact direction is always normal to master's surface. This kind of algorithm imposes the following restriction on the master surface: it must be element-based or analytical, generally the master should be chosen as the surface of the stiffer body or as the surface with coarser mesh if the two surfaces have comparable stiffness. Due to this reason, a rigid element should be always a master and the stiffness of the structure and the stiffness of the material are both taken into account in this choice. On the other side, slave surface should always be assigned to the deformable bodies or deformable bodies defined as rigid: when both the surfaces are deformable the chose has to be done carefully. The master surface cannot be made up of two or more disconnected regions: it must be always continuous and in 2D systems it should be either simple, without intersecting curve with two terminal ends or closed loop. The densely meshed body should be the slave: this is done because of Abaqus allows master to penetrate into slave: to avoid this penetration the slave meshing must be denser and the longer of these two surfaces should be master in order to prevent sliding slave nodes from sliding off the surface and falling behind. In conclusion, summarizing, the main characteristic that master surfaces must have are the following:

1. The larger of the two surfaces should act as a master surface;
2. Stiffer body should act as master;
3. Body with Coarser mesh should act as master;

4. Master surface should be smoothed;

In fact, Abaqus automatically smooths all master surfaces in finite-sliding simulations.

2.2.9 Module Load

You use the Load module to define and manage the following prescribed conditions:

- a. Loads;
- b. Boundary conditions;
- c. Predefined fields;
- d. Load cases;

Prescribed condition managers are dialog boxes that analyst use to organize and manipulate the prescribed conditions associated with a given model: each kind of prescribed condition that can be defined in the Load module has a separate manager. This module allows to fix the boundary conditions and to applied loads to the model: the BCs are used to fix some frames of the model and to let other parts free to move. Prescribed conditions in Abaqus/CAE are step-dependent objects, which means that the analysis steps in which they are active must always be specified. It is possible to use the load, boundary condition, and predefined field managers to view and manipulate the stepwise history of prescribed conditions. The Set and Surface toolsets in the Load module allow to define and name regions of the model to which you would like to apply prescribed conditions and the Analytical Field toolset and the Discrete Field toolset allow to create fields through which define spatially varying parameters for selected prescribed conditions. The wide range of useful applicable loads is shown below:

- Surface traction load;
- Body force;
- Line load;
- Gravity load;
- Connector moment;
- Surface heat flux;
- Surface current;
- Body current;
- Concentrated force;
- Moment;
- Pressure load;

The wide range of useful applicable boundary conditions is shown below:

- Symmetry/antisymmetric/Encastre boundary conditions;
- Displacement/ rotation boundary conditions;

- Velocity/angular velocity boundary conditions;
- Acceleration/angular acceleration boundary conditions;
- Connector displacement boundary conditions;
- Connector velocity boundary conditions;
- Connector acceleration boundary conditions;

2.2.10 Module Job

Once analyst has finished all of the tasks involved in defining a model (such as defining the geometry of the model, assigning section properties, and defining contact), the Job module can be used to analyze the model. The Job module allows to create a job, to submit it for analysis, and to monitor its progress: if desired, multiple models and jobs can be created and be ran and be monitored the jobs

3 MODELING

Before starting with the description of the models done in Abaqus it is important to specify the general features common to both the models, in order to avoid describing two times the same things. At the beginning, it is important to specify that Abaqus does not have really the unit referring system. It has been decided to build the model with the following measures: N, mm and MPa. It is necessary to be careful with units: if dimensions of the parts are specified in [mm], then the Young's modulus must be given in [MPa] and the resulting stress fields are expressed in [MPa].

3.1 General properties of FE-Models

There are some common features used in the modeling.

3.1.1 Material

The material used in this chapter are four:

1. Steel S355J2;
2. Concrete C35/45;
3. Concrete C45/55;
4. Concrete C140/150 UHPFRC

The steel S355J2 can be modelled as a homogeneous and isotropic elastic material, defined by the Young's modulus of elasticity $E = 210000$ MPa and Poisson's ratio $\nu = 0.3$.

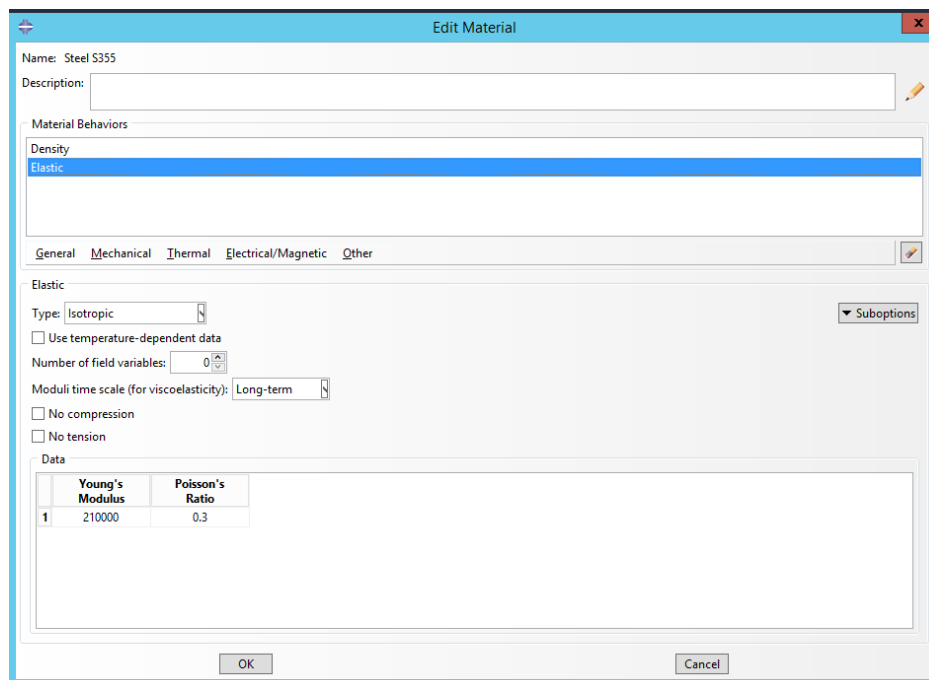


Figure 44 Description of the concrete and steel mechanical properties

In the bridge model, the density of the steel has been increased to taking into account the dead load of the steel bracings added every four meters along the span:

$$\gamma = 78.5 * 1.03 = 80.855 \frac{kN}{m^3}.$$

In the joint model, the elastic-perfectly plastic law is taking into account. In fact, in the joint there is the need to investigate the behavior also in the plastic field, to understand better the reliability of the results. The plastic analysis has been done introducing the elastic-perfectly-plastic behavior in the steel properties, as follows:

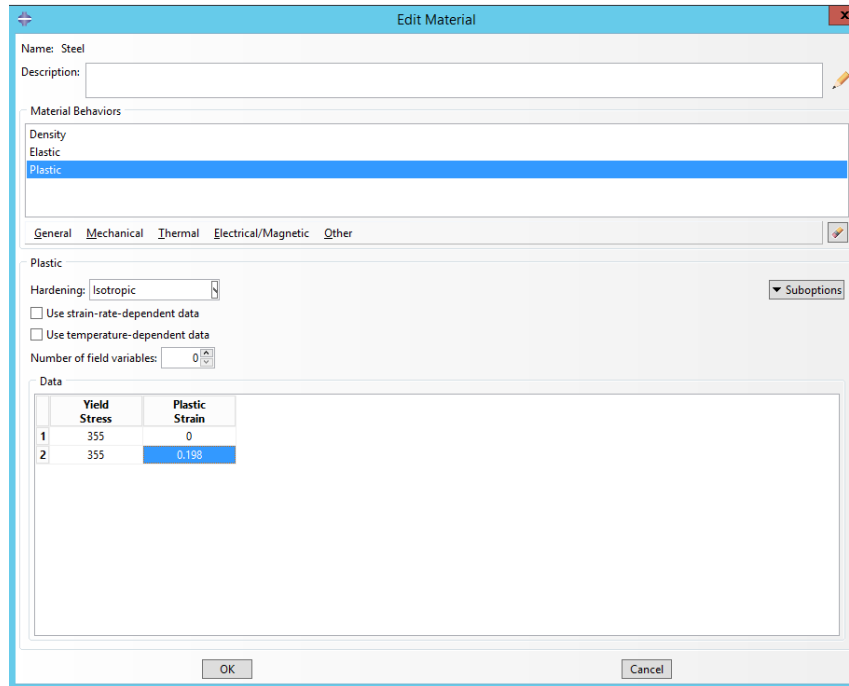


Figure 45 Plastic Properties

The concrete C35/45 is used for the slab of the bridge cast in situ and it has the following mechanical properties: it has been modelled as a homogeneous and isotropic elastic materials, defined by the Young's modulus of elasticity $E = 34000 \text{ MPa}$ and the Poisson's ratio $\nu = 0.15$. In fact, the analysis of the bridge is done assuming always an elastic behaviour: it is specified only the elastic modulus of the material and it is expressed in MPa on Abaqus. The density is supposed to be $\gamma = 25 \frac{\text{kN}}{\text{m}^3}$.

The concrete C45/55 is used for the prefabricated slab it has the following mechanical properties: it has been modelled as a homogeneous and isotropic elastic materials, defined by the Young's modulus of elasticity $E = 35500 \text{ MPa}$ and the Poisson's ratio $\nu = 0.15$. As said before, the analysis of the bridge is done assuming always an elastic behaviour: it is specified only the elastic modulus of the material and it is expressed in MPa on Abaqus. The density is supposed to be $\gamma = 25 \frac{\text{kN}}{\text{m}^3}$.

The Concrete C140/150 UHPFRC: it is ultra-high-performance fiber reinforced concrete. It has the following mechanical properties:

$$\gamma = 25 \frac{\text{kN}}{\text{m}^3}$$

$$E = F_{cm}^{\frac{1}{3}} * 10200 = 44000 \text{ MPa}$$

$$F_{ck} = 150 \text{ MPa}$$

$$F_{cd} = 0.85 * \frac{150}{1.5} = 85 \text{ MPa}$$

$$F_{ckt} \approx 10 \text{ MPa}$$

$$F_{cm} = F_{ck} + 8 \text{ MPa} = 94 \text{ MPa}$$

In the first basic model of the joint, the elastic behavior has investigated; indeed, the final model has been created to investigate the effect of the introduction of some more detailed properties for modelling the concrete behavior. The properties assigned to the concrete part, has been defined using the concept of Concrete Damage Plasticity. This command allows to describe the compressive behavior and also the tensile. Thanks to the tests done by the concrete company, it is possible to have the expected compressive and tensile behavior:

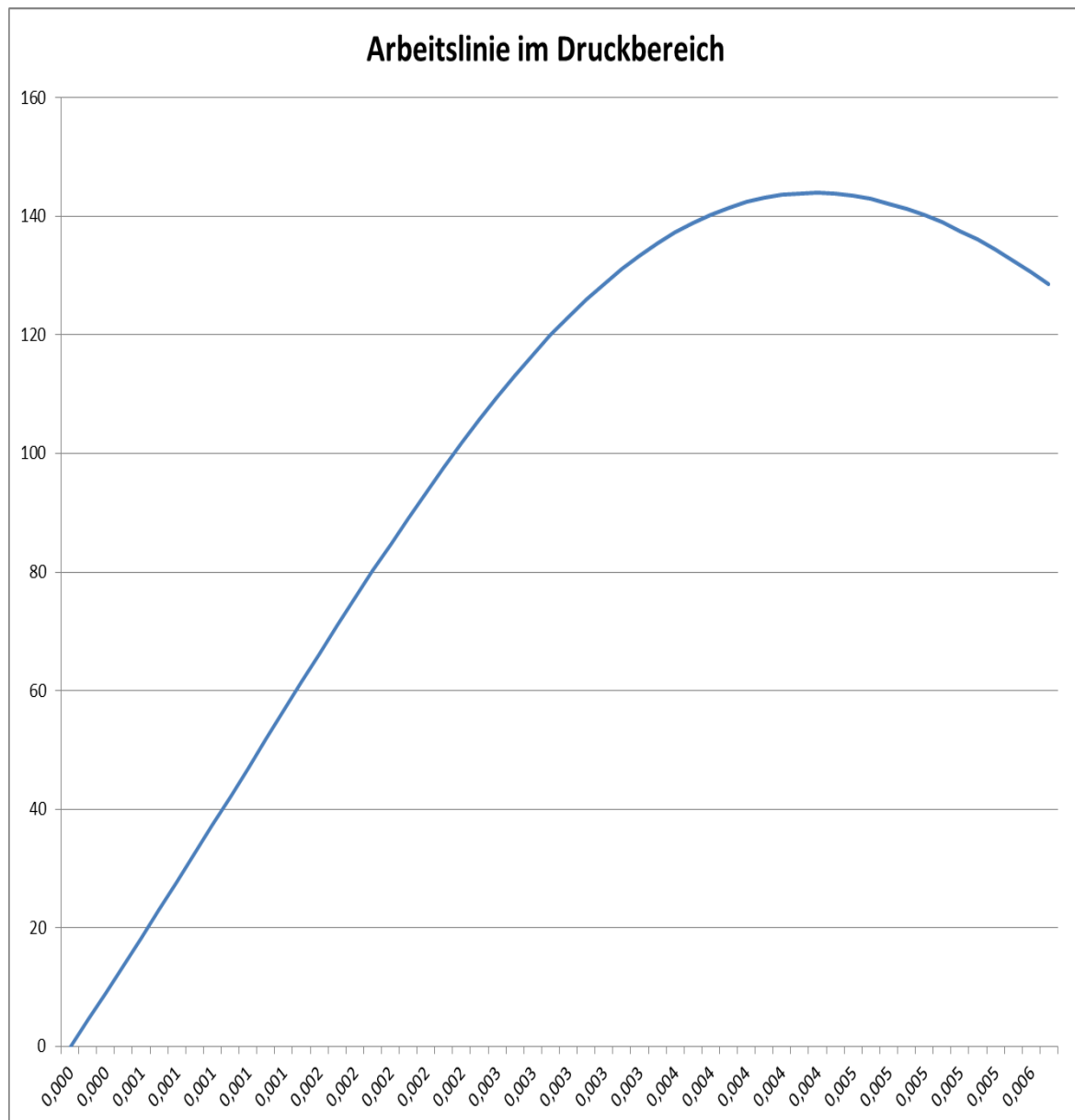


Figure 46 Working line in the printing area

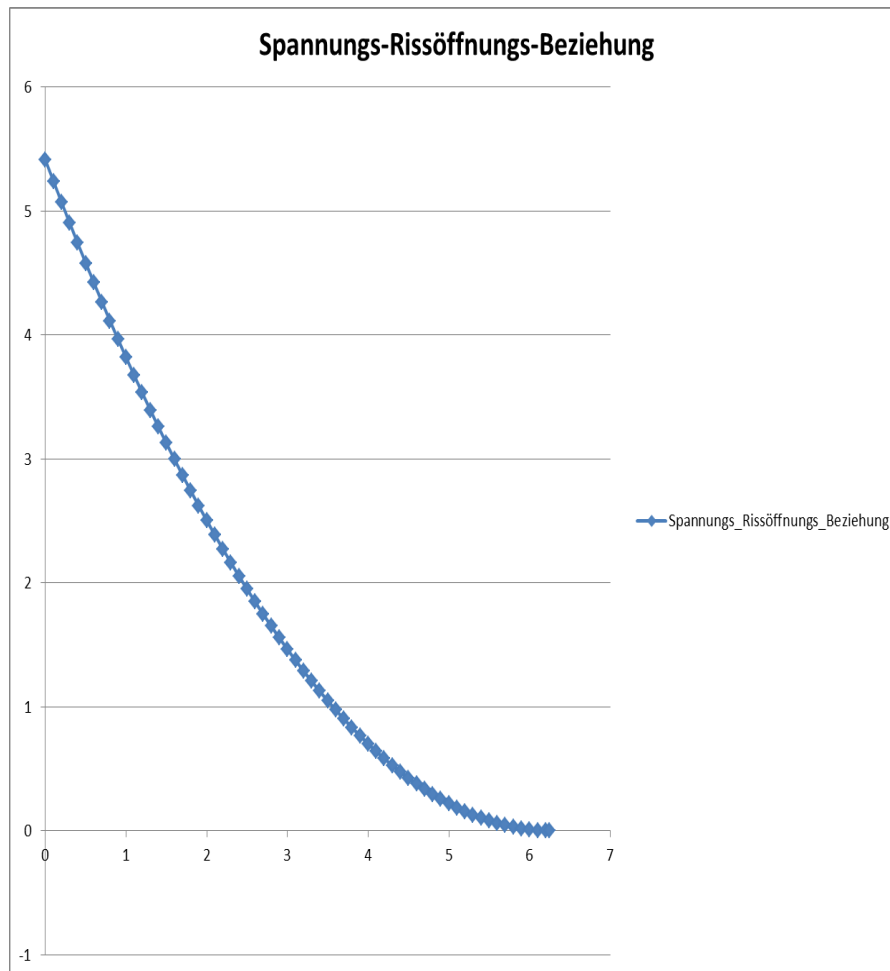


Figure 47 Stress-crack opening relationship

Inserting this on the Abaqus model, it is possible to define this kind of behavior. The other data inserted in the Abaqus input file are the following:

Material Behaviors

Density

Elastic

Concrete Damaged Plasticity

General Mechanical Thermal Electrical/Magnetic Other

Concrete Damaged Plasticity

Plasticity Compressive Behavior Tensile Behavior

☐ Use temperature-dependent data

Number of field variables: 0

Data

	Dilation Angle	Eccentricity	f_b/f_c	K	Viscosity Parameter
1	30	0.1	1.16	0.667	0

Figure 48 Parameters for Concrete Damaged Plasticity

3.1.2 Element

Another common feature is the element type used in the mesh of the model: the element type used in this case is C3D8I. In fact, there are not difference between the results obtained with this element and the ones obtained with C3D20R: and the latter require a far greater honor computing. In fact, the incompatible mode eight-node brick element is an improved version of the C3D8-element: in particular, shear locking is removed and volumetric locking is much reduced. This is obtained by supplementing the standard shape functions with so-called bubble functions, which have a zero value at all nodes and nonzero values in between. As reported in Abaqus guide, the C3D8I element should be used in all instances, in which linear elements are subject to bending. Giving a better explanation, it is plausible to say fully-integrated formulation (C3D8, CPS4, CPE4 & CAX4) and reduced integration formulation (C3D8R, CPS4R, CPE4R & CAX4R) are two different kinds of formulation in ABAQUS. The most important difference between these two typologies, is that the reduced integration elements use a lower order integration to form the element stiffness. In fact, comparing the fully-integrated formulation with the reduced formulation, it is possible to see that a first order fully integrated plane stress element will have four integration points as compared to first order reduced integration plane stress element with one integration point at the centroid of the element, taking less time to solve due to the reduced order of integration. The fundamental issue with these first order elements come up when used with pure bending or bending dominated problems, that is exactly the problem under investigation, in which there is a ratio between the bending moment and shear applied to the joint of $R = \frac{M_x}{V_y} \cong 10$. The fully integrated elements undergo excessively rigid behavior when the energy of the cut enters the element rather than bending it: this causes ‘shear locking’. Reduced integration elements on the other hand cannot detect strains at the center integration point due to bending, leading to the phenomena called ‘hour glassing’.

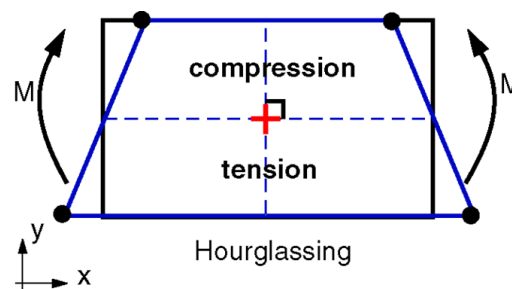


Figure 49 Hourglassing phenomena

Hour glassing effect can be significantly reduced by using more elements through the thickness experiencing bending load. A minimum of four reduced integration elements may be required to reduce hourglass effects. When using reduced integration elements, it is possible to evaluate how

much “hour glassing” happens with some energy results. However, Abaqus also offers ‘incompatible’ mode elements for the quadrilateral and hexahedral elements (C3D8I, CPS4I, CPE4I, CAX4I). These elements enhanced by incompatible model can capture bending more accurately with even one element through the thickness. These elements are fully integrated elements with added internal degrees of freedom (incompatible deformation modes) eliminating ‘parasitic shear stresses’ thereby eliminating the shear locking phenomena. They also remove artificial stiffening due to Poisson’s effect in bending. Since they are fully integrated, there is no question of hourglass effects. Hence, they can capture bending accurately. They can capture bending as accurately as second order elements, with reduced runtime. One of the significant disadvantages of using these elements is their shape. They tend to be less accurate with a parallelogram shape and poor if the elements have trapezoidal shape: the shape of the element needs to be near perfect. When it is possible, the first choice would be to use the reduced integration formulation and use at least four elements in the thickness. This is easier for 2D plane strain / plane stress and axisymmetric models since they are usually small. Since in the case under investigation it is not possible to use that many elements in the thickness, then the incompatible mode has been used. Summarizing, it is possible to state that the quality of the C3D8I element is far better than the C3D8 and C3D8R element, and even if the best results are usually obtained with quadratic elements (C3D20 and C3D20R), the choice to use these elements is a good compromise between the calculation time and the quality of the obtained result.

3.2 Global model of the bridge

According to preliminary studies, the bridge model has been designed as follow:

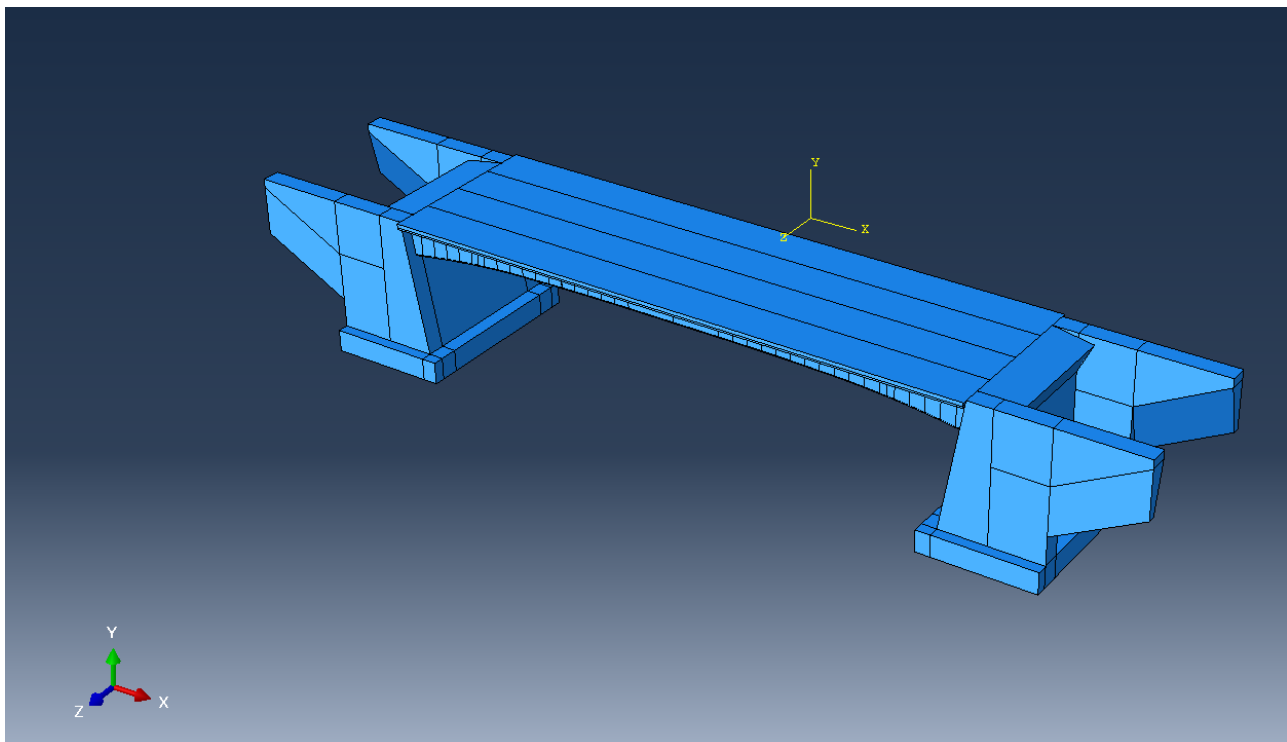


Figure 50 General and complete 3D model

The following simplifications have been done:

1. Perfect flatness of the span;
2. Perfect orthogonality of the girders regarding the abutments connections;

From the picture, it is important to notice that in the first place, the abutments were modelled. However, after that it was done another simplification in the first study approach: neglect the effect of the abutments on the bridge and use constraints on the ends of the span, in order to reduce the computational effort.

3.2.1 Model of only one girder

After the previous conclusion, the model of only one girder has been made:

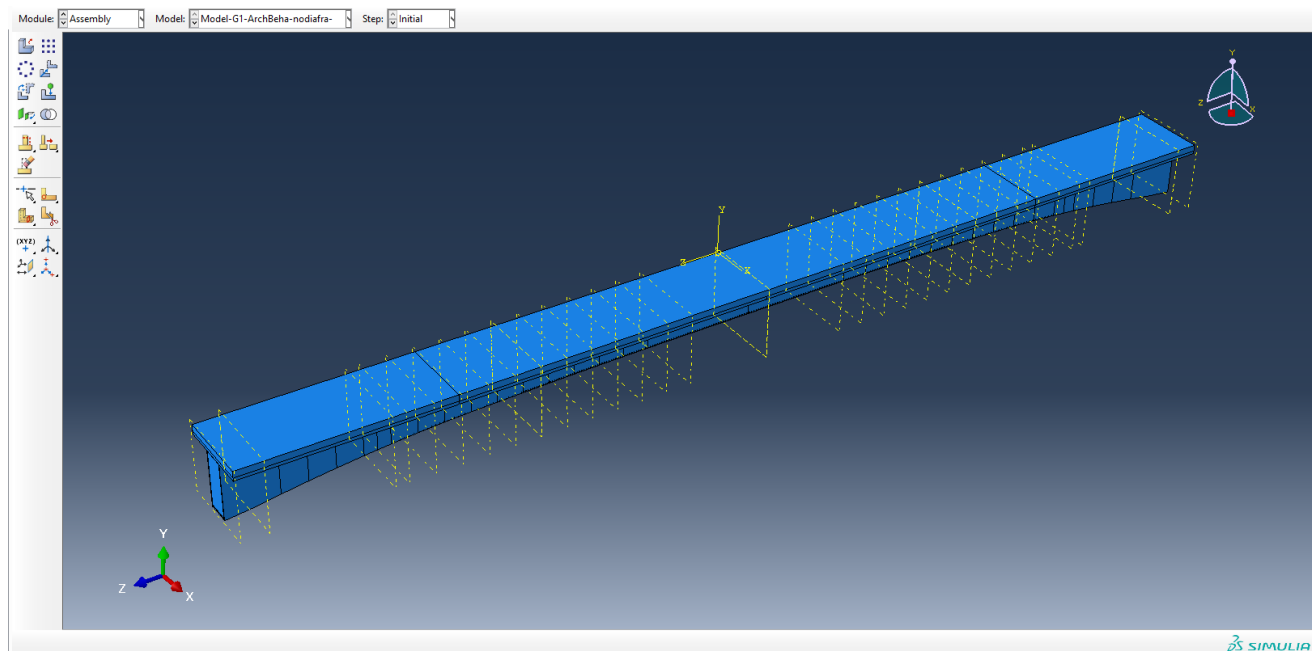


Figure 51 Only one of the four girders

The length of the span is 40419 mm and the steel section height varies from the initial one of 2200mm to 1150 mm in the middle section. This girder is modelled through the following steps: each of the components were modelled before in the module Part and after they are assembled all together in the assembly module. The beam has been split into some components due to the complex geometry of the span. Each element can be modeled as 3D deformable body and its geometry can be designed by selecting solid and extrusion. Agreeing upon that, the precast concrete slab and also the slab cast in situ are modelled as one single rectangle of dimensions 3000x120x40419 mm and 3000x250x40419 mm respectively. Instead, the box steel section is divided into 4 components: the top flange, the bottom flange and the lateral webs.

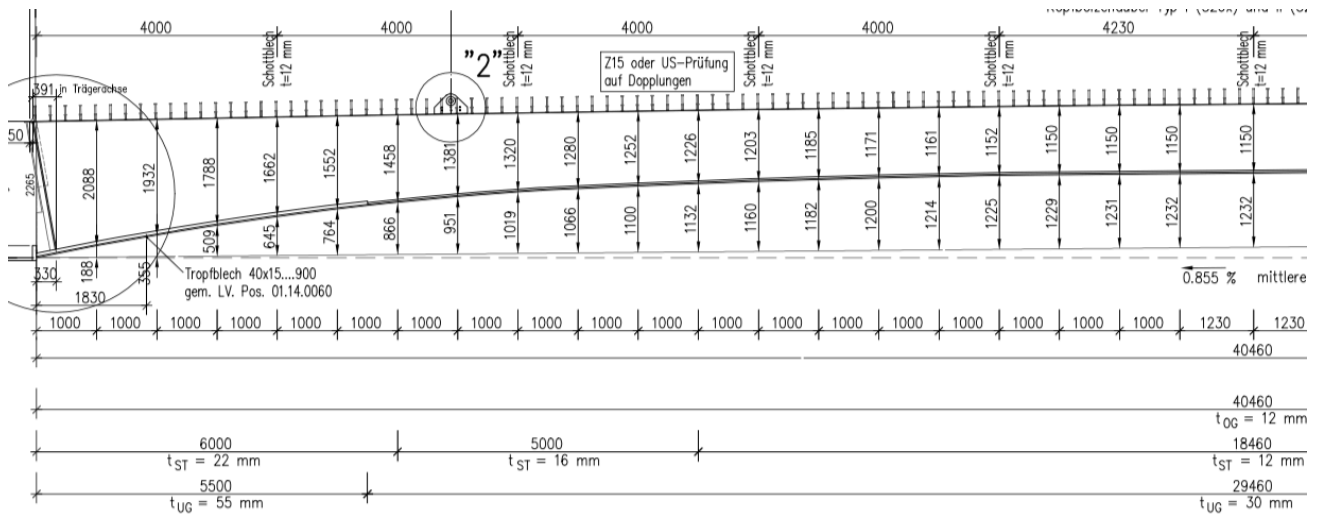


Figure 52 Half-span of the bridge

The top flange is modelled as a single rectangle of dimensions 900x12x40419 mm because its thickness and its transversal section are constant along the whole length. The side walls, instead, have been divided into three parts because they change the thickness three times:

- WebT22: it starts with a transverse section of 2188x22mm and it is extruded with a variable height for six meters where it ends with a transverse section of 1446x22mm;
- WebT16: it starts at six meters with a transverse section of 1446x16 mm and it is extruded with a variable height for 5 meters where it ends with a transverse section of 1214x16mm;
- WebT12: it starts at 11 meters with a transverse section of 1214x12 mm and it is extruded with a variable height until the middle section where it ends with a transverse section of 1138x12mm;

In fact, it has been modelled using the module Part, only half-span of the bridge due to symmetry reasons: these elements in fact are copied and mirrored in the assembly module in order to create the correct shape of the span. For the same reasons, the bottom flange has been portioned in 4 parts:

- Bottomflange1: it is modelled as a rectangle of 856x55 mm with linear inclination until 5.5 meters and it ends with the same transverse section with a horizontal gap of 695mm;
- Bottomflange2: it starts at 5.5m and it is modelled as a rectangle of 856x30mm with linear inclination until 6 meters and it ends with the same transverse section with a horizontal gap of 47mm;
- Bottomflange3: it starts at 6m and it is modelled as a rectangle of 868x30mm with linear inclination until 11 meters and it ends with the same transverse section with a horizontal gap of 232mm;

- Bottomflange4: it starts at 11m and it is modelled as a rectangle of 876x30mm with linear inclination until the middle section where it ends with the same transverse section with a horizontal gap of 76mm;

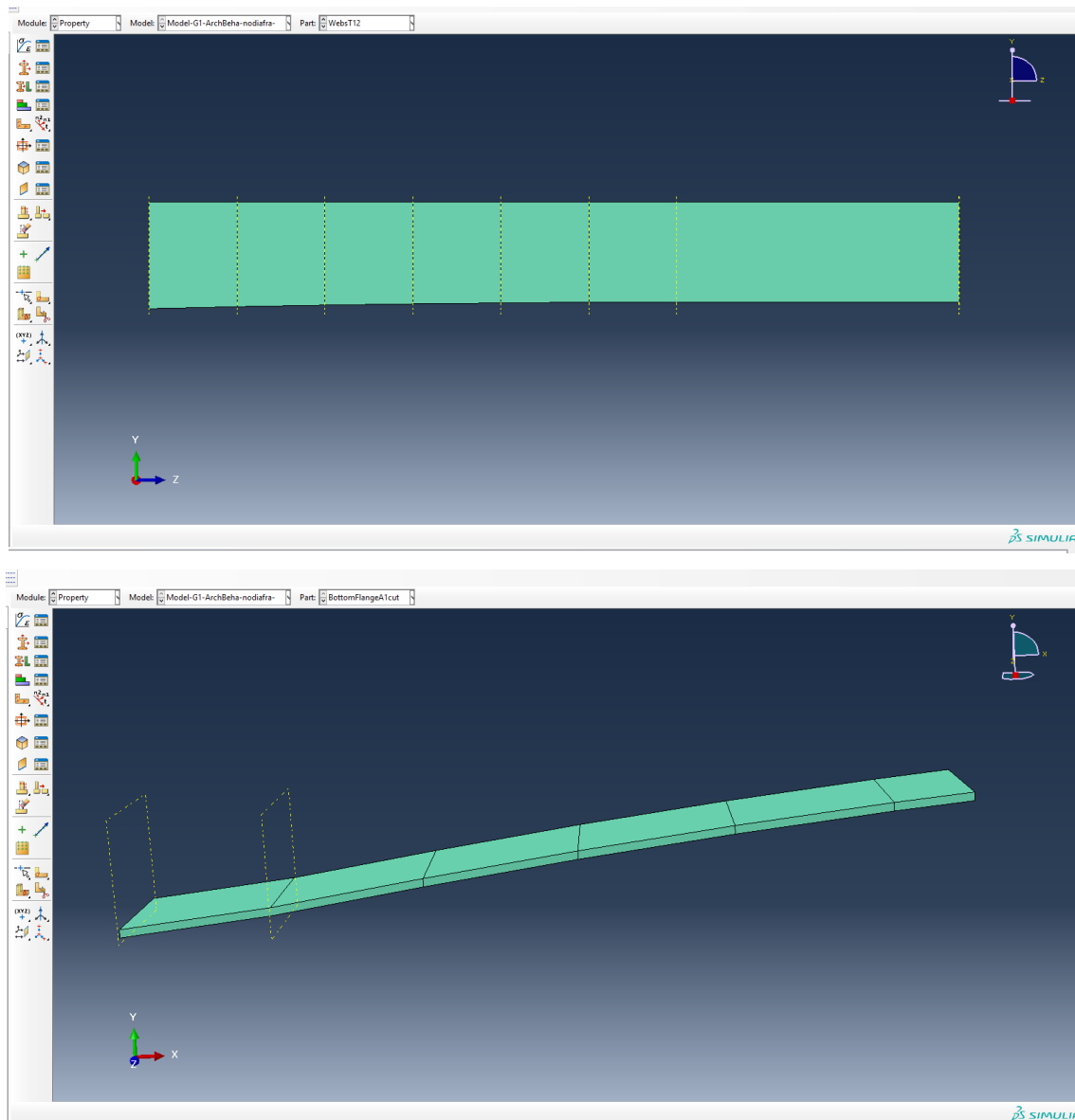


Figure 53 some components in details: the bottom flange of the bridge and the lateral side

The subsequent step is that to put all the element together in the assemble module, creating the entire girder. The problem related to the fragmentation of the section, is to understand how the whole girder behaves, in order to know if the section is working as it should. To connect the different elements a huge number of Tie constraints have been created one for each contact surfaces between different parts. Doing some test models, it was clarified that with the use of these type of connections, the section behaves as expected and in those models the results obtained are almost identical to those got by hand calculation. This is the reason, why ties constraints are used everywhere along the whole span. But before introducing the constraints it is better to figure out the best mesh for each single

element, thinking about what are the interest points in which using finer mesh and what will be the areas that contain the master surfaces in order to have a coarse mesh in it. The rules imposed by the program's guide are respected and thus reliable results are obtained. The choice of the 'Seed length' is important; clicking on Assign Mesh Controls, the mesh is applied to selected bodies.

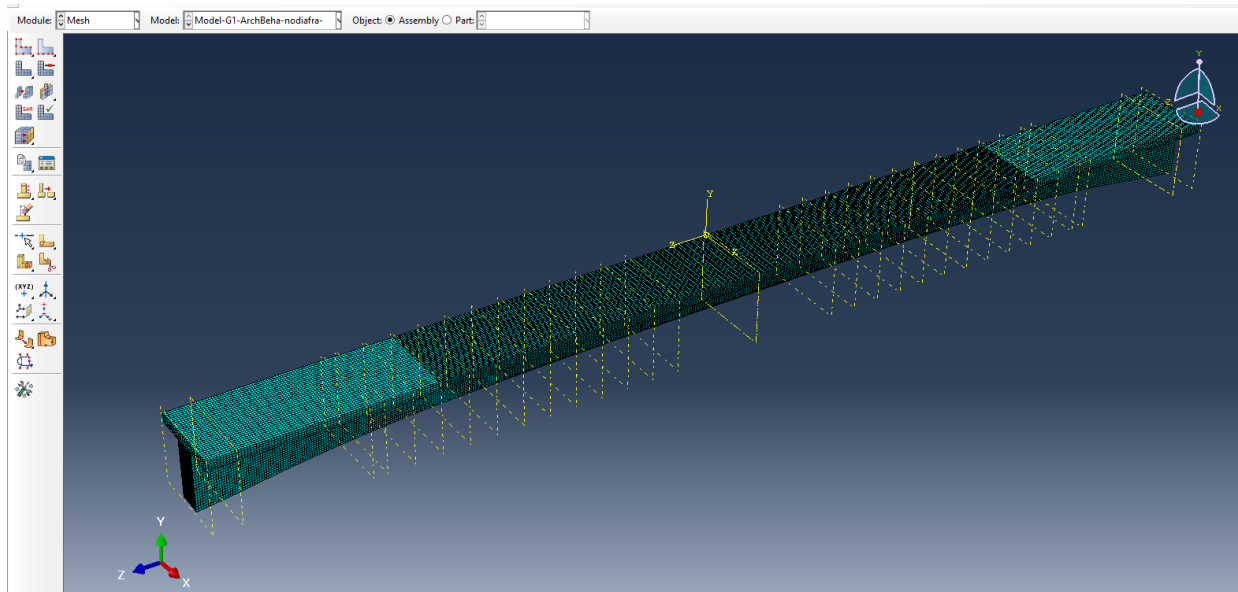


Figure 54 Girder with the final mesh

As visible in this picture, a finer mesh is chosen for the middle part of the span. By default, the type of the elements, using in the solver process is linear, 8-node continuum elements C3D8, in which C means continuum element, 3D means space model and 8 means 8 nodes. But as said in the chapter 3.1.1 the element used everywhere is C3D8I. As requested by Abaqus, the next move is the creation of the different analysis step: the initial step, Phase1, Phase2, Phase3 and Phase4. The initial one is unavoidable and it is used to apply the initial boundary conditions. The phase1, according to constructive staged of the bridge, allows the box steel and the precast slab to be analysed under their own dead load in the simply supported scheme. In the phase 2 the dead load due to the slab cast in situ at the boundaries is added; in the phase 3 there is the change of the static scheme and the introduction of the last part of the slab cast in situ. In the phase 4 there is the definitively change of the reagent section in the entire bridge. These steps are created in order to simulate in the correct way the real process of the building in construction site; each of them has its own loads, boundary conditions and interactions. Special attention is put on the concrete cast in situ: Abaqus in fact, does not allow to introduce a part in a subsequent step. All the parts should be added at the beginning and only after the introduction of the initial BCs, they could be removed or modified. In this case, the presence of this slab should be modelled only after the third phase and it is used the 'Model change' command, deactivated this part since the beginning.

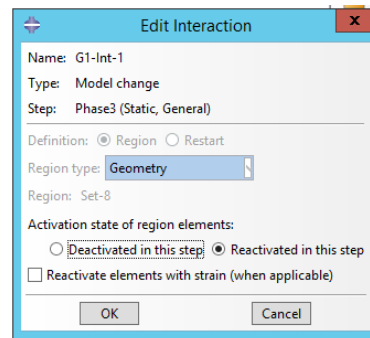


Figure 55 Model change command

The reintroduction of it, in the right step is done by the command ‘Reactivation of the element’ and ‘reactivated stress and strain free’. In this way, it is possible to obtain the expected behaviour of the structure: the bridge behaves with the first transverse section, composed by steel box and precast concrete in the phase1 and phase2, and after that there is a change in the reagent cross section. In the initial step, boundary conditions are defined in two different ways, in order to compare the two different expected behaviours: Beam Behaviour and Arch Behaviour. The first one is modelled imposing zero displacement $U_1 = 0$ and $U_2 = 0$ in the entire boundary cross sections, and leaving free the horizontal translation U_3 and rotations UR_1 UR_2 UR_3 . The second one is modelled imposing zero displacement $U_1 = 0$ and $U_2 = 0$ and $U_3 = 0$ in the bottom line of one of the two boundary sections and imposing $U_1 = 0$ and $U_2 = 0$ on the other side, leaving free rotations UR_1 UR_2 UR_3 everywhere. These displacements are still valid in the initial step and in the Phase1 and 2: in the phase 3, as said above, there is the change of static scheme through the application of the following BCs:

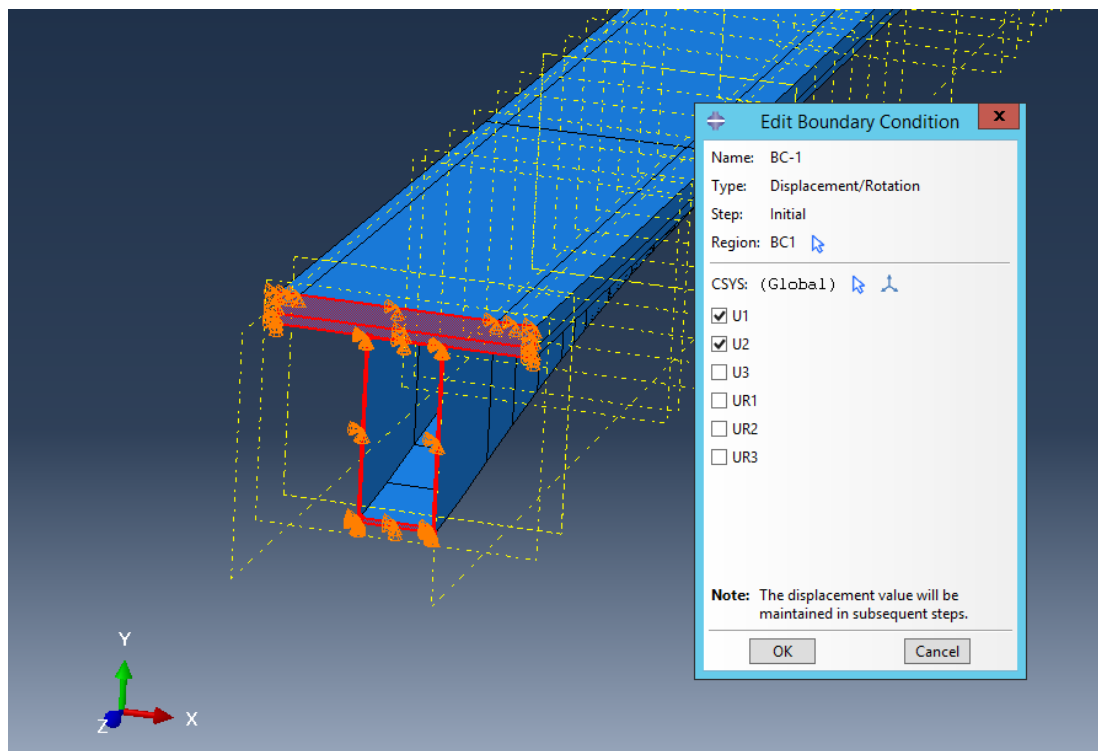


Figure 56 Boundary conditions on both sides: Beam behavior simulation

Although Encastre constrains all 6 degrees of freedom, three displacements and three rotations, in 3D case, it is necessary to remove just the three displacements: the reason is that the mesh will be formed by 8-node spatial continuum elements C3D8 and they have only three translations degrees of freedom. The last thing to do is to apply the load conditions: the external forces and other kinds of loads can only be entered in the user defined steps, for example in the phase1 which have defined previously. In the Initial step, only kinematic boundary conditions and interactions can be activated. Now the model of the girder 1 is ready to start the calculation: parameters of the calculation are specified in the module Job, select Create Job and name one job as “Girder1-BeamBehaviour” and another one “Girder1-ArchBehaviour”.

3.2.2 Model of the entire deck

Once the single girder has been processed and analysed, the whole model has been created. Through the prompt ‘linear pattern’ the others three girders are created, simply by copying the already modelled beam linearly, without any space between the two slabs of each girders that are in full contact and work together.

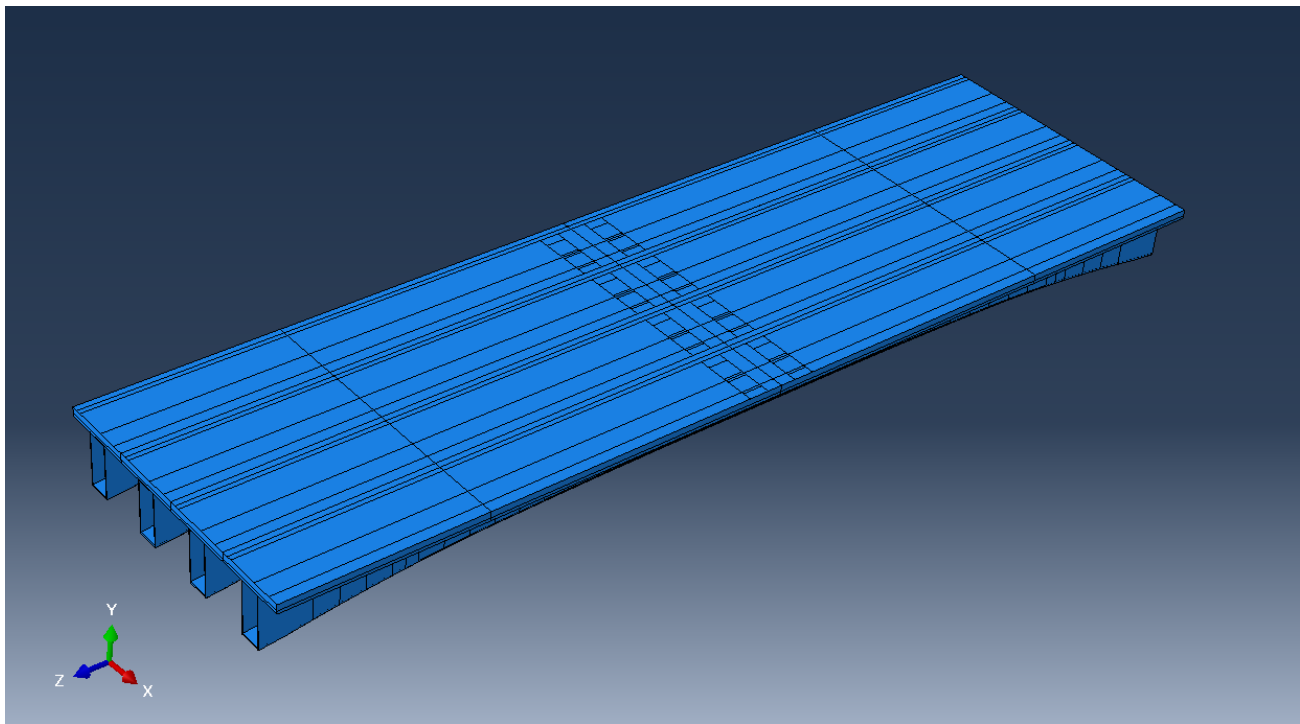


Figure 57 The whole deck

In the design of the whole bridge it is important to use the same procedure used for the construction of the first girder, in order to respect all the requirements introduced before. Of course, the parts and the properties are completely the same of the single girder, and so the assembly and the mesh as described above.

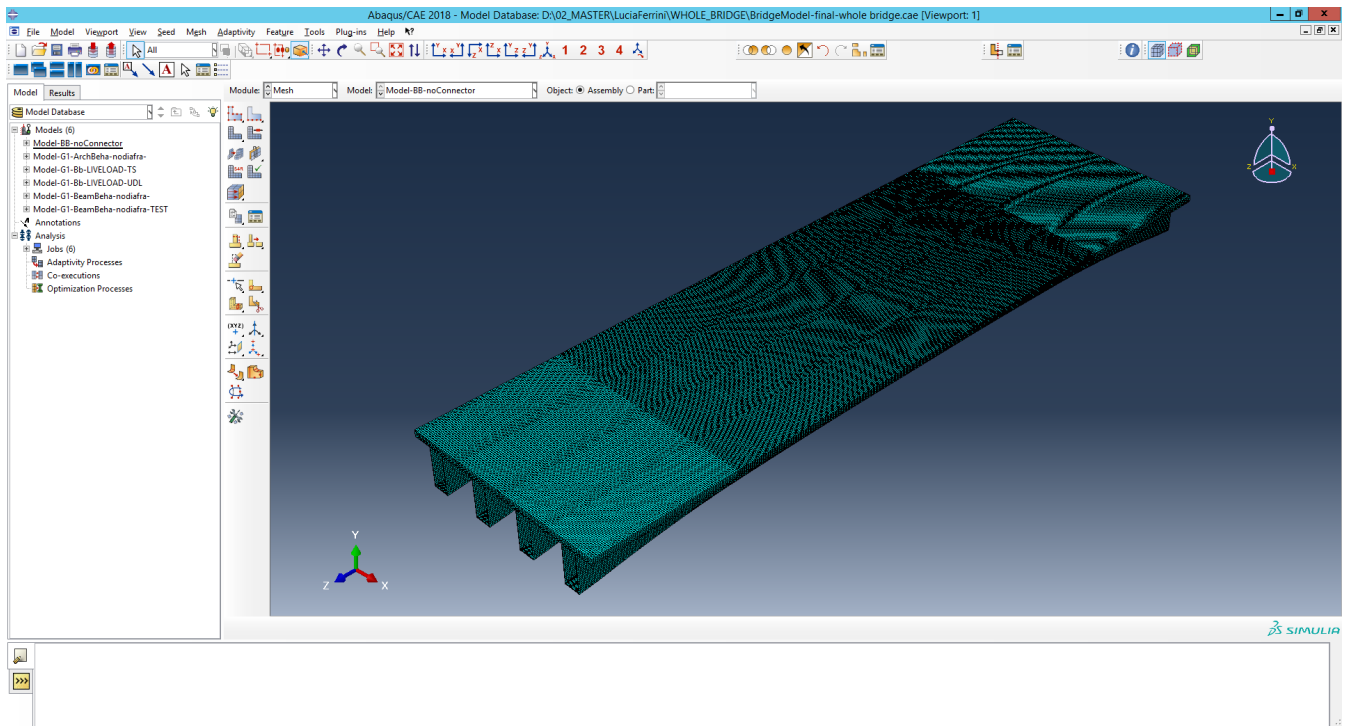


Figure 58 the global mesh of the 3D model

The final element type is always the C3D8I. The analyses steps are completely the same:

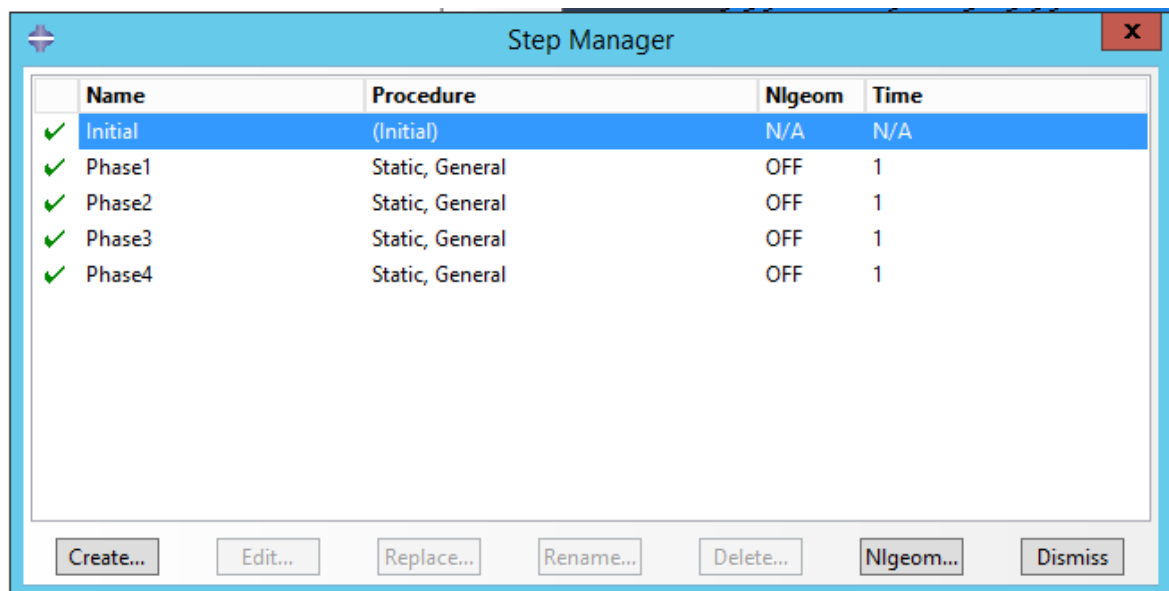


Figure 59 List of analysis steps

The interaction between the surfaces of the slabs of the girders in contact has to be modelled and taken into account: in this way, it is possible to create the collaboration between each slab, as shown in the picture 57. The picture 58, instead, it represents all the interaction ‘Model Change’ used for each girder.

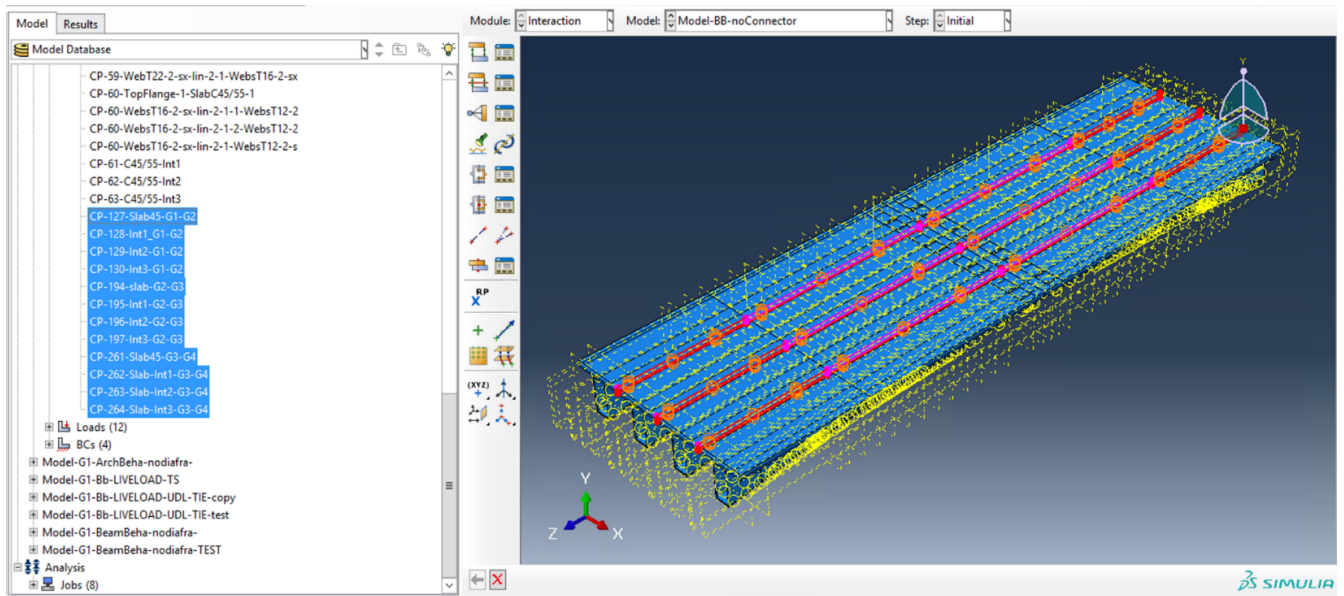


Figure 60 Constraint between the Girders

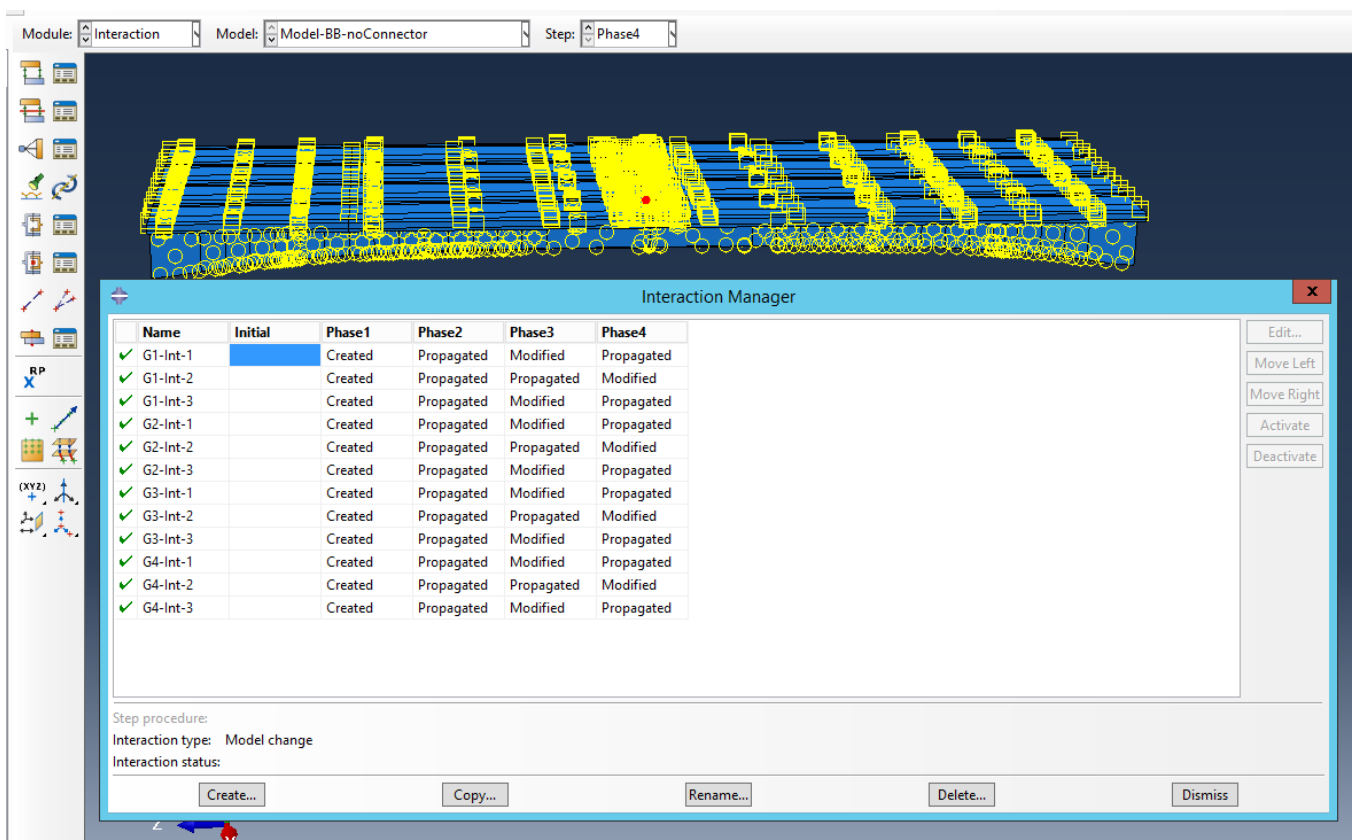


Figure 61 Model change in the entire bridge

All the four girders are working together and the distributed loads due to the substructure can be now inserted on the top surface. In fact, assign the loads and the boundary conditions is the next thing to do in the modelling.

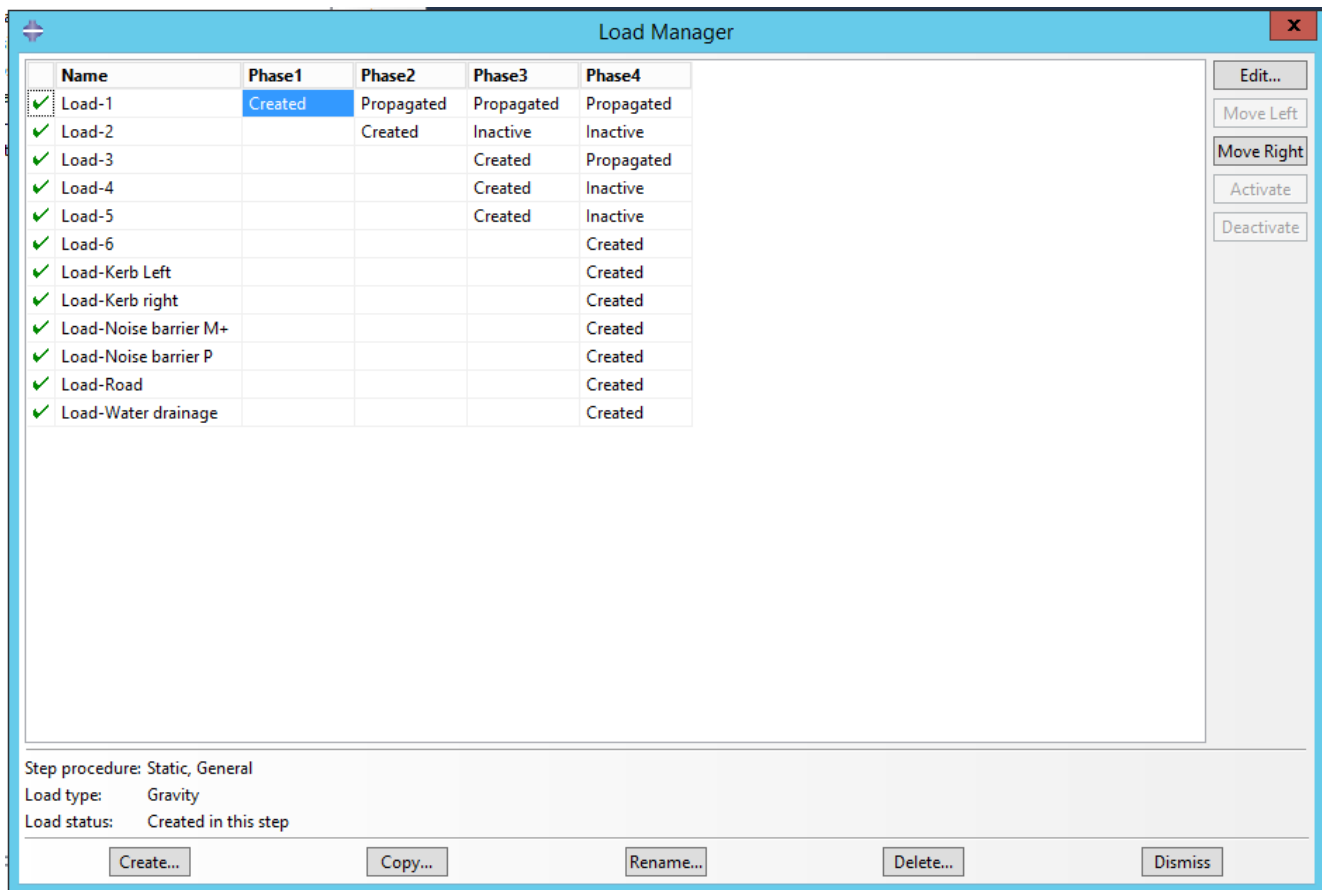


Figure 62 Description and list of applied loads

The boundary conditions adopted in this model are the same: there are two types of behavior that we want to describe and study. In the next picture, the beam behavior is taken into account.

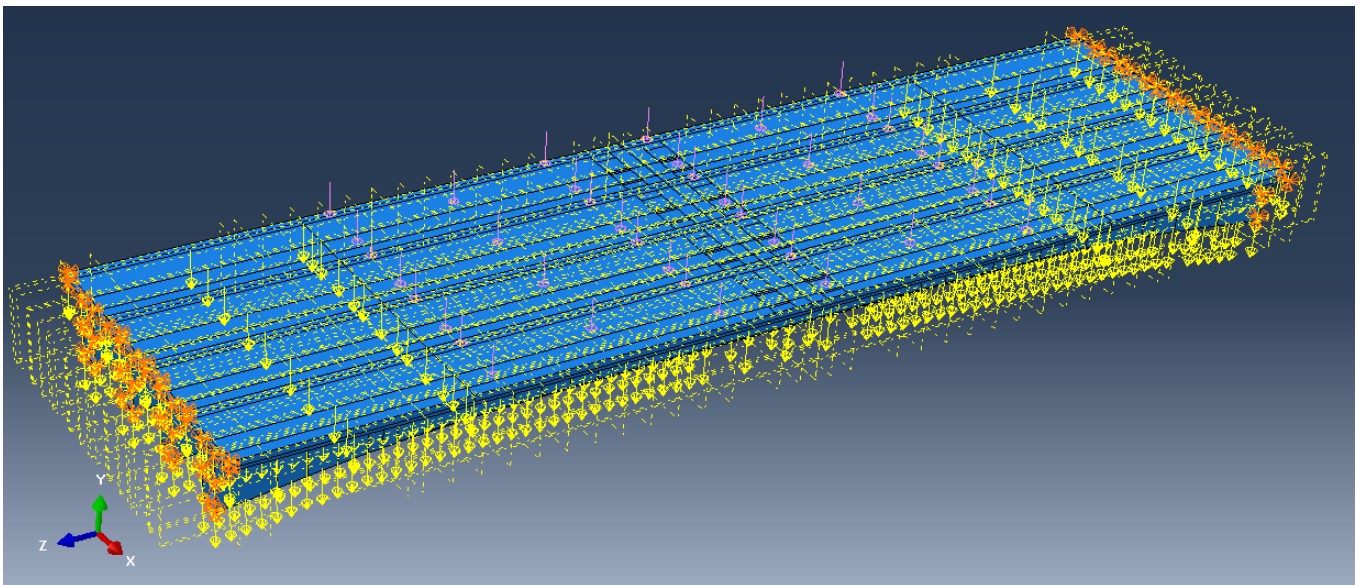


Figure 63 the entire and loaded bridge

The following two figures, instead, represent the changing of the reagent section during the different analyses constructive stages:

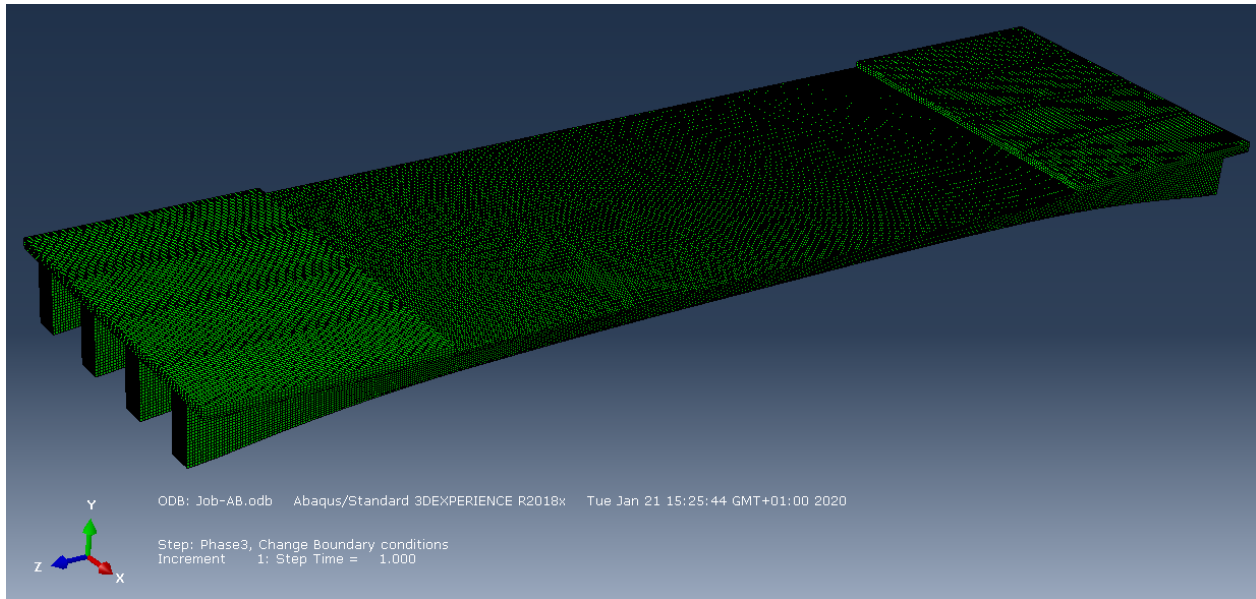


Figure 64 Reagent section in the first and in the second phase

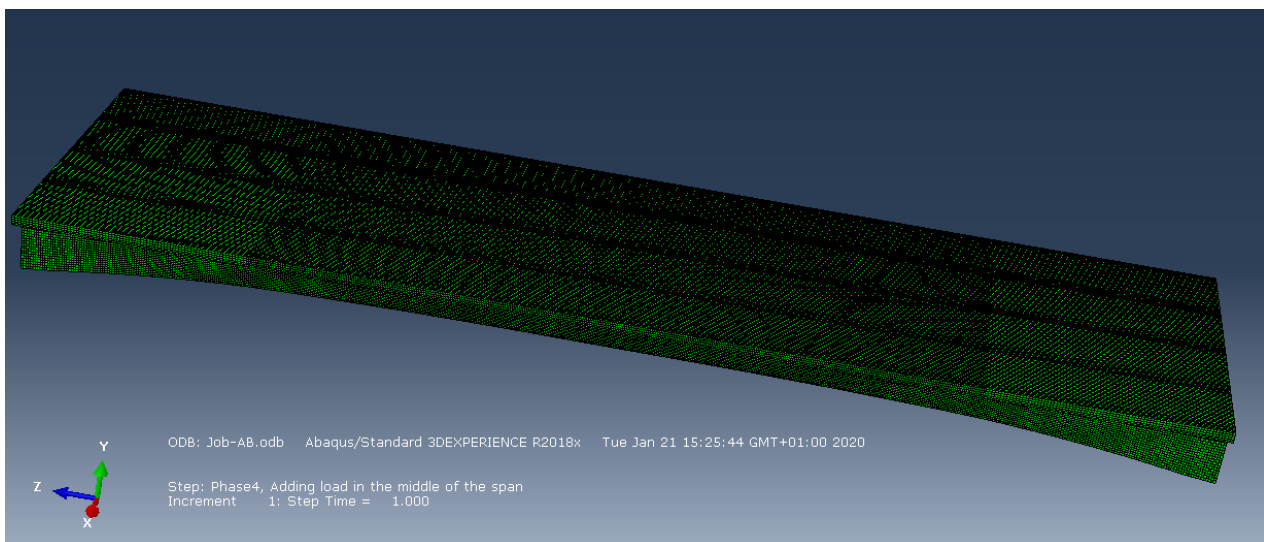


Figure 65 Reagent section in the third phase and on

The results obtained are post-processed in the following chapter, ‘Results’.

3.2.3 Model of the entire deck with the effect of the abutments

After the first model, it is necessary to move on and add some details to describe in the best way the influence of the abutments. In fact, the decision to take them off it is only to have a simplest and faster resolution, but their effect must be taken into account. According to a previous study on Sofistik, the behavior of the abutments on the deck can be simulated by the introduction of three springs of equivalent stiffness. This stiffness has been calculated on Sofistik model in the following way:

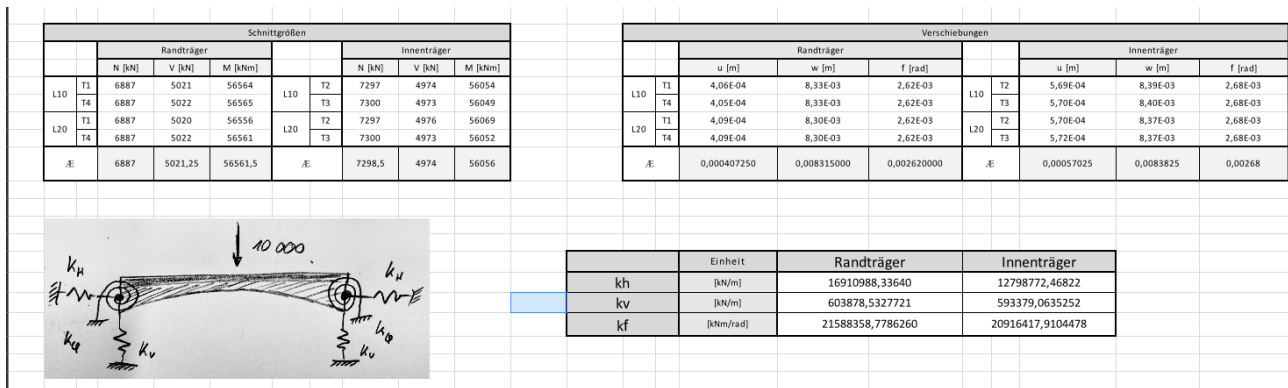


Figure 66 Definition of the equivalent stiffness of the spring

This model is the same of the one studied before, just with some modifications on the boundaries. In fact, eight reference points have been introduced: each of them is in the barycenter of the border section of each girder on both sides.

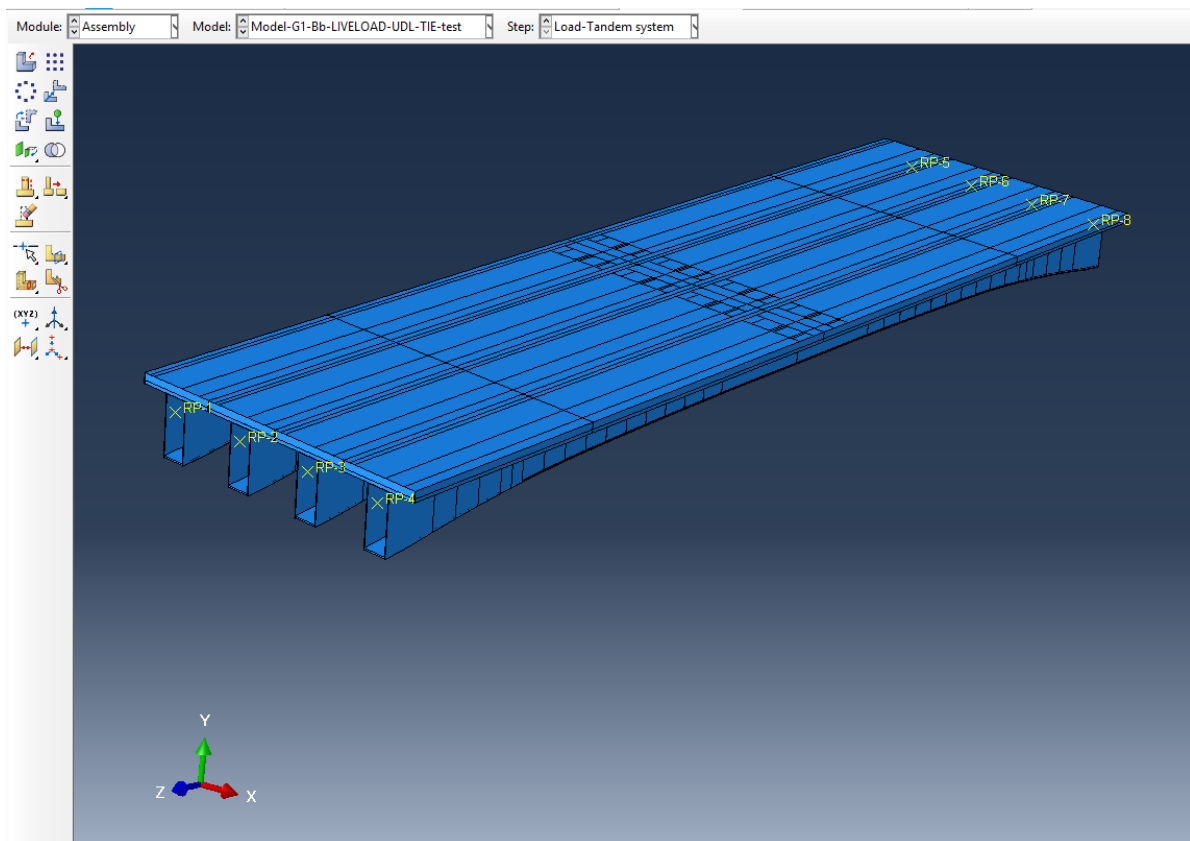


Figure 67 Reference points

These reference points are connected to the entire border section of each girders through the use of coupling kinematic connection:

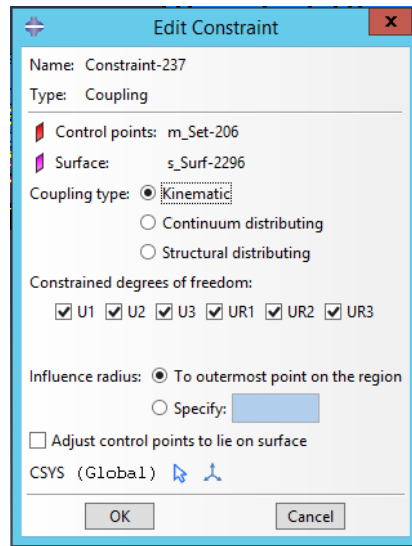


Figure 68 Kinematic constraint

To consider the abutments effects, three springs are modelled in each reference point, with Abaqus command Special → Springs → Connected points to the ground (Standard). 24 springs have been created according to the studies on Sofistik: there are two different set of springs, for the central girders and for the external ones.

Equivalent stiffness for the external girders:

$$K_H = 1.6911E + 07 \frac{N}{mm^2} \text{ d.o.f } U_3$$

$$K_V = 603879 \frac{N}{mm^2 d} \text{ o.f } U_2$$

$$K_R = 2.15884E + 13 \frac{N}{mm^2 mm} \text{ d.o.f } UR_1$$

Equivalent stiffness for the internal girders:

$$K_H = 1.27988E + 07 \frac{N}{mm^2 d} \text{ d.o.f } U_3$$

$$K_V = 593379 \frac{N}{mm^2 d} \text{ o.f } U_2$$

$$K_R = 2.09164E + 13 \frac{N}{mm^2 mm} \text{ d.o.f } UR_1$$

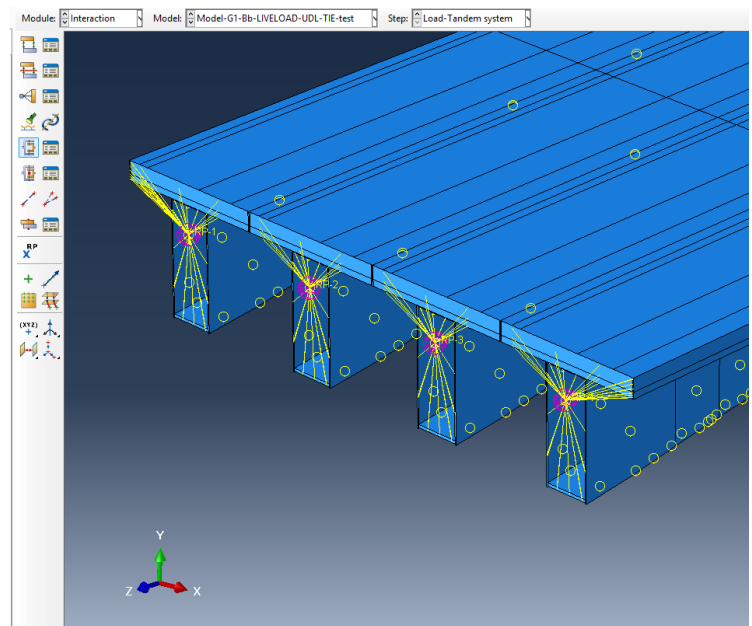


Figure 69 springs on reference points

The important thing, once the model has been created, is to add the traffic load, according to the Euro code explained before. To simply again the computational afford, it is considered only the worst load combinations. It is done by the uniform distributed load of 9 kN/m² on the first lane and the uniform distributed load of 3 kN/m² on the second lane and the uniform distributed load of 3 kN/m² everywhere. For the tandem load, the worst combination is when it is exactly in the middle of the girders. The tandem load is not considered as a concentrated force but as surface loads in the following way:

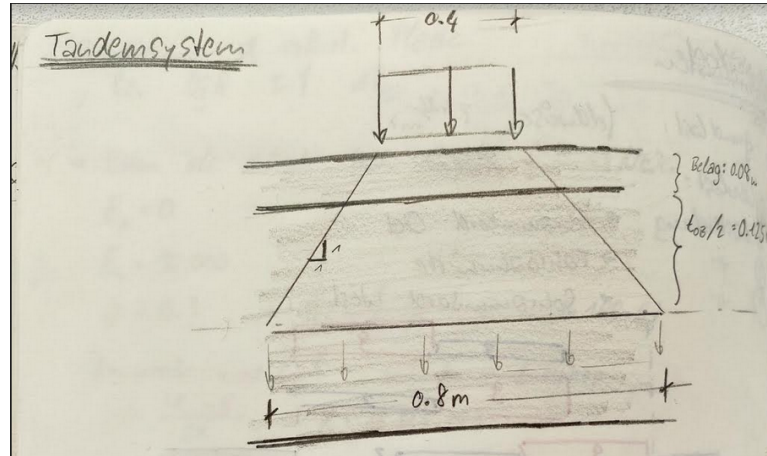


Figure 70 Diffusion of the tandem load

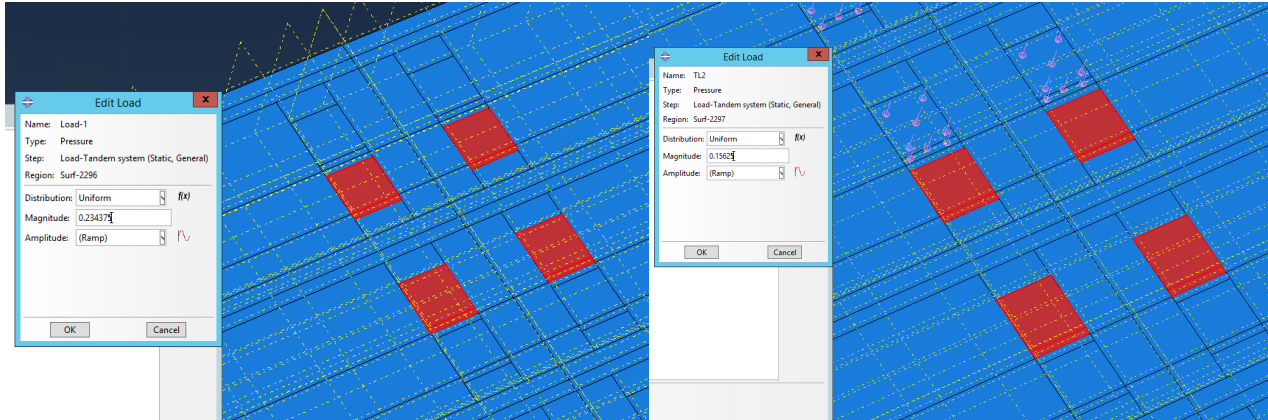


Figure 71 Tandem load

The values of the pressure loads are:

$$P_1 = \frac{600}{4} * \frac{1}{0.80^2} = 0.234375 \text{ MPa}$$

$$P_2 = \frac{400}{4} * \frac{1}{80^2} = 0.15625 \text{ MPa}$$

3.3 Simplified model and interaction between steel and concrete parts

Before starting the modelling of the entire joint, a smallest model of only the concrete and the T-stubs was done, in order to understand the general behaviour of the joint and to investigate the suitable interaction properties between steel and concrete parts. The geometry of the elements is chosen indicatively close to the one of the first approach, in order to respect the size of the problem.

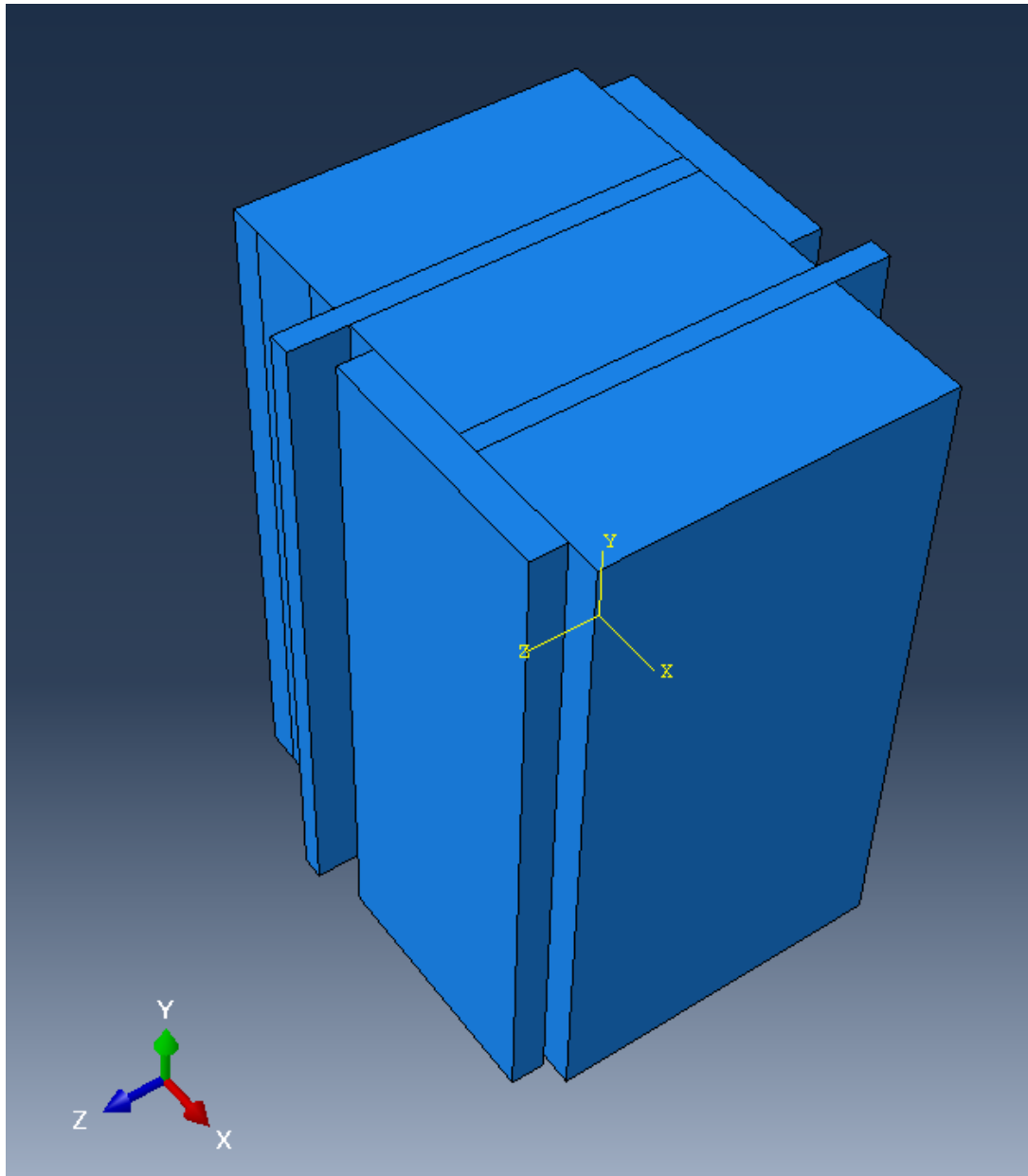


Figure 72 Simplified model

The most important thing to investigate thanks to this model are the interactions: generally, it is possible to say that three different contact types should be modelled in this joint. The first is the contact between T-stubs and concrete, the second one is the contact between the T-flange and the bottom flange of the bridge and at the end all the others contact. The last contact includes all those surfaces that in reality, will be welded to each other; the second and the third interactions are not

included in the simplified model: the focus is on the connection between T-stud and concrete. The simplified model allows a deeper investigation on the interaction between concrete and steel. Studying the concrete behavior, the load applied is a pressure load on both the T-web sides in the opposite directions. To respect the behavior of the all joint, the follow boundaries conditions have been applied:

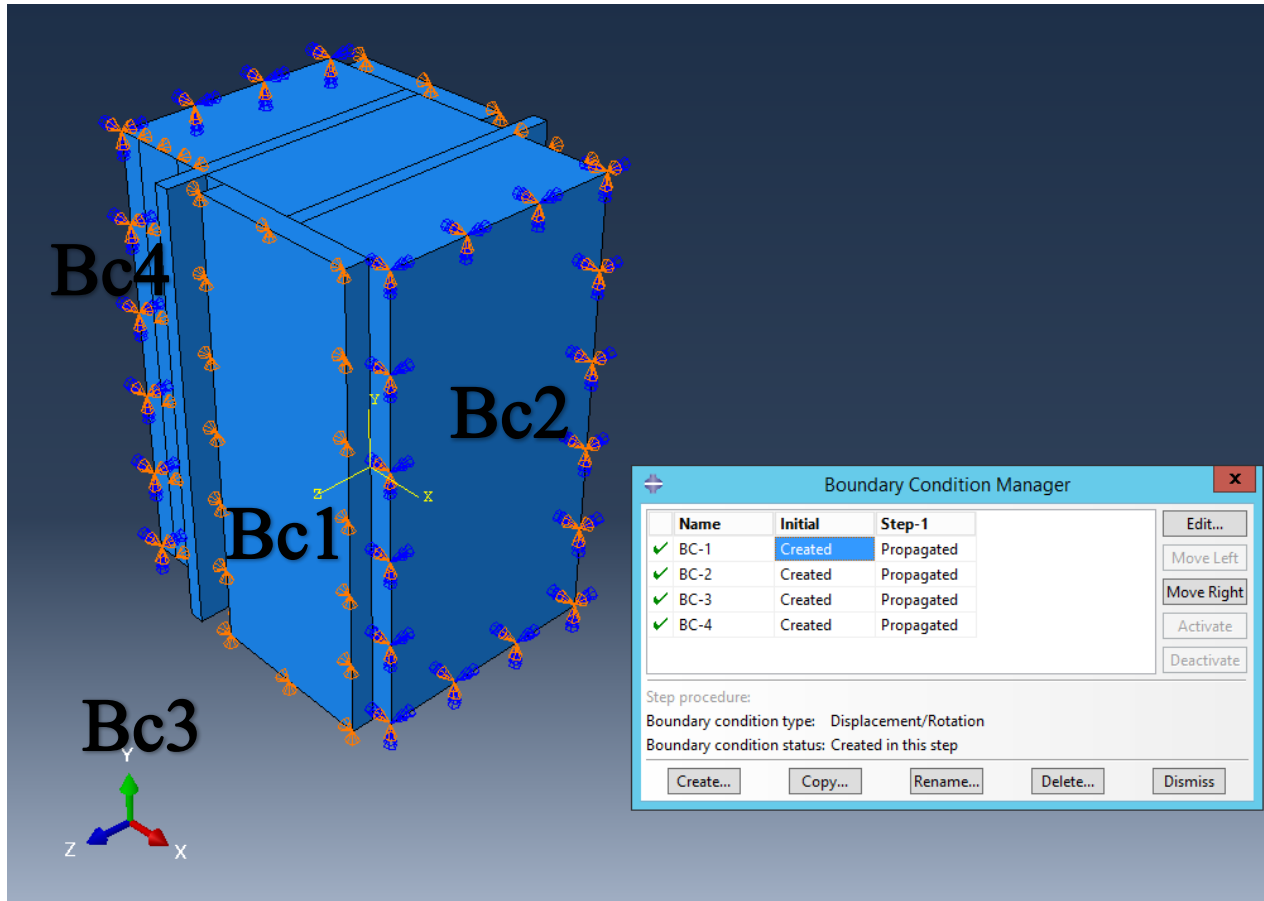


Figure 73 Boundary conditions

There are four types of boundary conditions:

BC1: it is applied on both the external surfaces of the T-flanges and it includes $U_1 = U_2 = 0$

BC2: it is applied on the concrete lateral sides and it is $U_1 = U_2 = UR_1 = UR_2 = UR_3 = 0$

BC3: it is applied on the concrete bottom surface and it is $U_2 = 0$

BC4: it is applied on the concrete transversal sides and it is $U_3 = 0$

At the beginning, it is possible to define the main properties that these connections should have: the contact between the concrete and the T-flange should be modelled in order to be activated only in case of compression and deactivated when some tension field grows. Defining the interaction, the choice of a tracking approach that will be used, will have a considerable impact on how contact surfaces interact. In Abaqus/Standard there are two tracking approaches to account for the relative motion of two interacting surfaces in mechanical contact simulations:

- finite sliding, which is the most general and allows any arbitrary motion of the surfaces;
- small sliding, which assumes that although two bodies may undergo large motions, there will be relatively little sliding of one surface along the other;

According to Abaqus guide it is possible to analyze which are the most plausible options available.

A contact can be defined by mechanical properties, and in this case the most important are:

- Tangential behavior;
- Normal behavior;

Tangential behavior: Abaqus allows to define some different tangential interactions. The common way to proceed, is starting with Frictionless property. In fact, it means to choose the absence of shear force transmission, it is the easiest kind of interaction and it allows the program to study the connection without taking into account transversal interaction. It could be a good starting point, despite admitting an approximation that must be checked carefully. Doing a little more detailed analysis, it is possible to use Penalty contact: it allows the friction coefficient between two surfaces to be taking into account. In this case, the tangential interaction between the two surfaces is considered and it depends on the chosen of the friction coefficient: $\mu \sim 0.2$ it could be a plausible value. The solution offered by this interaction, it can be very reliable. To achieve a good description of the tangential behavior, it is possible, at the end, to use the Shear stress limit property: it is an accurate solution but it may have higher computational efforts. In this case, shear stress τ_{max} can be imposed, for example as $\tau_{max} = \frac{f_{ck}}{\sqrt{3}}$ MPa.

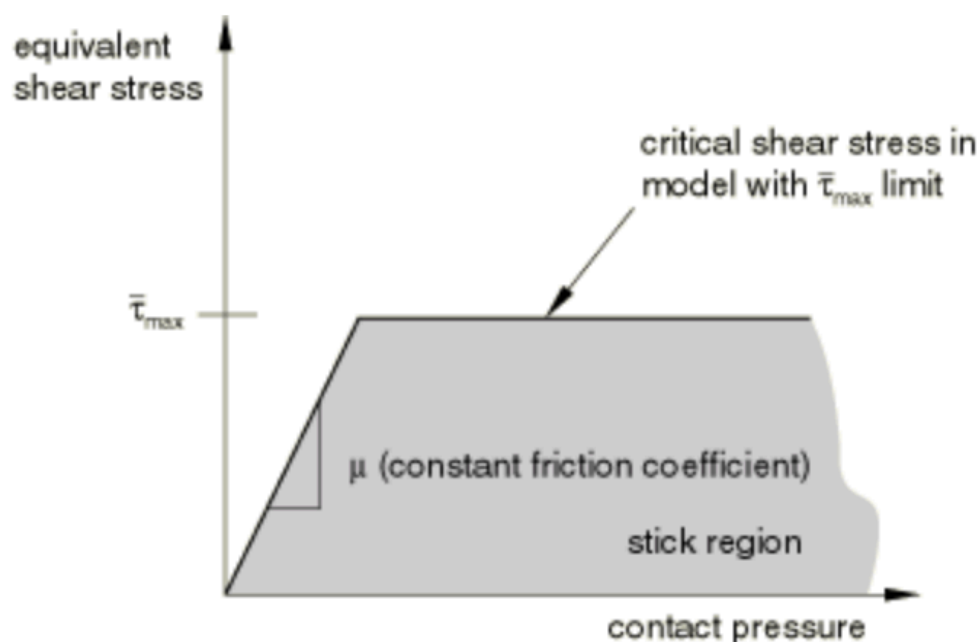


Figure 74 Shear stress limit

Normal behavior: it is possible to describe different normal contact, in such a way as to balance the computational cost and the precision sought in the results. The default one is Hard contact: the “hard” contact relationship minimizes the penetration of the slave surface into the master surface at the constraint locations and does not allow the transfer of tensile stress across the interface.

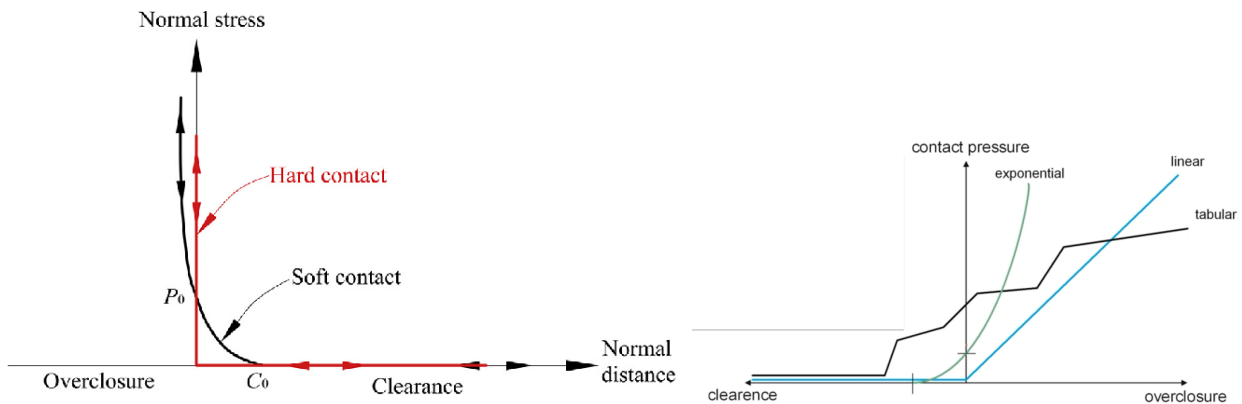


Figure 75 Description of the interaction between Clearance, Overclosure and Normal stress

Hard contact relationship can be assigned to pressure-overclosure with linear penalty method for surface behavior, exponential or tabular equation. Hence, surfaces will not be able to penetrate each other whereas separation is allowed when the contact pressure between them is tensile. Hard contact default is more accurate but the numerical solution could require a huge computational effort. On the other side, the soft contact formulation is useful since contact conditions are easier to fulfill from numerical point of view but it is less accurate, of course. Summing up, the constraint enforcement method could be described as follows:

1. Direct:

- Strictly fulfills the defined constraint;
- Struggles with over constraint problems;
- Hard and soft formulations;

2. Penalty:

- Uses penalty parameters;
- Hard formulation only;
- Penetration will occur for hard contact;

3. Augmented Lagrange:

- Combination of the methods stated above;
- Accurate and efficient;
- Hard formulation only;

These types of interactions must be studied carefully, analyzing the results and comparing it with some hand calculation to understand if they are plausible and if they produce more or less reliable results. Some models have been made, changing the interaction properties of the contact between concrete and steel. The models are described below, in a simplified way:

SM1:

Tangential behavior: Frictionless;

Normal behavior: Hard contact → Augmented Lagrange;

SM2:

Tangential behavior: Penalty, $\mu = 0.2$;

Normal behavior: Hard contact → Augmented Lagrange;

SM3:

Tangential behavior: Frictionless;

Normal behavior: Hard contact → Default;

SM4:

Tangential behavior: Frictionless;

Normal behavior: Linear → contact stiffness= 10^5

These four models are loaded with only the pressure load in the longitudinal direction, to simulate the traction inducted in the T-web by the total bending moment, and doing the hypothesis of uniform distributed pressure along the whole T-web section. After these models, another two simplified models have been created, to investigate the effect of the shear force on the entire system: the geometry of these models is the same of the previous one; the differences are in the boundary conditions and in the load applied.

3.4 Basic model for the parameter studies

After the introduction of the parametric relations between all geometric sizes introduced in the chapter 1.2.1, it is possible to create, definitely, a parametric model of the joint.

3.4.1 Geometry of steel parts

The joint has been model in the following way: all the parts, described in the previous chapter, have been created in the module part of Abaqus and the material properties have been assigned to each element. Each of the single part of the joint is developed in a parametric way, in order to obtain the best geometry with an optimization program maybe.

```
# FIXED PARAMETERS of the joint
Btot = 876
Sw = 30.0
tw = 20.0
Lj = 300.0
ts = 20.0
C = 20.0
tf = 30.0
Ls = 750.0
Gap = 5.0
hw=0.5*Havaiable
```

```
# PARAMETERS related to the bridge
h11 = 1226-12
h12 = 1203-12
h13 = 1185-12
Delta1213= 18
alfa1= 1.3175 # angle calculated between 11 and 12meters
alfa2=1.0312 # angle calculated between 12 and 13 meters
alfamedio = 1.174398985 # halfa calcolata manualmente come ljoint per tangente di alfa medio
halfa = 12.70 #----- Lcls per tangente alfa alfamedio
Havaiable = 1141.0

# Position of the Joint
Xjoint = 2209.5
Yjoint = Delta1213*(Xjoint-2000)/1000+(h11-h12)
Hjoint = Havaiable-Delta1213*(Xjoint-2000)/1000
Htotj= Hjoint+370
```

```
# DEPENDING PARAMETERS (in pianta)
Bf = (Btot-2*tw-6*Sw)/(3)
hw = 0.5*Havaiable
Bj= (Bf-tw)/2+Sw
D1 = 2*Sw+tw
Lw = Lj+tf+C
Ltstub = Lw+tf
Lcls = Ltstub+C # no matters this length anymore
Dgap = 2*tf+C
Bw=Bj-Sw

# DEPENDING PARAMETERS (in elevation)
Hf = hw+2*C
hs = Hf-C
Hcls = Havaiable-Hf
H2 = Havaiable -halfa #----- height of second stiffnerA, taking into account the inclination

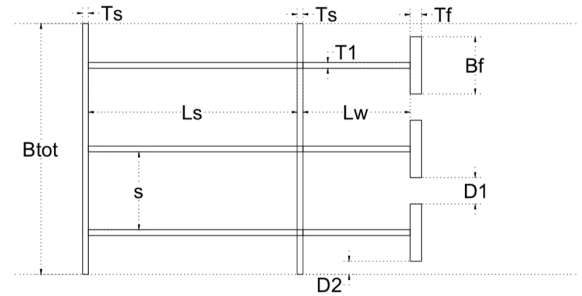
Ljoint = Lcls+2*ts # it has only drawings meaning
Ltot= (2*ts+2*Ls+2*ts+2*C+2*tf+Lj)+(Xjoint-1000-(C+2*ts+Ls))*2
delta1= 0.022998766*(ts*2+Ls+C)
delta2=0.017999778*(Lw+tf+2*ts+Ls)
```

Figure 76 Parameters of the joint, of the bridge and general position of the joint

According to the name in chapter 1.2.1, the elements which compose the joint are the following and they are introduced through the module Part as deformable 3D bodies:

Joint 1 (right part):

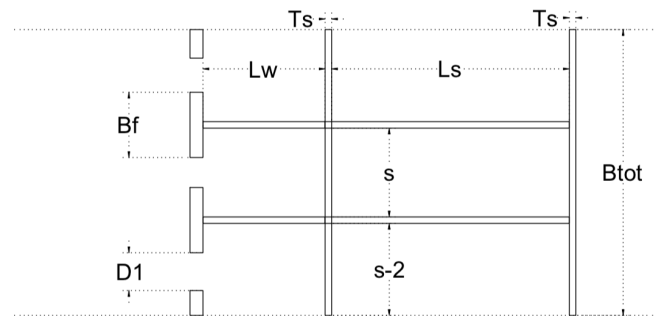
- 3 T-webs: t_w, h_w, L_w
- 3 T-flanges: t_f, B_f, h_f
- 1 stiffeners of total height: $t_s, B_{tot}, H_{available}$
- 1 stiffeners of half height: $t_s, B_{tot}, H_{available}/2$
- 3 links: $t_w, B_{tot}, H_{available}/2$



Picture 1 Joint-1

Joint 2 (left part):

- 2 T-webs: t_w, h_w, L_w
- 2 T-flanges: t_f, B_f, h_f
- 2 half T-flanges: $t_f, \frac{B_f - t_f}{2}, h_f$
- 1 stiffeners of total height: $t_s, B_{tot}, H_{available}$
- 1 stiffeners of half height: $t_s, B_{tot}, H_{available}/2$
- 2 links: $t_w, B_{tot}, H_{available}/2$



Picture 2 Joint-2

Bridge components:

- Top flange: 12x900x L_{tot}
- Slab C35/45: 250x3000x L_{tot}
- Slab C45/55: 120x3000x L_{tot}
- 2 Web_bridgeT12;
- Bottom flange;

3.4.2 Concrete

The concrete in the joint can be modelled in three different way, in order to simulate and understand the exact behavior of the joint. First Idea: the concrete could be modelled only in the region between the T-flanges of the two joints and without contact between T-webs and concrete. This model has not the advantage to take into account the biaxial behavior, and so it has been discharged.

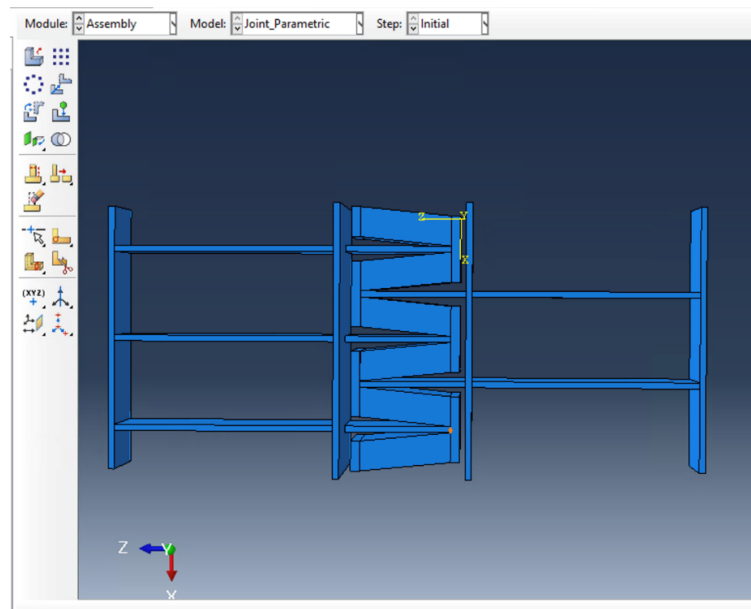


Figure 77 Model 1

Second Idea: the concrete inside the joint is modelled in the whole part between the joint1 and joint2, with the contact between T-webs and concrete. This model can be used to investigate the influence of the two parameters B_j and L_j on the stresses on the concrete and to investigate the real stresses distribution along the contact surface between the T-flange and the concrete itself. This model is used also to simulate two behaviour:

1. Uniaxial behavior: deactivated contact between T-webs and concrete;
2. Biaxial behavior: activated contact between T-webs and concrete;

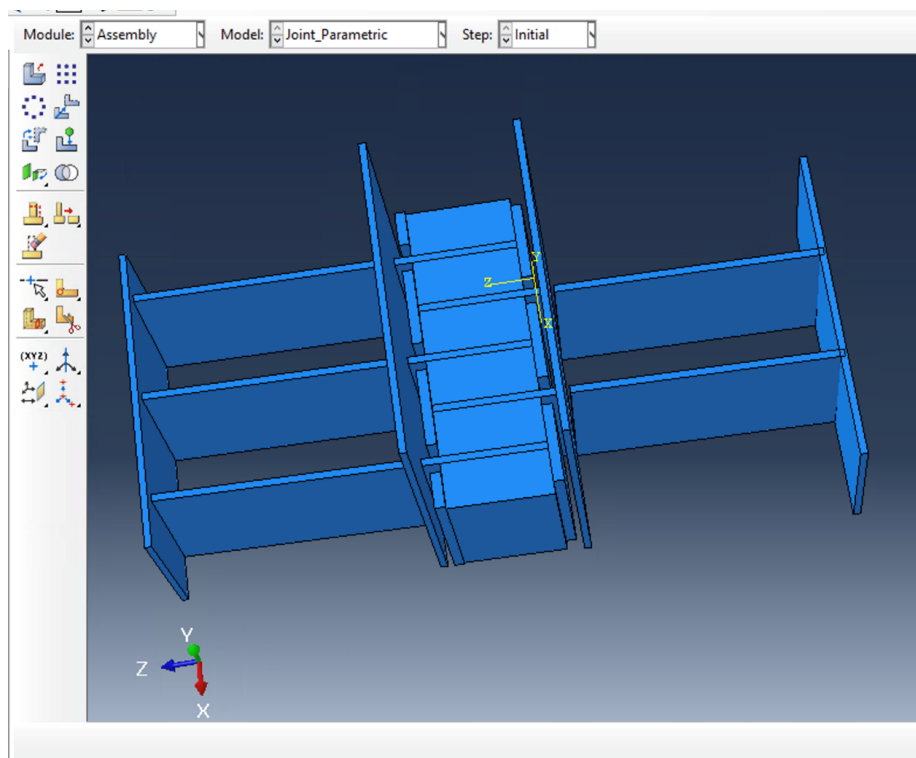


Figure 78 Model 2

Third Idea: the concrete can finally be modelled everywhere in order to describe the total and global behavior of the joint, before inserting it into the bridge.

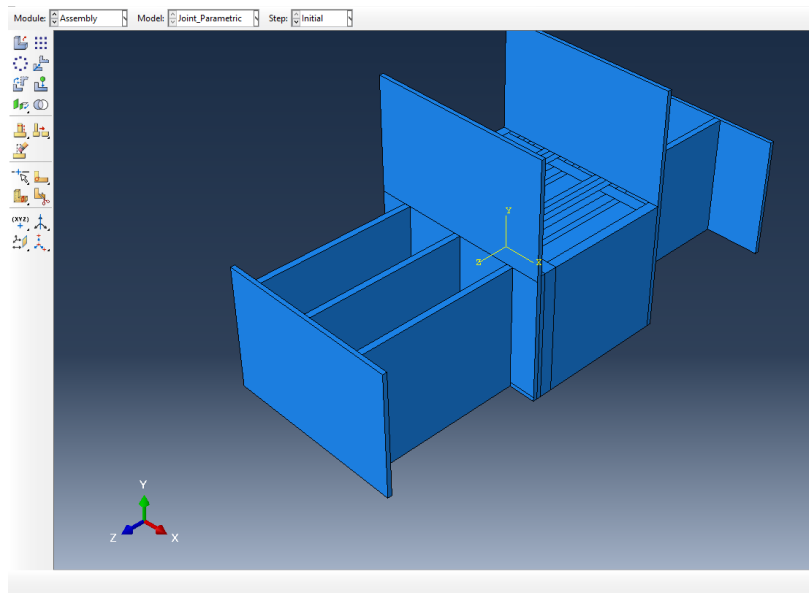


Figure 79 Model 3

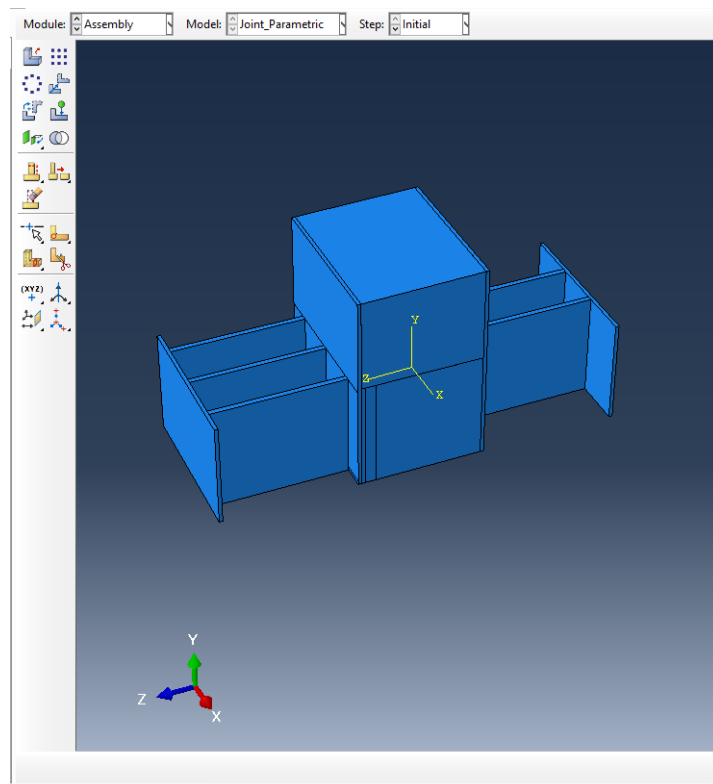


Figure 80 Model 3, complete

Regardless of how concrete is modelled, the real modeling issue is to assembly all these parts together. The origin of the referring system is fixed on one point on the bottom surface of the first T-flange of the joint1. Considering the whole bridge, the global position of the joint 1 is $L = 12.2095 \text{ m}$

from the abutments in the both sides, in order to have the two Joint1 exactly at a distance of 16 meters; in this way, the geometric limitation of the hot- galvanized tanks is completely respected.

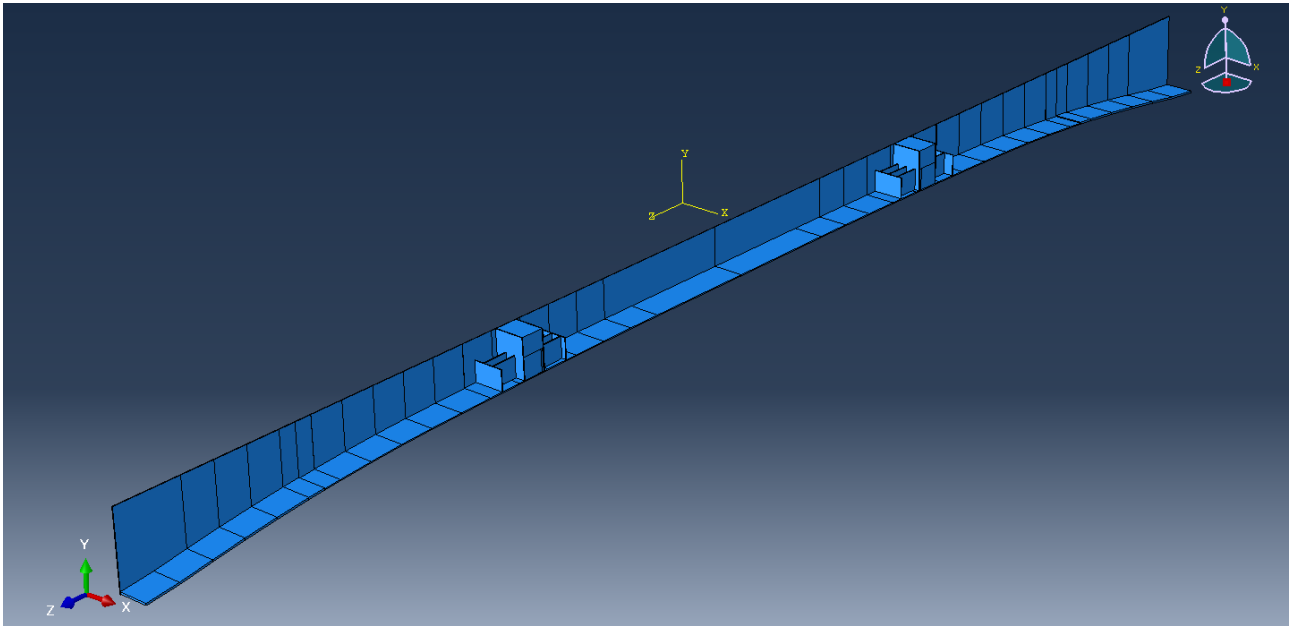


Figure 81 Position of the joints inside the girder

It is important to underline how the first idea is not applicable because the purpose of this thesis is to investigate the biaxial behavior of the concrete. The third idea is the best when the joint is inserted in the whole bridge, but it is not useful for the single investigation because it adds only computational afford to the program without provides any significate changes. The second idea indeed, is the best for our purpose.

3.4.3 Basic Model

All the various parts, described above, are assembled together according to their respective positions. All the elements are assembled together in their horizontal position, except the connecting parts between the two stiffeners, external to the actual joint. Therefore, it is necessary to specify that the links are rotated to respect the inclination of the bottom flange of the bridge. The links of Joint1 have a different inclination than those of Joint2 as the inclinations of the two sides of the bottom bridge are different. In fact, the links of the Joint2 lie on the bottom flange located between $L = 11$ m and $L = 12.2095$ m of the global length. The links of the Joint1 lie on the bottom flange located between $L = 12$ m and $L = 13$ m of the global length. The inclination of the links of the joint2 are calculated in this way:

$$\Delta h_2 = h_{11} - h_{12} = 1226 - 1203 = 23 \text{ mm}$$

$$L_1 = 1000 \text{ mm}$$

$$\alpha_2 = \arctan\left(\frac{\Delta h_2}{L_1}\right) = 1.3175^\circ$$

In the same way, the inclination of the links of the Joint1 are calculated in this way:

$$\Delta h_1 = h_{12} - h_{13} = 1203 - 1185 = 18 \text{ mm}$$

$$L_1 = 1000 \text{ mm}$$

$$\alpha_1 = \arctan\left(\frac{\Delta h_1}{L_1}\right) = 1.0312^\circ$$

One of the most important thing to do during the assembly, is the cut in the webs of the bridge and in the bottom flange, in order to divide the two parts of the bridge. This gap is insert at a hypothetical distance of $D_{gap} = 2t_f$ and it is considered a gap between the two parts of Gap= 5 mm.

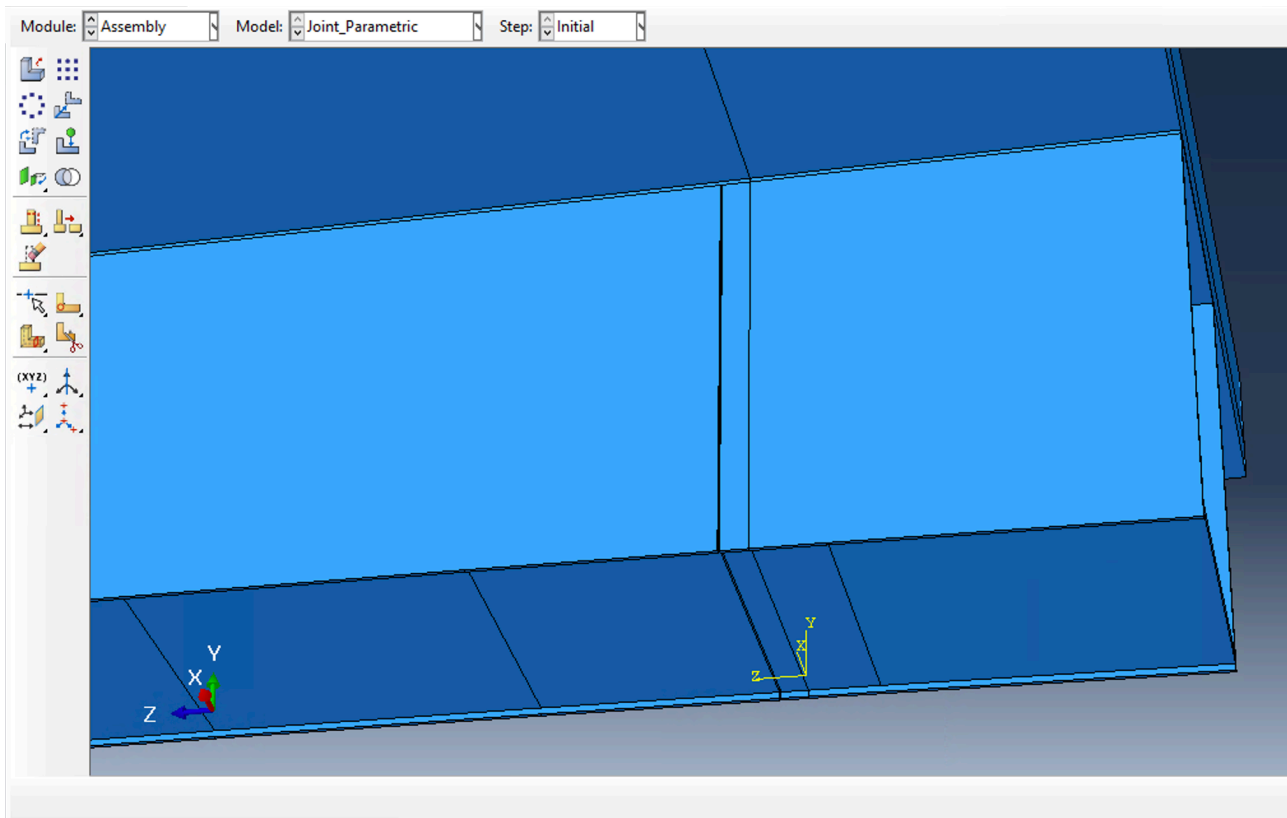


Figure 82 Gap in the Webs and in the bottom flange

Once complete the assemble part, it is important to specify the chosen mesh for each element, in order to respect the roles related to the master surfaces and slave surfaces and in order to have a finer mesh in the interested areas. Now it is possible to define the interaction between each part in the assembly shape: in this model, in fact, the interactions play an important role in order to define the real behavior of all the components. The geometry of this joint is complex and all the connections between all the surfaces has to be study carefully, investigating the results and finding out if the model has the

expected behavior. The interactions are chosen according to the results obtained by the simplified model. In fact, as reported above, tie constraint is used for all the surfaces that are welded in the reality: this interaction is perfect to simulate a perfect constraint between two surfaces. Tied contact for contact pair is used with no separation interaction behavior and tied surfaces require adjustment which was decided as 0.1 because tied surfaces should be defined precisely in contact. It is used to describe the contact between the stiffeners and the links, between the stiffeners A and the T-webs, between the steel parts of the joint and the surrounding bridge's components. On the other side, the contact between T-flange and bottom flange of the bridge should be as slip contact: it should allow only the vertical transmission of the shear forces from one part of the bridge to the other part. As shown thanks to the simplified model, the best kind of interaction could be this one: Tangential frictionless and normal hard contact. The following solicitants actions are considered:

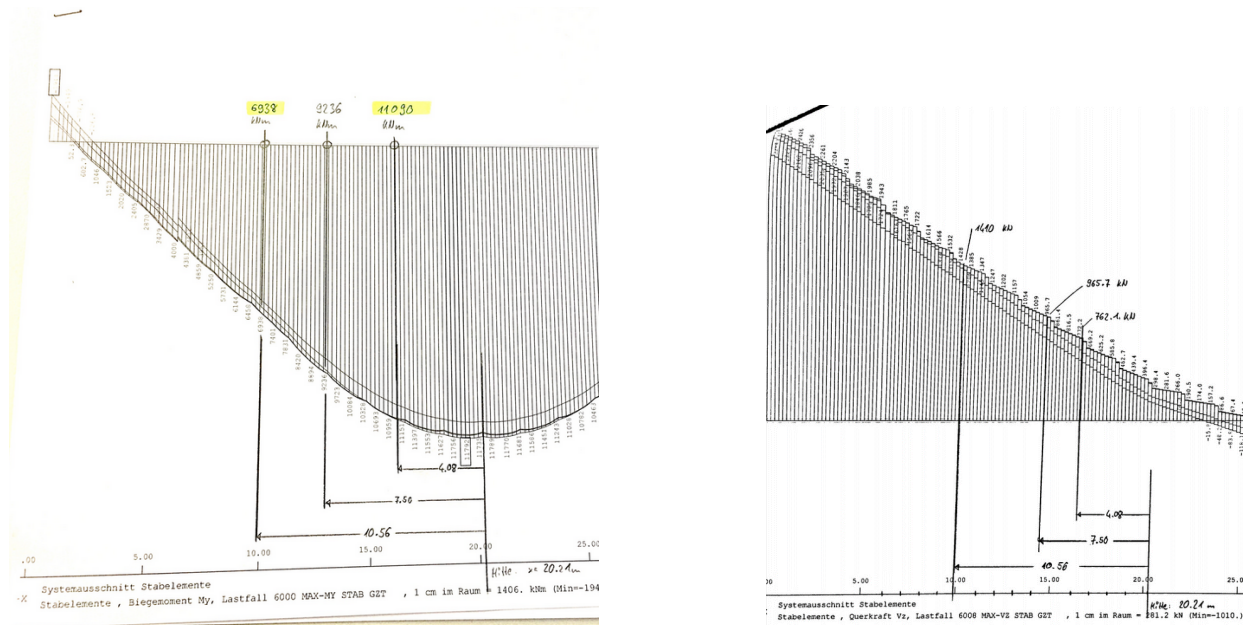


Figure 83 Solicitants actions taken directly from Sofistik model under the ultimate limit state

The joint is considered insert inside the bridge also in the small model. In order to avoid the influence of the D-regions in the joint itself, the theoretical distance of 2,250 meters is considered from the both sides of the end of the stiffeners B of the joint model. According to that, the following solicitants actions are taken by Sofistik model. The moment and the shear are applied to a reference point RP, which is coupled to the hole final section of the bridge in which is located. The position of the point is in the barycenter of the section under investigation. The surface-based coupling constraint, in fact, allows the motion of a series of nodes on a surface to be coupled to the motion of a reference node. It is of type kinematic when the group of nodes is coupled to the rigid body motion defined by the

reference node: kinematic coupling constrains the motion of the coupling nodes to the rigid body motion of the reference node. The constraint can be applied to defined degrees of freedom at the coupling nodes with respect to the global or a local coordinate system. Kinematic constraints are imposed by eliminating degrees of freedom at the coupling nodes: in fact, once any combination of displacement degrees of freedom at a coupling node is constrained, additional displacement constraints, as MPCs, boundary conditions, or other kinematic coupling definitions, cannot be applied to any coupling node involved in a kinematic coupling constraint. The same limitation applies for rotational degrees of freedom. To be sure to have a right behavior and transmission of these two loads in the joints this choice has been done:

$$V_y = 762.10 \text{ kN}$$

$$M^* = 11090 \text{ kNm}$$

On the other sides, the boundaries conditions are applied: the whole section of the bridge is considered fixed.

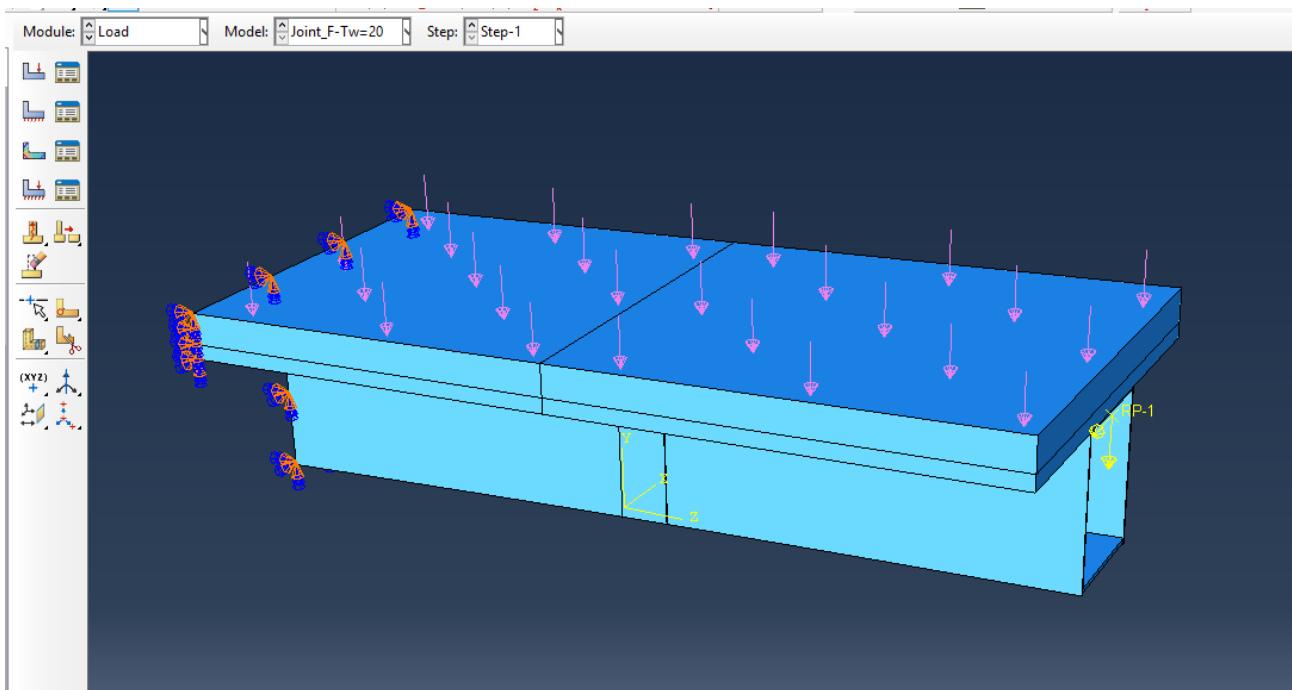


Figure 84 Loads and BCs

Studying the joint in an incremental way, the step created is considered divided in 5 calculation increment $\Delta = 0.25$. It allows to analyze the behavior of the joint not only for the final load but also in the intermediate calculations and it is a useful tool to investigate the joint in detail.

3.4.4 Variation models for the parameter studies

Some different models have been created in order to investigate the influences of the geometry of the T-webs. The purpose of this creation is related to the influence of the parameters t_w and h_w . The Model 1 that is considered the basic model has the following parameters:

```
# FIXED PARAMETERS of the joint
Btot = 876
Sw = 30.0
tw = 30.0
Lj = 300.0
ts = 20.0
C = 20.0
tf = 30.0
Ls = 750.0
Gap = 5.0
hw=0.5*Havaiable
```

Figure 85 Geometrical parameters of model 1

Model 2: it has the same initial geometry with the addition of a horizontal plate. Its purpose is to add horizontal stiffness, connecting horizontally, the two webs of the bridge nearby the vertical cut. This new part is inserted above the T-flanges of the Joint-2:

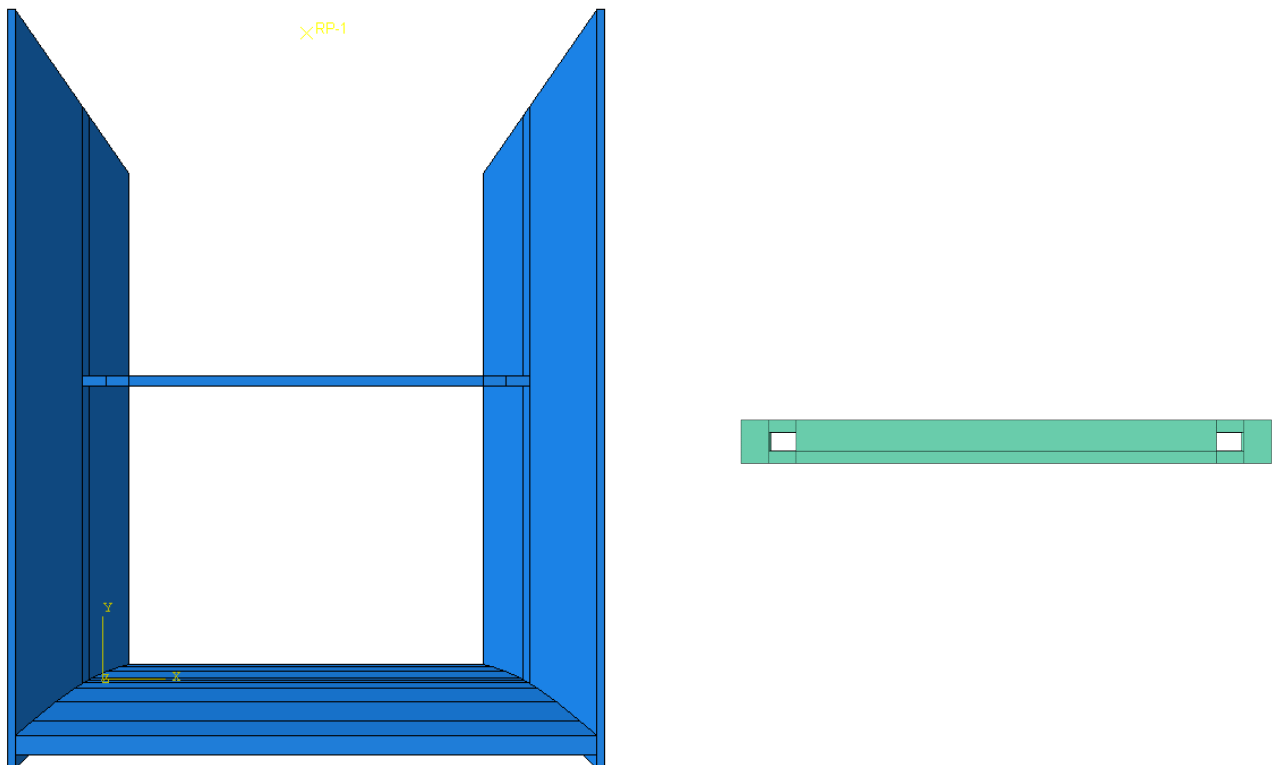


Figure 86 Horizontal Stiffener

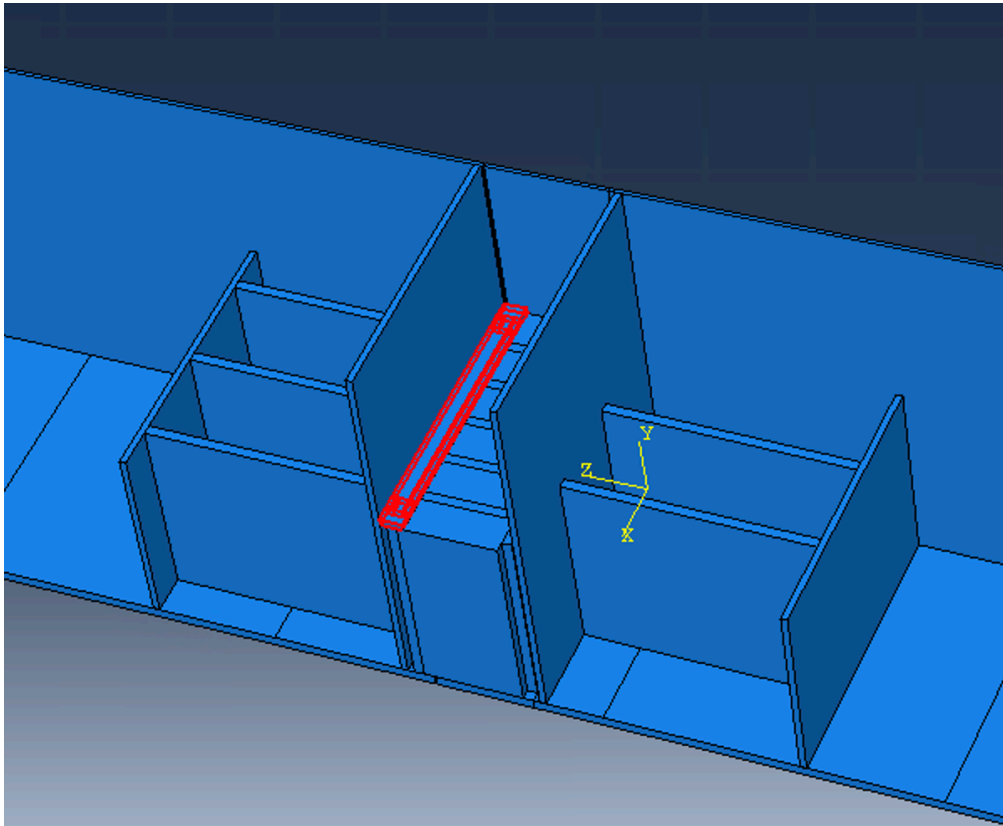


Figure 87 Positioning of the Horizontal stiffener

Model 3: It has the same geometry but the analysis is in the plastic field. While the model 2 and 3 have the same geometry of the basic model, the others have some changes.

Model 4: the height of the T-web is the same and the thickness is increased up to 35 mm. The model has run under elastic conditions.

Model 5: the thickness is now decreased to 400 mm and the thickness is again 30 mm. This model has been created to investigate how much is possible to reduce the height of the whole joint because it is, probably, necessary the introduction of a horizontal stiffeners plate above the T-flange, to reduce and contain the horizontal displacements of the webs of the bridge.

Model 6: both the thickness and the height of the T-web are changed and the plastic properties are considered to describe the steel behavior.

In this summary table are reported the quantities involved in each model created and the modified quantities are underlined in red.

MODEL	Tw [mm]	Hw [mm]	Analysis	New element
1	30	570.5	Elastic	
2	30	570.5	Elastic	x
3	30	570.5	Plastic	
4	35	570.5	Elastic	
5	30	400	Plastic	
6	35	400	Plastic	

4 RESULTS

4.1 The whole bridge

The aim of this chapter is to elaborate the data obtained by the Abaqus model, in order to compare the results with those obtained by the use of another program, Sofistik. In order to do that it is necessary to compare the results in terms of displacements [mm] and stresses [MPa]. At the same time, it is useful also to compare the bending moment along the span for the different loading phases and the reaction forces at the borders as to be sure of the correct functioning of the model and to be definitively able to validate it.

4.1.1 Comparison of the displacement

It is possible to compare the vertical displacement in the middle section obtained by Abaqus model with the displacement of Sofistik model.

Construction state 0				
Model	M_{\max} [kNm]	M_{\min} [kNm]	A_{\max} [kN]	u_{\max} [mm]
SOFiSTiK	2997.00	0.00	323.00	69.80
Abaqus	3050.00	0.00	322.42	72.55
err [%]	1.77%	0.00%	0.18%	3.94%

Construction state 1				
Model	M_{\max} [kNm]	M_{\min} [kNm]	A_{\max} [kN]	u_{\max} [mm]
SOFiSTiK	3612.00	0.00	477.60	85.80
Abaqus	3660.40	0.00	473.60	88.88
err [%]	1.34%	0.00%	0.84%	3.58%

Construction state 2				
Model	M_{\max} [kNm]	M_{\min} [kNm]	A_{\max} [kN]	u_{\max} [mm]
SOFiSTiK	4342.00	-2518.00	708.00	94.60
Abaqus	4362.00	-2454.67	702.53	95.97
err [%]	0.46%	2.52%	0.77%	1.44%

Construction state 3				
Model	M_{\max} [kNm]	M_{\min} [kNm]	A_{\max} [kN]	u_{\max} [mm]
SOFiSTiK	5227.00	-5771.00	1160.00	104.80
Abaqus	5128.00	-5960.00	1156.35	102.18
err [%]	1.89%	3.27%	0.31%	2.50%

Figure 88 Comparison of displacements

The deformation of the entire bridge is shown in the second construction phase, for information purposes.

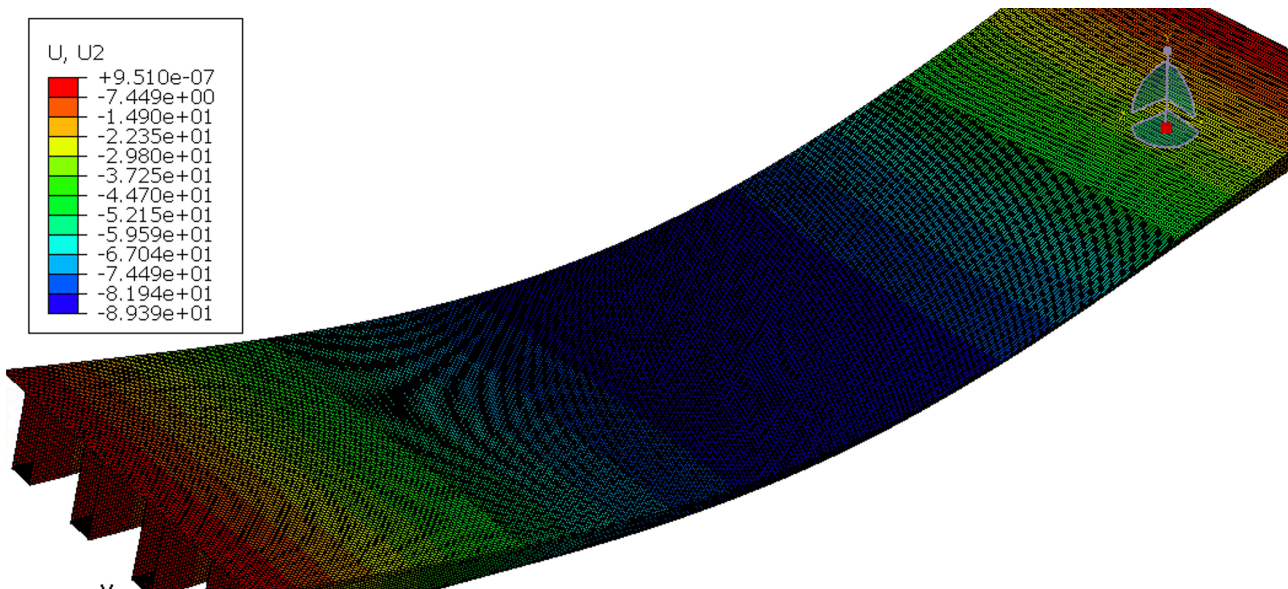


Figure 89 Displacement U2 in the second phase

4.1.2 Comparison of the Reaction forces

The history output allows to select a region and to calculate particular quantities for it: in this particular case, the sections at the borders in which the BCs are applied have been picked and the reaction forces have been calculated. The reaction forces below are calculated for all the girders on one side of the bridge:

	Girder 1	Girder 2	Girder 3	Girder 4
STEP	Reaction Force [N]	Reaction Force [N]	Reaction Force[N]	Reaction Force[N]
0	0	0	0	0
1	321626	320564	321626	322419
2	473601	469852	471860	473601
3	702527	693631	699998	702527
4	1097090	873.069	1156350	1156350

The bigger values are compared with the values obtained on the Sofistik model.

Construction state 0				
Model	M_{\max} [kNm]	M_{\min} [kNm]	A_{\max} [kN]	u_{\max} [mm]
SOFiSTiK	2997.00	0.00	323.00	69.80
Abaqus	3050.00	0.00	322.42	72.55
err [%]	1.77%	0.00%	0.18%	3.94%

Construction state 1				
Model	M_{\max} [kNm]	M_{\min} [kNm]	A_{\max} [kN]	u_{\max} [mm]
SOFiSTiK	3612.00	0.00	477.60	85.80
Abaqus	3660.40	0.00	473.60	88.88
err [%]	1.34%	0.00%	0.84%	3.58%

Construction state 2				
Model	M_{\max} [kNm]	M_{\min} [kNm]	A_{\max} [kN]	u_{\max} [mm]
SOFiSTiK	4342.00	-2518.00	708.00	94.60
Abaqus	4362.00	-2454.67	702.53	95.97
err [%]	0.46%	2.52%	0.77%	1.44%

Construction state 3				
Model	M_{\max} [kNm]	M_{\min} [kNm]	A_{\max} [kN]	u_{\max} [mm]
SOFiSTiK	5227.00	-5771.00	1160.00	104.80
Abaqus	5128.00	-5960.00	1156.35	102.18
err [%]	1.89%	3.27%	0.31%	2.50%

Figure 90 Comparison of Reaction forces

4.1.3 Comparison of the bending moment

It should be nice to compare directly the stresses in the sections, but it is better to compare the bending moment, because Sofistik returns, as outputs, the values of the bending moment, from which the stresses can be obtained by numerical operations. In order to do that, a Matlab program has been created: it contains the input of the bridge geometry along the span and so the information regarding the variation in height and thickness of the elements involved section by section.

L [mm]	H section [mm]	Hcls1 [mm]	Hcls2 [mm]	Hcls3 [mm]	t_top [mm]	t_bot [mm]	t_web [mm]	E1 [MPa]	E2 [MPa]	E3 [MPa]
0	2200	120	250	250	12	55	22	35500	34486	34486
1000	2088	120	250	250	12	55	22	35500	34486	34486
2000	1932	120	250	250	12	55	22	35500	34486	34486
3000	1788	120	250	250	12	55	22	35500	34486	34486
4000	1662	120	250	250	12	55	22	35500	34486	34486
5000	1552	120	250	250	12	55	22	35500	34486	34486
6000	1458	120	250	250	12	30	22	35500	34486	34486
7000	1381	120	250	250	12	30	16	35500	34486	34486
8000	1320	120	0	250	12	30	16	35500	35500	34486
9000	1280	120	0	250	12	30	16	35500	35500	34486
10000	1252	120	0	250	12	30	16	35500	35500	34486
11000	1226	120	0	250	12	30	16	35500	35500	34486
12000	1203	120	0	250	12	30	12	35500	35500	34486
13000	1185	120	0	250	12	30	12	35500	35500	34486
14000	1171	120	0	250	12	30	12	35500	35500	34486
15000	1161	120	0	250	12	30	12	35500	35500	34486
16000	1152	120	0	250	12	30	12	35500	35500	34486
17000	1150	120	0	250	12	30	12	35500	35500	34486
18000	1150	120	0	250	12	30	12	35500	35500	34486
19000	1150	120	0	250	12	30	12	35500	35500	34486
20209.5	1150	120	0	250	12	30	12	35500	35500	34486
21419	1150	120	0	250	12	30	12	35500	35500	34486
22419	1150	120	0	250	12	30	12	35500	35500	34486
23419	1150	120	0	250	12	30	12	35500	35500	34486
24419	1152	120	0	250	12	30	12	35500	35500	34486
25419	1161	120	0	250	12	30	12	35500	35500	34486
26419	1171	120	0	250	12	30	12	35500	35500	34486
27419	1185	120	0	250	12	30	12	35500	35500	34486
28419	1203	120	0	250	12	30	12	35500	35500	34486
29419	1226	120	0	250	12	30	16	35500	35500	34486
30419	1252	120	0	250	12	30	16	35500	35500	34486
31419	1280	120	0	250	12	30	16	35500	35500	34486
32419	1320	120	0	250	12	30	16	35500	35500	34486
33419	1381	120	250	250	12	30	16	35500	34486	34486
34419	1458	120	250	250	12	30	22	35500	34486	34486
35419	1552	120	250	250	12	55	22	35500	34486	34486

36419	1662	120	250	250	12	55	22	35500	34486	34486
37419	1788	120	250	250	12	55	22	35500	34486	34486
38419	1932	120	250	250	12	55	22	35500	34486	34486
39419	2088	120	250	250	12	55	22	35500	34486	34486
40419	2200	120	250	250	12	55	22	35500	34486	34486

In this way, the program can calculate the position of the neutral axis for each section and through this formulation it is possible to obtain the graphic of the bending moment in each section for the different reagent section:

$$M_{sec} = \frac{\sigma_{sec} \cdot J_{sec}}{n \cdot (H_{TOTsec} - x_{sec})}$$

It is important to specify the subsequent fact: this formulation allows to calculate directly the exact moment only in the section without change of the reagent section. So, it is ok for the first, the second and the third step along the whole span because in the middle section there is no change of section and at the boundaries the previous moment related to the first static scheme is zero. In the fourth step, this formulation it is not valid anymore, and a more complex operation should be done to calculate the moment in the middle section, starting from the σ_{33} .

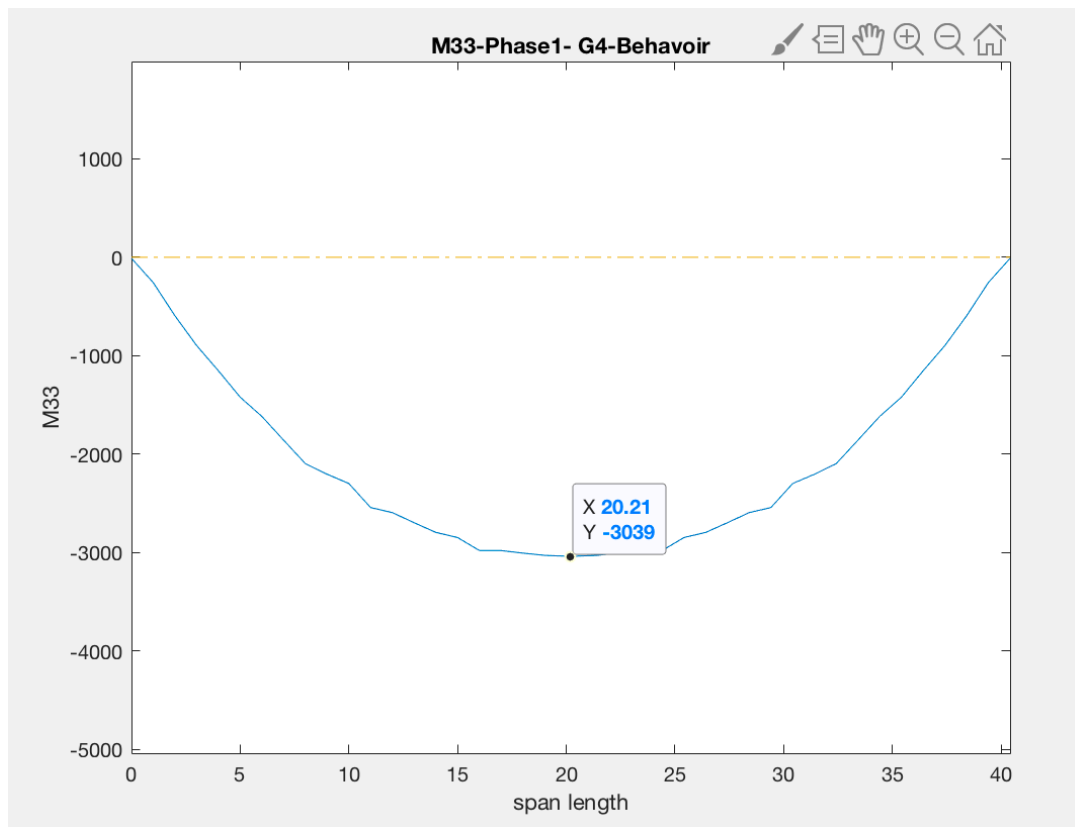


Figure 91 Bending Moment in the phase1

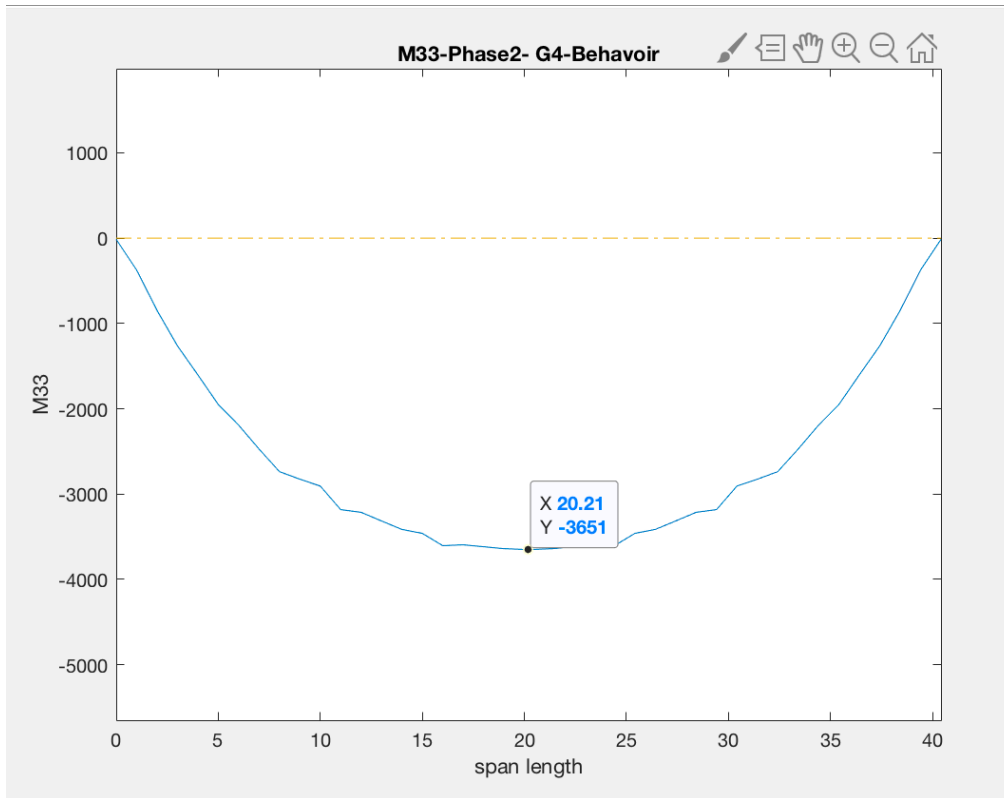


Figure 92 Bending moment in the phase2

The sign of the bending moment must be understood purely referred to the previous graphs, in such a way that at a positive bending moment corresponded a graph below the axis of the section. In the third and fourth phases the calculation is done by hand in the point of interest: in the middle section and in the boundary section. Analyzing the middle section, the bending moment M_{33} in the third phase is obtained by the same formulation:

$$M_{33.3} = \frac{\sigma_{33} \cdot J_2}{n \cdot (H_{TOT2} - x_2)} = \frac{111,7 \cdot 1,88 \cdot 10^{11}}{5,915 \cdot (1270 - 452)} \cdot 10^{-6} = 4340 \text{ kNm}$$

The formulation used for M_{33} in the final constructive step is, instead the follow:

$$\Delta M_{33} = \frac{\Delta \sigma \cdot J_3}{n_3 \cdot (H_{TOT3} - x_3)} = \frac{(128 - 111,7) \cdot 3,2369 \cdot 10^{11}}{6,089 \cdot (1520 - 416,9)} \cdot 10^{-6} = 820,251 \text{ kNm}$$

The sum $M_{33.3} + \Delta M_{33}$ is the final bending moment in the middle section, $M_{33.4}$, before the opening to the traffic and after the constructive phases. The same reasoning has been done for the border section in the third and fourth phases:

$$M_{33.3} = \frac{\sigma_{33} \cdot J_2}{n \cdot (H_{TOT2} - x_2)} = \frac{-14,52 \cdot 1,7957 \cdot 10^{12}}{6,089 \cdot (2570 - 887,95)} \cdot 10^{-6} = -2524,242 \text{ kNm}$$

$$M_{33.4} = \frac{\sigma_{33} \cdot J_2}{n \cdot (H_{TOT2} - x_2)} = \frac{-33.80 \cdot 1.7957 \cdot 10^{12}}{6.089 \cdot (2570 - 887.95)} \cdot 10^{-6} = -5926,05 \text{ kNm}$$

Of course, only a few of all the calculations made have been reported by way of example: these calculations have been done for all the four girders and for all the constructive phases. The results are display in the following table, in which the most loaded girder of Abaqus model, is compared with the most loaded girder on Sofistik model.

Construction state 0				
Model	M_{\max} [kNm]	M_{\min} [kNm]	A_{\max} [kN]	u_{\max} [mm]
SOFiSTiK	2997.00	0.00	323.00	69.80
Abaqus	3050.00	0.00	322.42	72.55
err [%]	1.77%	0.00%	0.18%	3.94%

Construction state 1				
Model	M_{\max} [kNm]	M_{\min} [kNm]	A_{\max} [kN]	u_{\max} [mm]
SOFiSTiK	3612.00	0.00	477.60	85.80
Abaqus	3660.40	0.00	473.60	88.88
err [%]	1.34%	0.00%	0.84%	3.58%

Construction state 2				
Model	M_{\max} [kNm]	M_{\min} [kNm]	A_{\max} [kN]	u_{\max} [mm]
SOFiSTiK	4342.00	-2518.00	708.00	94.60
Abaqus	4362.00	-2454.67	702.53	95.97
err [%]	0.46%	2.52%	0.77%	1.44%

Construction state 3				
Model	M_{\max} [kNm]	M_{\min} [kNm]	A_{\max} [kN]	u_{\max} [mm]
SOFiSTiK	5227.00	-5771.00	1160.00	104.80
Abaqus	5128.00	-5960.00	1156.35	102.18
err [%]	1.89%	3.27%	0.31%	2.50%

Figure 93 Comparison of positive and bending moment in the most loaded girder

The results show the error between Abaqus and Sofistik results:

$$err = \frac{M_{sofy} - M_{Abaq}}{M_{sofy}} * 100$$

The error [%] is always under the 5 %, for each of the quantities under investigation. According to that, it is possible to say that Abaqus model behaves well and in according to Sofistik model.

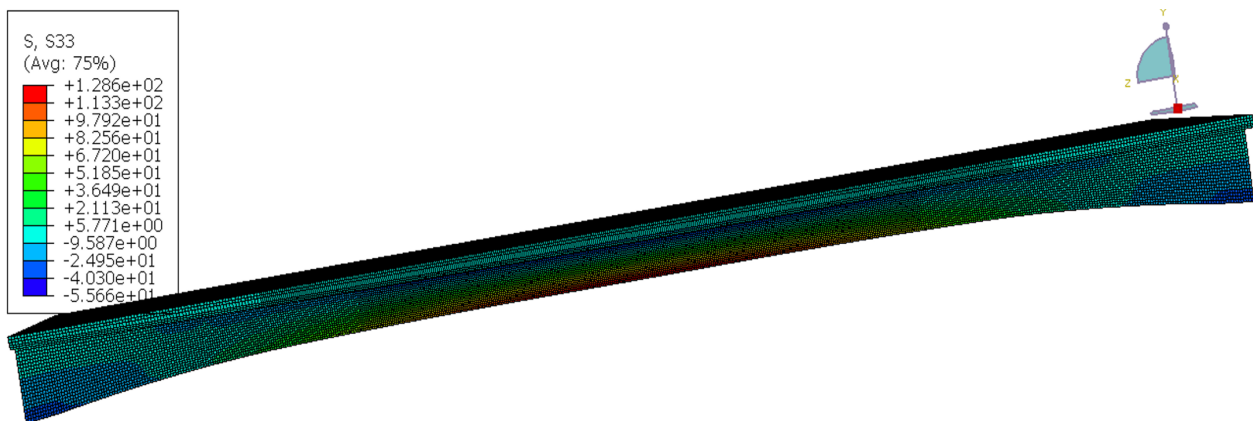


Figure 94 Display of the Stresses S_{33} in the final step

4.2 The whole bridge with the effect of abutments

In this chapter, the results of the traffic loads are verified apart from the results obtained before: this is useful to validate the model of the whole bridge with the springs as boundary conditions to take into account the effect of the abutments on the deck. The results under the traffic loads are studied separately in three different steps.

4.2.1 Comparison of the UDL

The behavior of the bridge under the uniformed distributed load $q = 3 \frac{kN}{m^2}$ is compared with the results obtained by Sofistik. As specified before, the bending moment in Abaqus model is calculated by this formulation:

$$M_{33.3} = \frac{\sigma_{33} \cdot J_3}{n \cdot (H_{TOT3} - x_3)}$$

According to that, the maximum bending moment and the minimum bending moment are:

$$M_{33.max} = \frac{\sigma_{33} \cdot J_3}{n \cdot (H_{TOT3} - x_3)} = \frac{8.373 \cdot 3,236 \cdot 10^{12}}{6.089 \cdot (1520 - 416.9)} \cdot 10^{-6} = 404.5 \text{ kNm}$$

$$M_{33.min} = \frac{\sigma_{33} \cdot J_3}{n \cdot (H_{TOT3} - x_3)} = \frac{-8,21 \cdot 1.7957 \cdot 10^{12}}{6.089 \cdot (2570 - 887.95)} \cdot 10^{-6} = -1439.435 \text{ kNm}$$

	M max [kNm]	M min [kNm]	Displacement [mm]
Sofistik	409,6	-1394	-3,63
Abaqus	404,5	-1439,43	-3,996
err [%]	1,2%	-3,3%	-7,5%

The behavior of the bridge to the entire distributed traffic load is describe by the following picture, in terms of displacements.

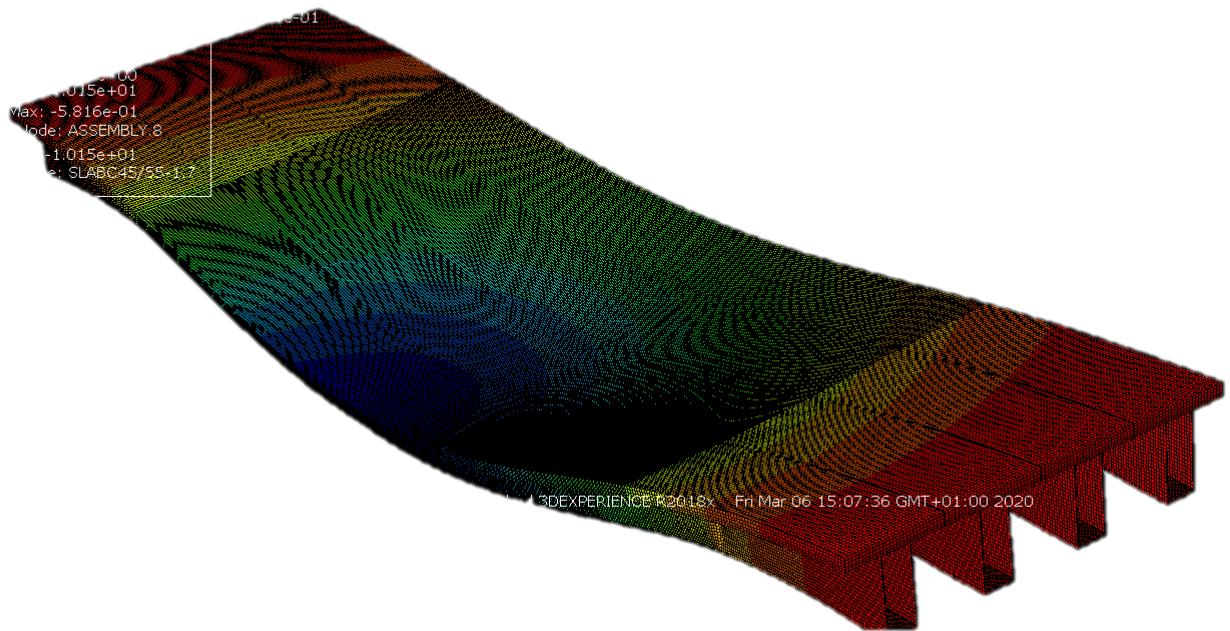


Figure 95 Displacement of the whole bridge under the UDL

The maximum bending moment and the minimum bending moment are:

$$M_{33.max} = \frac{\sigma_{33} \cdot J_3}{n \cdot (H_{TOT3} - x_3)} = \frac{21.5 \cdot 3,236 \cdot 10^{12}}{6.089 \cdot (1520 - 416.9)} \cdot 10^{-6} = 1035.82 \text{ kNm}$$

$$M_{33.min} = \frac{\sigma_{33} \cdot J_3}{n \cdot (H_{TOT3} - x_3)} = \frac{-19,8613 \cdot 1.7957 \cdot 10^{12}}{6.089 \cdot (2570 - 887.95)} \cdot 10^{-6} = -3482.22 \text{ kNm}$$

In the following tabs the results are compared with the one obtained by Sofistik model.

Model	M max [kNm]	M min [kNm]	Displacement [mm]
Sofistik	1009	-3463	-9,27
Abaqus	1035,82	-3482,22	-10,15
err [%]	-2,7%	-0.6%	-8,6%

4.2.2 Comparison of the TS

Once the model is validated for the uniform distributed load, the same verification has to be done for the tandem load.

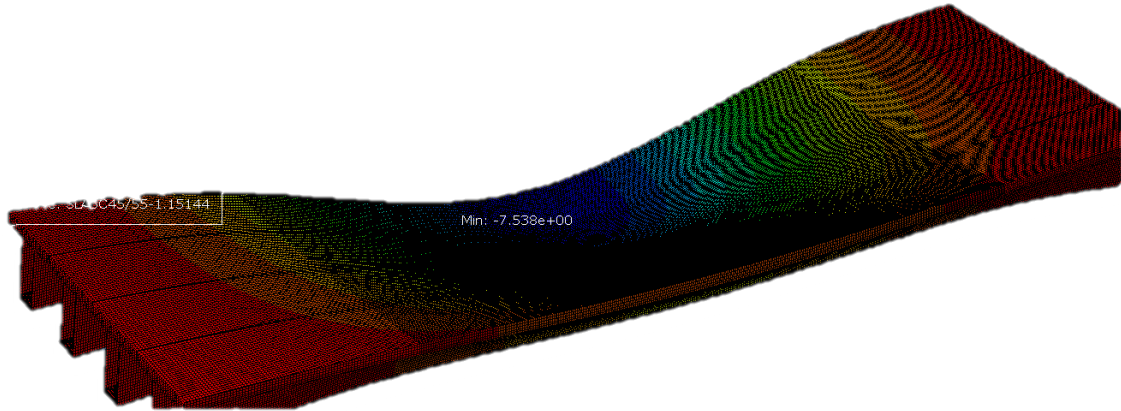


Figure 96 Displacement due to the application of the tandem load

The most relevant bending moment are calculated: the bending moment in the middle section of the most loaded girder and the bending moment at the boundaries of each girder, to validate definitively the exact behavior of the springs in this model.

$$M_{33.max} = \frac{\sigma_{33} \cdot J_3}{n \cdot (H_{TOT3} - x_3)} = \frac{26,80 \cdot 3,236 \cdot 10^{12}}{6,089 \cdot (1520 - 416,9)} \cdot 10^{-6} = 1291,2 \text{ kNm}$$

$$M_{33.minG1} = \frac{\sigma_{33} \cdot J_3}{n \cdot (H_{TOT3} - x_3)} = \frac{-12,002 \cdot 1,7957 \cdot 10^{12}}{6,089 \cdot (2570 - 887,95)} \cdot 10^{-6} = -2103,9 \text{ kNm}$$

$$M_{33.minG2} = \frac{\sigma_{33} \cdot J_3}{n \cdot (H_{TOT3} - x_3)} = \frac{-10,4 \cdot 1,7957 \cdot 10^{12}}{6,089 \cdot (2570 - 887,95)} \cdot 10^{-6} = -1823 \text{ kNm}$$

$$M_{33.minG3} = \frac{\sigma_{33} \cdot J_3}{n \cdot (H_{TOT3} - x_3)} = \frac{-7,85 \cdot 1,7957 \cdot 10^{12}}{6,089 \cdot (2570 - 887,95)} \cdot 10^{-6} = -1376,0 \text{ kNm}$$

$$M_{33.minG3} = \frac{\sigma_{33} \cdot J_3}{n \cdot (H_{TOT3} - x_3)} = \frac{-3,42 \cdot 1,7957 \cdot 10^{12}}{6,089 \cdot (2570 - 887,95)} \cdot 10^{-6} = -599,78 \text{ kNm}$$

Model	M max [kNm]	M min [kNm] G1	M min [kNm] G2	M min [kNm] G3	M min [kNm] G4	Displacement [mm]
Sofistik	1408	-2103,9	-1823	-1376	-599	-8
Abaqus	1291	-2050	-1821	-1301	-584	-7,53
err [%]	8,3%	2,6%	0,1%	5,5%	2,5%	5,9%

The small quantities of the errors show that the model is totally valid and reliable.

4.3 Simplified model

Comparison of Abaqus simplified model results and simplified hand calculation. In this chapter, it is possible to analyze Abaqus results, in order to validate or neglected the previous starting hypothesis for the first-hand calculation approach. Under the hypothesis of the first geometry choses it is possible to have some results obtained by the hand calculation.

4.3.1 Simplified model results

The simplified model has done to study the exact behavior of the concrete in relation with the different kind of interaction that it is possible to use in Abaqus. It is possible to report the comparison of the results obtained with the all different kind of model. The first is thing is to report the hand calculation, used as unit of length to compare the results. The pressure load applied on both the T-webs is the following that implies the others results:

$$\sigma = 100 \text{ MPa}$$

$$F_M = \frac{\sigma}{A_w} = \frac{\sigma}{t_w * h_w} \approx 1141 \text{ kN}$$

$$\alpha = 23^\circ \text{ and } F_{c\perp} = \frac{F_M}{2} \quad F_C = F_{c\perp} * \cos(\alpha) \quad F_C = \frac{F_M}{2} * \frac{1}{\cos(\alpha)} \approx \frac{1141}{2} * \frac{1}{\cos(23)} \approx 620 \text{ kN}$$

$$\sigma_c = \frac{F_C}{A_{cls}} = \frac{F_C}{b_w * h_w} \approx -11 \text{ MPa}$$

It is important to understand that these results are valid only far from the D-regions: it is necessary to compare the results in these regions to validate or invalidate the results. In fact, near the corners there are of course some singularities that should be investigate apart from these results. Comparing the results of the different models, three different paths on the concrete were chosen.

PATH-1				
	Sigma_33			
Position	SM1	SM2	SM3	SM4
0	-32,9506	-31,9129	-32,996	-32,937
15	-19,4583	-19,2047	-19,444	-19,463
30	-12,8811	-12,6678	-12,879	-12,882
44	-9,94817	-9,74917	-9,947	-9,949
58	-7,88205	-7,77725	-7,882	-7,882
72	-5,55072	-5,47839	-5,552	-5,551
85	-2,20148	-2,4117	-2,199	-2,202
99	-0,35699	-0,41169	-0,357	-0,357
114	0,022377	-0,01513	0,022	0,022
129	0,341443	0,33852	0,341	0,341

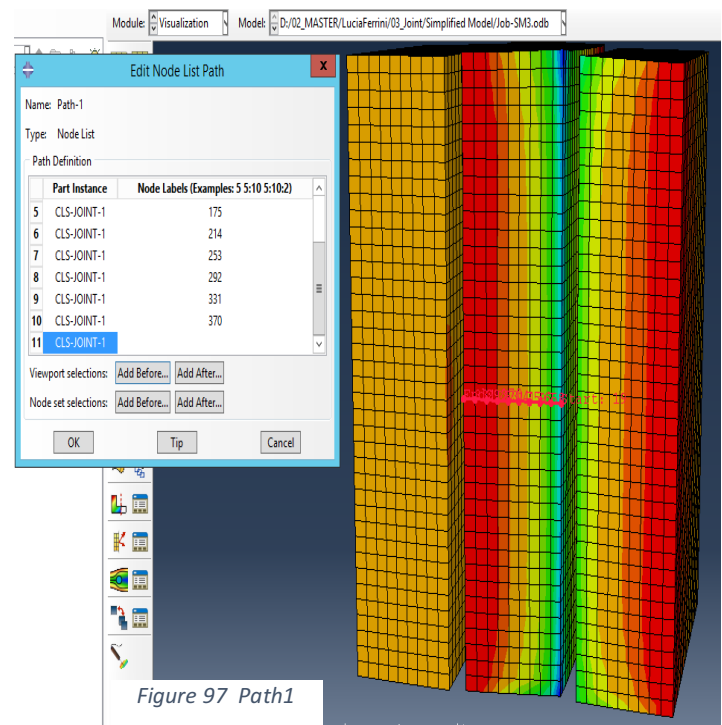


Figure 97 Path1

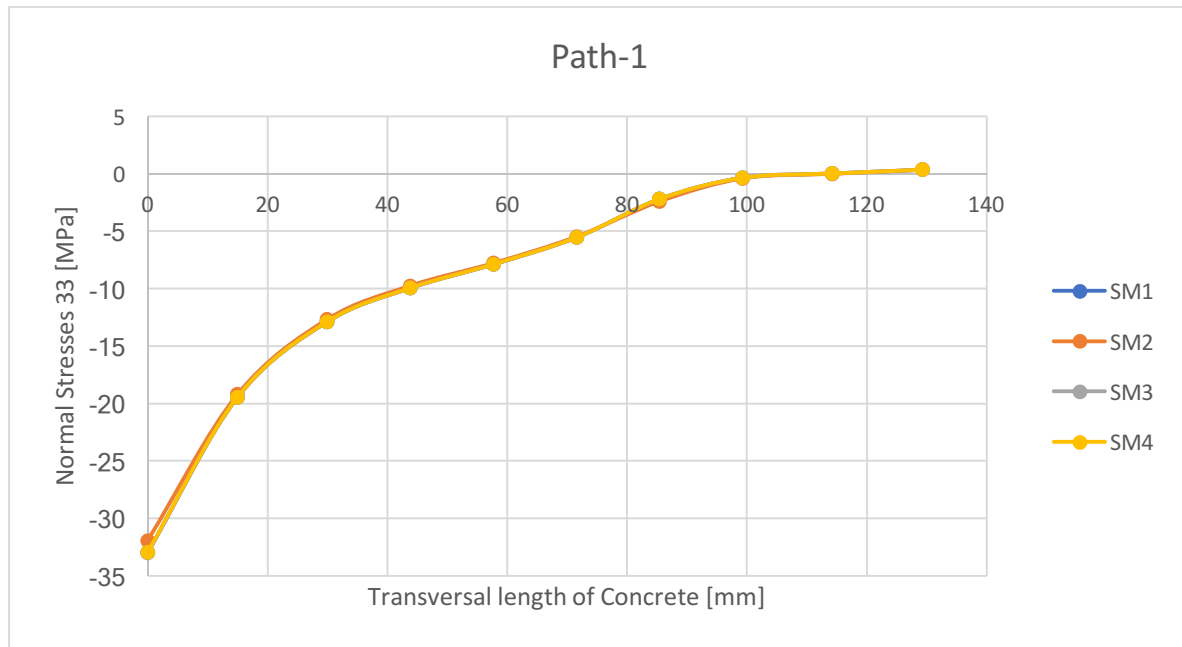


Figure 3 Comparison of the results in the path-1

It is possible to notice that there is almost perfect match between the four results. So the same investigation is done also for the path-2 and the path-3, neglecting the tables and reporting only the graphs of the trends of the stresses along that specified path.

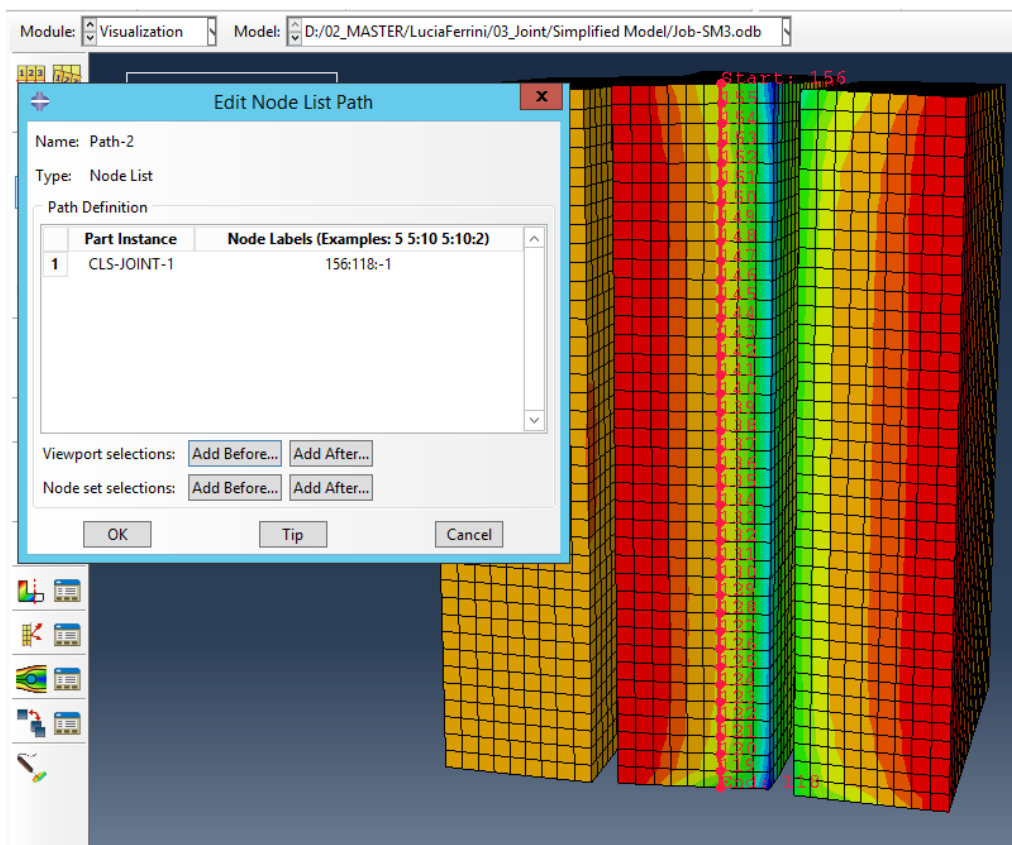


Figure 98 Path2

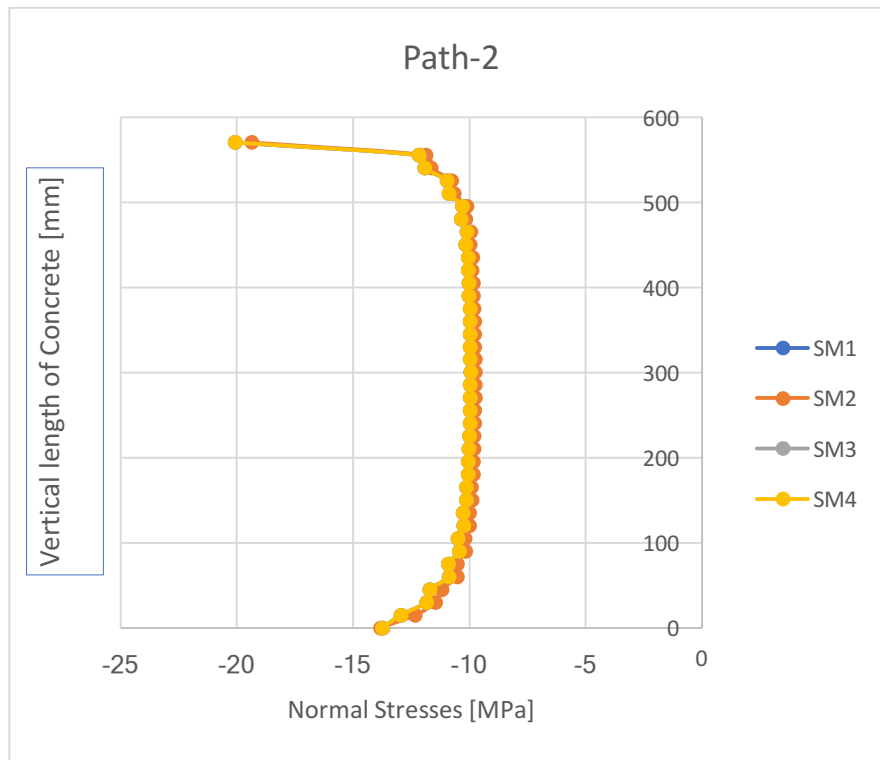


Figure 99 description of the stresses along the path-2

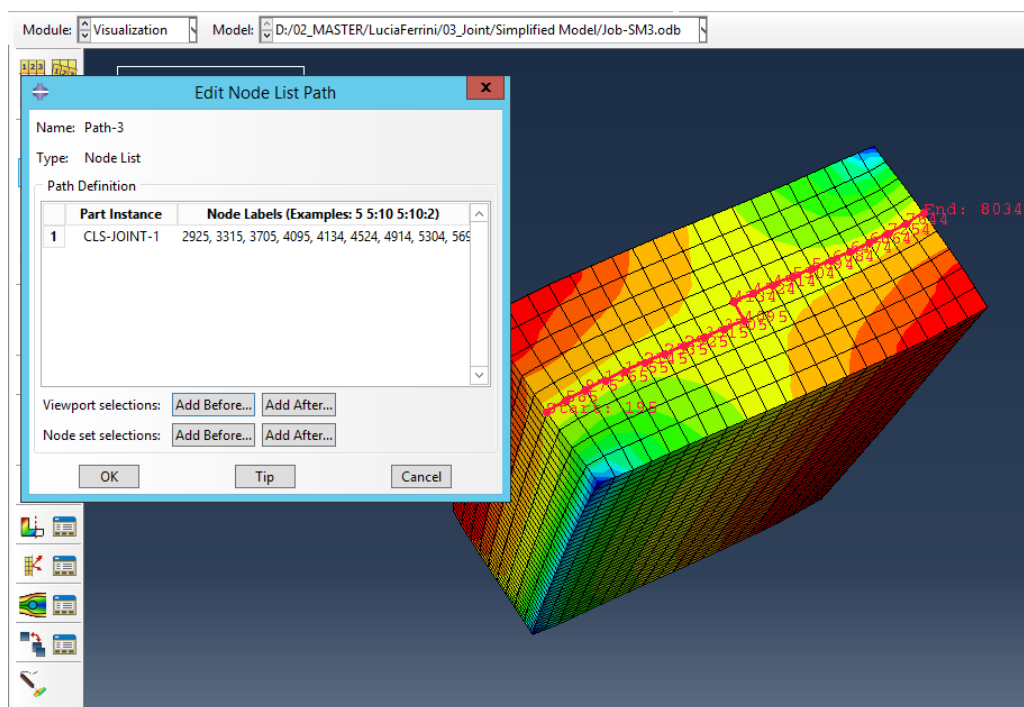


Figure 100 Path3

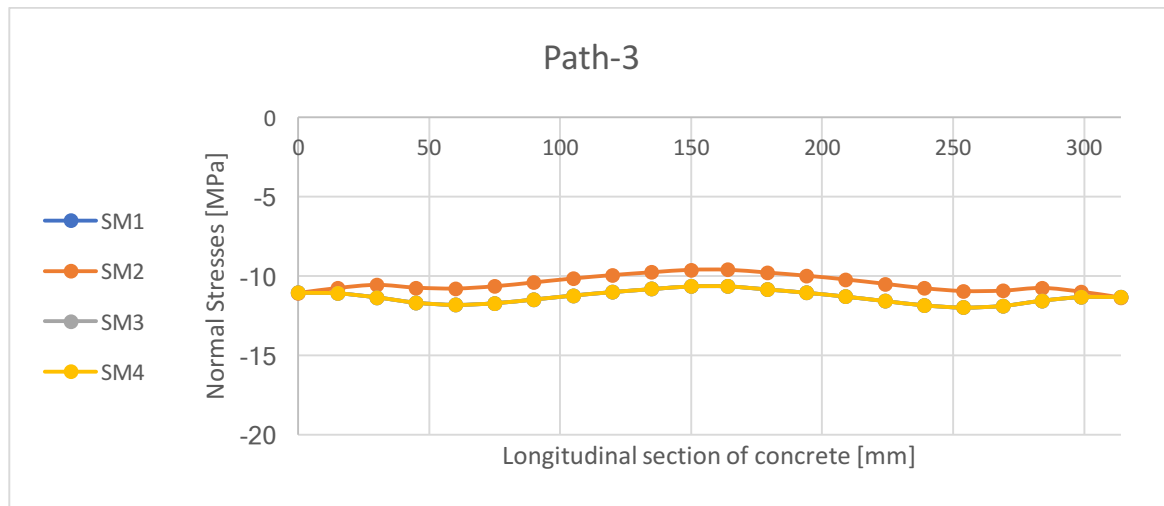


Figure 4 description of the stresses along the path-3

The first one is in the middle section of the concrete surface in contact with the T-flange, along the transversal axis, in order to underline how the stresses are spreading in the longitudinal direction. The second one is on the same surface but along the vertical axis and in a section far enough from the contact between the concrete and the T-web, to avoid some singularities. The third one is chosen on the bottom surface of concrete, in order to underline how the stress develops in the longitudinal direction. For each path and for each single simplified model introduced before, σ_{33} has been calculated and all the results are collected in three summary tables shown below. The numbers underline are the values far from the discontinuities regions: and they are really close to the values obtained by hand calculations. In fact, far enough from the D-regions, in each of the three paths under investigation the stresses are closed to $\sigma_{33} \sim (-)11 \text{ MPa}$.

4.4 Joint Basic Model

The basic model, the model 2 and the model 3 are investigated separately before of the comparison. In order to investigate all the effect, the following models are compared in the results chapter:

Model 1- Model 2: the comparison underlines the difference in the horizontal displacement between the two models and it shows the benefits of the presence of the new added part.

Model 1- Model 3: the comparison underlines the effect of the plastic investigation taking into account the same geometry.

Model 2- Model 4: the comparison underlines the effect of the increasing of the thickness of the T-web in an elastic analysis.

Model 3- Model 5: the comparison underlines the effect of the decreasing of the height of the T-web in a plastic analysis.

Model 5- Model 6: the comparison underlines the effect of the increasing of the thickness of the T-web in a plastic analysis.

4.4.1 Results of Basic Model: elastic analysis

The basic model is the one described above, with the same geometry thinking at the beginning of the studies. The analysis has been done in the elastic field.

4.4.1.1 Results on the steel: T-web behavior

It is possible to state that the behavior is different from the one estimated for the first approach. The hand calculation is now almost complete and so it is possible to analyzed Abaqus results. The behavior of the five T-webs is shown in the next picture and the graphical stresses limits were printed in the range from 0 to 355 MPa.

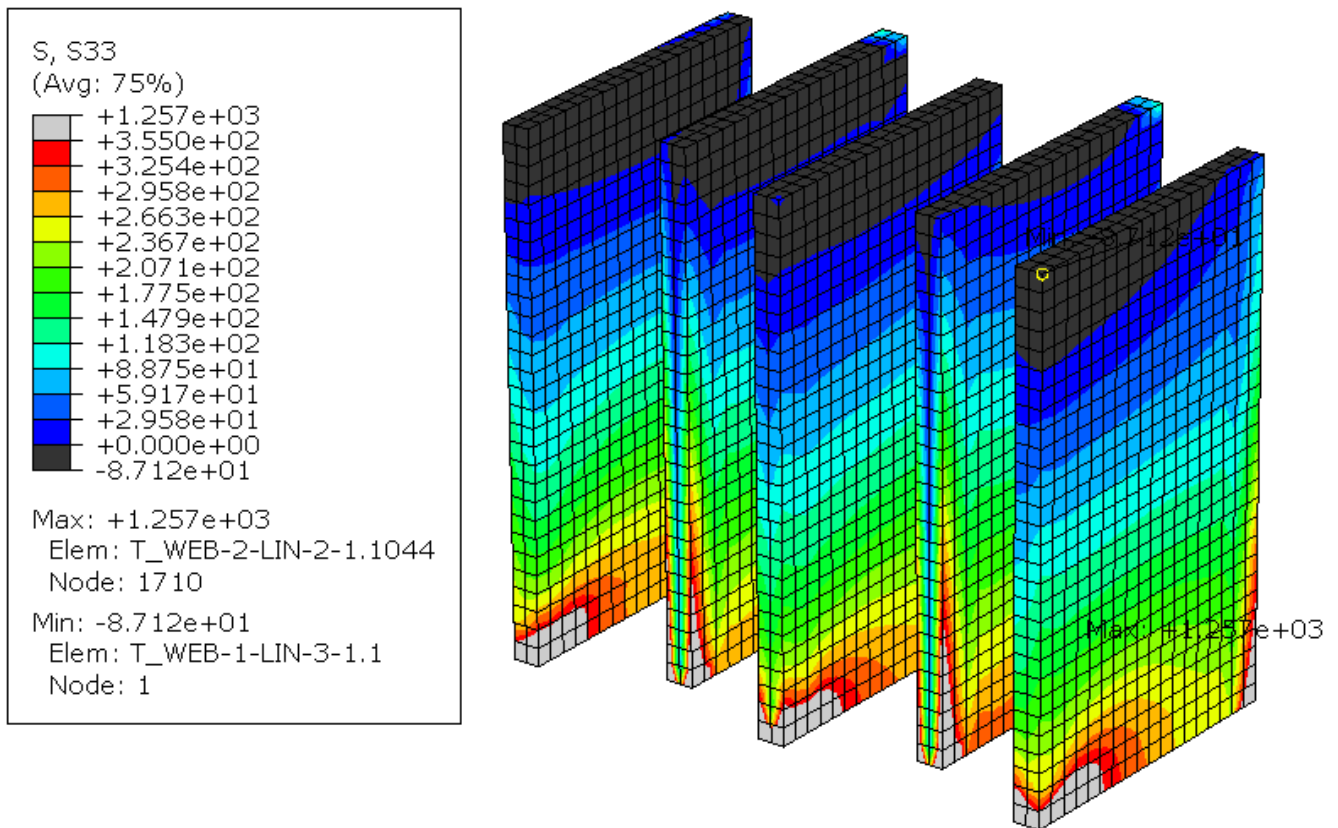


Figure 101 Upper limit of the stresses

In this picture, it is possible to see that the regions outside the upper limits are almost closed to the edges and so are nearby to some singularities points.

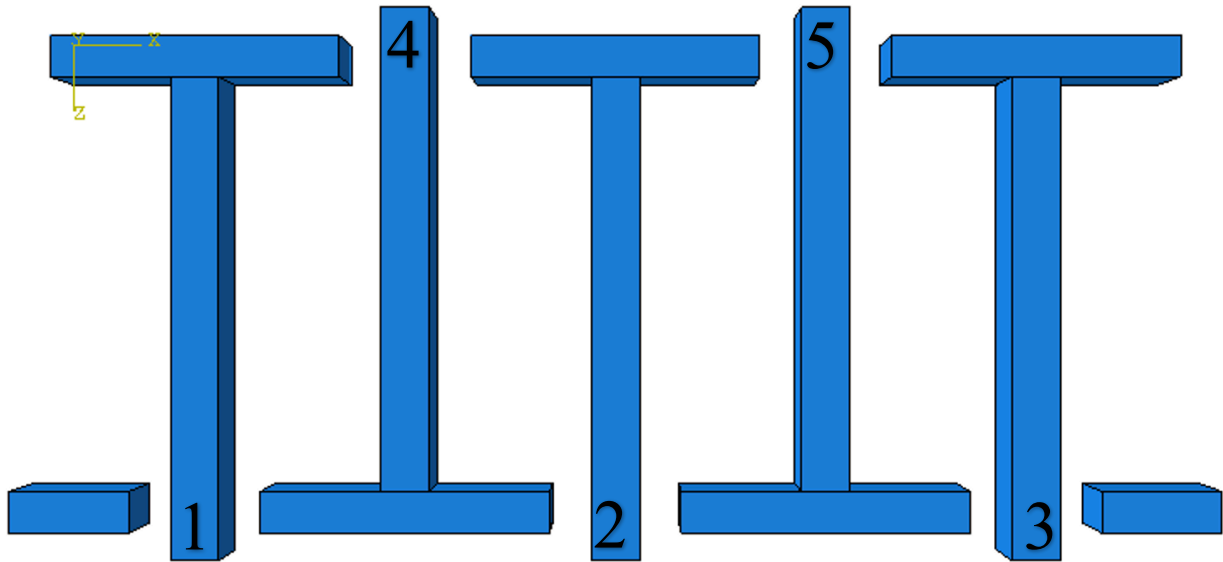


Figure 102 Numbering of the T-webs

This is an important thing, and probably these results can be perfected through a plastic analysis. However, in this chapter, it is important to give some numerical results. In order to do that, 5 paths have been determined in each of the T-web surfaces, far enough from the D-regions. The horizontal length is around 350 mm, and the concrete begins after 50 cm c.a. The path is considered to be in a section 6 cm away from the edge. Now, it is possible to compare the results obtained for each path and see the distribution of the stresses along the height of the T-web.

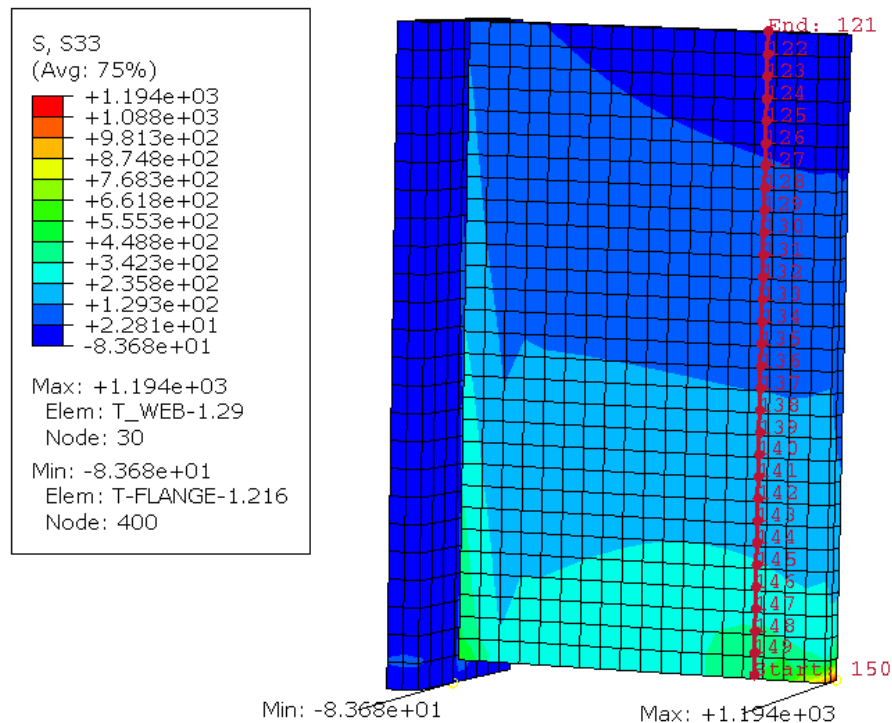


Figure 103 Chosen Path along the T-web height

The results of each T-web are compared in the following graph

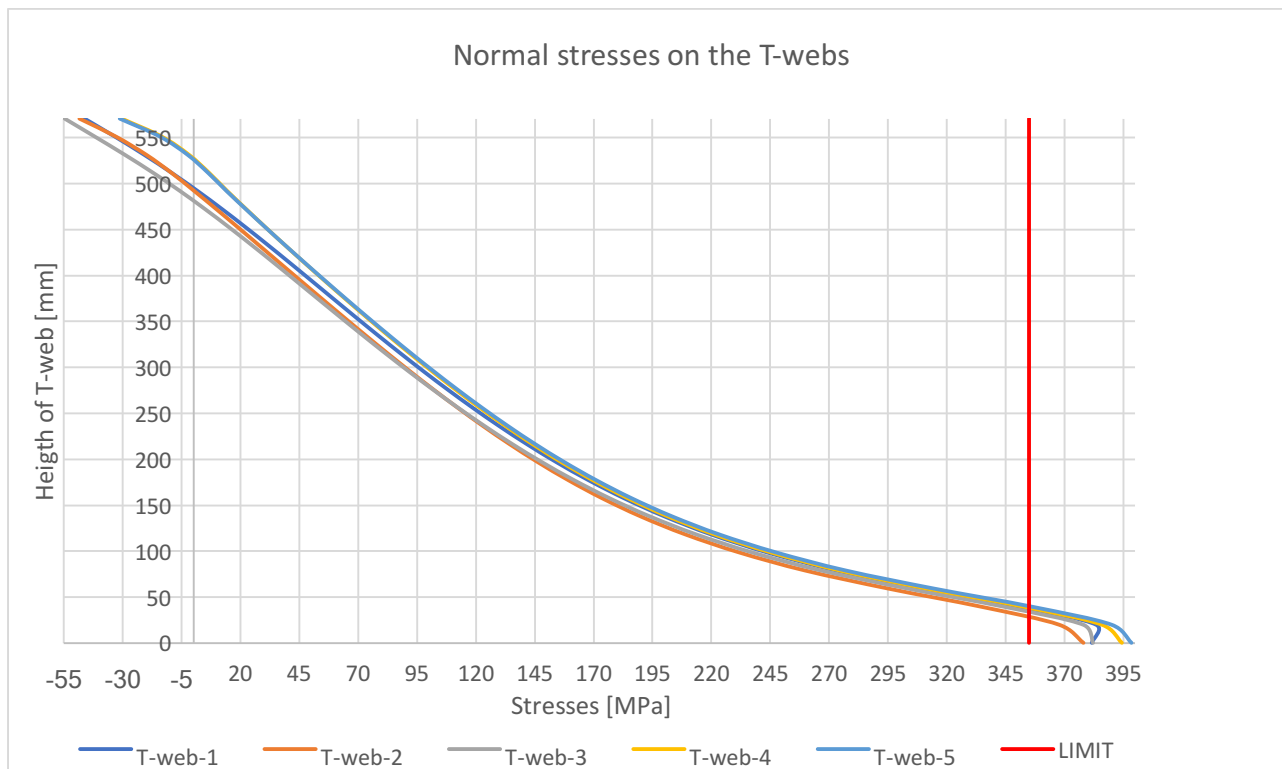


Figure 104 Comparison of the stresses on the T-webs

The results are numerically explained also through the following tabs:

Height T-web	Stresses [MPa]				
	Path1	Path2	Path3	Path4	Path5
0	381.754	378.023	382.041	394.373	398.471
19.6724	383.651	367.732	377.916	385.945	390.041
39.3448	350.814	334.508	344.134	352.589	356.1
59.0172	310.309	295.201	303.432	311.577	314.58
78.6897	273.33	259.845	266.578	274.517	277.086
98.3621	243.895	231.823	237.293	245.242	247.472
118.034	219.962	208.89	213.467	221.234	223.201
137.707	200.1	189.86	193.681	201.409	203.165
157.379	183.029	173.58	176.663	184.46	186.035
177.052	167.914	159.223	161.579	169.571	170.988
.....
.....
413.121	41.225	36.7911	34.3225	47.2777	47.3898
432.793	31.7858	27.802	24.7677	38.7776	38.7958
452.466	22.1397	18.7811	14.9775	30.4169	30.3389
472.138	12.1835	9.65499	4.83139	22.2436	22.0642

491.81	1.80369	0.322079	-5.79385	14.1974	13.9088
511.483	-9.1712	-9.30833	-17.1226	6.53749	6.1152
531.155	-20.8523	-20.023	-29.1944	-2.02108	-2.59764
550.828	-33.2383	-32.8444	-41.8549	-13.5169	-14.2491
570.5	-46.1888	-48.4208	-54.7175	-30.5987	-31.4354

It is possible to see that the red values are the one that overcome the yielded stress of the steel used. However, it is also possible to underline how the values are not so far from the upper limit:

$$ratio = \frac{\sigma_{33}}{f_{yd}} \approx \frac{388,451}{355} \approx 1.092$$

4.4.1.2 Results on the Concrete

Abaqus model is very important to describe the interaction between the T-stud and the concrete and to know how the stresses are actually distributed along the interface between the T-flange and the concrete. The results of the concrete are reported graphically before: the upper and the lower limits are settled according to Euro code.

$$F_{cd} = \alpha_{cc} * \frac{F_{ck}}{\gamma_c} = 85 \text{ MPa}$$

$$F_{ctd} = \alpha_{ct} * \frac{F_{ctk0.05}}{\gamma_c} = 6,67 \text{ MP}$$

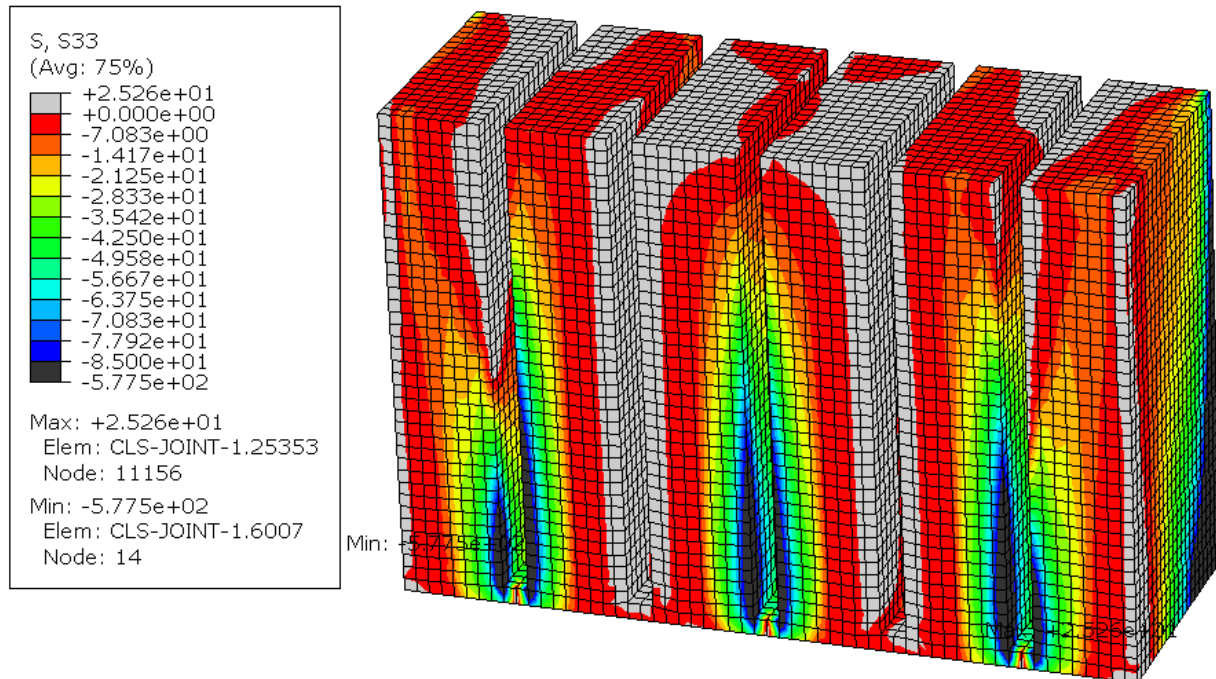


Figure 105 Compression Stresses on concrete

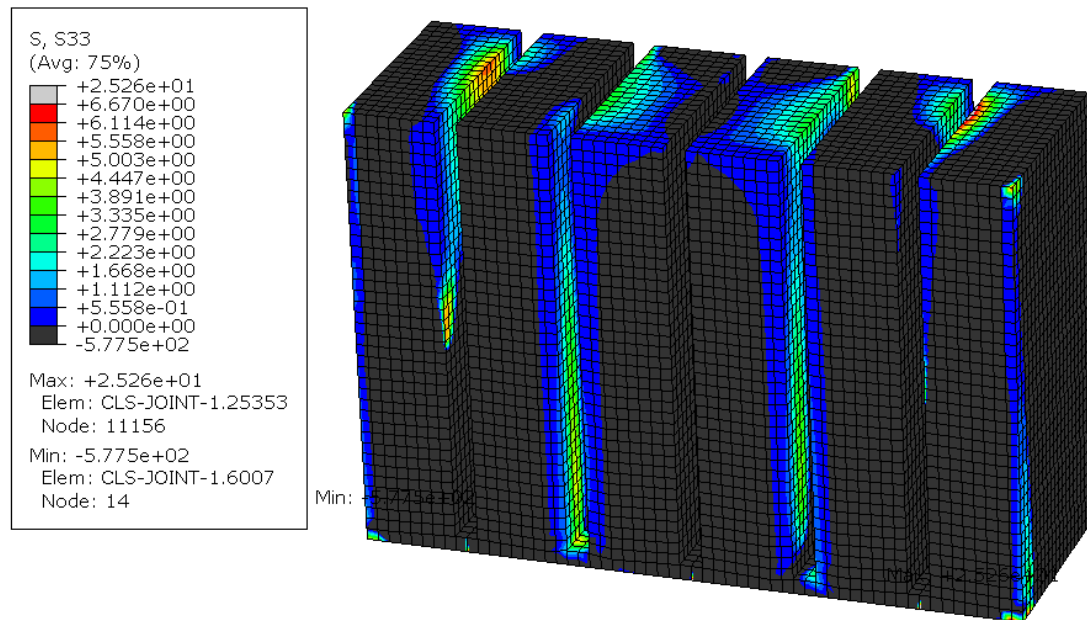


Figure 106 Tension Stresses on concrete

In this model, the concrete is modeled through elastic properties. As done in the simplified model, there are considered different paths along the vertical directions, the transversal direction and the longitudinal direction, in order to describe completely the stresses on the concrete. The vertical path is chosen up to a distance of 3 cm from the hole due to the T-web presence. The stresses on the vertical line are plotted as follow:

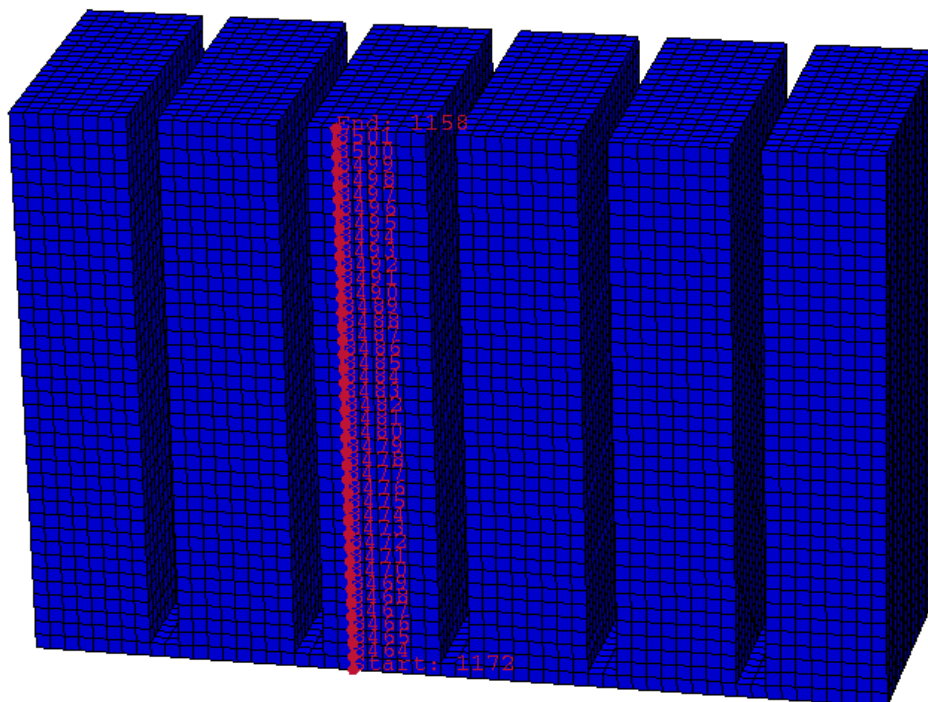


Figure 107 Vertical Path

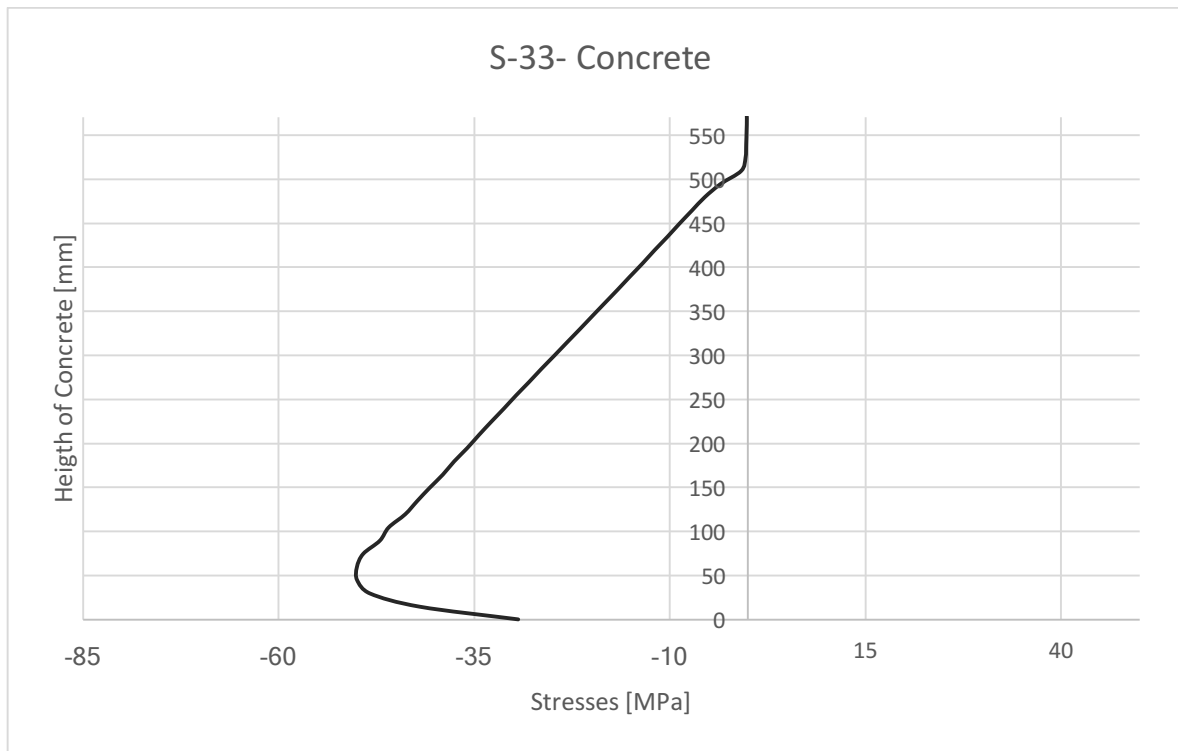


Figure 108 concrete distribution of normal stress

In this picture, it is important to underline why the stresses at the bottom are so smaller: this happens because in the bottom part, there is not anymore, the T-web because it ends before.

The horizontal path is chosen at a distance of 10 cm from the bottom surface. The graphical distribution of stresses in this horizontal section can be represented thanks to the command 'cut view' of Abaqus.

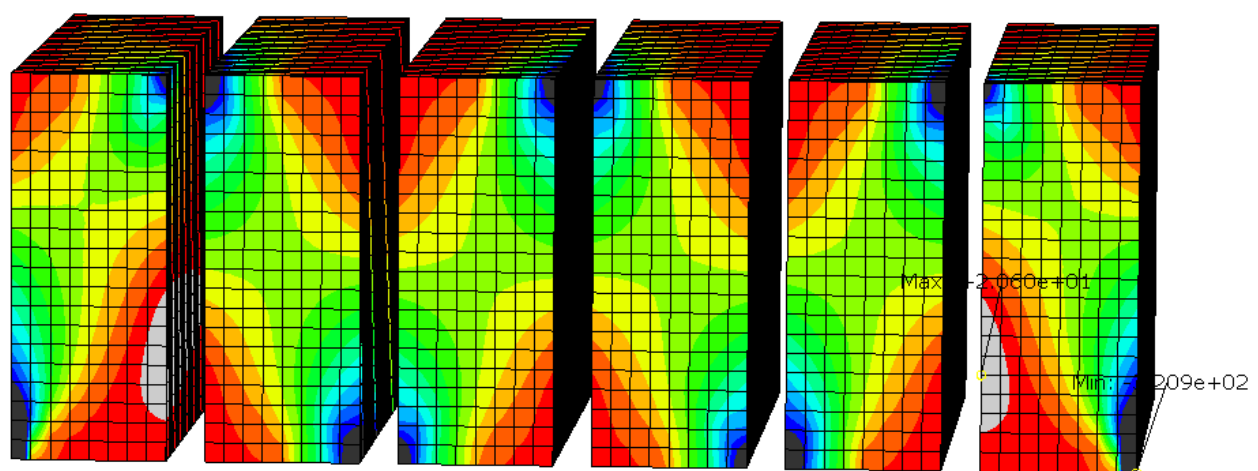


Figure 109 Horizontal Section y= 10 cm

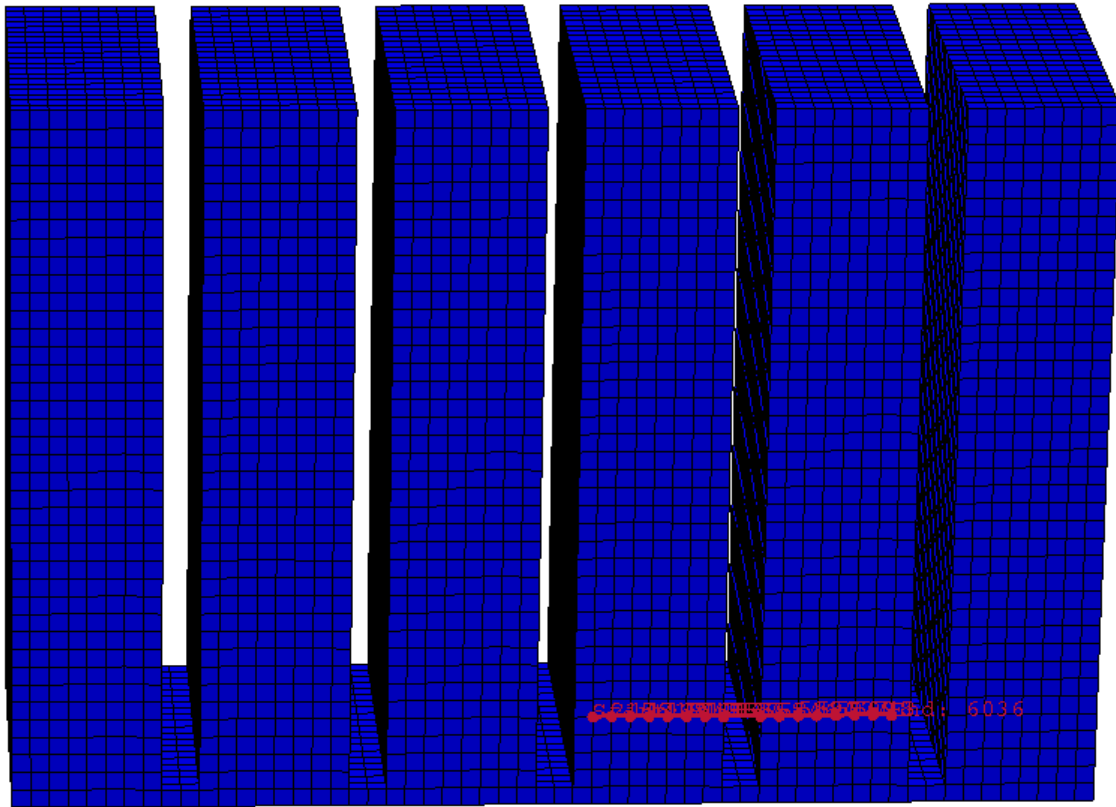


Figure 110 Path-7: in contact with the T-flange-5

The picture above it shows how the stresses are distributed along the contact surface between the T-flange and the concrete in the section mentioned before.

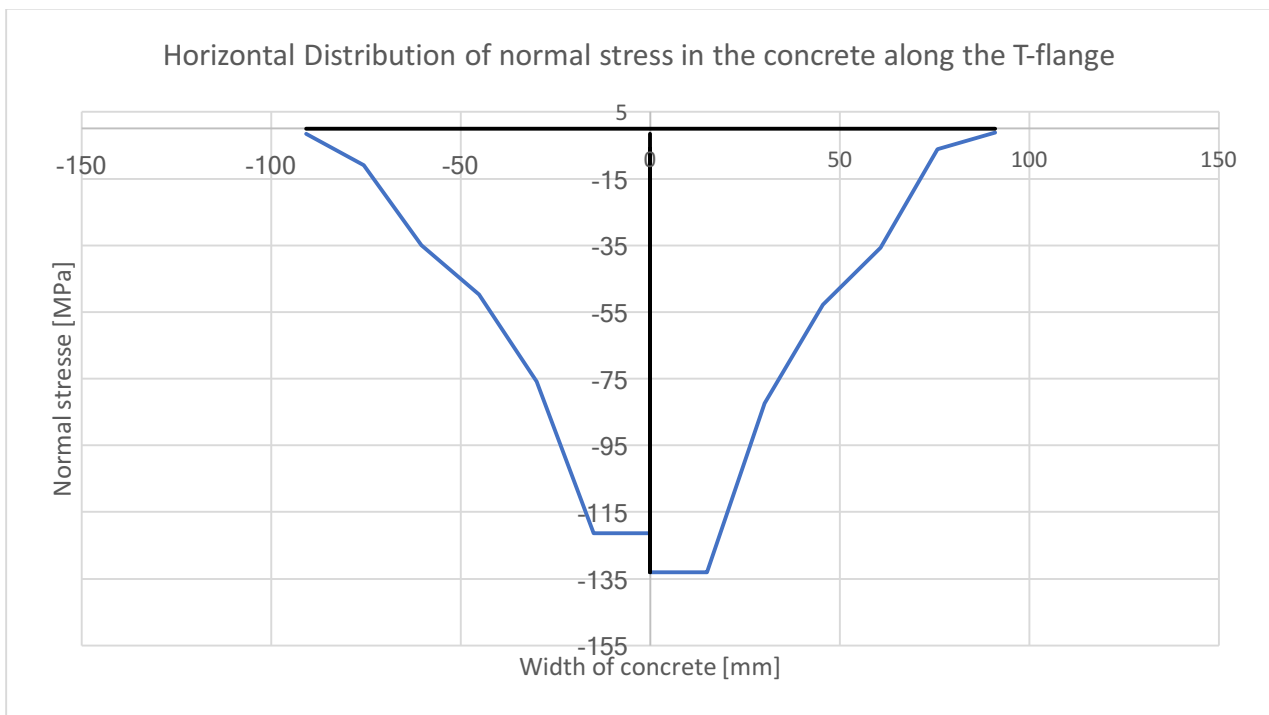


Figure 111 Stresses in the contact surface concrete-T-flange

Another relevant aspect is to investigate the horizontal displacement in the webs of the bridge due to the pressure exerted by the two half flanges at the borders, before the cut.

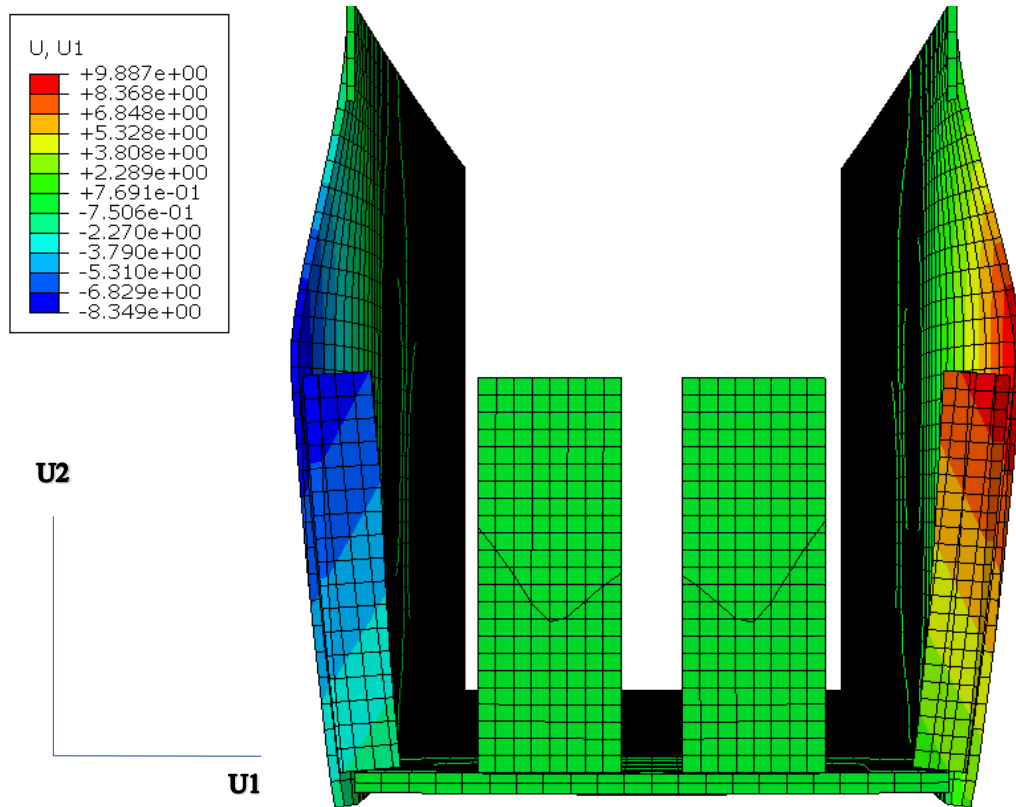


Figure 112 Horizontal displacement

4.4.2 Results of Model 2: Influence of the addition of horizontal stiffener

The most important result to investigate is the horizontal displacement of the webs near the cut region. As said before, the dimension of this horizontal stiffness as chosen according to the available space above the T-flange. In fact, the full height vertical stiffener nearby the T-flange does not allow it to be too deep. The dimensions are the following:

The thickness: $t_h = t_f + 2 * C$;

The length: $L_h = B_{tot}$;

The height: $h_h = C$;



Figure 113 Horizontal Stiffener

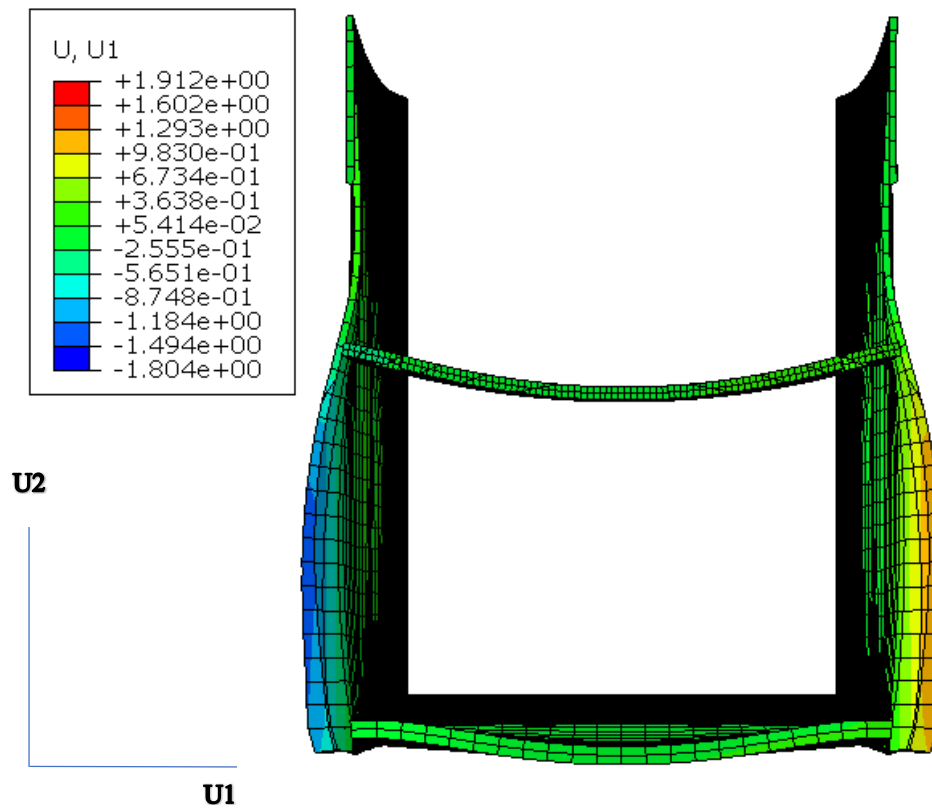


Figure 114 Horizontal displacement of the new model

It is possible now to compare numerically the results obtained:

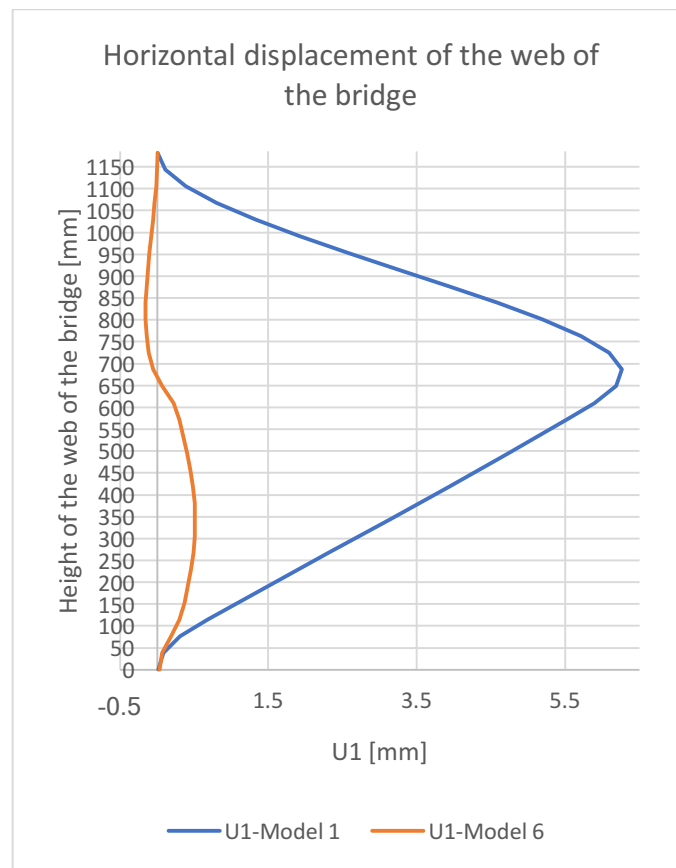


Figure 115 Comparison between the horizontal displacements

Height Web	Model-1	Model-6	Height Web	Model-1	Model-6
0	0.0194381	0.0321842	610.09	5.89128	0.221578
38.1306	0.0862692	0.0675543	648.22	6.18371	0.069371
76.2612	0.308407	0.187832	686.351	6.26445	-0.0508727
114.392	0.684966	0.299185	724.482	6.08835	-0.111021
152.522	1.0882	0.366193	762.612	5.71171	-0.141758
190.653	1.48769	0.416488	800.743	5.19578	-0.153972
228.784	1.89422	0.458492	838.873	4.58835	-0.152414
266.914	2.30514	0.489406	877.004	3.92777	-0.140933
305.045	2.71712	0.507484	915.135	3.24538	-0.122792
343.176	3.12774	0.512386	953.265	2.56792	-0.100686
381.306	3.53556	0.504139	991.396	1.9196	-0.0768037
419.437	3.93952	0.481902	1029.53	1.32382	-0.0529889
533.829	5.12578	0.355563	1143.92	0.10938	0.000779125
571.959	5.51374	0.30235	1182.05	0.00874669	0.00728943

In the first case, the maximum horizontal displacement is $U_{1Max} = 6,26 \text{ mm}$ and it is collocated more or less in the middle of the available height, between the two fixed points of the web of the bridge. In the second case the maximum $U_{1Max} = 0.512 \text{ mm}$ is located in the middle of the T-flange height.

4.4.3 Results of Model 3: plastic analysis

4.4.3.1 Results on the steel: T-web behavior

The graphical visualization allows to see some important effect in the model under plastic analysis.

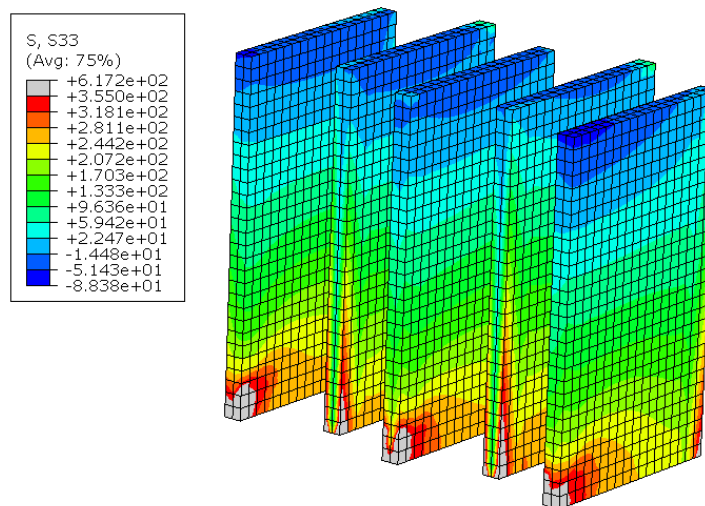


Figure 116 Normal stresses under the upper limit on the T-webs

The same analysis operation has been done in this chapter and for this model: the same paths have been studied, in a graphical way before and in a numerical way after, in order to compare the difference between these two models.

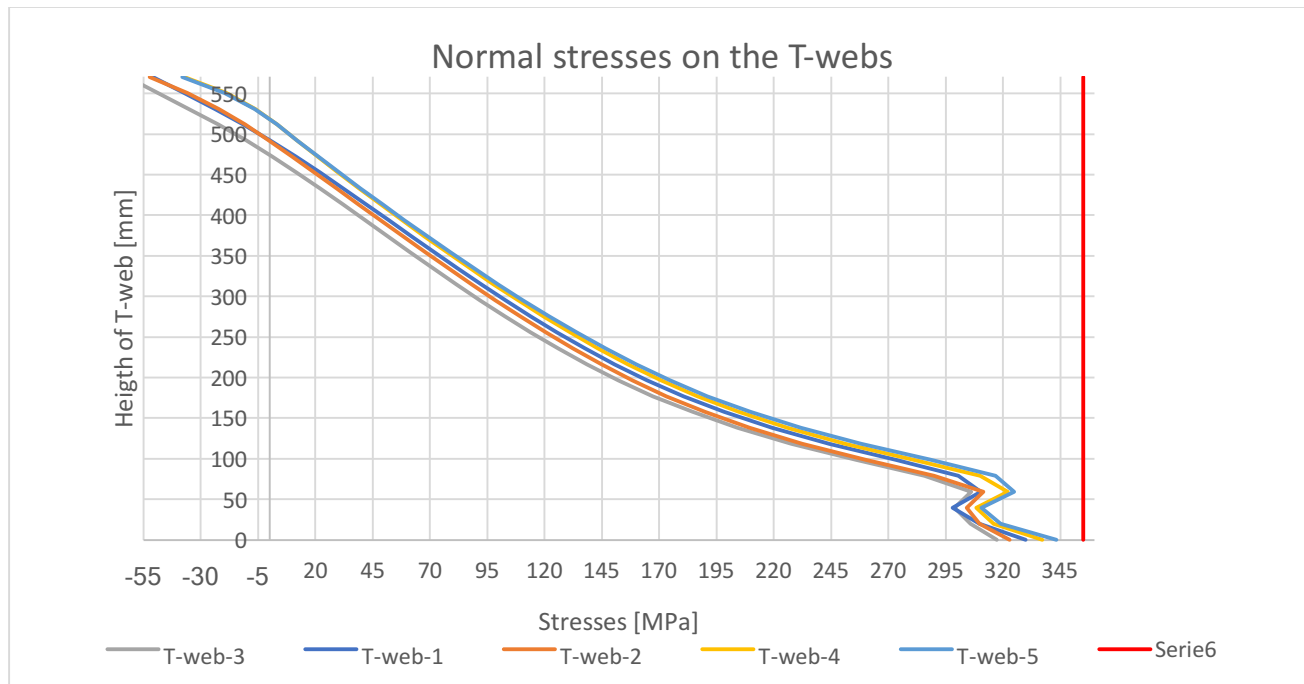


Figure 117 Normal Stresses on the T-webs

It is possible now to have a look at the numerical results:

Height T-web	Stresses [MPa]				
	Path1	Path2	Path3	Path4	Path5
0	329.933	323.007	317.238	337.257	343.385
19.6724	309.902	309.913	305.757	316.013	318.879
39.3448	297.956	304.208	298.977	308.432	310.519
59.0172	310.255	311.561	306.096	322.015	324.86
78.6897	300.702	289.881	285.709	309.949	316.742
98.3621	273.304	260.027	255.802	280.941	288.532
118.034	244.011	232.323	227.611	251.211	257.99
137.707	219.251	209.346	204.211	226.008	231.8
157.379	198.426	189.979	184.482	204.824	209.83
177.052	180.563	173.209	167.418	186.741	191.126
.....
511.483	-11.455	-10.6358	-22.3267	3.36051	3.19409
531.155	-23.9519	-22.1003	-35.1985	-6.1839	-6.59951
550.828	-37.2231	-35.7849	-48.6518	-18.8015	-19.5143
570.5	-51.0842	-52.3937	-62.1236	-37.1542	-38.2048

It is possible now to compare the results of the two most loaded T-webs analyzed under elastic and plastic conditions. In both model, the T-web 5 is the most loaded:

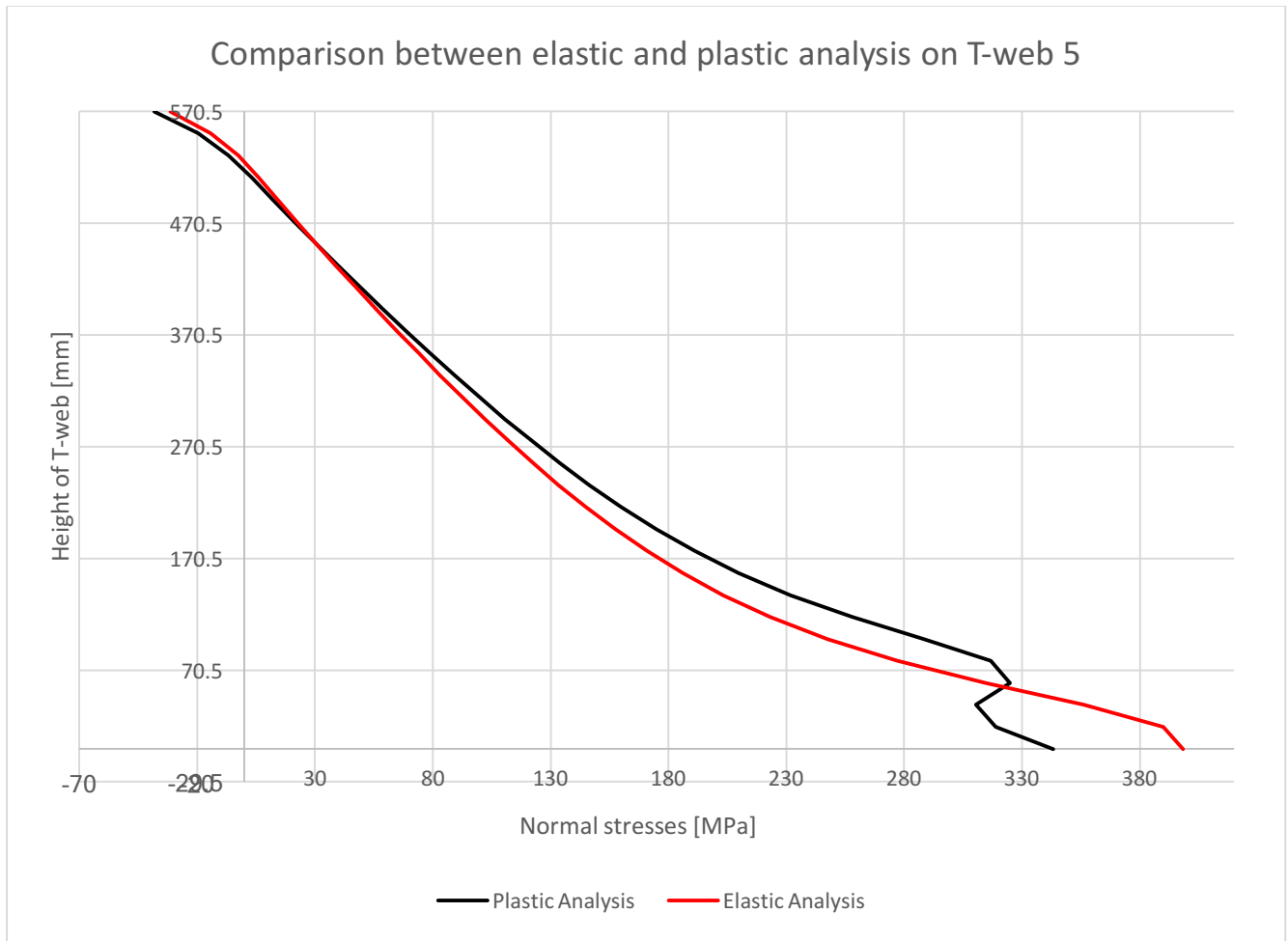


Figure 118 Comparison between elastic and plastic analysis

H-web	5-EL [MPa]	5-PS [MPa]	Decrease %
0	398.471	343.385	13.82
19.6724	390.041	318.879	18.24
39.3448	356.1	310.519	12.80
59.0172	314.58	324.86	-3.27
78.6897	277.086	316.742	-14.31
98.3621	247.472	288.532	-16.59
118.034	223.201	257.99	-15.59
137.707	203.165	231.8	-14.09
157.379	186.035	209.83	-12.79
177.052	170.988	191.126	-11.78
196.724	157.439	174.71	-10.97

From this numerical comparison, it is possible to notice that the biggest difference, according to the expectations, are in the first 20 cm from the bottom surface, in contact with the concrete. The decrease in the lower part is around the 13% in the model under plastic analysis.

4.4.3.2 Results on the Concrete

The same investigation of the model 1, is done in the concrete of this second model. The same procedure is adopted and the same limits are used.

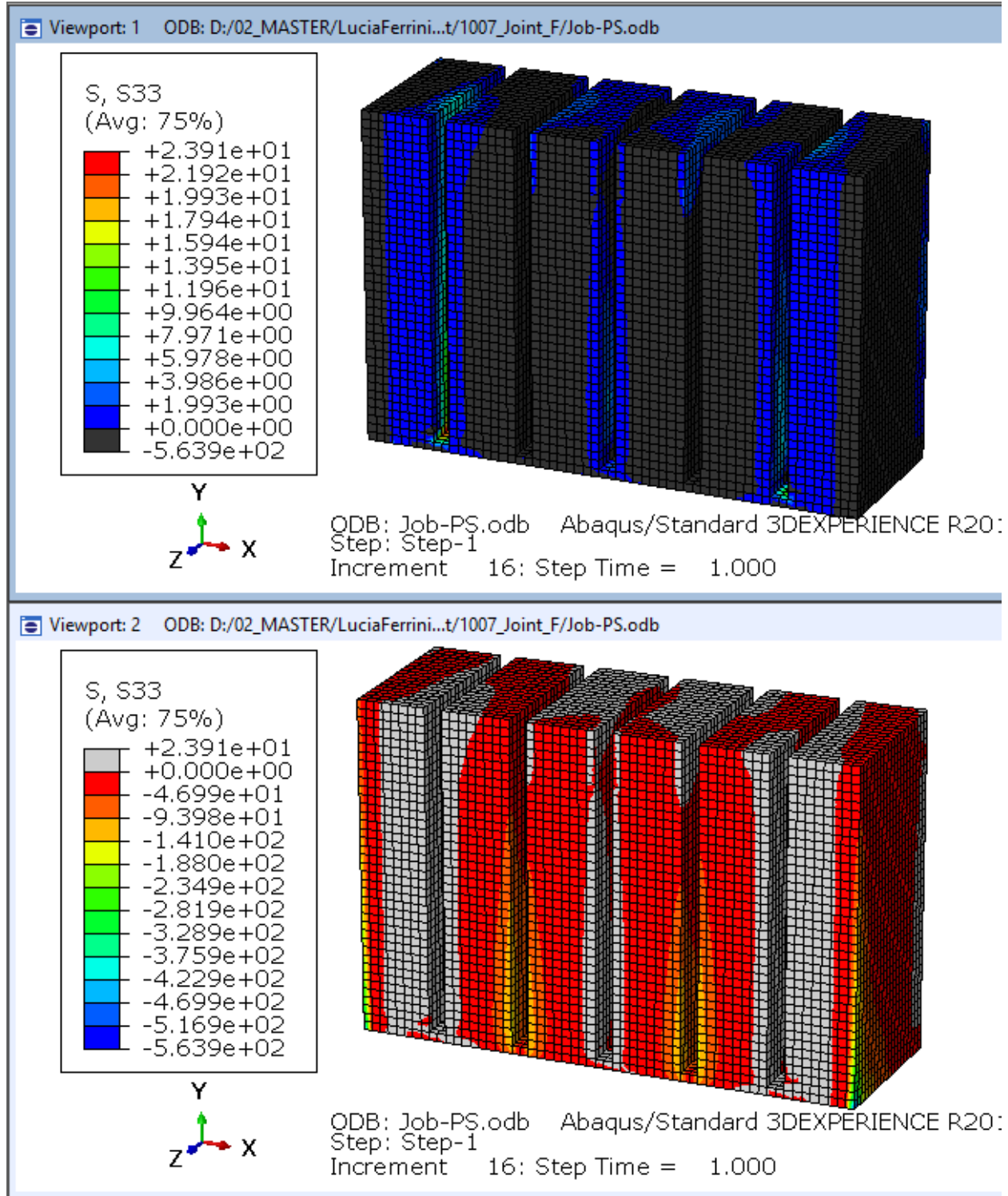


Figure 119 Compressive regions of concrete and tensile part

The same paths on concrete are chosen: the vertical one and the horizontal.

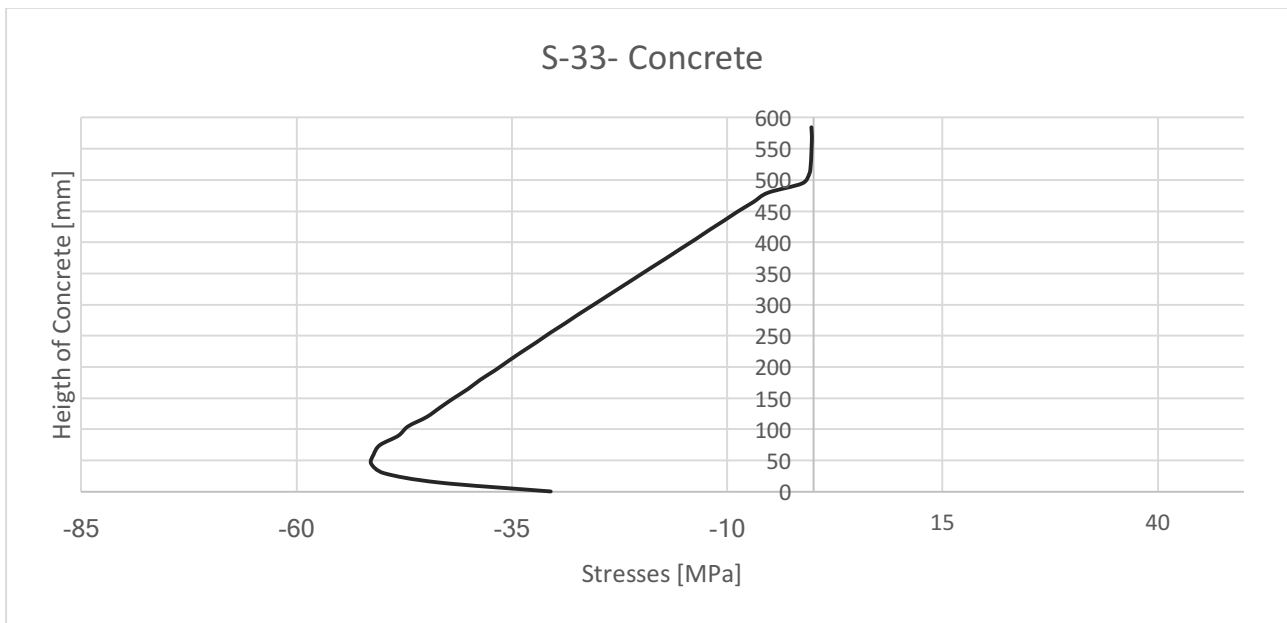


Figure 120 Normal stresses on the vertical path of concrete

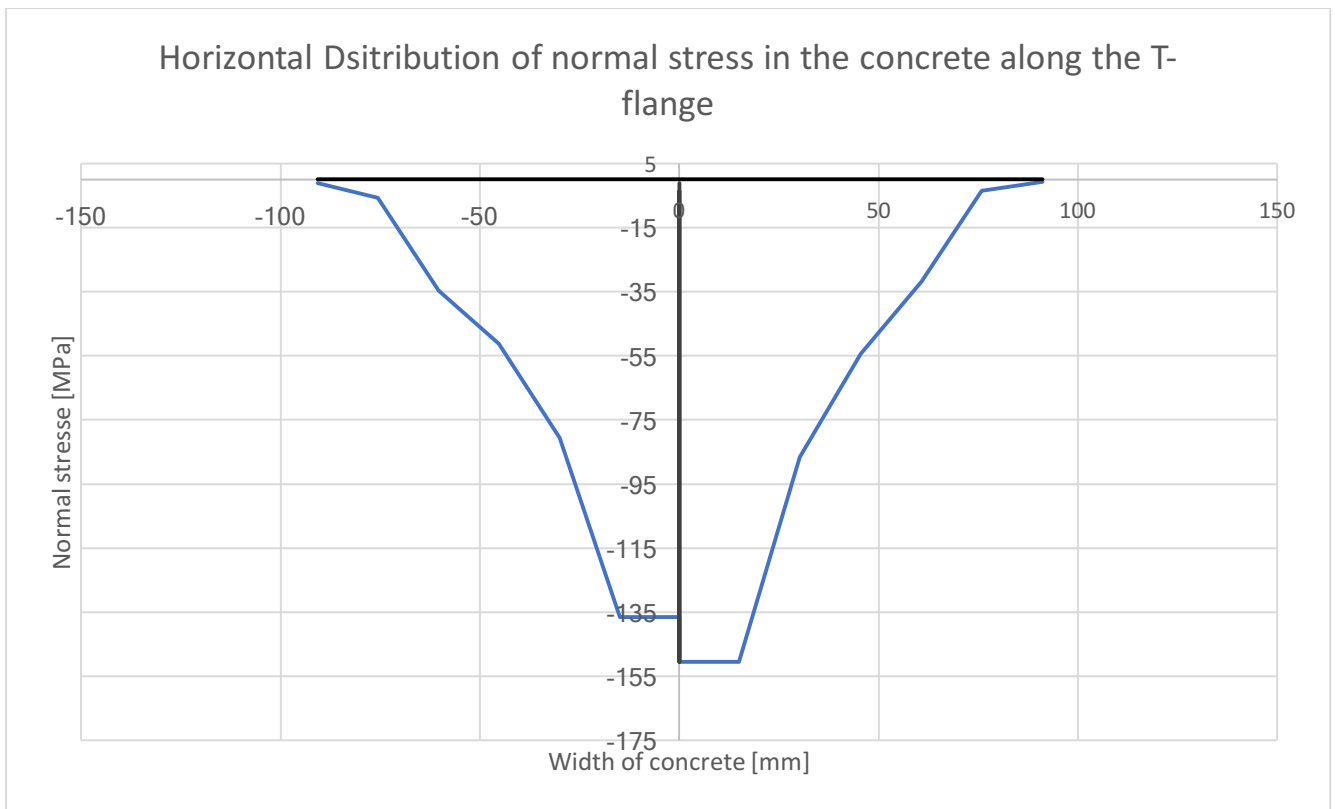


Figure 121 Horizontal distribution of stresses in the contact surface between T-flange and concrete

4.4.4 Model1-Model4: Influence of t_w in the elastic analysis

4.4.4.1 Comparison of normal stresses on the steel

The same paths are investigated under the same limits, to underline what are the regions of the model affected by some singularities and which parts are overcome the yielding stresses of material. The comparison between these two models is useful to investigate how the stresses are affected by change in the thickness size in elastic analysis. The stresses on the T-web 1, 2 and 5 are investigated and compared to the results obtained in the model 2:

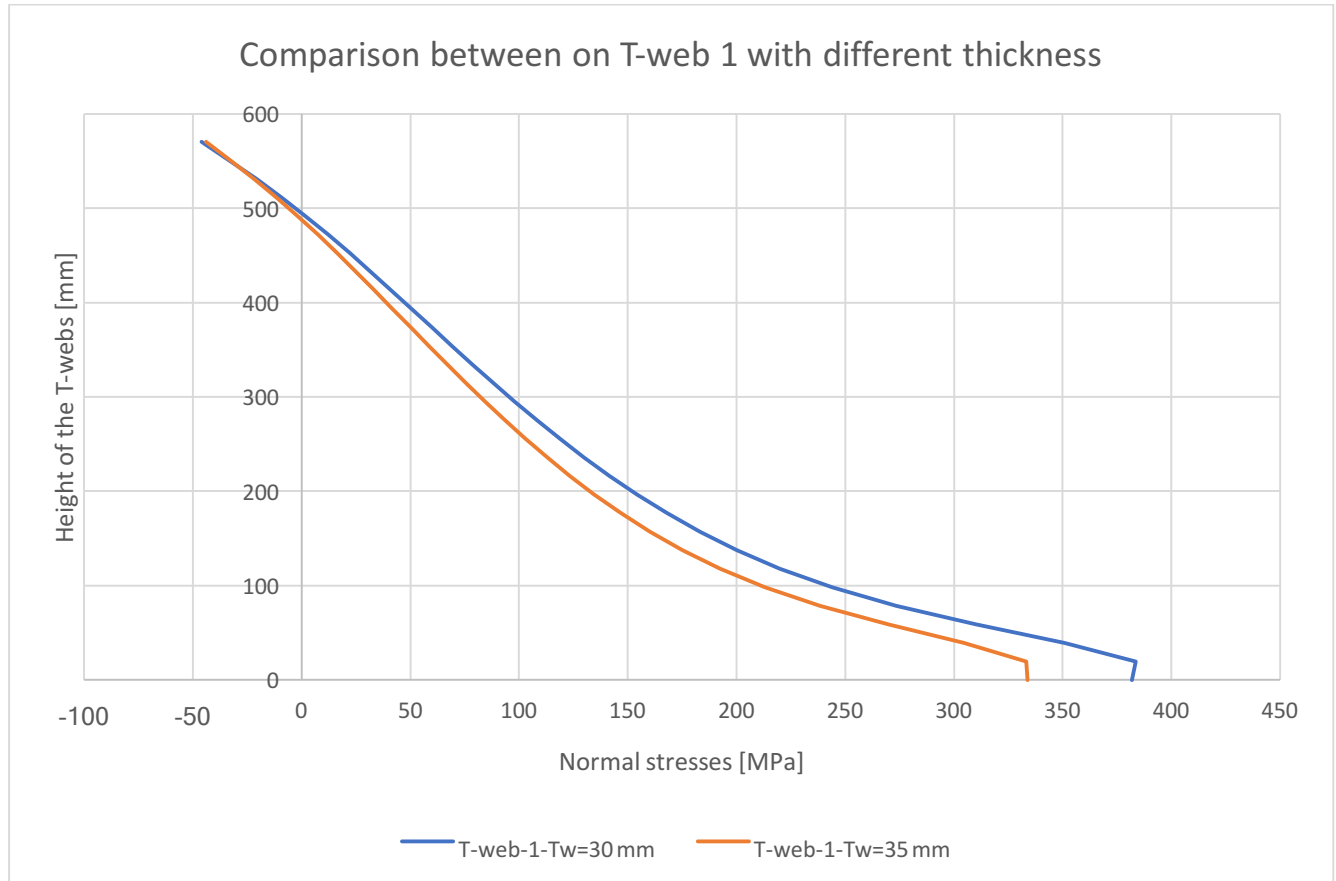


Figure 122 Comparison of stresses on the T-webs

Height T-web	Stresses [Mpa]		
	T-web-1-Model1	T-web-1-Model-4	Decrease %
0	381.754	333.893	12.5
19.6724	383.651	333.289	13.1
39.3448	350.814	304.756	13.1
59.0172	310.309	269.934	13.0
78.6897	273.33	238.346	12.8
98.3621	243.895	213.121	12.6
118.034	219.962	192.396	12.5
137.707	200.1	175.05	12.5
157.379	183.029	160.062	12.5
177.052	167.914	146.726	12.6
196.724	154.235	134.603	12.7

216.397	141.645	123.403	12.9
354.103	69.1485	58.4909	15.4
373.776	59.8295	50.1292	16.2
393.448	50.5459	41.8035	17.3
413.121	41.225	33.4503	18.9
432.793	31.7858	24.9986	21.4
452.466	22.1397	16.3694	26.1
531.155	-20.8523	-22.008	5.5
550.828	-33.2383	-32.9221	1.0
570.5	-46.1888	-44.0964	4.5

The numerical results show a decrease of the normal stresses inside the T-webs around the 14%. It is an expected consequence of the increase of the thickness:

$$\sigma_1 = \frac{F_M}{t_{w1} * h_w} + \frac{6 * M}{t_{w1} * h_w^2} \quad \sigma_4 = \frac{F_M}{t_{w2} * h_w} + \frac{6 * M}{t_{w2} * h_w^2}$$

$$\frac{\sigma_1}{\sigma_4} = \frac{\frac{F_M}{t_{w1} * h_w} + \frac{6 * M}{t_{w1} * h_w^2}}{\frac{F_M}{t_{w2} * h_w} + \frac{6 * M}{t_{w2} * h_w^2}} = \frac{F_M * h_w + 6 * M}{t_{w1} * h_w^2} * \frac{t_{w2} * h_w^2}{F_M * h_w + 6 * M} \approx \frac{t_{w2}}{t_{w1}}$$

This relation implies:

$$\sigma_4 \approx \frac{t_{w1}}{t_{w2}} \sigma_1 \approx \frac{30}{35} \sigma_1 \approx 0.857 \sigma_1$$

The theoretical formulation estimates a difference between the two stresses around the 15%.

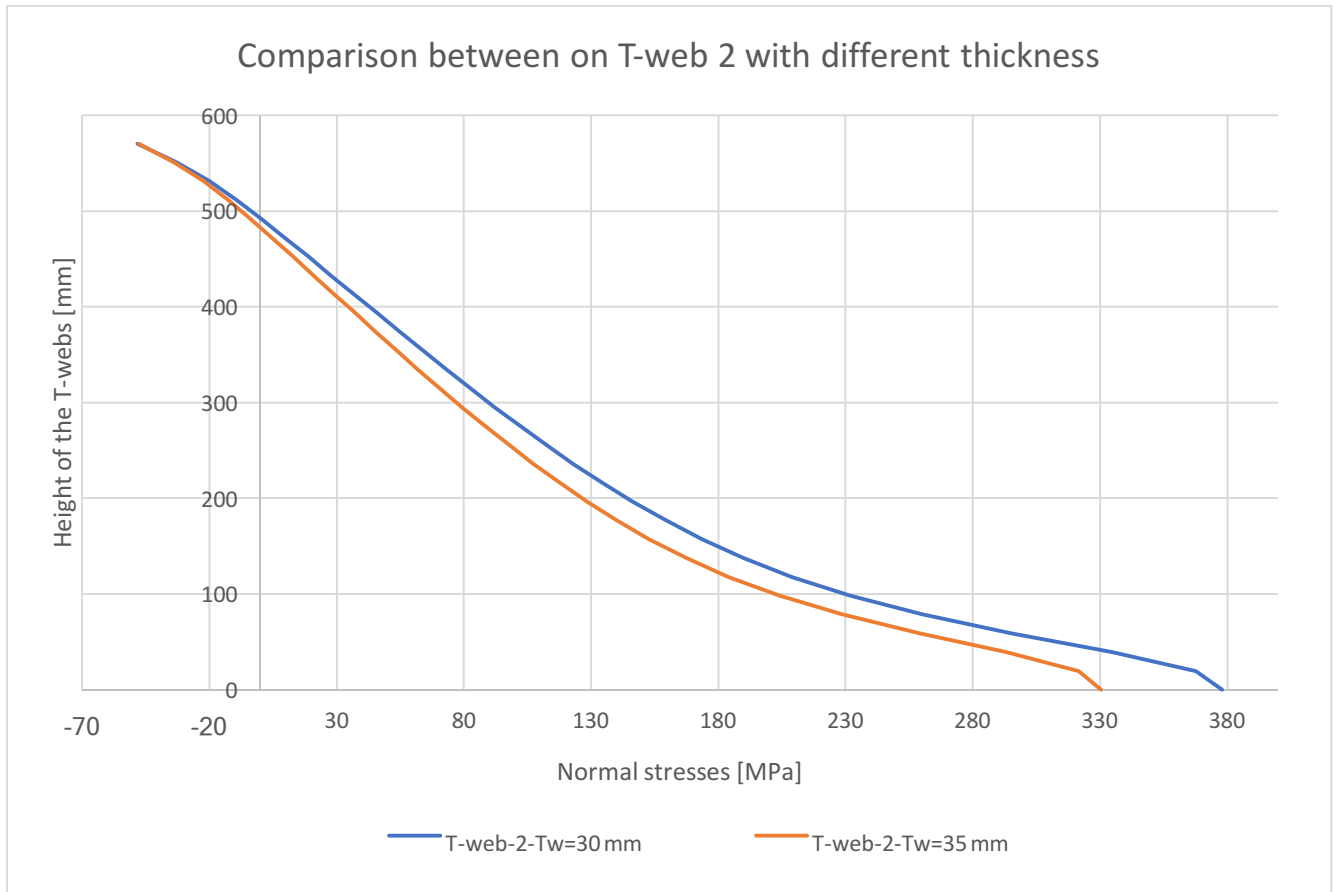


Figure 123 Comparison of the stresses according to the thickness of the web

Height T-web	Stresses [MPa]		
	T-web-2-Model1	T-web-2-Model-4	Decrease %
0	378.023	330.533	12.6
19.6724	367.732	321.645	12.5
39.3448	334.508	293.039	12.4
59.0172	295.201	259.13	12.2
78.6897	259.845	228.518	12.1
98.3621	231.823	204.146	11.9
118.034	208.89	184.081	11.9
137.707	189.86	167.306	11.9
157.379	173.58	152.845	11.9
177.052	159.223	139.973	12.1
196.724	146.208	128.247	12.3
216.397	134.187	117.411	12.5
236.069	122.938	107.229	12.8
255.741	112.293	97.5415	13.1
275.414	102.092	88.2584	13.6
295.086	92.2116	79.2917	14.0
.....
550.828	-32.8444	-33.8873	-3.2
570.5	-48.4208	-47.7675	1.3

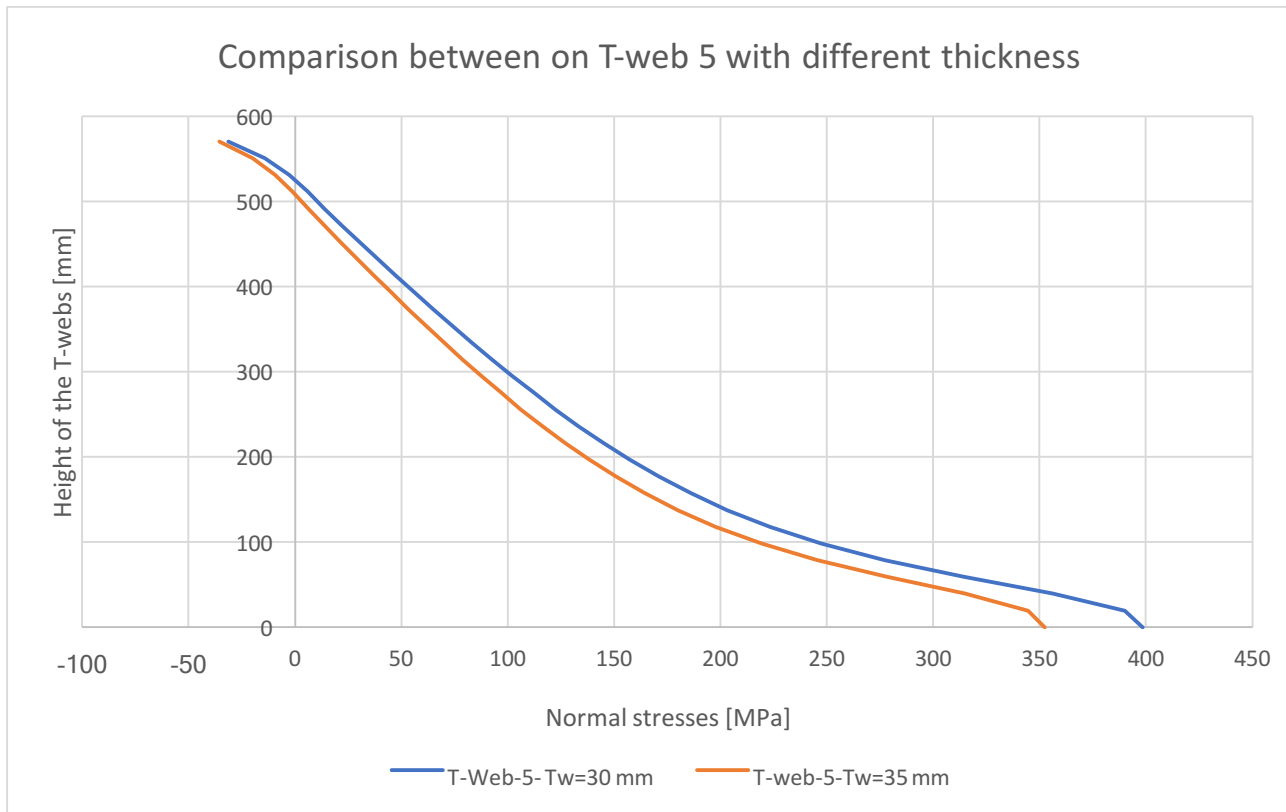


Figure 124 Comparison of the stresses according to the thickness of the web

The numerical results are commented below, comparing the most stressed bracket:

Height T-web	Stresses [MPa]		
	T-web-5-Model1	T-web-5-Model-4	Decrease %
0	398.471	352.371	11.6
19.6724	390.041	344.635	11.6
39.3448	356.1	314.904	11.6
59.0172	314.58	278.526	11.5
78.6897	277.086	245.582	11.4
98.3621	247.472	219.442	11.3
118.034	223.201	197.839	11.4
137.707	203.165	179.864	11.5
157.379	186.035	164.401	11.6
177.052	170.988	150.746	11.8
196.724	157.439	138.396	12.1
216.397	145.019	127.032	12.4
236.069	133.455	116.42	12.8
255.741	122.55	106.39	13.2
275.414	112.158	96.8148	13.7
295.086	102.175	87.6057	14.3
314.759	92.5218	78.694	14.9
334.431	83.1352	70.0255	15.8
354.103	73.9623	61.5551	16.8

The benefits of increasing the thickness of the T-webs are shown respect to the lower part of the section, in which the stresses difference is around the 12 %, and this difference is decreasing, going up to the top.

4.4.4.2 Comparison of normal stresses on the concrete

Two different paths are analyzed in this chapter: the vertical and the horizontal one.

$$\sigma_1^- = -121.387 \text{ MPa} \quad \sigma_1^+ = -133.034 \text{ MPa}$$

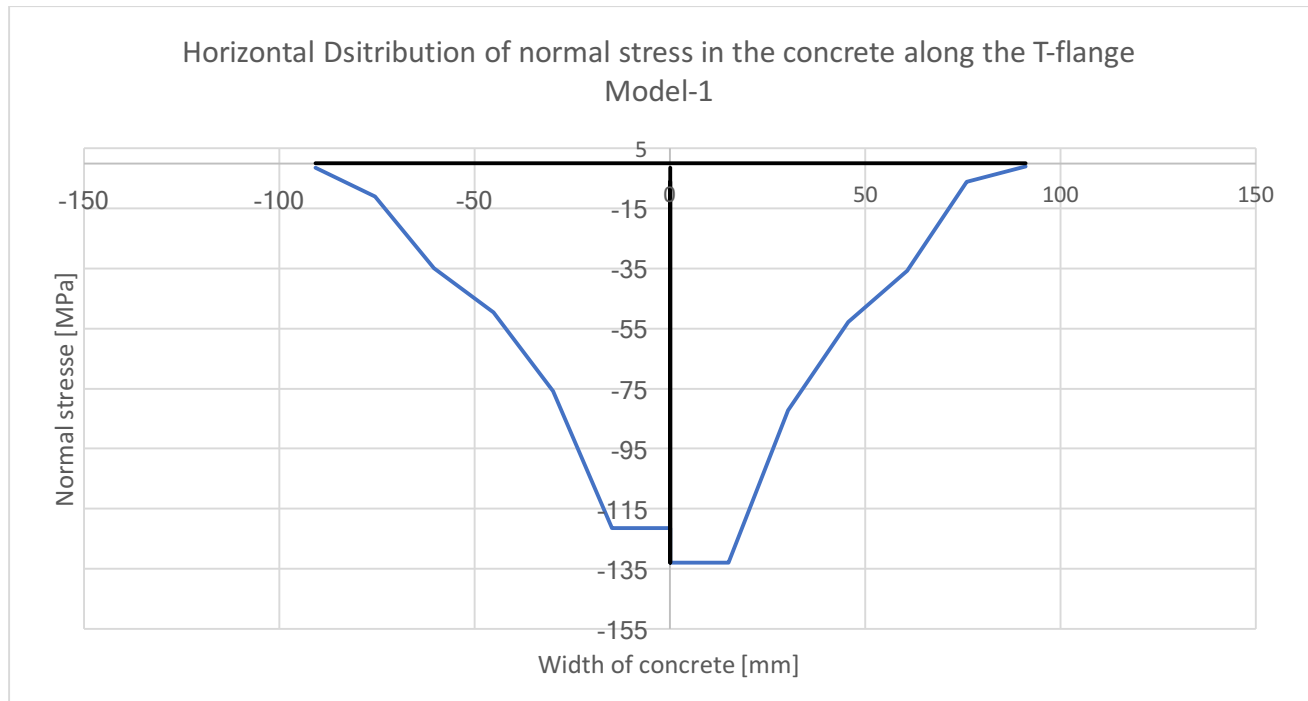


Figure 125 Horizontal distribution

$$\sigma_4^- = -139.66 \text{ MPa} \quad \sigma_4^+ = -152.76 \text{ MPa}$$

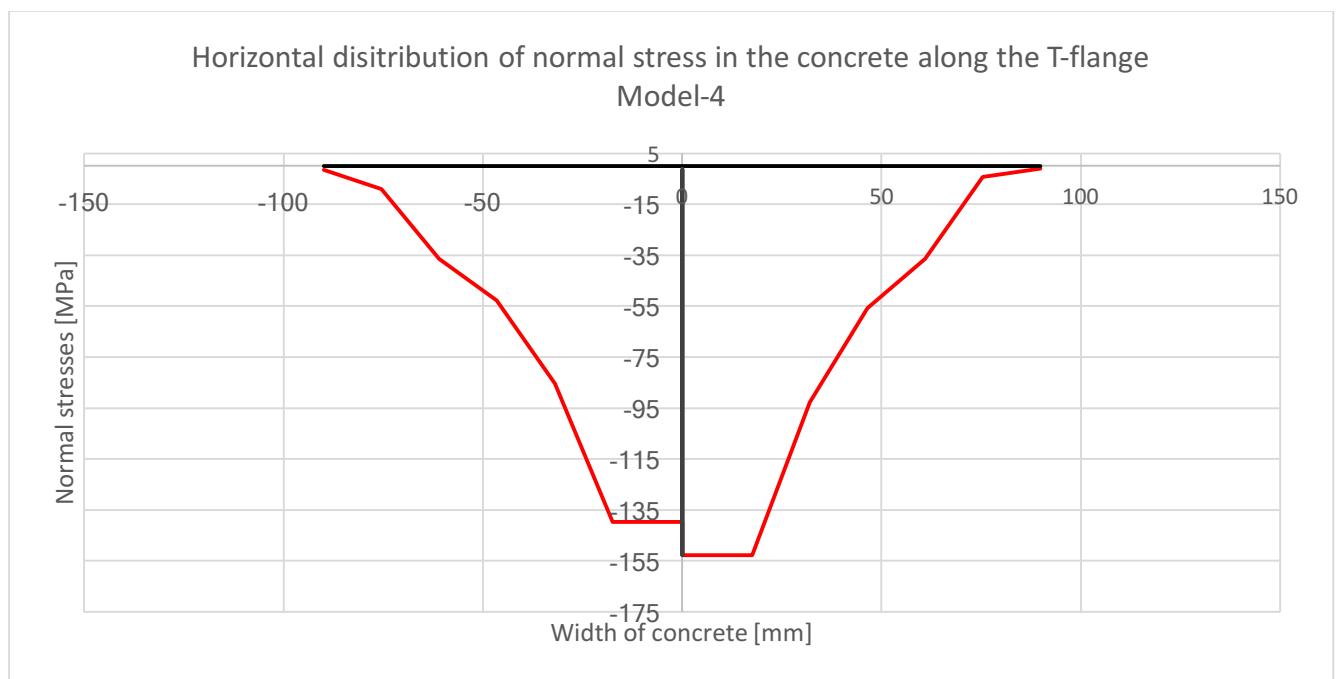


Figure 126 Stresses at the interface between concrete and T-flange

The vertical path is instead investigated in comparison with what happened in the previous model:

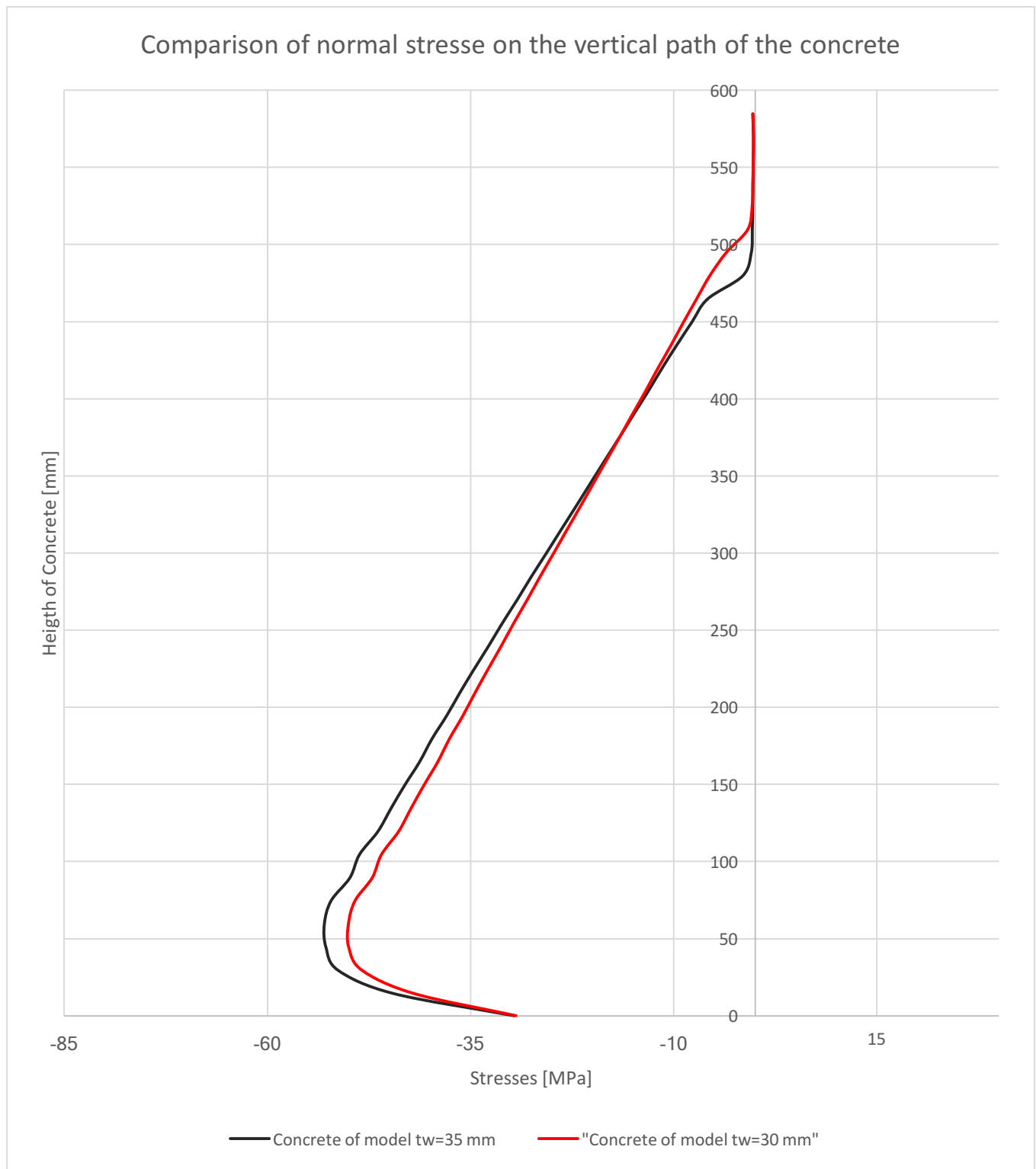


Figure 127 Comparison of stresses on concrete

As shown in the picture, the stresses on the concrete in this model are reduced. Let's introduce also the numerical comparison.

Height T-web	Stresses [MPa]		
	Concrete Model-1	Concrete Model-4	Increase %
0	-29.4058	-29.667	0.9
19.6724	-41.9573	-44.4854	6.0
39.3448	-48.3274	-51.287	6.1
59.0172	-49.9739	-52.7939	5.6
78.6897	-50.0106	-52.9867	6.0
98.3621	-49.2119	-52.169	6.0
118.034	-47.08	-49.842	5.9
137.707	-45.9538	-48.6661	5.9
157.379	-43.8364	-46.395	5.8
177.052	-42.3092	-44.7772	5.8
196.724	-40.7201	-43.0957	5.8
....
550.828	-11.9695	-11.4505	-4.3
570.5	-10.3497	-9.64243	-6.8

The stresses are increasing in the bottom region and decreasing a bit in the top direction. However, it is possible to say that the changes in concrete stresses are not so relevant. From this comparison, it is possible to state that the change of the thickness has beneficial effect on the stresses of the T-webs: its increment has benefits on the order of the 15% on the normal stresses in the bottom region of the steel. On the other side, it is possible to say that the effect on the concrete stress is more or less irrelevant: it does not help, of course, but not in a relevant way. This discovery is in accordance with the initial expectations: the stresses in concrete are highly dependent on other geometric parameters, B_j and L_j .

4.4.5 Model3-Model5: Influence of hw in the plastic analysis

4.4.5.1 Comparison of normal stresses on the steel

The models 3 and 5 have the same thickness of the webs, but different heights. Both the models are investigated under plastic behavior. The comparison between these two models is useful to investigate how the stresses are affected by change in the height size.



Figure 128 Comparison of stresses on T-web-1

Height T-web	Stresses [MPa]		
	T-web-1-Model-3	T-web-1-Model-5	Increase %
0	329.933	357.358	8.3
20	309.902	332.981	7.4
40	297.956	304.867	2.3
60	310.255	320.669	3.4
80	300.702	321.193	6.8
100	273.304	297.058	8.7
120	244.011	262.336	7.5
140	219.251	231.892	5.8
160	198.426	206.198	3.9
180	180.563	184.04	1.9
200	164.828	164.272	-0.3
220	150.637	146.059	-3.0
240	137.598	128.801	-6.4

Numerical results show a maximum around 9% of increase of the stresses in the lower region of the T-web-1. They also show that the compressive stresses on the top is lower than the maximum compressive stress reach at the top of the T-web with the bigger height.

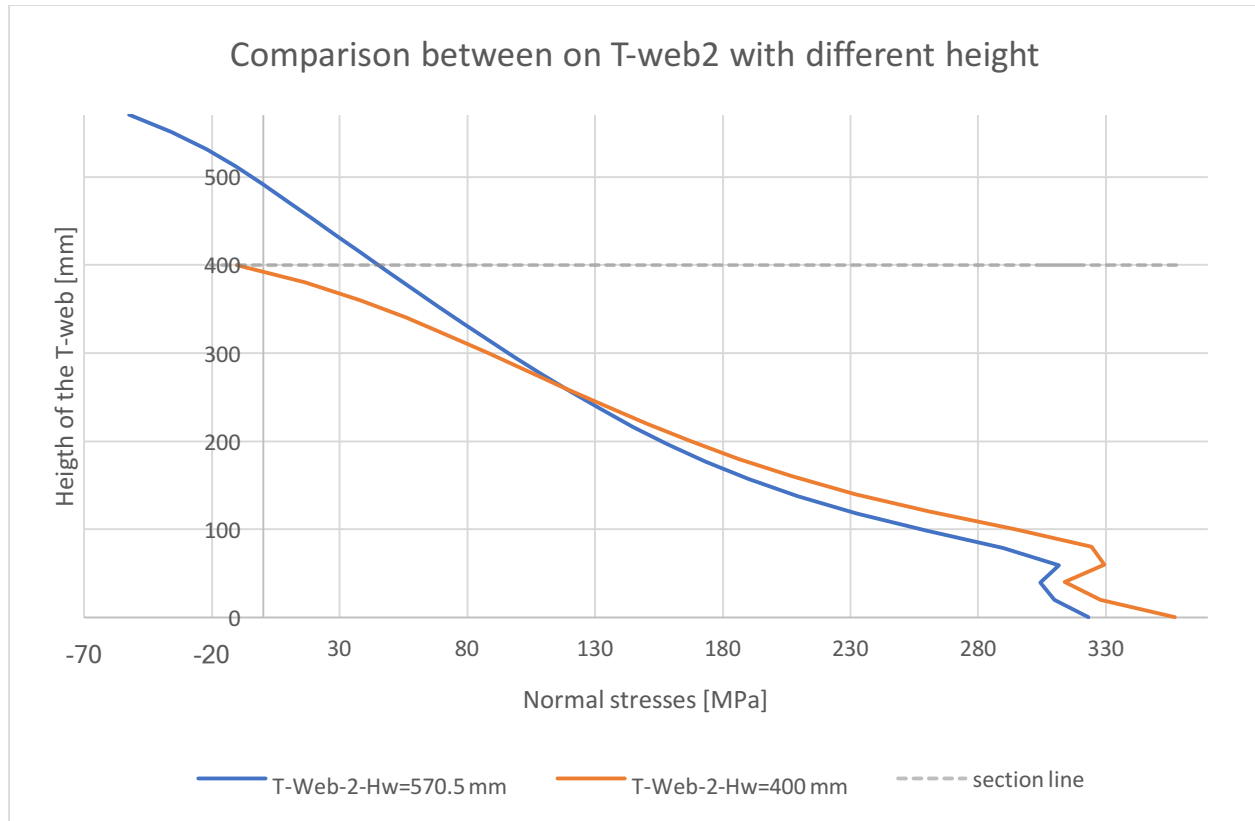


Figure 129 Comparison of stresses on T-web-2

	Stresses [MPa]		
Height T-web	T-web-2-Model-3	T-web-2-Model-5	Increase %
0	323.007	356.961	10.5
20	309.913	327.916	5.8
40	304.208	313.964	3.2
60	311.561	329.389	5.7
80	289.881	324.264	11.9
100	260.027	294.707	13.3
120	232.323	260.931	12.3
140	209.346	231.885	10.8
160	189.979	207.414	9.2
180	173.209	186.333	7.6
200	158.312	167.562	5.8

Numerical results show a maximum around 11% of increase of the stresses in the lower region of the T-web-2.

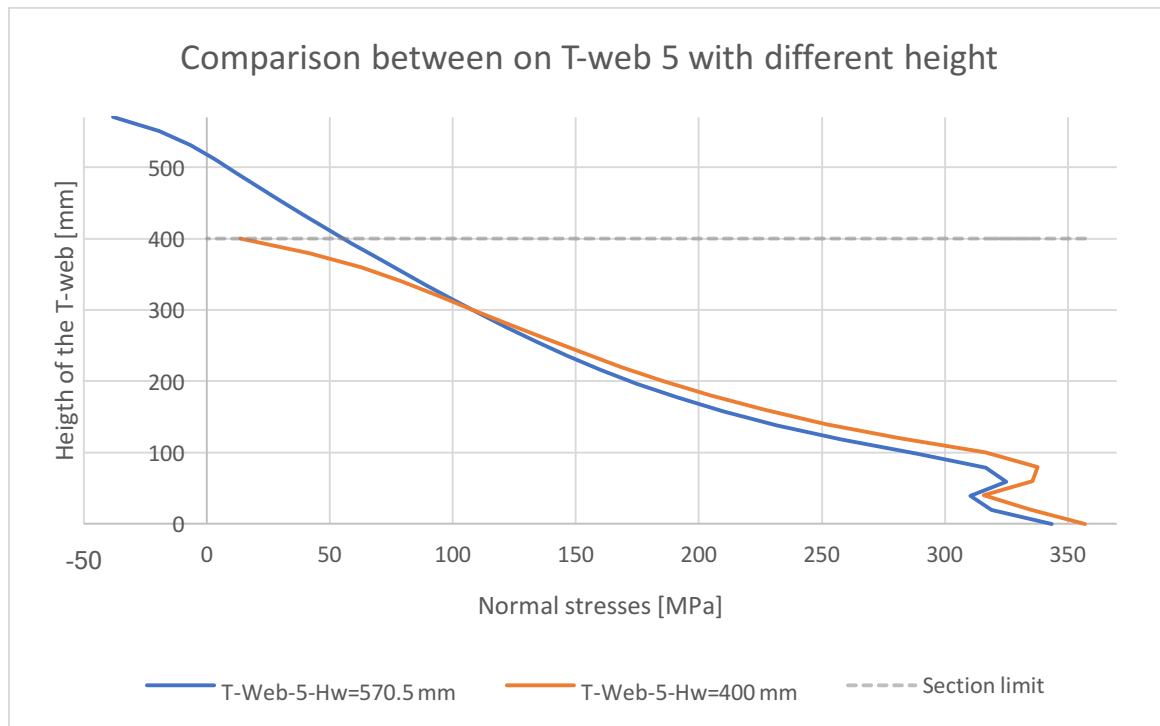


Figure 130 Comparison of the stresses on the T-web-5

Height T-web	Stresses [MPa]		
	T-web-5-Model-3	T-web-5-Model-5	Increase %
0	343.385	356.959	4.0
20	318.879	334.415	4.9
40	310.519	315.949	1.7
60	324.86	335.729	3.3
80	316.742	337.727	6.6
100	288.532	316.273	9.6
120	257.99	281.827	9.2
140	231.8	251.551	8.5
160	209.83	226.211	7.8
180	191.126	204.684	7.1
200	174.71	185.743	6.3
220	159.978	168.596	5.4
240	146.474	152.634	4.2
260	133.892	137.458	2.7

Numerical results show a maximum around 10% of increase of the stresses in the lower region of the T-web-5. Another relevant conclusion is that in each case, the lower height of the model implies a lower compressive stress on the top of the T-web section: even in the last case, the section is completely tense.

4.4.5.2 Comparison of normal stresses on the concrete

The same comparison is done for the concrete. First the vertical path is analyzed:

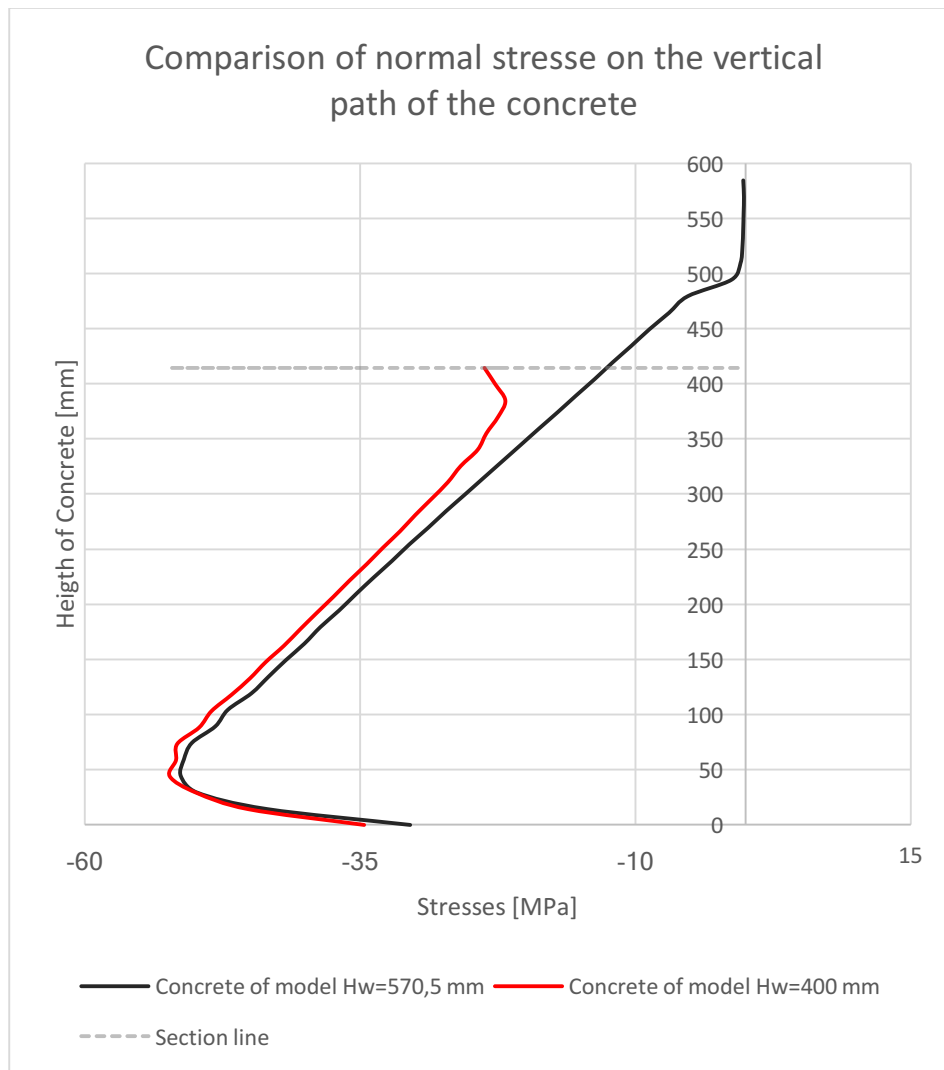


Figure 131 Comparison of normal stresses on the vertical path

Height Concrete	Stresses [MPa]		
	Concrete Hw=570.5 mm	Concrete Hw=400 mm	Increase %
0	-30.4676	-34.6337	13.7
14.3696	-43.4518	-45.1512	3.9
29.3746	-49.8237	-49.8472	0.0
44.3796	-51.2978	-52.263	1.9
59.3846	-51.0174	-51.7033	1.3
74.3896	-50.2953	-51.5834	2.6
89.3946	-48.1619	-49.5961	3.0
104.4	-47.0272	-48.4838	3.1
119.405	-44.8761	-46.6636	4.0
134.41	-43.334	-44.995	3.8

149.415	-41.7614	-43.5637	4.3
164.42	-40.0734	-41.9082	4.6
179.425	-38.6237	-40.4471	4.7
194.43	-36.9306	-38.9475	5.5

Numerical results show a maximum around 5.5 % of increase of the stresses in the lower region of the concrete: the effect due to the decrease of the total height pf the joint is not so relevant.

After that the horizontal path is investigated:

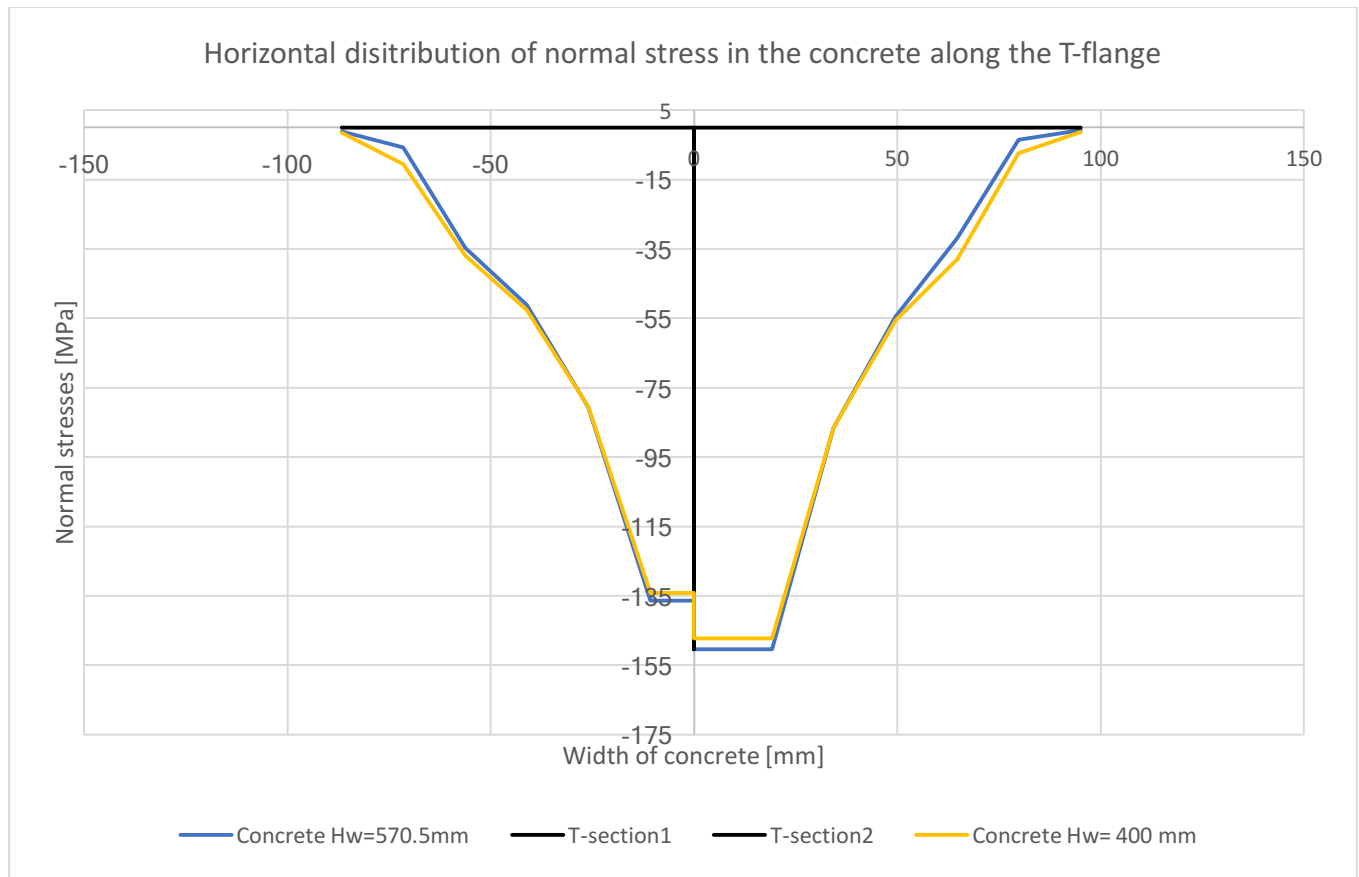


Figure 132 Comparison of the stresses in the concrete along the horizontal path

$$\sigma_3^- = -134.141 \text{ MPa} \quad \sigma_3^+ = -147.205 \text{ MPa}$$

$$\sigma_5^- = -136.412 \text{ MPa} \quad \sigma_5^+ = -150.482 \text{ MPa}$$

The numerical results show that the stresses in the two models are much closed, especially near the T-webs. It is important to underline also that the results show a little, but better distribution of the stresses in the border regions of the T-flange. Of course, the stresses mentioned above, in the point of contact between concrete and T-flange, can be affected by some calculation singularities and these values are not quantitative but only qualitative.

4.4.6 Model5-Model6: Influence of t_w in the plastic analysis

4.4.6.1 Comparison of normal stresses on the steel

The height is 400 mm for both the model and the thickness of the T-web is 30 mm and 35 mm respectively. Both the models are investigated under plastic conditions.

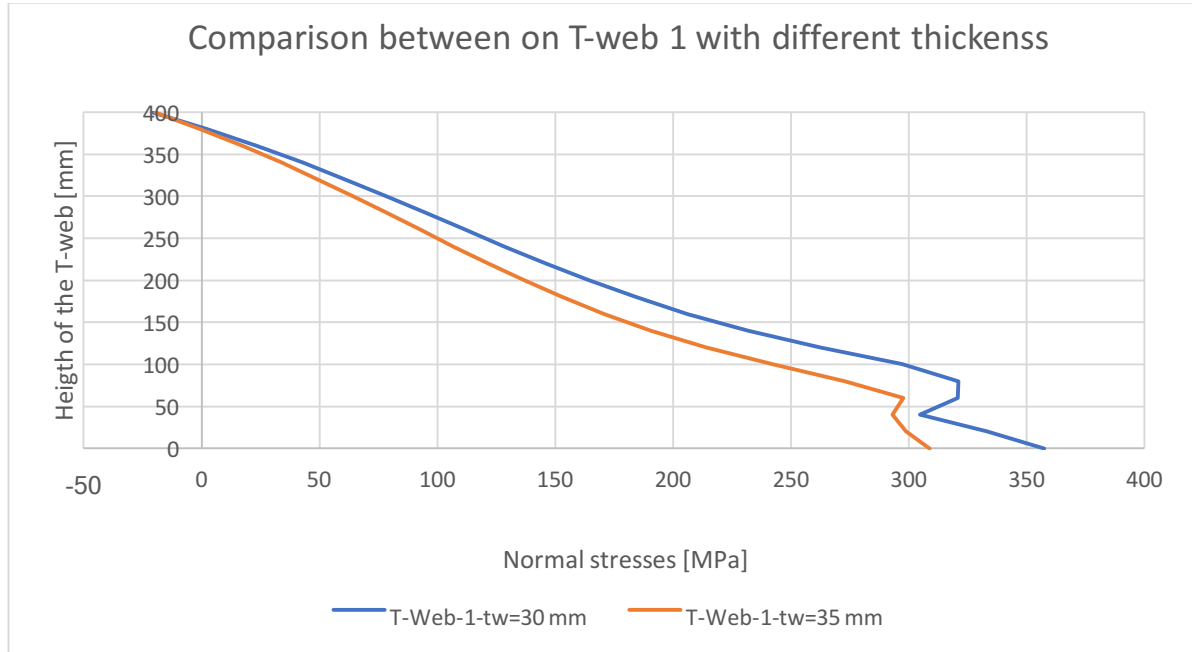


Figure 133 Comparison of the normal stresses in the T-web 1

Height T-web	Stresses [MPa]		
	T-web-1-Model-5	T-web-1-Model-6	Decrease %
0	357.358	308.706	13.6
20	332.981	298.711	10.3
40	304.867	293.089	3.9
60	320.669	297.726	7.2
80	321.193	273.01	15.0
100	297.058	241.922	18.6
120	262.336	214.03	18.4
140	231.892	190.742	17.7
160	206.198	170.735	17.2
180	184.04	153	16.9
200	164.272	136.816	16.7
220	146.059	121.65	16.7
240	128.801	107.104	16.8
400	-20.5958	-19.6466	4.6

The numerical results show an average benefit of 17 % in the normal stresses of the T-web 1, when the thickness is increased.

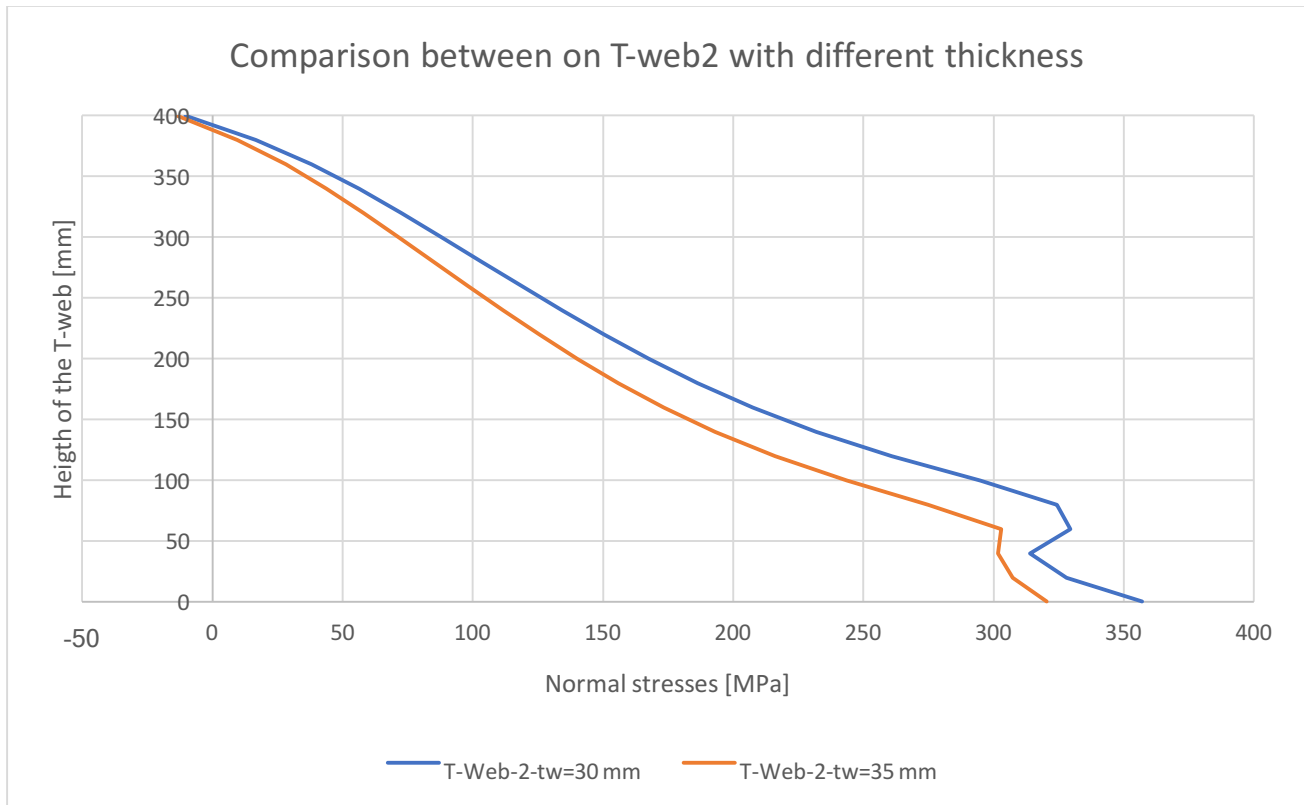


Figure 134 Comparison of normal stress in the T-web 2

Height T-web	Stresses [MPa]		
	T-web-2-Model-5	T-web-2-Model-6	Decrease %
0	356.961	320.325	10.3
20	327.916	307.372	6.3
40	313.964	301.666	3.9
60	329.389	302.874	8.0
80	324.264	274.928	15.2
100	294.707	243.682	17.3
120	260.931	216.076	17.2
140	231.885	193.068	16.7
160	207.414	173.326	16.4
180	186.333	155.962	16.3
200	167.562	140.225	16.3
220	150.366	125.6	16.5
240	134.188	111.672	16.8
260	118.606	98.1727	17.2
280	103.288	84.8485	17.9

The numerical results show an average benefit of 16 % in the normal stresses of the T-web 2, when the thickness is increased.

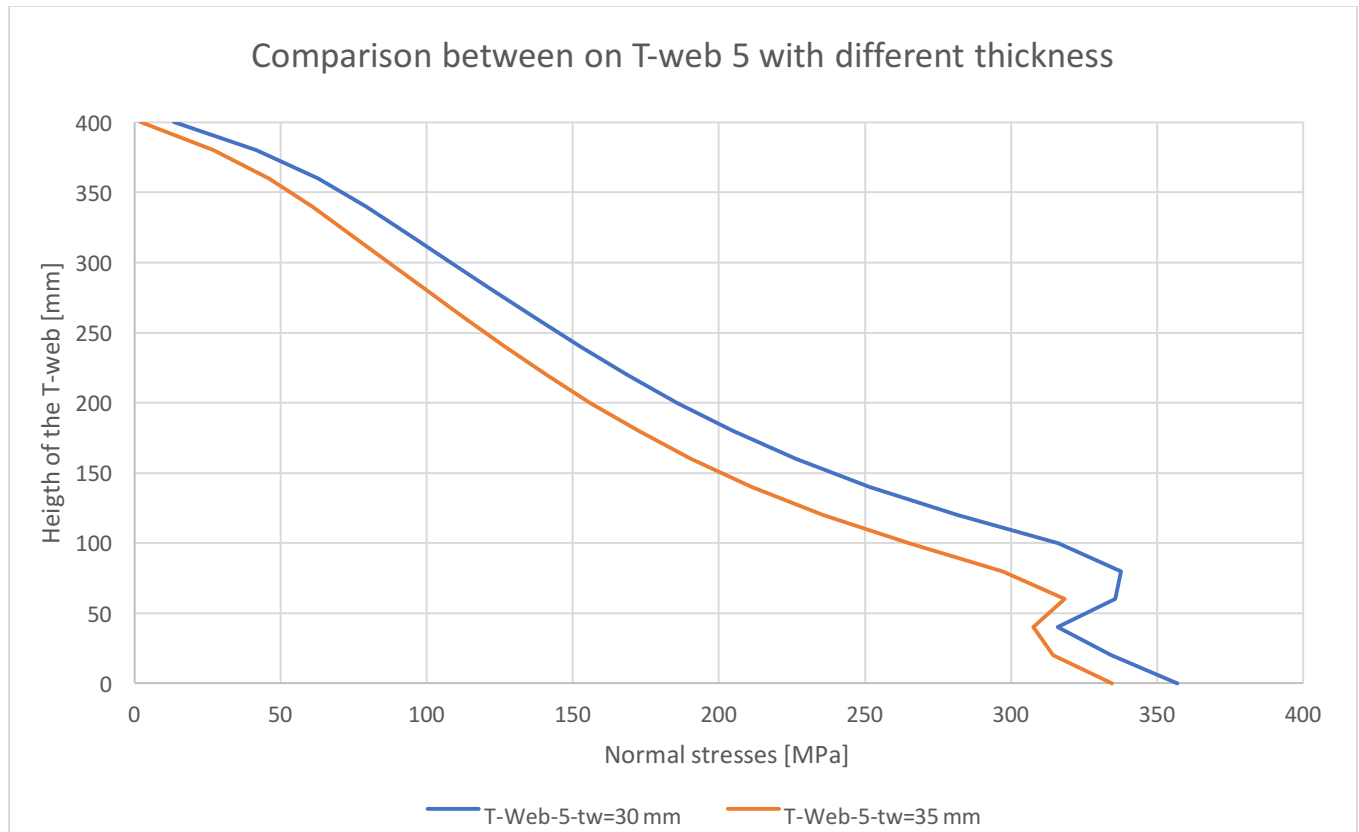


Figure 135 Comparison of normal stress in the T-web 5

Height T-web	Stresses [MPa]		
	T-web-5-Model-5	T-web-5-Model-6	Decrease %
0	356.959	334.475	6.3
20	334.415	314.462	6.0
40	315.949	307.672	2.6
60	335.729	318.317	5.2
80	337.727	296.996	12.1
100	316.273	265.084	16.2
120	281.827	235.693	16.4
140	251.551	211.206	16.0
160	226.211	190.402	15.8
180	204.684	172.294	15.8
200	185.743	156.011	16.0
220	168.596	141.012	16.4
240	152.634	126.875	16.9

260	137.458	113.314	17.6
280	122.756	100.105	18.5
300	108.348	87.1079	19.6

The numerical results show an average benefit of 16 % in the normal stresses of the T-web 2, when the thickness is increased. In each of these illustrative cases, the bigger differences in the stresses in these two models, are over 10 cm of the t-web height: this is reasonable and it could be due to the discontinued region due to the presence of concrete below the bottom surface.

4.4.6.2 Comparison of normal stresses on concrete

The stresses on the vertical path of concrete are investigated:

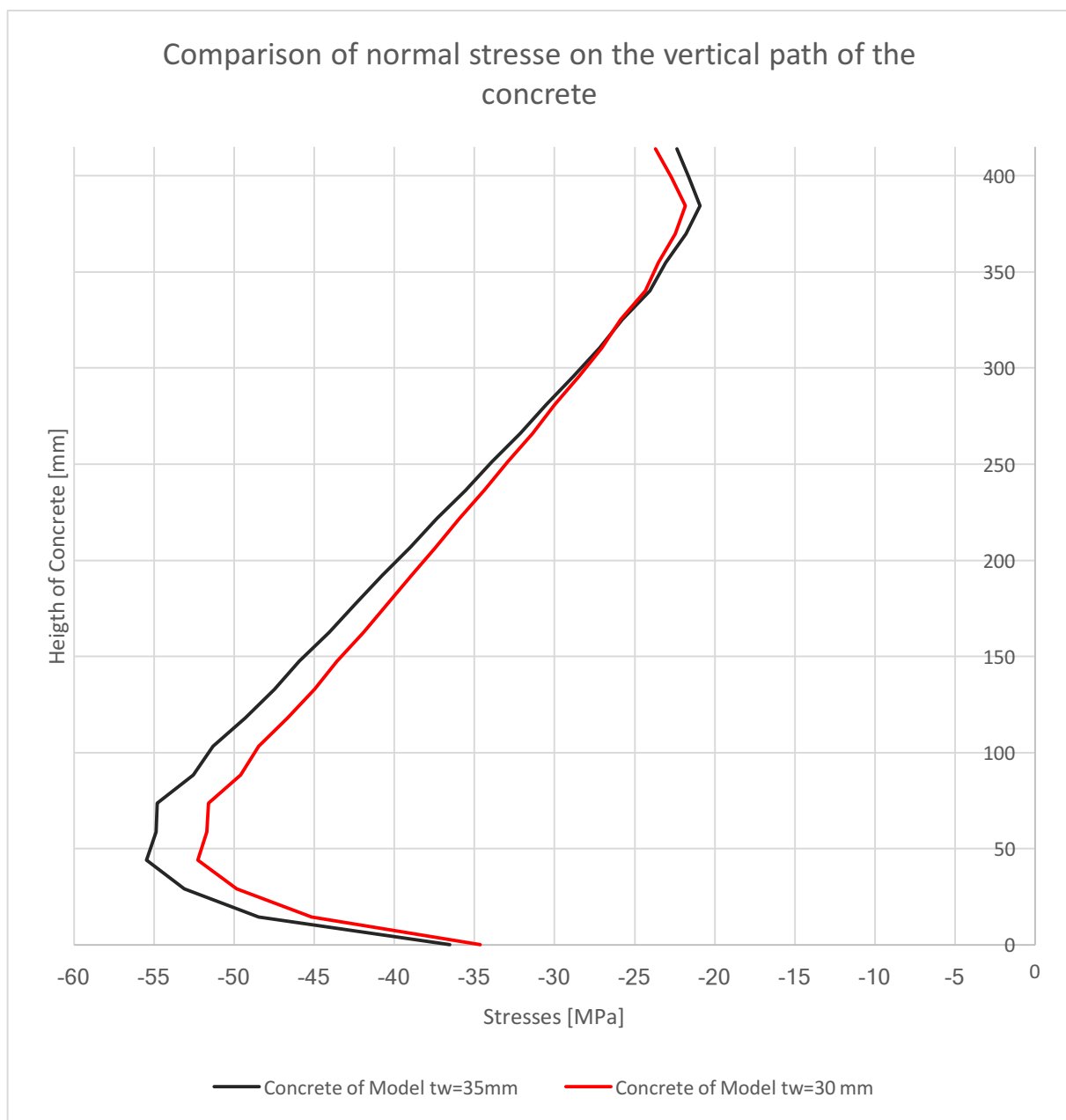


Figure 136 Comparison of normal stress on the concrete

Height Concrete	Stresses [MPa]		
	Concrete Model tw= 30 mm	Concrete Model tw=35 mm	Increase %
0	-34.6337	-36.5246	5.5
14.3026	-45.1512	-48.4549	7.3
29.1084	-49.8472	-53.1022	6.5
43.9143	-52.263	-55.4868	6.2
58.7201	-51.7033	-54.8831	6.2
73.5259	-51.5834	-54.8133	6.3
88.3318	-49.5961	-52.5498	6.0
103.138	-48.4838	-51.3283	5.9
117.943	-46.6636	-49.3183	5.7
132.749	-44.995	-47.482	5.5
147.555	-43.5637	-45.9257	5.4
177.167	-40.4471	-42.4506	5.0
191.973	-38.9475	-40.7622	4.7
.....

Numerical and graphical results show an increment in the stresses due to the increase of the thickness of the web on the concrete in the lower region and a reduction of the values in the upper regions. The result is in accordance with the theory: increasing the thickness it means to have a smaller width of reagent concrete and it means to have more stresses inside of it.

$$\sigma_{c5} = \frac{F_c}{B_{j1} * H_{cls}}$$

$$\sigma_{c6} = \frac{F_c}{B_{j2} * H_{cls}}$$

$$\frac{\sigma_{c5}}{\sigma_{c6}} = \frac{F_c}{B_{j1} * H_{cls}} * \frac{B_{j2} * H_{cls}}{F_c} \approx \frac{B_{j2}}{B_{j1}}$$

$$B_{ji} = \frac{B_{fi} - t_{wi}}{2}$$

→

$$\frac{B_{j2}}{B_{j1}} \approx \frac{86.8335}{94.3335} \approx 0.92$$

It implies, theoretically an increment around the 8 %:

$$\sigma_{c6} \approx 1.08 \sigma_{c5}$$

As seeing in the numerical results and in the theoretical formulation, the increase it is not so relevant and in the model, it is not never more than the 6 %.

The horizontal path is now investigated:

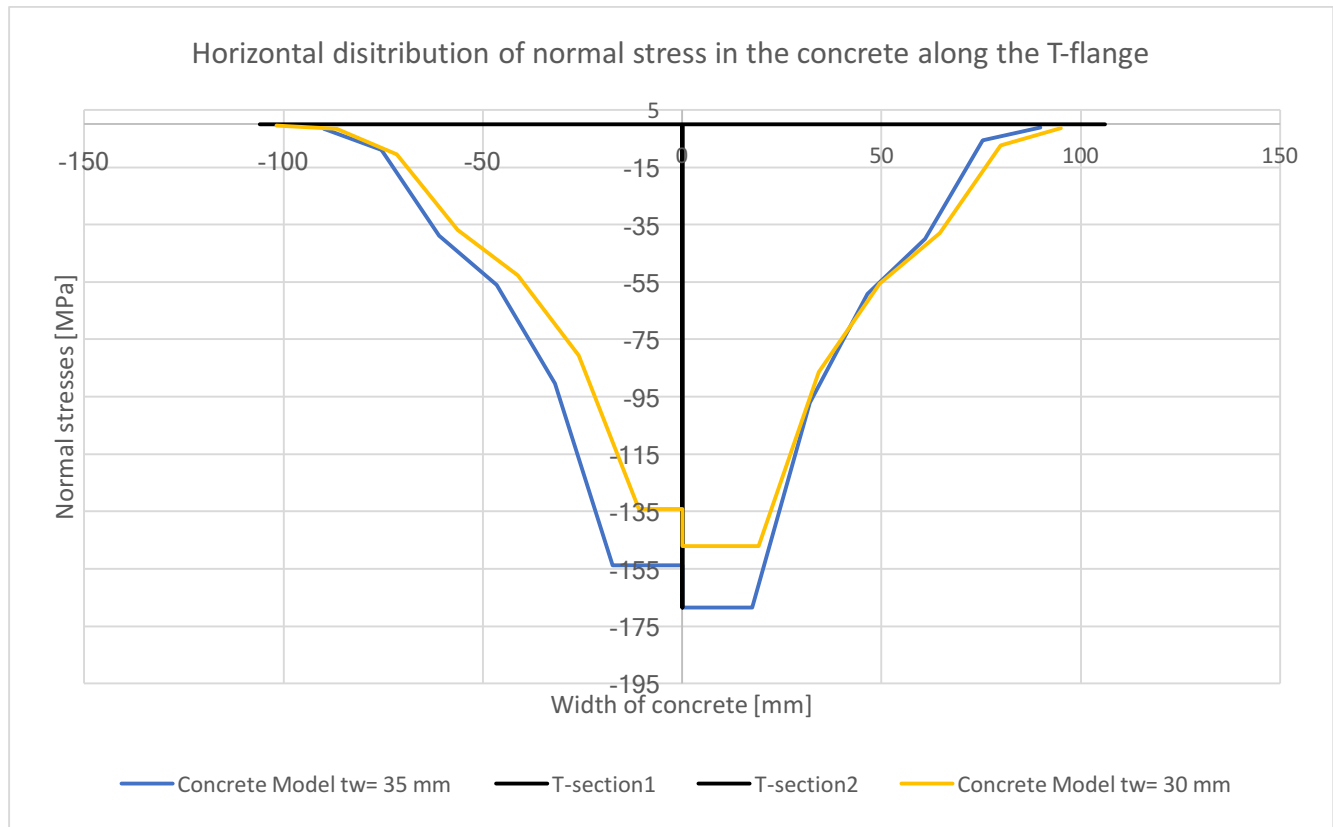


Figure 137 Comparison of stresses in the contact surface between concrete and T-flange

Height T-web	Stresses [MPa]		
	Concrete Model-6	Concrete Model-5	Increase %
30.173	-1.59974	-1.59689	0.2
45.3404	-9.0519	-10.4923	-15.9
60.5077	-38.8391	-36.9444	4.9
75.675	-56.1004	-52.664	6.1
90.8422	-90.3629	-80.573	10.8
106.01	-153.753	-134.141	12.8
136.01	-168.616	-147.205	12.7
151.177	-97.1746	-86.4915	11.0
166.344	-59.0674	-55.6523	5.8
181.511	-40.0219	-37.9512	5.2
196.679	-5.63329	-7.35891	-30.6
211.846	-1.24993	-1.2607	-0.9

The numerical comparison shows an increase around the 6% between the two stresses, in a region far enough from the singularities.

5 CONCLUSIONS

In the first part of the thesis the model of the whole bridge has been validate, comparing the results obtained on the Sofistik model. The reliability of the model is confirmed by the calculation of the error between Abaqus results and Sofistik results. It does not overcome, ever, the 10% and it is a good result, considering the large size of the model and the huge forces involved. Once the model has been declared valid, the parametric model of the joint has been done. At the beginning, three models have been analysed: they have the same geometry. The changes between the three models are as follows: the first one is analysed under elastic conditions, the second one has an additional component to control the horizontal displacement and the third one is investigated under plastic conditions with regard to steel. After that, the geometry has been changed to investigate the effect of each single parameter on the stresses on the steel and on the concrete. The first important thing found out thanks to this Abaqus model, is the need to use an additional horizontal plate to increase transverse stiffener and connect the two lateral walls of the bridge behind the vertical cut. In fact, in this way, the horizontal displacement can be reduced from 6.26 mm to 0.512 mm, with a decrement of 90 %. The first comparison and the third show the benefits in the T-web due to the increase of its the thickness in the elastic and plastic analysis, respectively. The decrease of the stresses can be estimated around the 15% for the first comparison and around the 17% for the third. The stresses on the concrete are not influenced in a relevant way: the increment is around the 6%. The second comparison shows the consequences due to the increase of the height in a plastic analysis. The stresses on the steel are increasing of the 10%, more or less; on the other side the compressive region in the top of the T-web is reducing. The stress distribution on the vertical height of the concrete is close to a uniform distribution than the previous model: the stresses on the top are not near zero anymore. To complete the geometrical study can be important to investigate how the change of B_w , L_j or t_f modifies the trend and the distribution of stresses on concrete. Finally, it is possible to state that this thesis allows who comes next, to insert the joint into the validate bridge model in order to investigate the influence of the joint in the bridge's components and also to understand how the bridge itself affects the joint behavior.

Bibliography

- Abaqus Analysis User's Guide** [Online] / auth. Abaqus. - Dassault Systèmes, Aprile 2, 2013. - Aprile 2, 2013. - <http://dsk.ippt.pan.pl/docs/abaqus/v6.13/books/usb/default.htm>.
- Behavior of the concrete under biaxial stresses** [Journal]. - 1 8, 1969. - Vol. 66.
- Bridge Engineerin: A Global Perspective** [Book] / auth. Troyano Leonardo Fernandez. - 2003.
- Concepts and Applications of Finite Element Analysis** [Book] / auth. R.D. Cook. - [s.l.] : John Wiley & Sons, 1989. - third edition.
- Eurocodice 3 EN 1993-1-1**. - 1993.
- Finite element modeling for stress analysis** [Book] / auth. Cook Robert D.. - Madison : John Wiley & sons, inc, 1995. - Vol. 1.
- Finite element modeling for stress analysis** [Book] / auth. Cook Robert D.. - Madison : John Wiley & sons, 1995. - Vol. 1.
- Girder Bridge** [Journal] / auth. Technology Argentina: National Istitute of Industrial. - Ottobre 26, 2012.
- Incompatibile Displacements Models** [Book] / auth. Wilson E.L. R.L.Taylor, W. Doherty and J. Ghaboussi. - Illinois : [s.n.], 1971.
- Integral bridges** [Article] / auth. society The concrete // concrete society current practice sheets. - 02 12, 2018.
- Integral Bridges and the Modelling of Soil-Structure Interaction** [Book] / auth. Rhodes Steve. - 2018.
- Integral Railway bridges in Germany** [Journal] / auth. Marx Steffen. - Berlino : [s.n.].
- Introduction to finite element methods** [Book] / auth. Felippa Carlos A.. - Boulder : ASEN 5007, 2001. - Vol. 1.
- La zincatura a caldo: cosa è e perchè sceglierla?** [Interview] / interv. Ricciolino Carmine / ed. Ingenio. - 12 11, 2013.
- Lezioni ponti e grandi strutture** [Book] / auth. Rossi Pier Paolo. - Catanuia : [s.n.], 2014.
- Manuale di ingegneria civile** [Book]. - [s.l.] : Zanichelli. - Vol. 2.
- Ponti integrali: analisi statica e sismica** / auth. Condoleo Alberto. - Padova : Università degli studi di Padova, 2011. - Vol. 1.
- Popular Cable-Stay Bridges Rise Across U.S. to Replace Crumbling Spans** [Journal] / auth. American Scientific. - Aprile 2, 2017.
- Port Authority of New York and New Jersey- George Washington Bridge** [Journal] / auth. York The Port Authoriry of New. - September 13, 2013.
- Revolutionized the finite Finite Element Method by introducing a natural coordinate reference system** [Book] / auth. Irons Bruce. - 1968.
- Rigid Frame Bridges** [Book] / auth. Transportation Maryland Department of. - Maryland : [s.n.].
- Strutture in acciaio** [Book] / auth. G.Ballio F. Mazzolani. - [s.l.] : Hoepli, 1987.
- The Finite Element Method in Plane Stress Analysis** [Book] / auth. R.W. Clough. - Pittsburg : [s.n.], 1960.
- Zincatura a caldo** / auth. Pernice Lello. - [s.l.] : poligrafia ruggiero, 2014.